Geo-information Science and Remote Sensing

Thesis Report GIRS-2023-27

Influence of forest management on canopy gap dynamics

Uncovering the potential of the AHN to map, characterize and compare canopy gap dynamics

Niek Koelewijn

17 May 2023

WAGENINGEN
UNIVERSITY & RESEARCH

Influence of forest management on canopy gap dynamics

Uncovering the potential of the AHN to map, characterize and compare canopy gap dynamics

Niek Koelewijn BSc

Registration number 1039084

Supervisors:

L. C. Vreugdenhil MSc
dr. ir. J. den Ouden

A thesis submitted in partial fulfilment of the degree of Master of Science
at Wageningen University and Research,
The Netherlands.

17 May 2023
Wageningen, The Netherlands

Thesis code number: GRS-80436
Thesis Report: GIRS-2023-27
Wageningen University and Research
Laboratory of Geo-Information Science and Remote Sensing

Abstract

In the Netherlands, a country-wide, multi-temporal, and publicly available Areal Laser Scanning (ALS) dataset exists, the Actueel Hoogtebestand Nederland (AHN). ALS has been shown to provide highly suitable data to investigate canopy gap dynamics. However, the AHN has currently not been used to study canopy gap dynamics in the Netherlands. Accurate assessment of canopy gap dynamics is shown to provide useful insights in a number of ecological processes in forests. Understandings in canopy gap dynamics on large spatiotemporal scales can considerably be improved with the use of ALS data. In this study, a comparison is made between canopy gap dynamics derived from two CHM-based canopy gap detection methods. Furthermore, the added value of combining these methods is explored. It was found that the combination of methods was highly accurate in detecting canopy gaps from AHN data. It was further revealed that the combination of canopy gap detection methods provided information about the presence of a tree layer in the detected canopy gap, information that could not be derived from the methods separately. This study further aimed to determine the influence of forest management on canopy gap dynamics. In the study area, the Speulderbos, forest plots were situated with different conditions in terms of management type, dominant tree species and age. The influence of forest management was disentangled from the influence of tree species and age, and it was thereby found that forest management leads to an increased canopy gap density, while it does not lead to an increased canopy gap area. This investigation revealed that canopy gaps detected from the AHN can be used to adequately study the influence of forest conditions on canopy gap dynamics.

Acknowledgements

I want to thank L. C. Vreugdenhil MSc and dr. ir. J. den Ouden for supervising this thesis research. The enthusiasm of both supervisors for this topic helped me to stay motivated for this project, and inspired me to think creatively. The discussion that we had about the content of this study were much appreciated. The skills that I have acquired in the process of this theses would not have been achieved without the help of the supervisors. I want to thank dr. ir. S. de Bruin for examining this thesis. I want to thank Staatsbosbeheer for cooperating in this thesis research project by providing access to data about the Speulderbos. Lastly, I want to thank my wife, who took care of me while finalising this study, and the Lord, who gave me every day that the project lasted the necessary strength and inspiration.

Table of contents

1. Introduction

Forest ecosystems are globally under influence of human-induced stressors. Climate change, land use change, the biodiversity crisis and the combination of these processes cause large-scale alterations in forest systems (Hasan et al., 2019). Climate change causes forest systems to adapt in a complex and non-linear fashion (Bonan, 2008). Land use change has led to increased forest fragmentation, to altered biochemical and biophysical cycles, and to reduced forest ecosystem-service provisioning (da Cruz et al., 2021; Haddad et al., 2015). Human activities in forests, such as hunting and logging, are leading to changes in the forest structure and species composition (Ripple et al., 2015; Thiollay, 1992). High precision data can be used to monitor how forests develop under these different stressors, and therefore it can be used to support forest management, and to guide forest ecosystem system conservation (Leiterer et al., 2015; Zielewska-Buttner et al., 2016).

1.1. Background canopy gaps

High precision data can e.g. be used to assess the development of canopy gaps in forests over time, which can lead to an improved insight in the ecological state of forests (Blackburn et al., 2014). Canopy gaps can be defined as openings within a continuous and relatively mature canopy, in which trees are absent or markedly smaller than their immediate neighbours (St-Onge et al., 2014). Canopy gaps influence the ecological characteristics and structure of a forest (Spies, 1998). Insights in forest processes, such as tree regeneration and disturbance regimes, can be increased by investigating canopy gaps (Blackburn et al., 2014). Canopy gaps locally adapt the soil and air temperature, soil moisture content, soil nutrient concentration and soil light availability, and are thus an important factor to explain tree species composition, species heterogeneity, and successional dynamics in forests (Lombard et al., 2019; Muscolo et al., 2014; Vepakomma et al., 2008). The degree of impact of a canopy gap on local conditions in a forest is dependent on the size, orientation, and shape of the canopy gap (Frolking et al., 2009).

Canopy gap dynamics can be defined as the continuous process of canopy gap formation and closure over time (St-Onge et al., 2014). Canopy gaps can emerge, remain, expand, shrink, be displaced and disappear over the course of time (St-Onge et al., 2014). Canopy gap emergence is caused by the disappearance of a tree, either due to natural and or human factors (Mao et al., 2020). Natural factors include wind storms, fires, insect or pest outbreaks, or individual tree mortality (Blackburn et al., 2014). Wind storms, fires, and insect or pest outbreaks often result in relatively large canopy gaps, whereas individual tree mortality often results in relatively small gaps (Muscolo et al., 2014). Human activities that can lead to the emergence of canopy gaps are thinning, rejuvenation cutting, and girdling. Thinning, or improvement cutting, is the practice of decreasing the stem density in a forest plot by cutting trees, with the aim to stimulate the growth of the remaining trees in the plot (Subedi et al., 2018). Thinning operations often lead to the formation of small canopy gaps with a high density and a regular pattern (Wilkinson et al., 2016). Rejuvenation cutting is the practice of wood harvest at the end of a forest management cycle. The area and shape of canopy gaps emerged due to rejuvenation cutting is dependent on the forest management system. In a clear cutting system, large continuous canopy gaps are formed (Rosenvald & Lohmus, 2008). In other management systems, in which live trees remain in the cutting area, such as shelter wood systems or selection systems, canopy gaps can either emerge as large interrupted patches, or as multiple smaller patches (Beaudet et al., 2004; Weis et al., 2006). Girdling is the removal of a strip of bark from a tree with the aim to prevent transportation of photosynthesis products to the roots of a tree (Li et al., 2003). After applying girdling, the tree stem is not removed from the forest, with the aim minimise the impact of this management activity on the forest ecosystem

(Fujii et al., 2021). Girdling leads to a gradual decay of the targeted tree, which eventually leads to the emergence of small canopy gaps.

When a canopy gap emerges, the physical stress on the trees surrounding the gap increases. This increased level of stress at the edges can lead to canopy gap expansion (St-Onge et al., 2014). Canopy gap closure can either be caused by lateral growth or by vertical growth. Lateral gap closure is the inward expansion of the crowns of the trees surrounding the canopy gap. Vertical gap closure is the growth of tree juveniles in the canopy gap (St-Onge et al., 2014). The combination of canopy gap closure and expansion can occasionally lead to canopy gap displacement (Vepakomma et al., 2012).

1.2. Canopy gap detection methods

Studying canopy gap dynamics is a complex task. To start, the effort needed to map and delineate canopy gaps in field studies is high (Zielewska-Buttner et al., 2016). For this reason, field studies of canopy gaps are often carried out on low spatial and temporal scales (Bonnet et al., 2015). Field studies of canopy gaps require a high degree of expertise, and occasionally lead to subjective results (Leiterer et al., 2015; Mao et al., 2020). Furthermore, the methods used to delineate canopy gaps, and the thresholds used to determine what is considered to be a canopy gap, are inconsistent between different studies (Hunter et al., 2015).

Passive remote sensing can be used as an alternative to field studies to detect canopy gaps. However, identifying canopy gaps by visually interpreting aerial images is considered to be a complicated task (Mao et al., 2020). The use of passive remote sensing techniques in canopy gap studies is hampered by their spatial resolution, which complicates the detection of small canopy gaps (Lombard et al., 2019). Moreover, the influence of shadows, illumination conditions and spectral inseparability obstructs the accuracy of passive remote sensing techniques in detecting canopy gaps (Vepakomma et al., 2008).

LiDAR (Light Detection and Ranging) is an active remote sensing technique that can be used to derive three dimensional (3D) data about the forest structure (Leiterer et al., 2015). High resolution information of the vertical and horizontal structure of forests can be derived making use of LiDAR (Gaulton & Malthus, 2010). Therefore, LiDAR has the potential to spatially delineate canopy gaps with high precision (Vehmas et al., 2011). The main principle behind LiDAR is the transmittance of light pulses to determine the distance to an object (Akay et al., 2009). With these pulses, the distance to an object is determined by taking the product of the speed of light and the time required for an emitted pulse to travel to an object (Lim et al., 2003). LiDAR can amongst others be acquired making use of Terrestrial Later Scanning (TLS) or Airborne Laser Scanning (ALS). TLS is more suitable to derive information about the sub canopy structure of a forest (Alonso-Rego et al., 2021), while ALS is more suitable to derive information about the canopy height (Brede et al., 2017). The advantage of ALS is that it can be used to determine the canopy height at a high spatial resolution (Koukoulas & Blackburn, 2004). Therefore, ALS has opened the way to study canopy gaps at large spatial and temporal scales (Bonnet et al., 2015).

1.3. Canopy gap detection thresholds

Methods and thresholds to derive canopy gaps from ALS data is not standardized. Inconsistencies exists in the definition of canopy gaps, and in the thresholds used to delineate canopy gaps from ALS data (White et al., 2018). This inconsistency hampers the comparability between different canopy gap studies, as the use of different canopy gap definitions and thresholds can lead to significantly different results (Hunter et al., 2015; Koukoulas & Blackburn, 2004).

Runkle (1981) defined canopy gaps as the ground area under the canopy, extending to the bases of canopy trees surrounding the canopy opening. The advantage of this definition is that it includes areas directly and indirectly affected by canopy gaps, and therefore this definition is often used to study the ecological effects of canopy gaps (de Lima, 2005; Gaulton & Malthus, 2010). However, using ALS, it is challenging to detect the stems of trees surrounding canopy gaps (Gaulton & Malthus, 2010). Therefore, the canopy gap definition of Brokaw (1982) is often used in ALS-based canopy gap detection studies. In this definition, canopy gaps are defined as holes in the forest, with irregularly shaped, vertical sides. The sides of the gap are situated at the innermost place reached by the crown of trees surrounding the gap (Brokaw, 1982). This definition is considered to be objective and convenient, although it has received critique for its lack of realism in determining the effects of canopy gaps (de Lima, 2005).

The shapes of canopy gaps are typically irregular, which complicates the canopy gap delineation process (Seidel et al., 2015). Canopy gaps continuously develop over time, and therefore subjective choices must be made to determine what still counts as a canopy gap, and what not (Senecal et al., 2018). To determine which gaps in the forest are considered to be canopy gaps and which not, most studies make use of predefined thresholds (White et al., 2018). Common thresholds used are a minimum and maximum for the canopy gap area, and an absolute or relative vegetation height maximum within the canopy gap (St-Onge et al., 2014). A minimum canopy gap area could for example be used to exclude gaps from the analysis that are unlikely to have emerged due to the loss of an entire tree, or to exclude natural spaces between trees (Gaulton & Malthus, 2010; St-Onge et al., 2014). The threshold for the minimum canopy gap area ranged from 2 to 50 m2 in earlier published literature (White et al., 2018). The threshold for the maximum canopy gap could be used to distinguish the disappearance of one or several trees from the disappearance of a large cohort of trees, because the ecological consequences of these two events differ (McCarthy, 2001). In literature, the threshold for the maximum canopy gap area ranged from 200 to 1000 m2, although it is also common to not use this threshold in the canopy gap delineation process (St-Onge et al., 2014). A threshold for the maximum vegetation height within canopy gaps is used to determine when a canopy gap is considered to be closed. Absolute and relative height thresholds have been used in literature for the maximum vegetation height (St-Onge et al., 2014). An absolute height threshold could for example be determined based on knowledge about the field conditions (Vepakomma et al., 2008). Some authors preferred the use of a height threshold relative to the canopy height, as canopy gaps are defined as openings in the canopy that has a significantly lower canopy height compared to its surroundings (St-Onge et al., 2014). The absolute threshold for the maximum vegetation height in a canopy gap ranges in literature from 1 to 20 m. Studies that worked with a relative canopy gap vegetation height threshold used either a percentage of the maximum canopy height (Gaulton & Malthus, 2010), or using classes of absolute height thresholds depending on the height of the trees surrounding the gap (Zielewska-Buttner et al., 2016).

Canopy gaps can either be derived directly from a pointcloud, or indirectly using a Canopy Height Model (CHM) (Gaulton & Malthus, 2010). As it is possible to derive high precision canopy height information from ALS data, CHM-based methods have been shown to be efficient and accurate methods to detect canopy gaps (Gaulton & Malthus, 2010; Leitold et al., 2018; Vepakomma et al., 2012). There are two possible strategies to derive canopy gap dynamics from a time series of CHMs. Either the canopy gaps are selected in each CHM version separately, or the canopy gaps are directly selected from the difference between the CHM versions.

The first strategy, described by Vepakomma et al. (2008), uses as threshold the maximum vegetation height in a canopy gap to select areas that are considered to be canopy gaps in each CHM version. By comparing the selected canopy gaps of each CHM version, it is possible to study canopy gap dynamics over time, as was described by Vepakomma et al. (2012). An R

package was developed by Silva et al. (2019) to derive canopy gap dynamics following this method, therefore in this study this method will be referred to as the Silva method.

The second strategy is based on the difference in height between two CHM versions. A threshold for the minimum canopy height decrease in a canopy gap is used to select canopy gap areas in the difference CHM. This strategy was described by Leitold et al. (2018), and is therefore further referred to as the Leitold method.

1.4. Canopy gap detection in the Netherlands

In the Netherlands, a country-wide ALS dataset exists that is openly available, and that is updated every few years. The name of this dataset is Actueel Hoogtebestand Nederland (AHN) which can be translated to Dutch Current Elevation Model. The Netherlands was the first country to be entirely covered by an ALS dataset (van der Sande et al., 2010). Originally, the AHN was primarily acquired to support water safety management (Swart, 2010). However, the AHN is shown to be of use in a variety of fields, such as mapping tidal dynamics (Pearson et al., 2022), quantifying urban heath islands (Steeneveld et al., 2011), and deriving forestry related metrics (Meijer et al., 2015; Nolet & Spliethof, 2020). To the best of our knowledge, the AHN has not been used to map canopy gap dynamics to this date, even though ALS datasets with comparable characteristics to the AHN have earlier been shown to be highly suitable to map canopy gap dynamics (e.g. Vehmas et al., 2011; Vepakomma et al., 2012). Currently, canopy gap emergence caused by natural factors is not systematically registered in the Netherlands. Wood removal practices that cause canopy gaps to emerge are registered in a decentralized way, and only on forest plot level. Currently, there is no country-wide dataset available with information of the location were canopy gaps exist, were new canopy gaps have formed, or were canopy gaps have disappeared in Dutch forests. This data could, amongst other reasons, be used to learn to what extent forest management systems succeeds to mimic natural canopy gap dynamics, by making comparisons between canopy gaps in managed and unmanaged forests (Senecal et al., 2018).

1.5.Research aims

This study had two aims. First, it was aimed to derive canopy gap dynamics from the AHN. Two CHM-based methods, the Silva and Leitold method, were combined to compare the canopy gap detection results of these methods, and to derive what additional insights there could be derived from the combination of these methods. It was hypothesized that different canopy gap delineation methods would result in different spatial patterns of identified gaps, and that this difference would provide information of the ecological conditions in the canopy gaps.

Second, it was aimed to derive the influence of forest management on canopy gap dynamics, by comparing the canopy gap dynamics in forest plots with different management types. It was hypothesized that in managed forest plots, the canopy gaps would be larger in area, higher in density, and more regularly shaped compared to canopy gaps in unmanaged forest plots (Muscolo et al., 2014; St-Onge et al., 2014). It was further hypothesized that in managed forest plots, no tree layer would remain after a canopy gap emerging event, while this would be the case in unmanaged plots, as managed plots often lack different tree layers in the forest structure (Johann, 2006).

2. Methods

2.1. Study area

To investigate the potential of the AHN to study canopy gap dynamics, a 304 ha study area was selected in the Speulderbos (52.25ºN, 5.67ºE) (Figure 1). The Speulderbos is subdivided in forest plots with different management types, dominant tree species and germination year. It was selected as study area, as access to data was provided for this study containing the dominant tree species, age, and management type per forest plot. This data provided the possibility to disentangle the influence of management, dominant tree species and forest plot age on canopy gap dynamics. The forest plots are labelled with codes that consist out of a number and a letter. The codes that start with 10 are part of the forest reserve of the Speulderbos. These forest plots are strictly unmanaged. Outside the strict unmanaged reserve, there are other old beech and oak plots found in the Speulderbos. These plots are labelled with germination year 1835, the first documentation year of the Speulderbos. In these forest plots, no wood removal practices as thinning or rejuvenation cutting takes place. However, girdling takes place in these forest plots, for example to stimulate tree species diversity (J. den Ouden, personal communication, 14 September, 2022). Therefore, beech and oak forest plots in the study area that are situated outside the strict forest reserve with germination year 1835 are considered to be pseudo-unmanaged in this study. In the remaining forest plots, thinning and rejuvenation cutting frequently takes place, and therefore these plots are considered to be managed in this study. There is a gradient in forest management intensity between the three management types in the Speulderbos, with managed plots as most intensely managed, pseudo-unmanaged in-between, and unmanaged as least intensely managed.

The Speulderbos is part of a larger forested area; the Veluwe. It is situated in the humid temperate climatic zone, classified as Cfb in the Köppen-Geigner climatic classification (Beck et al., 2018). The average yearly temperature is 10.1 ºC, the average temperature in the coldest month is 2.9 ºC, the average temperature in the warmest month is 18.1 ºC, and the average yearly precipitation is 868.0 mm. These climatic characteristics were measured over the period 1990-2020, and were derived from the Deelen weather station of the Royal Dutch Meteorological Institute (KNMI), which is the nearest weather station to the Speulderbos. The soil is described as a Typic Dystrochrepts on thick heterogenous sandy loam formed by iced-pushed river sediments (Cisneros Vaca et al., 2018).

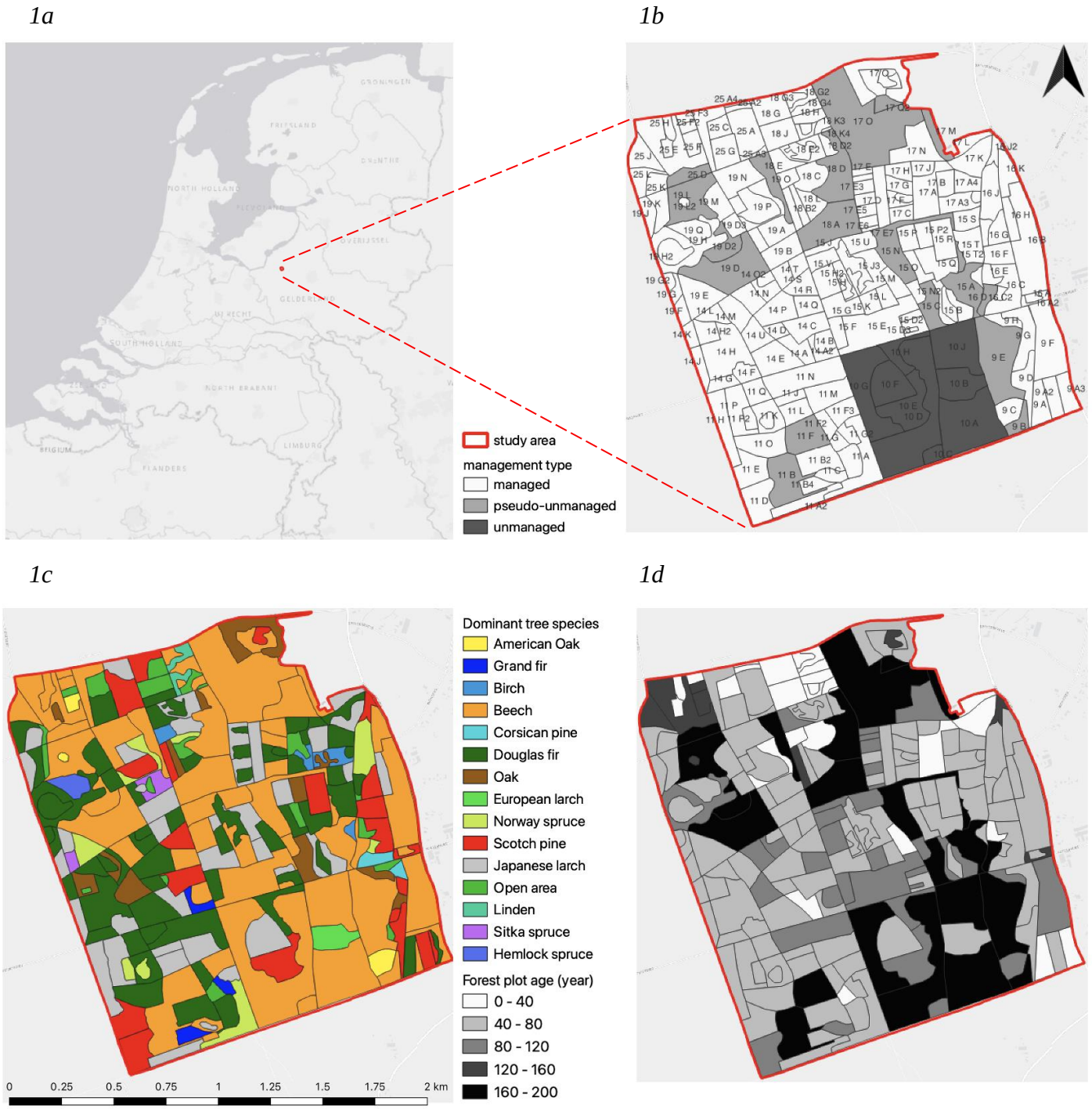

Figure 1 Location of study area in the Netherlands (1a), management type per forest plot with forest plot code (1b), dominant tree species per forest plot (1c), and age class per forest plot (1d).

2.2. Input data

2.2.1. AHN

Four versions of the AHN have been released since 1997. In 2023, the acquisition of the fifth version has started. In this study, two versions of the AHN, version 3 and 4, were included to derive insights about the development of canopy gaps over the time interval between these two AHN versions. For the Speulderbos, the date of acquisition was the 28th of January in 2018 for AHN3, and the 6th of April in 2020 for AHN4. The average point density was 28.7 points/m^2 for AHN3 and 60.3 points/m^2 for AHN4. The AHN is publicly available data, which means that it can openly be used. The data has been made available in 5 x 6.25 km tiles. The AHN data used in this study was remixed by GeoTiles (www.geotiles.nl). The advantages of GeoTiles AHN data are that it can be downloaded in smaller subtiles, 1 x 1.25 km, and that it has a 25 m overlap with the neighbouring (sub)tiles. To fully cover the extent of the study area, AHN3 and AHN4 was downloaded from seven subtiles, 26HZ2_21, 26HZ2_22, 32FN2_01, 32FN2_02, 32FN2_03, 32FN2_06, and 32FN2_07.

2.2.2. State forestry data

Three datasets provided by the Dutch independent governmental organisation Staatsbosbeheer (State Forestry) were used in this study: (1) an Excel sheet with a logbook with all management interventions in the Speulderbos since 2018, (2) a shapefile of the delineation and the code of forest plots in the Speulderbos, and (3) a shapefile with the delineation of dominant tree species and germination year per forest plot. The management intervention data was used as a first exploration of the validity of the location of identified new canopy gaps. The two shapefiles with forest plot data were used to make statistical comparisons between canopy gap dynamics in forest plots with different characteristics.

2.2.3. Yield tables

A book with yield tables per tree species in the Netherlands under different growth conditions and thinning intensities was used to determine the threshold for maximum vegetation height in a canopy gap, and to determine whether canopy gap closure occurred due to lateral or vertical growth (Jansen et al., 2018).

2.2.4. Orthophoto images

Publicly available high resolution orthophotos from 2018 and 2021 were used to visually assess the identified new canopy gaps before and after the gap emergence event. The image of 2018 had a 25 cm spatial resolution, and the image of 2021 had a 8 cm resolution. The data was provided by PDOK, the national geoportal of the Netherlands.

2.3.Software

Open-source software was used in the process of this study. Data preprocessing, data analysis and data visualising was done using R, Python, and QGIS (QGIS Development Team, 2023; R Core Team, 2023; Van Rossum, 2009). Pointcloud processing and analysis was performed using the R package lidR (Roussel et al., 2020). Raster and vector based processing was performed using the R packages terra and sf (Hijmans et al., 2023; Pebesma, 2018). Data structuring, analysis and visualisations were performed using the R packages belonging to the tidyverse (Wickham et al., 2019). For reproducibility purposes, the code of this study has been developed using the version control system GitLab, within the environment of the Wageningen University (git.wur.nl/niek.koelewijn/ahncanopygaps).

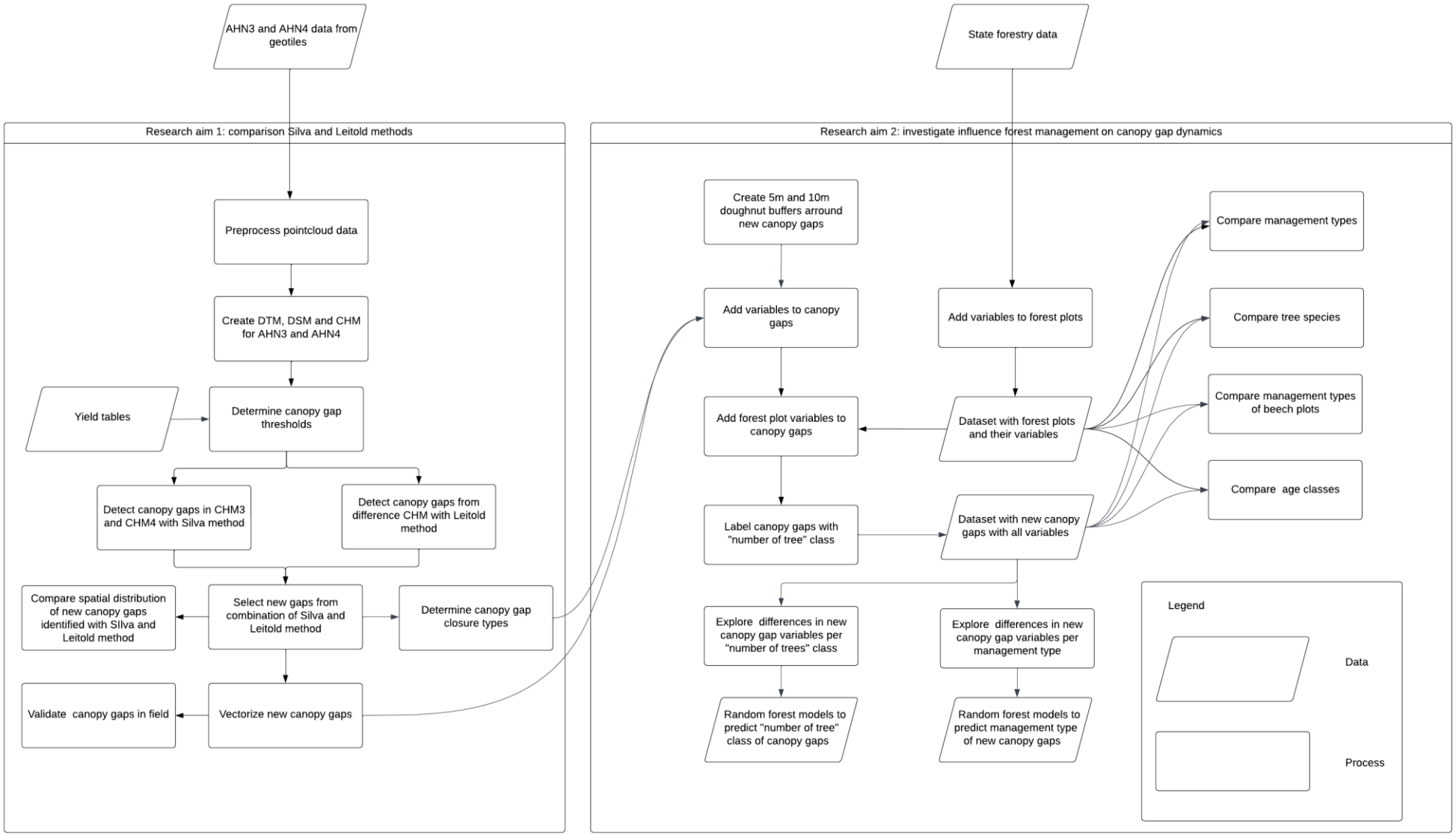

Figure 2 flow chart of the methods

2.4. Comparison Silva and Leitold method

The data analysis steps are summarised in a flow chart (Figure 2).

2.4.1. Pointcloud preprocessing

Using a Python script, the AHN data was decompressed to increase computation speed of further analysis steps. The 25 meter overlap between different AHN subtiles was useful for the development of Digital Elevation Models (DEM). However, for each identified new canopy gap, pointcloud metrics were derived, and the difference in point density between caused by the overlap hampered the acquisition of pointcloud variables. Therefore, AHN subtiles with overlap were used for the DEM development, and filtered AHN subtiles, without overlap, were used for further analysis steps. The filtered AHN subtiles were normalised for ground height to prepare the pointcloud variable acquisition.

2.4.2. Digital elevation models

As the Silva and Leitold methods are both CHM-based canopy gap detection methods, Digital Elevation Models (DEMs) had to be created from AHN3 and AHN4 to create the CHMs. The DEMs were developed with the *rasterize_terrain* function from the lidR package (Roussel et al., 2020). Digital Terrain Models (DTM) and Digital Surface Models (DSM) were created on a 1 meter resolution. Different subfunctions to create DTMs and DSMs were compared in terms of speed, output realism and smoothness. For the DTMs, it was decided that the k-nearest neighbour inverse-difference weighting (knnidw) algorithm, developed by Shepard (1968), with default parameters k = 10, and p = 2, was the most suitable for this study. For the DSMs, it was decided that the lidR point to raster (p2r) was the most suitable for this study. The p2r function takes the height of the highest point found for each pixel of the output DSM (Roussel et al., 2020). Two methods were used fill the missing values of the p2r output. First, a 0.2 meter subcircle was used. This meant that all points in the input pointcloud are replace with a disk of 20 cm. This operation is meant to simulate the fact that the laser footprint is not a point, but rather a circular area (Roussel et al., 2020). To fill the remaining gaps, the triangular irregulated network (tin) algorithm was used, developed by (Franklin, 1973).

After the development of the DEMs, the CHM could be created. The CHM of both AHN versions were created by subtracting the DSMs from the DTMs. To create a difference CHM raster, CHM4 was subtracted from CHM3.

2.4.3. Threshold selection

In this study, the Silva method and Leitold method were combined and compared, with the aim to increase the derived insights in canopy gap dynamics from a time series of CHMs. As both the Silva method and Leitold method were used in this study, four thresholds had to be selected for delineating canopy gaps: (1) the maximum vegetation height in a canopy gap, (2) the minimum canopy decrease in a canopy gap, (3) the minimum canopy gap area, and optionally (4) the maximum canopy gap area. To determine the threshold for the Silva method, the maximum vegetation height in a canopy gap, data from the yield tables by Jansen et al. (2018) was investigated. For the six most important tree species in the Speulderbos, which are beech (*Fagus sylvatica* L.), oak (*Quercus robur* L.), Scotch pine (*Pinus sylvestris* L.), Japanese larch (*Larix kaempferi* Camp.), Douglas fir (*Pseudotsuga menziesii* Mirb.) and Norway spruce (*Picea abies* L.), and for the average of these species, a linear model was created for the relation between tree height and Diameter at Breast Height (DBH). Trees are often defined as woody species with DBH largen than 5 cm (see e.g. Ryan & Williams, 2011). For this reason the height at which the tree species reached a DBH of 5 cm was sought. This was done by subtracting 5

cm from all DBH values, so that the intercept of the linear models showed the height of the trees at which they reached a DBH of 5 cm. The values ranged between 4.04 m (Norway spruce) and 5.90 m (Japanese larch), and the overall height at a DBH of 5 cm was 4.86 m (see Appendix A). For this reason, the threshold for maximum vegetation height in a canopy gap was set at 5 m.

The threshold for the Leitold method, minimum canopy decrease, was mainly based on expert knowledge. This method was previously only applied in tropical forest studies, and these studies used a threshold of 3 m (Huertas et al., 2022; Leitold et al., 2018). The error margin of the AHN is 0.05 m, with a standard deviation of 0.05 m (van der Sande et al., 2010). Canopy gap decreases larger than 0.15 m can therefore be assumed to reflect actual canopy gap decreases in the field. Because this study focusses on canopy gap emergence as the disappearance of trees instead of small branches, the threshold for minimum canopy decrease was set at 2 m.

The threshold for the minimum area of a canopy gap was mainly based on previous studies. White et al. (2018) reviewed the thresholds used in LiDAR-based canopy gap studies, and found out that the minimum gap area ranged from 2 to 50 m2, with the majority of studies within the range from 5 to 10 m2. It was decided to set the threshold for minimum gap area at 10 m2 in this study, because it was assumed that this would be the minimum footprint of a tree in the Speulderbos.

It was decided to not include a maximum area for the canopy gaps in this study, as analysis of the canopy gap detection results showed that this threshold could hamper the quality of the canopy gap delineation. When high density thinning interventions were carried out in a forest plot, the canopy gaps could form large contiguous clusters, especially if they were situated beside an open field, or another forest plot with large scale interventions. These situations can accidentally be excluded from the canopy gap analysis due to the implementation of a threshold for maximum gap area, and therefore it was decided to not use this threshold.

The threshold to distinguish lateral from vertical canopy gap closure was based on an estimation of the maximal tree height growth in the interval between AHN3 and AHN4, based on data from the yield tables by Jansen et al. (2018). For the six most important tree species in the Speulderbos, and for the average of these species, a linear model was created for the relation between tree height and age. The slopes of these linear models showed the annual tree height growth. The largest annual height growth was 0.58 m (Douglas fir). The interval between AHN3 and AHN4 was 2 years and 2 months. To make a conservative estimate about the maximal height growth in this time interval, the annual height growth was multiplied by three. The fasted growing tree species, Douglas fir, can grow 1.73 m in three years (Appendix A). Therefore, the threshold to distinguish lateral from vertical canopy gap closure was set at 2 m.

2.4.4. Canopy gap dynamics mapping

To map canopy gap dynamics in the study area, four steps were undertaken: (1) the Silva method was used to derive gaps in CHM3 and CHM4, (2) the output of these two binary gap rasters was combined, (3) the Leitold method was used to derive gaps from the difference CHM, and (4) the output of the Leitold method binary gap raster was combined with the combination of Silva method gap layers.

Canopy gap detection with the Silva method was performed by labelling CHM raster cells > 5 m as “no gap” and cells ≤ 5 m as “gap” in both CHM versions. The combination of these two binary gap rasters resulted in a canopy gap dynamics raster with four classes: (1) no canopy gap detected in both CHM versions (NoG), (2) canopy gap disappeared between CHM3 and CHM4 (DG), (3) canopy gap remained between CHM3 and CHM4 (RG), and (4) new canopy gap detected in CHM4 (NG). In this classification, raster cells that received the label NoG had CHM3 and CHM4 values > 5 m. Raster cells that received the label DG had CHM3 heights ≤ 5 m and CHM4 heights > 5 m. Raster cells that received the label RG had CHM3 and CHM4

heights ≤ 5 m. Raster cells that received the label NG had CHM3 heights > 5 m and CHM4 heights ≤ 5 m (Table 1).

Canopy gap detection with the Leitold method was performed by labelling difference CHM raster cells > -2 m as "no gap" and cells ≤ -2 m as "gap". The combination of the Silva method canopy gap dynamics raster and the Leitold method binary gap raster resulted in a canopy gap dynamics raster with seven classes: (1) NoG, (2) DG, (3) RG, (4) new canopy gap detected with both methods (NGBM), (5) new canopy gap only detected with Silva method (NGSM), (6) new canopy gap only detected with Leitold method (NGLM), and (7) remaining canopy gap according to Silva method, but new canopy gap according to Leitold method (RGLM). In this classification, raster cells that are labelled with one of the first three classes had the same characteristics as these classes in the Silva combined gap raster, with the added characteristic that difference CHM values were > -2 m. Raster cells that received the label NGBM had CHM3 heights > 5 m, CHM4 heights ≤ 5 m and difference CHM values ≤ -2 m. Raster cells that received the label NGSM had CHM3 heights > 5 m, CHM4 heights ≤ 5 m and difference CHM values > -2 m. Raster cells that received the label NGLM had CHM3 heights > 5 m, CHM4 heights > 5 m and difference CHM values ≤ -2 m. Raster cells that received the label RGLM had CHM3 heights ≤ 5 m, CHM4 heights ≤ 5 m and difference CHM values ≤ -2 m (Figure 3, Table 1).

The distinction between lateral and vertical gap closure was performed by labelling DG raster cells with a difference CHM value > 2 m as LC, and cells ≤ 2 m as VC (Figure 3, Table 2).

Table 1 Values for CHM3, CHM4 and difference CHM per canopy gap dynamic class

Class	*Meaning*	*Value CHM3 (m)*	*Value CHM4 (m)*	*Value difference CHM (m)*
NoG	No canopy gap detected in both CHM versions with both methods	> 5	> 5	> -2
DG	Canopy gap disappeared between CHM3 and CHM4	≤ 5	> 5	> -2
RG	Canopy gap remained between CHM3 and CHM4	≤ 5	≤ 5	> -2
NGBM	New canopy gap detected with both methods	> 5	≤ 5	≤ -2
NGSM	New canopy gap only detected with Silva method	> 5	≤ 5	> -2
NGLM	New canopy gap only detected with Leitold method	> 5	> 5	≤ -2
RGLM	Remaining canopy gap according to Silva method, but new canopy gap according to Leitold method	≤ 5	≤ 5	≤ -2

Table 2 Value for difference CHM values per DG class

DG class	*Meaning*	*Value difference CHM*
LC	Lateral canopy gap closure	> 2
VC	Vertical canopy gap closure	≤ 2

2.4.5. New canopy gap selection

The raster cells labelled with NGBM, NGSM, NGLM or RGLM were considered to be potential new canopy gap raster cells. A binary raster was created by labelling these cells as "new canopy

gap" and all other cells as "no new gap detected". This binary raster was used to derive new canopy gaps with a minimum area of 10 m2 from the study area. New canopy gaps were required to consist out of minimal 10 contiguous cells in 8 directions. The gaps that fulfilled the requirement were thereafter vectorized to polygons.

2.4.6. Validation

The identified new canopy gaps were validated using the management intervention logbook of State Forestry and with a field visit. The spatial distribution of the in the logbook described management interventions was compared to the spatial distribution of identified new canopy gaps. This comparison provided a first impression of the accuracy on forest plot level of the used canopy gap detection method. To further explore the accuracy, a subset of the identified new canopy gaps was taken. This subset was validated in a field visit. The subset was taken by intersecting the identified new canopy gaps with ten randomly selected forest plots, five managed and five (pseudo-)unmanaged (Appendix B). For each visited identified new canopy gap, it was verified whether they were present or absent in the field.

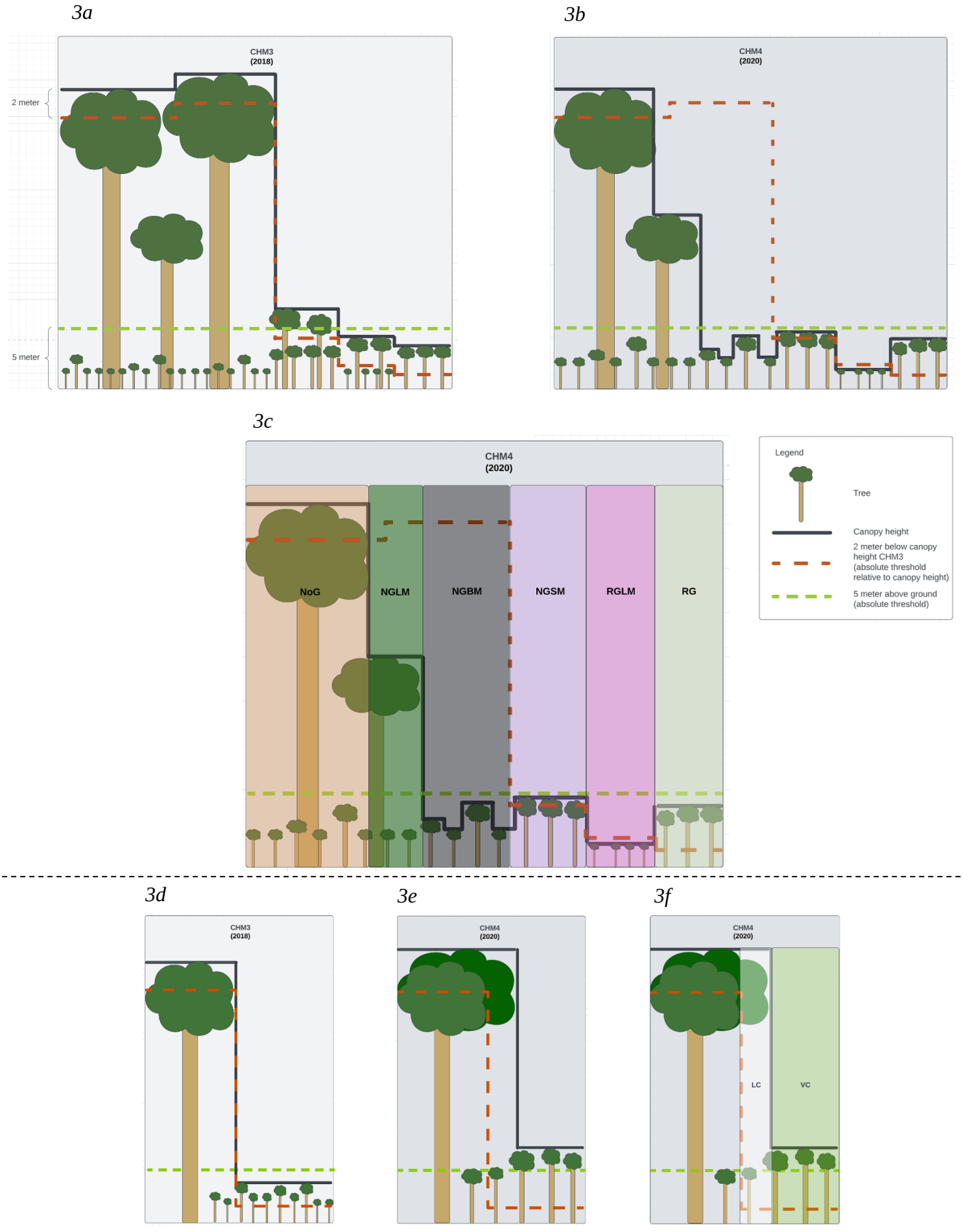

Figure 3 Graphical overview of the seven canopy gap dynamic classes. Figure 3a, 3b and 3c show the canopy height changes between CHM3 and CHM4 of the six classes NoG, NGLM, NGBM, NGSM, RGLM and RG. Figure 3d, 3e and 3f show the difference between the two DG classes LC and VC.

2.5. Determining the influence of forest management

The identified new canopy gaps were used to derive the influence of forest management on canopy gap dynamics. This was carried out in four steps. First, the identified new canopy gaps were visually assessed, and classified in a "number of trees" class. Second, a list of variables was assigned to each identified canopy gap, and to each forest plot in the study area. Third, Random Forest (RF) models were created to determine the most important variables in the classification of identified new canopy gaps in a "number of trees" class and management type. Fourth, statistical comparisons were made between management types, dominant tree species and age classes on canopy gap level and forest plot level.

2.5.1. "Number of trees" labelling

For all identified new canopy gaps, it was manually assessed and labelled whether it had formed due to the disappearance of a part of a tree, one individual tree, or a group of trees, and thus whether it fell in the class "part of tree", "one tree", or "group of trees". This was done by comparing the CHM3 and CHM4, and by comparing the orthophoto of 2018 and 2021 in each identified canopy gap. The labelling of all identified new canopy gaps provided the opportunity to cross validate the "number of trees" RF models with all identified new canopy gaps.

2.5.2. Deriving attributes

Pointcloud variables, shape variables, CHM variables, forest plot level variables and fraction variables were added to the identified new canopy gaps for further statistical analysis.

2.5.2.1. Pointcloud variables

The R package lidR provides a list of standard metrics that can be used to characterize a pointcloud. These variables can be derived with the *stdmetrics* function within the *plot_metrics* function (Roussel et al., 2020). The list consists out of 56 variables, and these variables have the potential to provide information about the structure of trees within a pointcloud. For an overview with description of the variables, see https://github.com/r-lidar/lidR/wiki/stdmetrics. The standard metrics were derived from a clip of the pointcloud within the identified canopy gaps for AHN3 and AHN4.

To derive insights in the development of the forest structure in the direct vicinity of the identified new canopy gaps, 5 and 10 m doughnut buffers around the new canopy gaps were created. These doughnut buffers were created by buffering the new canopy gap polygons with a 5 m and 10 m distance, and erasing the new canopy gap polygons from the buffer (see scheme below). This erasing was done in such a way that the parts of the buffers that overlapped with neighbouring new canopy gap polygons were not erased from the buffer. The buffer distances of 5 and 10 meter were chosen, as these distances are equivalent to one time and two times the minimum height of a tree. The standard metrics were derived from a clip of the pointcloud within the doughnut buffers for AHN3 and AHN4, and these variables were added to the

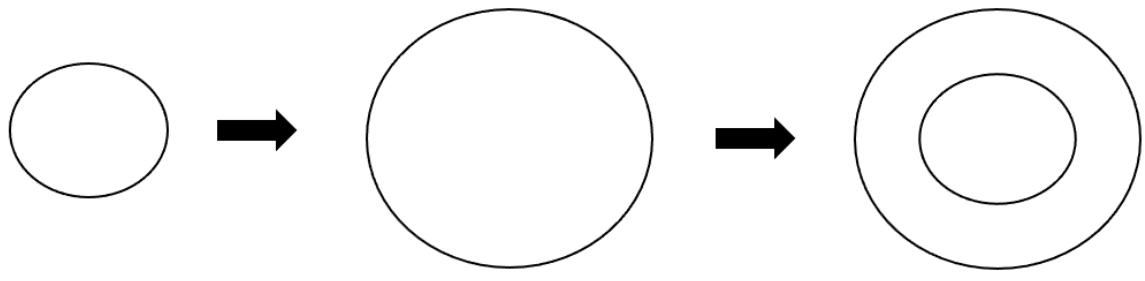

Identified new canopy gap *Buffered new canopy gap* *Doughnut buffer of new canopy gap*

identified new canopy gaps. Furthermore, the relative area of the doughnut buffers per identified new canopy gap that overlapped with neighbouring new canopy gaps was determined to derive information about the gap density. Moreover, the distance to the nearest neighbour was determined per identified new canopy gaps using the function *st_nn* from the nngeo package (Dorman, 2023).

2.5.2.2. Shape variables

Of the identified new canopy gaps, shape variables were determined describing the 3D shape of a clip of the pointcloud for AHN3 and AHN4, and the 2D shape of the canopy gap polygons. The 3D shape variables were derived with the *stdshapemetrics* function within the *plot_metrics* function from the lidR package (Roussel et al., 2020). The 2D shape variables were the area, perimeter, and variables derived from the area and perimeter. The area in m2 was derived by using the *st_area* function from the sf package, the perimeter in m using the *st_perimeter* function from the VLSM package (Knevels et al., 2020; Pebesma, 2018). To see how the 2D shape parameters were derived, see Appendix C.

2.5.2.3. CHM variables

Variables were added to the identified new canopy gap describing a clip of CHM3 and CHM4 within the canopy gaps. The mean, minimum, maximum, standard deviation, Gini coefficient, and range were calculated of CHM3, CHM4 and the difference CHM, inspired by Silva et al. (2019). The Gini coefficient was originally developed as a measurement for income inequality (Gini, 1921). However, it has been shown that the coefficient can be used as measurement for tree size inequality as well (Valbuena et al., 2017). The higher the Gini coefficient of a forest plot, the higher the inequality of tree sizes, which is used as an indicator of disturbance events in forests (Silva et al., 2019).

2.5.2.4. Forest plot variables

For each forest plot in the study area, variables were derived describing the canopy gap dynamics in the plot, inspired by Blackburn and Milton (1996) (Appendix C). Furthermore, the same CHM variables that were determined for the new canopy gap polygons were determined on forest plot level as well.

2.5.2.5. Fraction variables

On canopy gap level, the fraction of each of the four new canopy gap classes, NGBM, NGSM, NGLM and RGLM, was determined, to investigate the difference in forest structure per gap class. On forest plot level, the fraction of each of the seven canopy gap dynamics classes, NoG, DG, RG, NGBM, NGSM, NGLM, and RGLM, was determined. Besides, The fraction LC and VC of the fraction DG was determined per forest plot.

2.5.3. Random forest models

The dataset of identified canopy gaps and their attributes was used to train Random Forest (RF) models. The RF algorithm was described by Breiman (2001). Five RF models were developed: (1) “number of trees” model with all variables included, (2) “number of trees” model with only the three most important variables included, (3) management type model with all variables included, (4) management type model with only the four most important variables included, and (5) management type model without forest plot variables included. The RF models were created with the intention to derive insights in the variables that differed most between the different classes. The algorithm is suitable for this purpose, as this algorithm is able to determine the importance per variable in the distinction between classes, which reveals which

variables are most important in the classification, and which are possibly redundant. To create train and test data, the identified canopy gaps were split in a 70/30 ratio. The RF models trained on new canopy gap data with only the four most important variables were developed to observe the accuracy of the classification with less input data. The RF model without forest plot variables was developed to observe the management type classification accuracy with only the variables that were directly or indirectly derived from the AHN. The RF models were created using the *train* function from the caret package (Kuhn, 2008). The confusion matrix of the RF models were developed following the methods of Du et al. (2021).

2.5.4. Statistical comparisons

As can be observed in figure 1, the representation of forest plot dominant tree species and age classes is not equally distributed over the different management types. Therefore, to determine the influence of forest management on canopy gap dynamics, the influence of forest management had to be disentangled from the influence of dominant tree species and age. Variables that were derived directly from the new canopy gaps, or from the doughnut buffers that belonged to these canopy gaps, were statistically compared on canopy gap level. The forest plot variables were compared on forest plot level instead of new canopy gap level, as the comparison of forest plot variables on new canopy gap level would result in an overrepresentation of forest plots in which new canopy gaps have formed, and an underrepresentation of forest plots in which no new canopy gaps have formed. On new canopy gap level, fourteen variables were compared, namely the area, perimeter, distance to nearest neighbour, overlap of 5 and 10 m doughnut buffer with neighbouring new canopy gaps, mean of CHM3, mean of CHM4, mean of difference CHM, fraction NGBM, and fraction NGLM. Besides, the four most important variables in the management type RF model without forest plot variables were compared. On forest plot level, the variables fraction in gap, gap density, dispersion index, canopy edge, mean of CHM3, mean of CHM4, mean of difference CHM, Gini coefficient of CHM4, fraction NoG, fraction DG, fraction RG, fraction NGBM, fraction NGLM, and fraction VC of fraction DG were compared. These variable lists of new canopy gap level and forest plot level were selected, as there were reasons to expected differences in these variables between different management types. Furthermore, the comparison of these variables indirectly provides information of other variables. For example, the comparison of new canopy gap area and perimeter would provide information in all shape variables derived from the area and perimeter.

To study the influence of forest management, the new canopy gaps and forest plots were split up in the classes managed, unmanaged and pseudo-unmanaged. To study the influence of dominant tree species, the new canopy gaps and forest plots were split up in the six most tree species of the Speulderbos. The influence of forest management was as well investigated for the tree species beech separately. This comparison helped to disentangle the influence of forest management and dominant tree species on canopy gap dynamics. Beech was the only tree species for which there were observations in forest plots with all three management types (Appendix I). To study the influence of forest plot age, the new canopy gaps and forest plots were split up in five age classes; 0-40 years, 40-80 years, 80-120 years, 120-160 years, and 160-200 years.

Between the different classes, the medians of the variables were compared with the non-parametric Kruskal-Wallis test (Kruskal & Wallis, 1952). The Kruskal-Wallis test was selected, as the variables were not normally distributed. When the Kruskal-Wallis test was rejected, which means that there were observed significant differences between groups, the Dunn's test was used to make pairwise comparisons between classes (Dunn, 1964). The Bonferroni method was used to derive adjusted p-values (Bonferroni, 1936). The functions *dunnTest* from the FSA package and *ggbetweenstats* from the ggstatplots package were used for the statistical comparisons (Ogle D.H. et al., 2023; Patil, 2021).

3. Results

3.1. Comparison Silva and Leitold method

The combination of the Silva and Leitold methods resulted in a total number of 2473 identified new canopy gaps in the study area, with a total area of 150,463 m2. The new canopy gap area identified with only the Silva method was 79,876 m2 in the study area, or 53.09% of the total new canopy gap area identified with both methods. The new canopy gap area identified with only the Leitold method was 150,184 m2, or 99.81% of the identified new canopy gap area with both methods. The use of the Leitold method resulted in the spatial distribution of two canopy gap dynamic classes, namely the distribution of new canopy gaps and of no new canopy gaps. The use of the Silva method resulted in the spatial distribution of two additional canopy gap dynamic classes, namely the distribution of disappearing and remaining canopy gaps (Table 3, Figure 4).

Table 3 The seven classes of canopy gap dynamics identified with either the Silva method, the Leitold method, or the combination of these two methods.

Class	*Meaning*	*Fraction of study area*	*Average fraction of new canopy gap area*	*Identified with method*
NoG	No canopy gap detected in both CHM versions with both methods	0.8585	-	Both
DG	Canopy gap disappeared between CHM3 and CHM4	0.0160	-	Silva
RG	Canopy gap remained between CHM3 and CHM4	0.0737	-	Silva
NGBM	New canopy gap detected with both methods	0.0281	0.432	Both
NGSM	New canopy gap only detected with Silva method	0.0003	0.003	Silva
NGLM	New canopy gap only detected with Leitold method	0.0227	0.543	Leitold
RGLM	Remaining canopy gap according to Silva method, but new gap according to Leitold method	0.0008	0.021	Both

4a

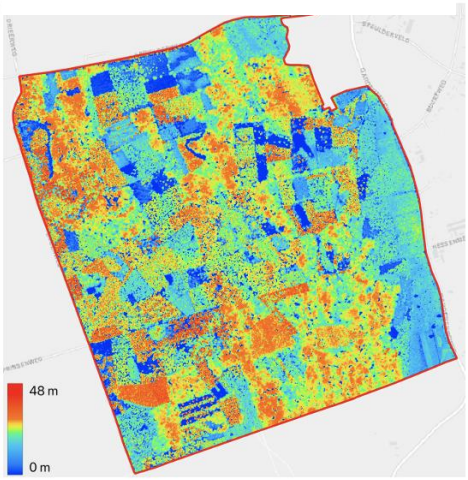

4b

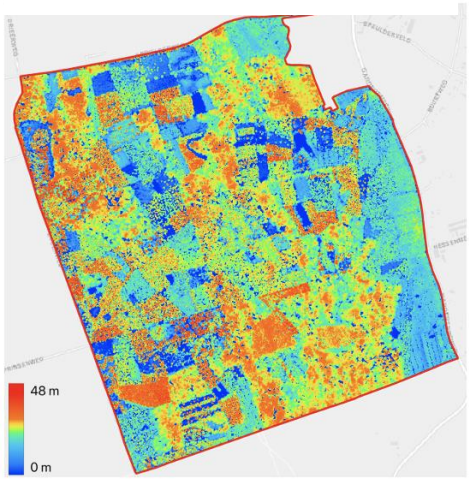

4c

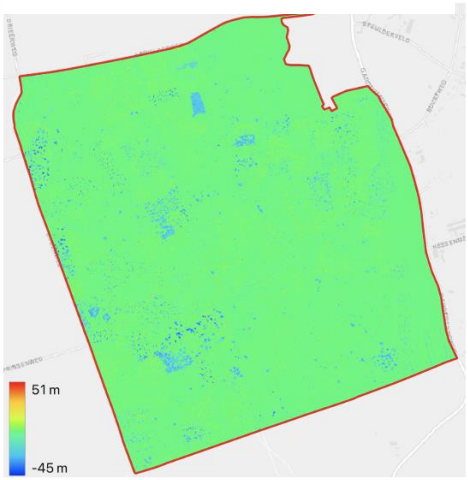

4d

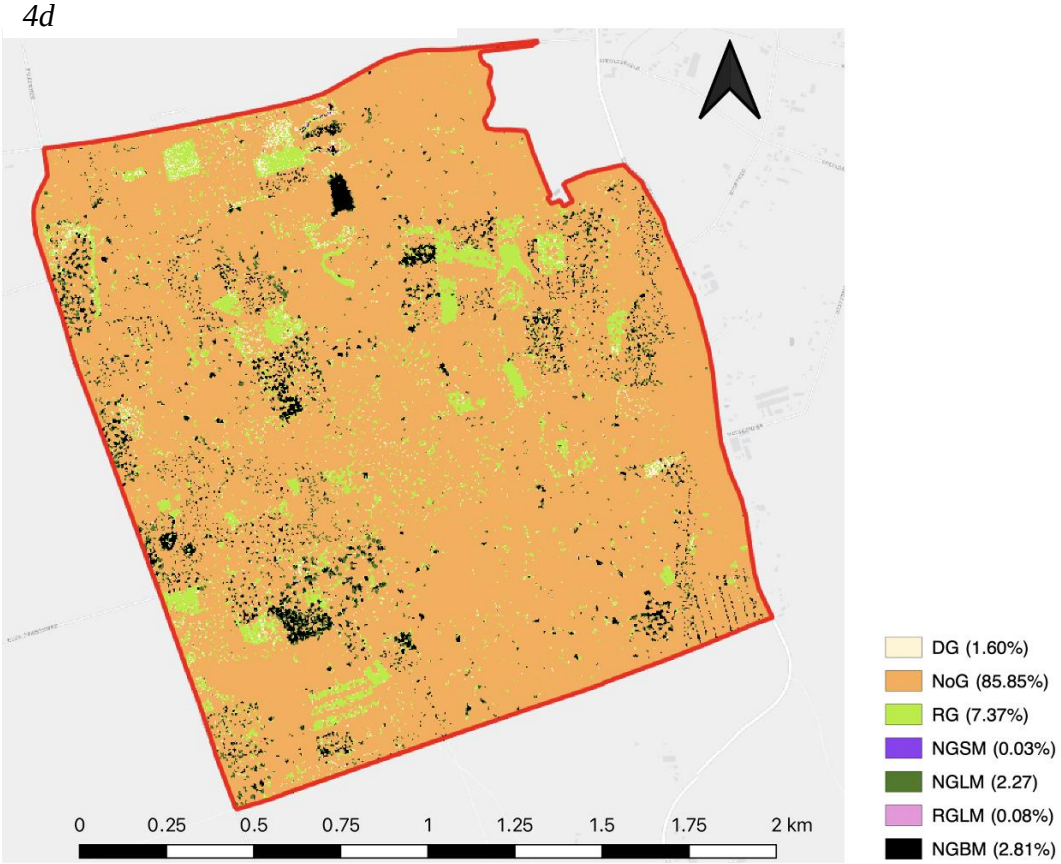

Figure 4 Result of the combination of the Silva and Leitold method to detect canopy gap dynamics. Figure 4a, 4b and 4c show the data on which the canopy gap detection was based. Figure 4a and 4b show the CHM of respectively AHN3 and AHN4. Figure 4c shows the difference CHM. Figure 4d shows the spatial distribution of the seven identified canopy gap dynamic classes in the study area. The percentage of study area that felled within each canopy gap dynamic class can be found in the legend of figure 4d.

3.1.1. Validation

First, the spatial distribution of forest plots with registered management interventions was compared to the spatial distribution of identified new canopy gaps (figure 5). The result of this comparison generally revealed that large new canopy gaps, and clusters with high densities of new canopy gaps, are often situated in forest plots with registered management interventions. However, there were identified large new canopy gaps, and clusters with high densities of new canopy gaps, that were not situated in forest plots with registered management interventions. This was the case in forest plots 9F and H, 11Q and K, 14D and P, 15R, 17E2-E6, 18E2, G4, and H, 19H2, J, K and M, and 25E. Besides, there were forest plots in which a management intervention was registered, but fewer new canopy gaps were identified than expected based on the registered intervention. This was the case in forest plots 11A2, H and P2, and 15P2.

Second, a selection of the identified new canopy gaps was validated during a field visit. The selected 5 managed forest plots were 9D, 11F2, 17A3 and E3, and 25E2. A total of 140 new canopy gaps were identified in these selected managed forest plots. The selected 5 pseudo-unmanaged and unmanaged forest plots were 10J, 11B, 15N and X, and 17M (Appendix B). A total of 61 new canopy gaps were identified in these selected pseudo-unmanaged and unmanaged forest plots. For all 201 identified new canopy gaps that were visited, the presence in the field was confirmed. There were no identified new canopy gaps that were absent in the field. However, there were new canopy gaps observed in the field in forest plot 10J and 15X that were not identified with either the Silva or the Leitold method.

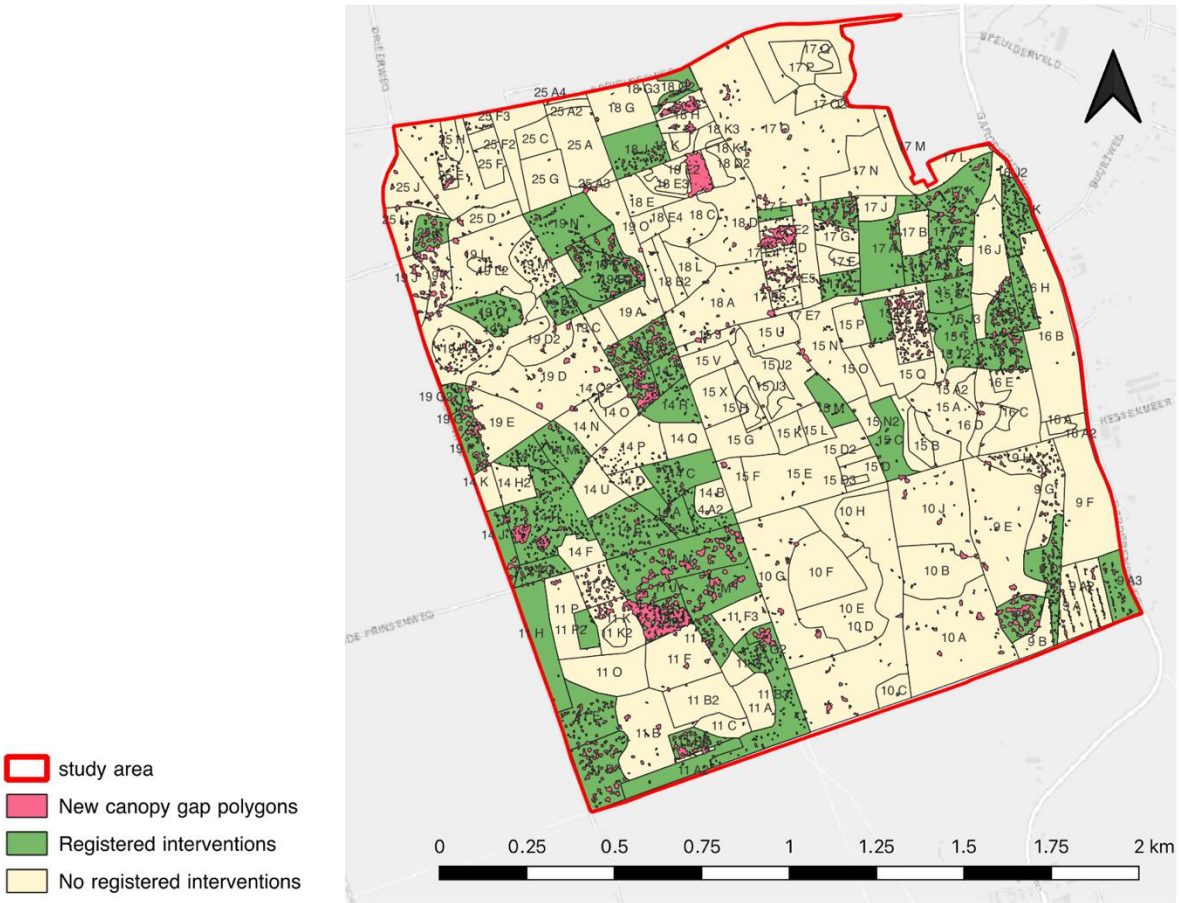

Figure 5. Spatial distribution of identified new canopy gaps, and of forest plots in which management interventions were registered since 2018.

3.2. Determining the influence of forest management

3.2.1. "Number of trees" classification

The result of the "number of trees" labelling of the identified canopy gaps can be found in figure 6. The new canopy gaps with the label "part of tree" was relatively evenly distributed over the different management types, while the labels "one tree" and "group of trees" were overrepresented in managed plots (Table 4).

Table 4 The number of new canopy gaps per "number of tree" class and per management type

Class	*Part of tree*	*One tree*	*Group of trees*	*Total*
Managed	236	1201	701	2138
Pseudo-unmanaged	170	60	7	237
Unmanaged	81	16	1	98
Total	487	1277	709	2473

3.2.2. RF models

Five RF models were developed: (1) "number of trees" model with all variables included, (2) "number of trees" model with only the three most important variables included, (3) management type model with all variables included, (4) management type model with only the four most important variables included, and (5) management type model without forest plot variables included. To create train and test data, the identified canopy gaps were split in a 70/30 ratio. Of the total 2473 new canopy gaps, 1732 were used as train data, and 741 as test data. The variable importance per variable per model can be found in Appendix D.

3.2.2.1. "Number of trees" model, all variables

The result of the "number of trees" classification with all variables can be found in table 5. The RF model had a Kappa coefficient of 0.757, and the total accuracy on test data was 0.846. The fifteen most important variables in the classification can be found in figure 7. Out of the fifteen most important variables, ten variables were shape variables. Out of the ten shape variables, four were pointcloud shape variables, describing the shape of AHN3 or AHN4 within the new canopy gaps, while six shape variables described the 2D shape of the new canopy gaps. Three variables were forest plot variables, describing the forest plots in which the new canopy gaps were situated. The remaining two variables were pointcloud variables, describing AHN3 within the new canopy gaps (Figure 7). The canopy gap shape area and perimeter differed significantly between the three "number of trees" classes. Therefore, variables derived from the area and shape had a high importance in this RF model (Appendix J).

Table 5 Confusion matrix RF model "number of trees" with all variables

Class	*Part of tree*	*One tree*	*Group of trees*	*User accuracy*
Part of tree	269	61	11	0.789
One tree	41	804	49	0.900
Group of trees	10	82	405	0.815
Producer accuracy	0.840	0.849	0.871	Total accuracy: 0.853

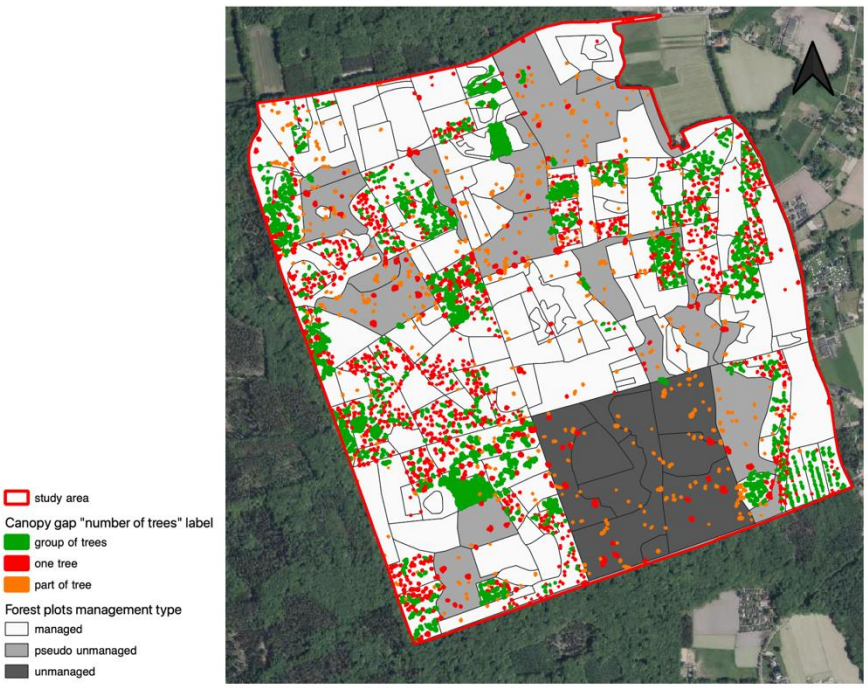

Figure 6. Spatial distribution of new canopy gaps per "number of trees" class in the study area. The basemap is the 8 cm resolution areal orthophoto of the study area from the year 2021 provided by PDOK.

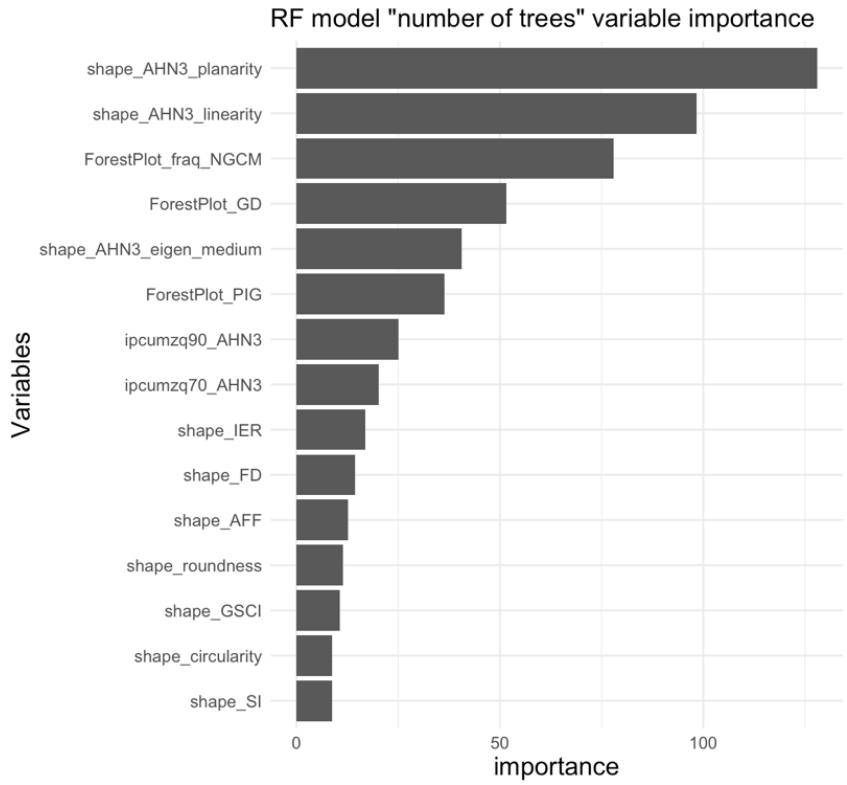

Figure 7 The fifteen most important variables, and their importance, in the "number of trees" RF model with all variables.

3.2.2.2. "Number of trees" model, most important variables

The result of the "number of trees" classification with only the three most important variables can be found in table 6. The three variables included in the model were the planarity of the AHN3 shape within the new canopy gaps, the canopy gap forest plot fraction NGLM, and the canopy gap forest plot gap density. Three instead of four variables were included in this model, as multicollinearity existed between the two most important variables. The correlation between the planarity and the linearity of the AHN3 shape within the new canopy gaps was 0.96, and therefore the linearity was left out of this model. The RF model had a Kappa coefficient of 0.576, and the total accuracy on test data was 0.791. For the statistical comparison of these three variables between the "number of trees" classes, see Appendix D2.

Table 6 Confusion matrix RF model "number of trees" with only the most important variables

Class	*Part of tree*	*One tree*	*Group of trees*	*User accuracy*
Part of tree	209	94	38	0.613
One tree	98	712	84	0.796
Group of trees	26	98	373	0.751
Producer accuracy	0.628	0.788	0.754	Total accuracy: 0.747

3.2.2.3. Management type model, all variables

The result of the management type model with all variables included can be found in table 7. The RF model had a Kappa coefficient of 0.946, and the total accuracy on test data was 0.986. The fifteen most important variables in the classification can be found in figure 8. Out of the fifteen most important variables, twelve were forest plot variables, describing the forest plots in which the new canopy gaps were situated. The other three variables were doughnut buffer pointcloud variables, describing AHN3 or AHN4 in a 5 or 10 m doughnut buffer around the new canopy gaps.

Table 7 Confusion matrix RF model management type with all variables

Class	*Managed*	*Pseudo-unmanaged*	*Unmanaged*	*User accuracy*
Managed	1499	1	1	0.999
Pseudo-unmanaged	10	149	0	0.937
Unmanaged	4	1	67	0.931
Producer accuracy	0.991	0.987	0.985	Total accuracy: 0.990

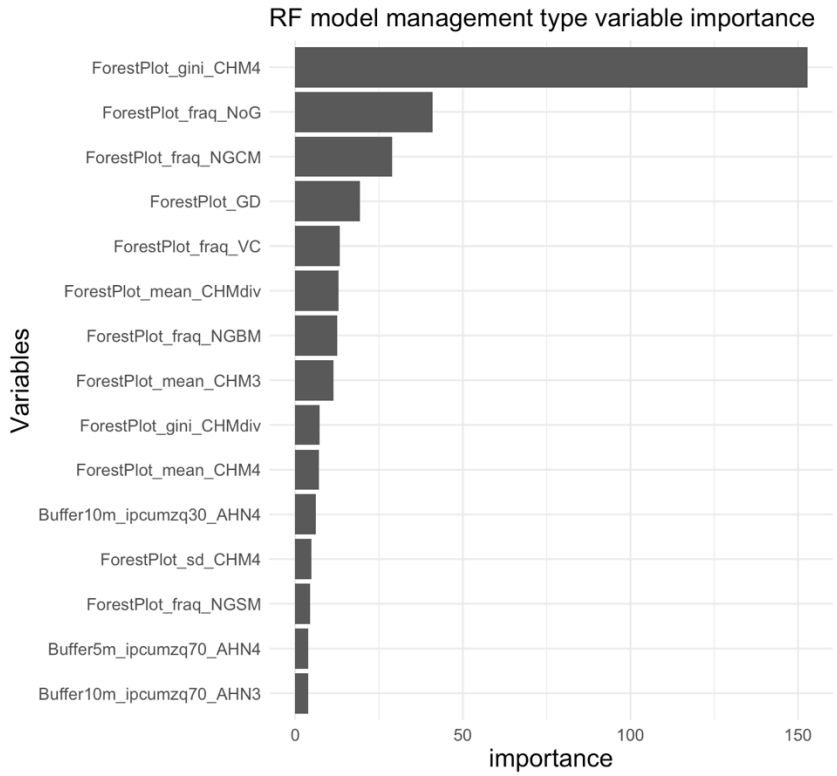

Figure 8 The fifteen most important variables, and their importance, in the management type RF model with all variables.

3.2.2.4. Management type model, most important variables

The result of the management type model with only the four most important variables can be found in table 8. The four variables included in the model were the forest plot Gini coefficient of CHM4 within the new canopy gaps, the forest plot fraction NoG, the forest plot fraction NGLM, and the forest plot gap density. The RF model had a Kappa coefficient of 0.986, and the total accuracy on test data was 0.997. The accuracy of the management type RF model with only the 4 most important variables had a higher total accuracy than the model with all variables included. For the statistical comparison of these four variables between the management types, see Appendix D4.

Table 8 Confusion matrix RF model management type with only the most important variables

Class	*Managed*	*Pseudo-unmanaged*	*Unmanaged*	*User accuracy*
Managed	1500	0	1	0.999
Pseudo-unmanaged	2	157	0	0.987
Unmanaged	1	1	70	0.972
Producer accuracy	0.998	0.994	0.986	Total accuracy: 0.998

3.2.2.5. Management type model, no forest plot variables

The influence of forest plot variables in the management type RF model was high. To investigate whether it still would be possible to distinguish the three management classes without forest plot variables, an RF model was developed without forest plot variables. Only the variables directly derived from the new canopy gaps and their doughnut buffers were

included in this model. The result of this management type model without forest plot variables can be found in table 9. The RF model had a Kappa coefficient of 0.587, and the total accuracy on test data was 0.913. The producer and user accuracies of the classes pseudo-unmanaged and unmanaged were low in this model. The fifteen most important variables in the classification can be found in figure 9. All of these fifteen variables were doughnut buffer pointcloud variables, of which eleven described AHN4, and four AHN3.

Table 9 Confusion matrix RF model management type with forest plot variables excluded

Class	*Managed*	*Pseudo-unmanaged*	*Unmanaged*	*User accuracy*
Managed	1468	28	5	0.978
Pseudo-unmanaged	58	93	8	0.585
Unmanaged	25	36	11	0.153
Producer accuracy	0.946	0.592	0.458	Total accuracy: 0.908

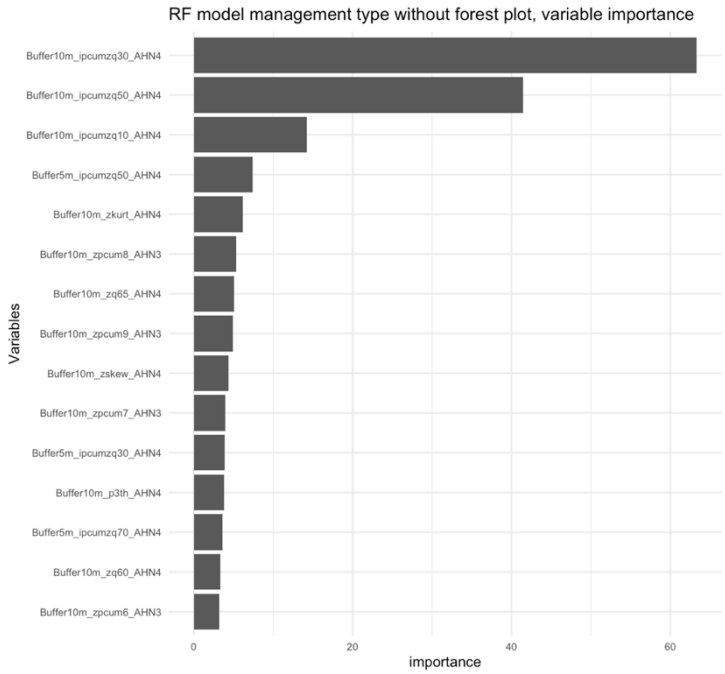

Figure 9 The fifteen most important variables, and their importance, in the management type RF model without forest plot

3.2.3. Statistical analysis influence different forest characteristics

The identified new canopy gaps were used to make statistical comparisons of different forest plot characteristics to disentangle the influence of different forest plot characteristics on canopy gap dynamics. Comparisons have been made on canopy gap and forest plot level between (1) management types, (2) dominant tree species, (3) management types for beech only, and (4) age classes. For each of these, comparisons of fourteen variables on canopy gap and forest plot level were made (Appendix E-H). The number of canopy gaps and forest plots for combinations of management type, dominant tree species, and age class, can be found in Appendix I.

Of the fourteen variables that were compared on canopy gap level, four were the most important variables in the management type RF model without forest plot variables. These were

the 10 m doughnut buffer percentage of intensity returned below the 90th height percentile in AHN4 (10m dbuffer ipcum90 AHN4), 5 m doughnut buffer percentage of intensity returned by points classified as 'ground' in AHN4 (5m dbuffer ipground AHN4), 10 m doughnut buffer skewness of intensity distribution in AHN4 (10m dbuffer iskew AHN4), and 10 m doughnut buffer 25th percentile of height distribution in AHN3 (10m dbuffer zq25 AHN4). These four doughnut buffer pointcloud variables were selected after investigation of the variable importance of the variables in the management type RF model without forest plot variables (Figure 9). The four most important variables were selected, but only if the statistic of the variable was unique in the selection. This was done to prevent that different variations of the percentage of intensity returned below the xth height percentile (ipcumx) would be compared.

3.2.4. Management type

The number and area of new canopy gaps and forest plots per management type can be found in table 10. The fraction of area in new canopy gap for managed forest plots was higher compared to pseudo-unmanaged and unmanaged forest plots. This fraction for pseudo-unmanaged plots was higher compared to unmanaged plots (Table 10).

Table 10 Number and area of new canopy gaps and forest plots per management type

Management type	*Number of new canopy gaps*	*Number of forest plots*	*Area of new canopy gaps (m2)*	*Area of forest plots in study area (m2)*	*Fraction area in new canopy gap*
Managed	2138	174	134544	2085964	0.064
Pseudo-unmanaged	237	19	11043	559562	0.020
Unmanaged	98	9	4876	365465	0.013
Total	2473	202	150463	3010991	0.050

3.2.4.1. New canopy gap level

The distance to the nearest neighbour of new canopy gaps in managed forest plots was significantly lower compared to pseudo-unmanaged plots, and this distance was also significantly lower in pseudo-unmanaged plots compared to unmanaged plots (Figure 10). This pattern was also observed for the 5 and 10 m doughnut buffer overlap with neighbouring new canopy gaps (Appendix E1). The mean difference CHM within the new canopy gaps was significantly higher in unmanaged plots compared to managed and pseudo-unmanaged plots (Figure 10). The fraction NGBM of new canopy gaps was significantly higher in unmanaged plots compared to managed and pseudo-unmanaged plots (Figure 10). The opposite pattern was observed for the fraction NGLM (Appendix E1). The 10m dbuffer ipcum90 AHN4 was significantly lower in managed plots compared to pseudo-unmanaged and unmanaged plots (Figure 10). The same pattern is observed for the three other important variables in the management type RF model without forest plot variables (Appendix E1). There is no significant difference observed in new canopy gap area or perimeter between the management types (Appendix E1).

3.2.4.2. Forest plot level

The gap density was not significantly lower in unmanaged forest plots compared to managed and pseudo-unmanaged plots, but the median gap density value was lower (Figure 11). The same pattern is observed for the fraction in gap (Appendix E2). The forest plot mean CHM4 was significantly lower in managed plots compared to pseudo-unmanaged and unmanaged plots (Figure 11). The same pattern was observed for the mean CHM3 (Appendix E2). The

Gini coefficient of CHM4 was significantly higher in managed plots compared to pseudo-unmanaged and unmanaged plots (Figure 11). The fraction NoG was significantly lower in managed plots compared to pseudo-unmanaged and unmanaged plots (Figure 11).

10a

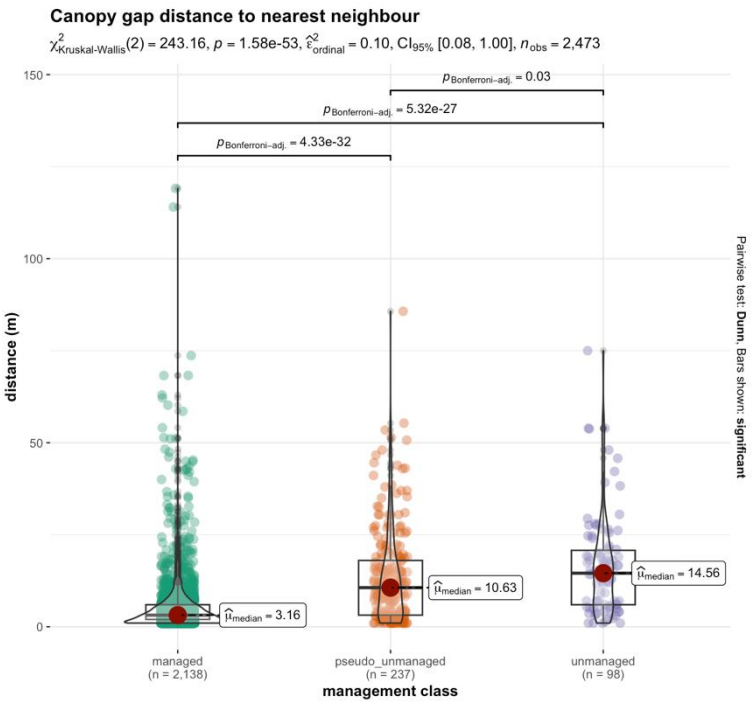

10b

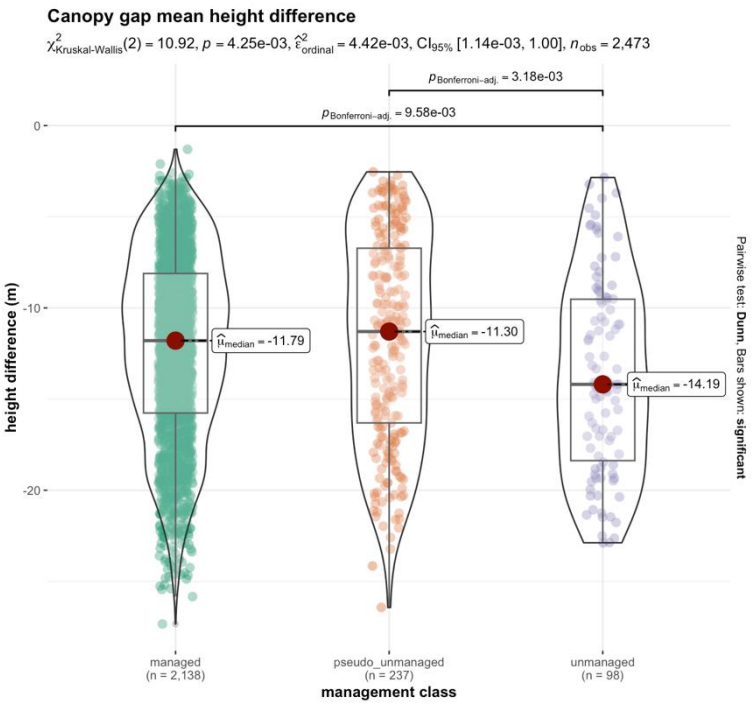

10c

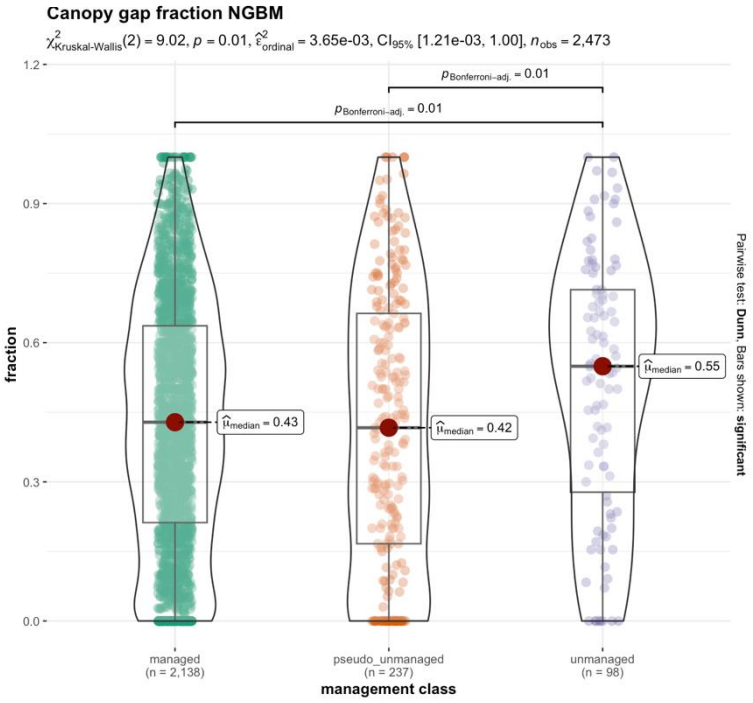

10d

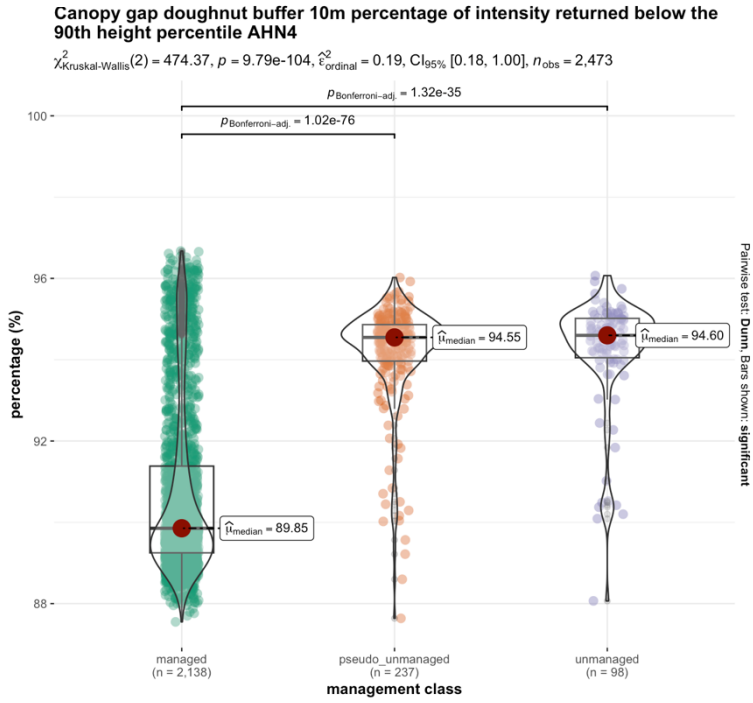

Figure 10 Statistical comparisons of management types on canopy gap level for the variables distance to the nearest neighbour (10a), mean difference CHM (10b), fraction NGBM (10c), and 10 m doughnut buffer percentage of intensity returned below the 90th height percentile AHN4 (10d). For additional variable comparisons of management types on canopy gap level, see Appendix E1.

11a

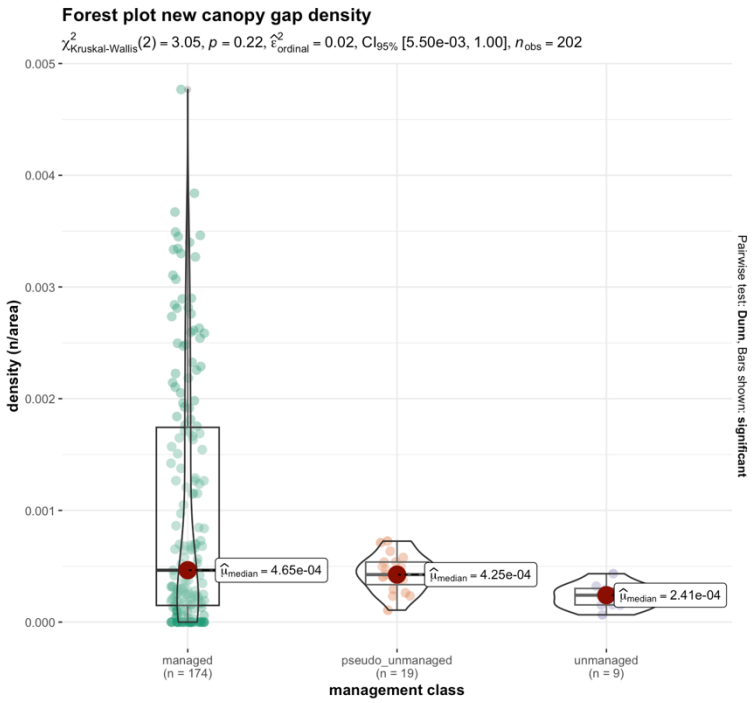

11b

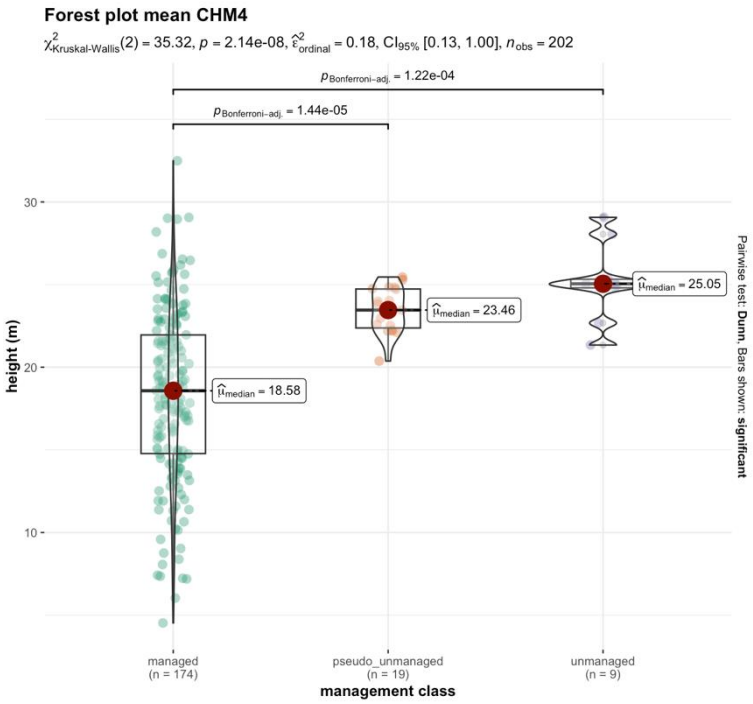

11c

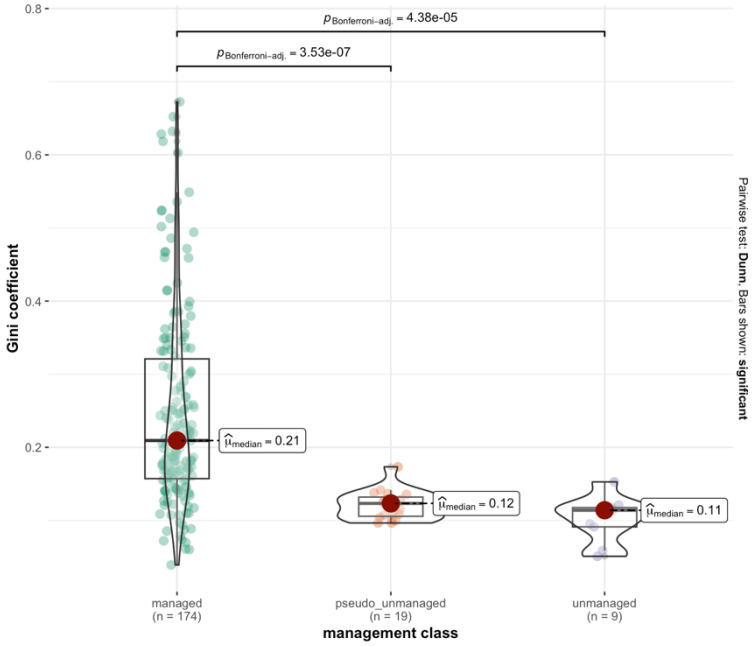

11d

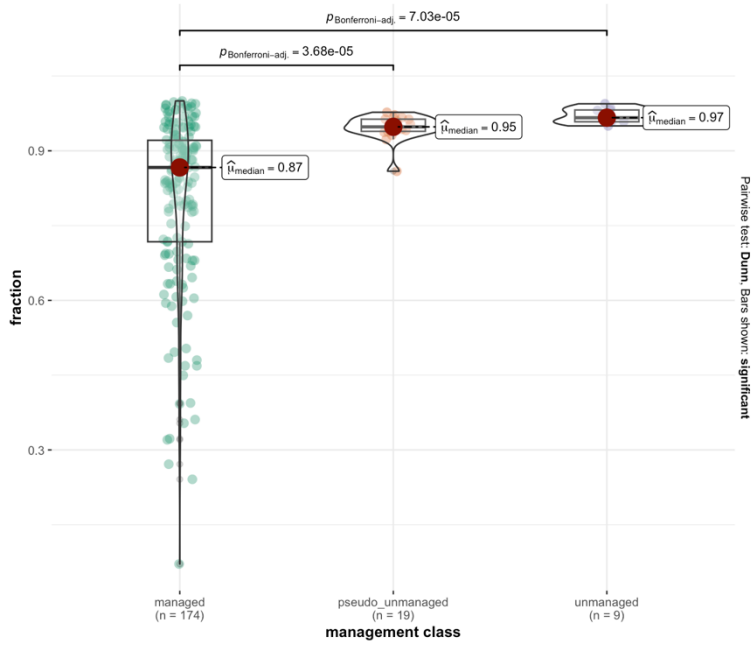

Figure 11 Statistical comparisons of management types on forest plot level for the variables new gap density (11a), mean CHM4 (11b), Gini coefficient CHM4 (11c), and fraction NoG (11d). For additional variable comparisons of management types on forest plot level, see Appendix E2.

3.2.5. Dominant tree species

The number of new canopy gaps and forest plots per dominant tree species and management type can be found in table 11. The fraction of area in new canopy gap for deciduous tree species, beech and oak, was lower compared to coniferous species, Scotch pine, Japanese larch, Douglas fir and Norway spruce. Beech was the only tree species that was represented in all three management types with multiple forest plots. Oak was represented in the pseudo-unmanaged area with one forest plot, all other oak forest plots were situated in the managed area. Scotch pine, Douglas fir and Japanese larch were represented in the unmanaged area with one forest plot, all other forest plots of these species were situated in the managed area. Norway spruce was only represented in the managed area (Appendix I1 & I2).

Table 11 Number and area of new canopy gaps and forest plots per tree species

Tree species	*Number of new canopy gaps*	*Number of forest plots*	*Area of new canopy gaps (m2)*	*Area of forest plots in study area (m2)*	*Fraction of area in new canopy gap*
Beech	595	59	27590	1290718	0.021
Oak	41	8	1518	99129	0.015
Scotch pine	412	19	22112	295250	0.075
Japanese larch	280	35	42492	392712	0.108
Douglas fir	776	52	36092	604129	0.060
Norway spruce	87	7	5173	99640	0.052
Total	2191	180	134977	2781578	0.049

3.2.5.1. New canopy gap level

The distance to the nearest neighbour of new canopy gaps in forest plots with deciduous dominant tree species was higher compared to coniferous tree species (Figure 12). This pattern was also observed for the 5 and 10 m doughnut buffer overlap with neighbouring new canopy gaps (Appendix F1). The mean difference CHM within the new canopy gaps was significantly higher in Douglas fir and Japanese larch forest plots compared to forest plots with other tree species (Figure 12). There were no significant differences in fraction NGBM of new canopy gaps between the different tree species, except between Scotch pine and Japanese larch forest plots (Figure 12). The 10m dbuffer ipcum90 AHN4 was significantly higher in forest plots with deciduous dominant tree species compared to coniferous tree species (Figure 12). The same pattern was observed for the three other important variables in the management type RF model without forest plot variables (Appendix F1). The area of new canopy gaps in Scotch pine and Japanese larch forest plots was significantly larger compared to forest plots with other tree species (Appendix F1).

3.2.5.2. Forest plot level

There were no significant differences in gap density between forest plots with different dominant tree species. However, beech forest plots had lower median gap density values compared to forest plots with other tree species (Figure 13). The forest plot mean CHM3 and CHM4 was significantly higher in Douglas fir and beech plots compared to other tree species, while the forest plot mean difference CHM did not differ significantly between the different tree species (Figure 13, Appendix F2). The Gini coefficient of CHM4 was significantly lower in beech forest plots compared to Scotch pine, Japanese larch and Douglas fir forest plots (Figure 13). The fraction NoG was significantly higher in forest plots with deciduous dominant tree species compared to coniferous tree species (Figure 13).

12a

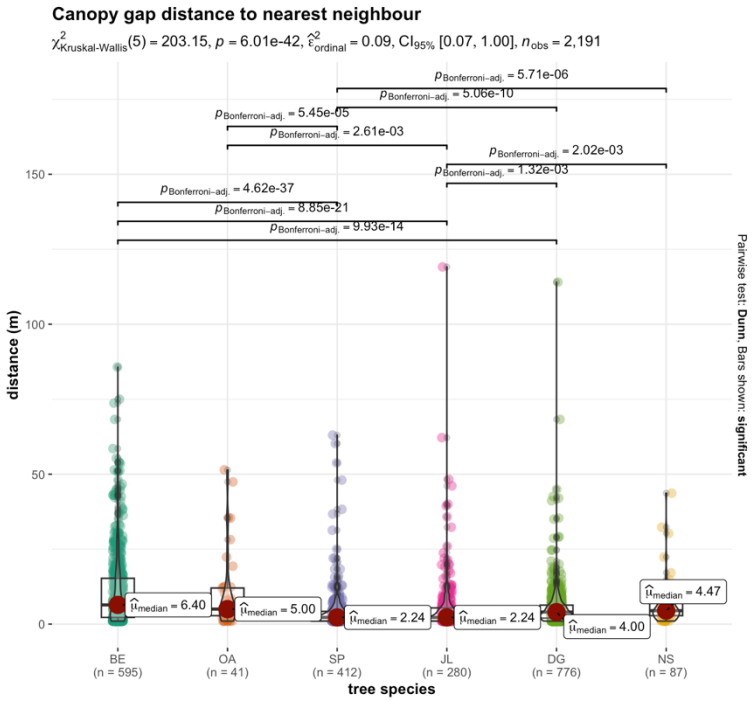

12b

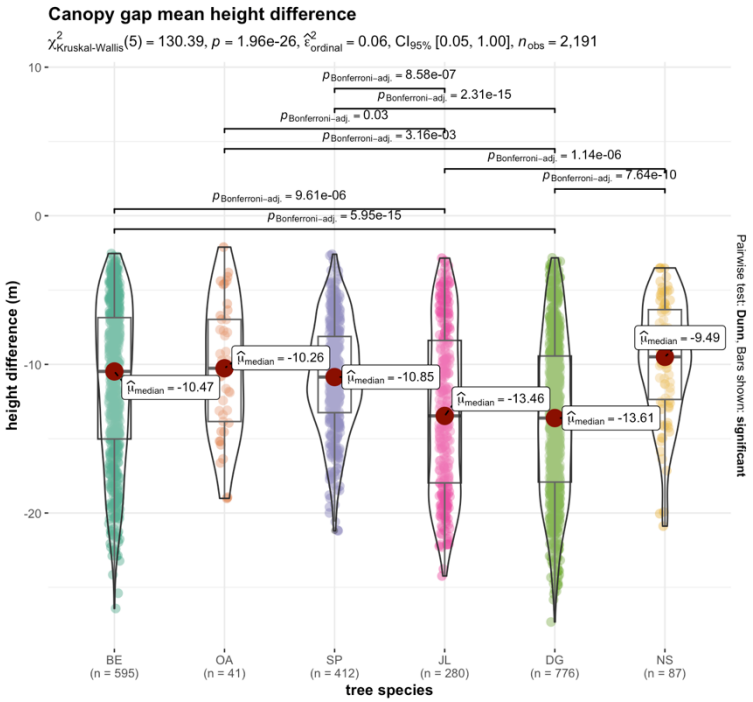

12c

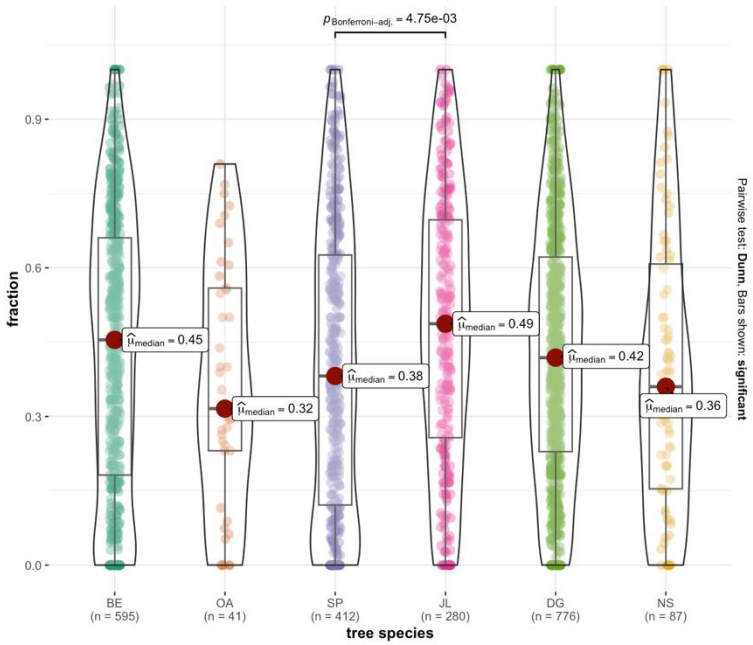

12d

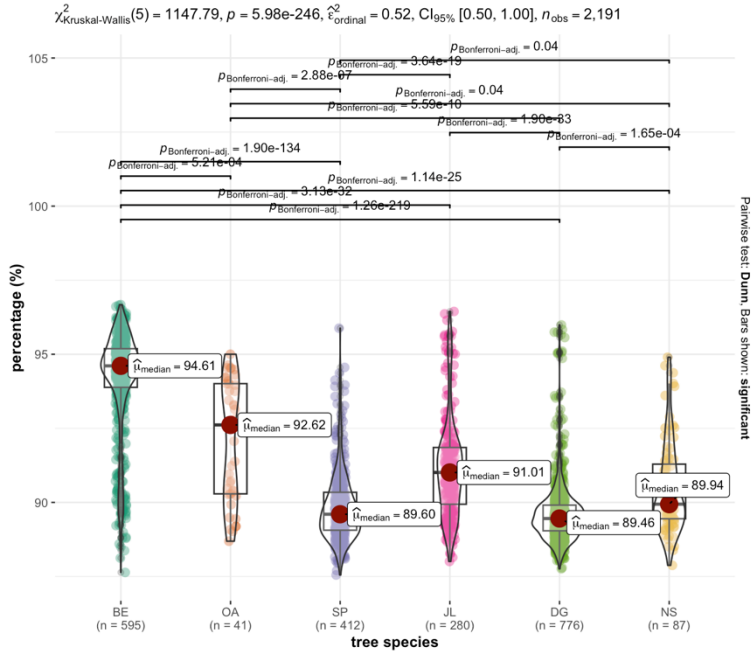

Figure 12 Statistical comparisons of dominant tree species on canopy gap level for the variables distance to the nearest neighbour (12a), mean difference CHM (12b), fraction NGBM (12c), and 10 m doughnut buffer percentage of intensity returned below the 90th height percentile AHN4 (12d). For additional variable comparisons of dominant tree species on canopy gap level, see Appendix F1.

13a

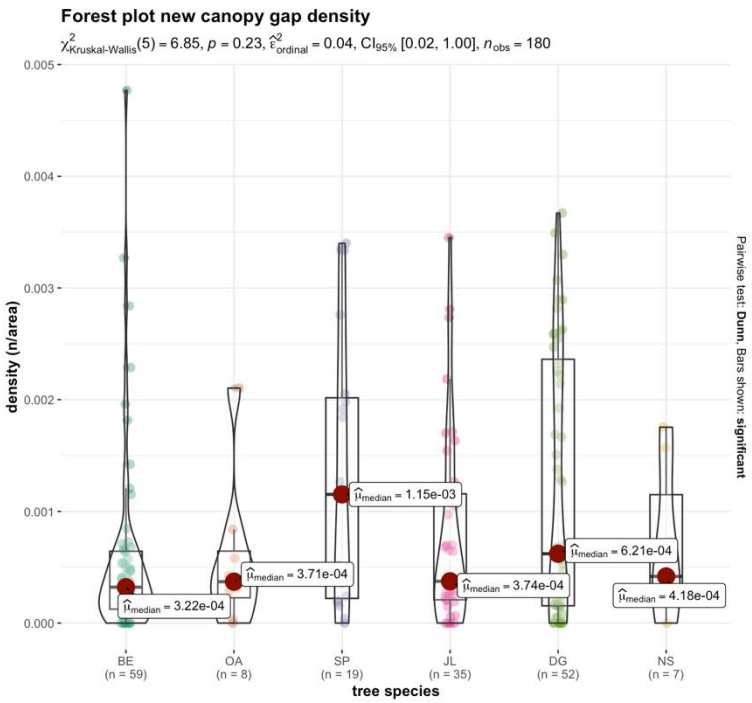

13b

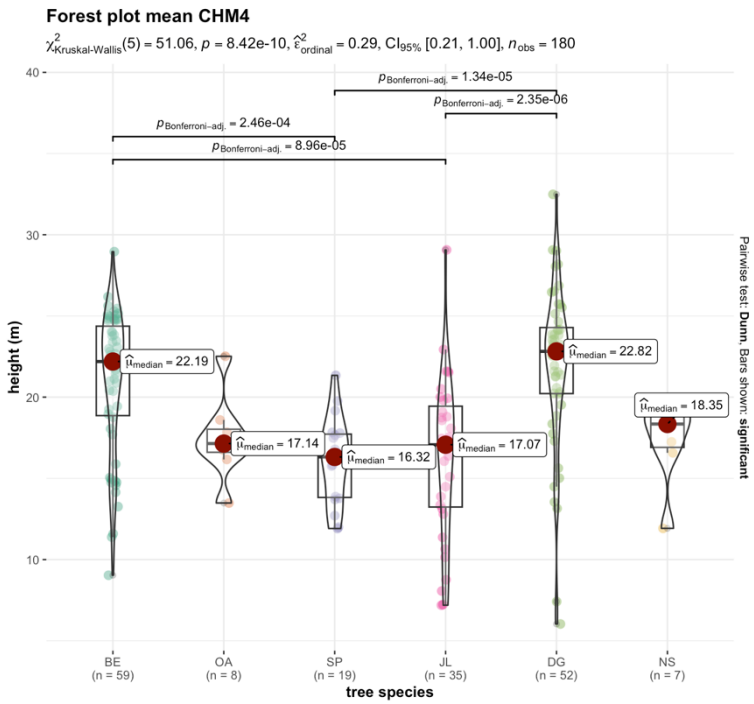

13c

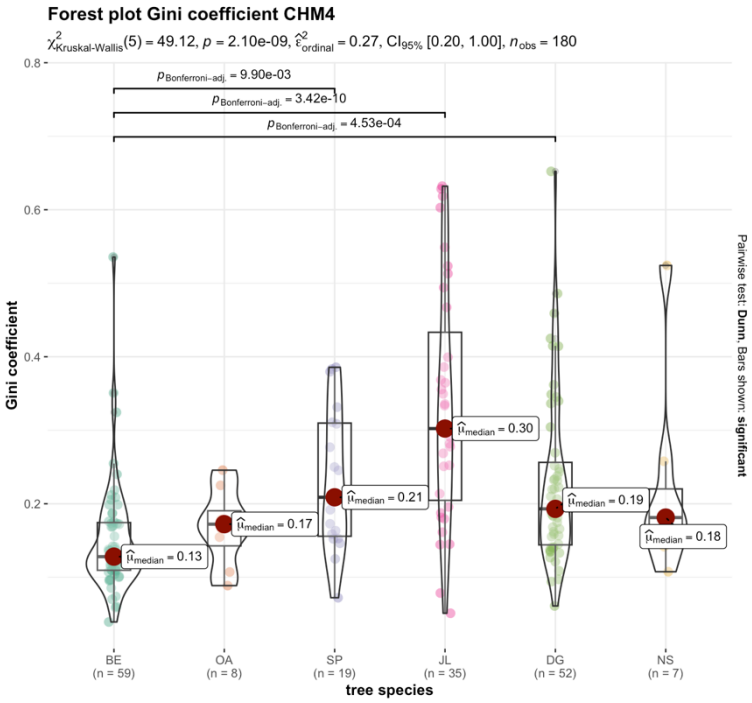

13d

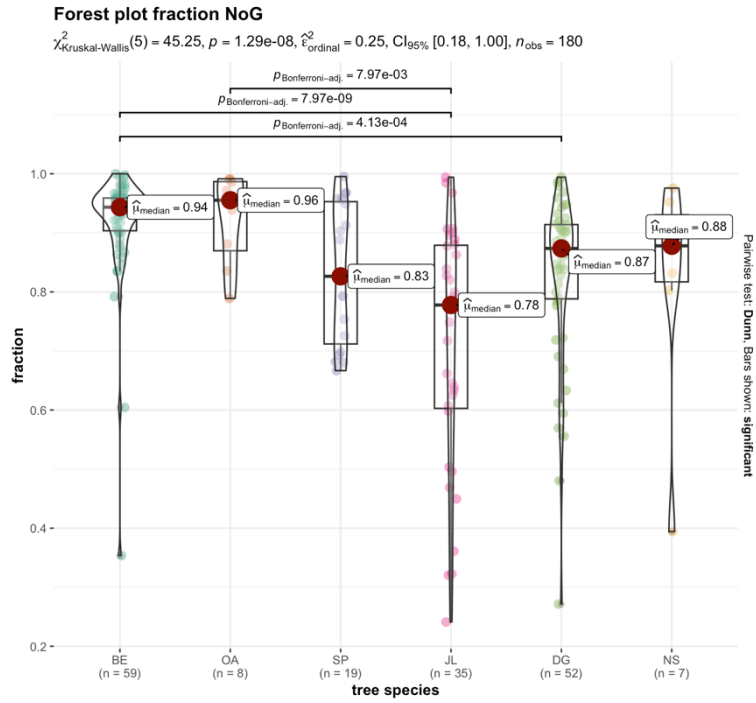

Figure 13 Statistical comparisons of dominant tree species on forest plot level for the variables new gap density (13a), mean CHM4 (13b), Gini coefficient CHM4 (13c), and fraction NoG (13d). For additional variable comparisons of dominant tree species on forest plot level, see Appendix F2.

3.2.6. Beech management type

To disentangle the influence of management type and dominant tree species on canopy gap dynamics, the three management types were compared in beech forest plots only. The number of new canopy gaps and forest plots per beech management type can be found in table 12. The fraction of area in new canopy gap for managed beech forest plots was higher than for the pseudo-unmanaged and unmanaged forest plots. This fraction for pseudo-unmanaged beech plots was higher compared to unmanaged beech plots (Table 12).

Table 12 Number and area of new canopy gaps and forest plots per management type for beech

Management type	*Number of new canopy gaps*	*Number of forest plots*	*Area of new canopy gaps (m2)*	*Area of forest plots in study area (m2)*	*Fraction area in new canopy gap*
Managed	284	36	12369	485915	0.025
Pseudo-unmanaged	230	18	10868	543101	0.020
Unmanaged	81	5	4353	261702	0.017
Total	595	59	27590	1290718	0.021

3.2.6.1. New canopy gap level

The distance to the nearest neighbour of new canopy gaps in managed beech forest plots was significantly lower compared to pseudo-unmanaged and unmanaged beech plots (Figure 14). This pattern was also observed for the 5 and 10 m doughnut buffer overlap with neighbouring new canopy gaps (Appendix G1). The mean difference CHM within the new canopy gaps was significantly higher in unmanaged beech plots compared to pseudo-unmanaged beech plots, and also significantly higher for pseudo-unmanaged compared to managed beech plots (Figure 14). The fraction NGBM of new canopy gaps was significantly higher in unmanaged beech plots compared to managed and pseudo-unmanaged beech plots (Figure 14). The opposite pattern was observed for the fraction NGLM (Appendix G1). There was observed a significant difference in 10m dbuffer ipcum90 in AHN4 of new canopy gaps between managed and pseudo-unmanaged beech plots, but not between managed and unmanaged beech plots (Figure 14). The 5m dbuffer ipground in AHN4 and the 10m dbuffer iskew in AHN4 was still significantly different between managed beech plots compared to pseudo-unmanaged and unmanaged beech plots, but the p-values were clearly lower when compared to the p-values of these statistical comparisons with all tree species included. No significant differences were found in the comparison of 10m dbuffer zq25 in AHN3 between beech management types (Appendix G1). There was no significant difference observed in new canopy gap area or perimeter between the beech management types (Appendix G1).

3.2.6.2. Forest plot level

The gap density of unmanaged beech forest plots was not significantly lower compared to managed and pseudo-unmanaged plots, but the median value is lower compared to pseudo-unmanaged plots (Figure 15). The forest plot mean CHM4 was significantly lower in managed beech plots compared to pseudo-unmanaged and unmanaged beech plots (Figure 15). The same pattern was observed for the mean CHM3 and CHM4 (Appendix G2). The Gini coefficient of CHM4 was significantly higher in managed plots compared to pseudo-unmanaged and unmanaged plots (Figure 15). There was no significant difference observed in forest plot fraction NoG between the beech management types, but the median value of managed beech plots was lower compared to pseudo-unmanaged and unmanaged plots (Figure 15).

14a

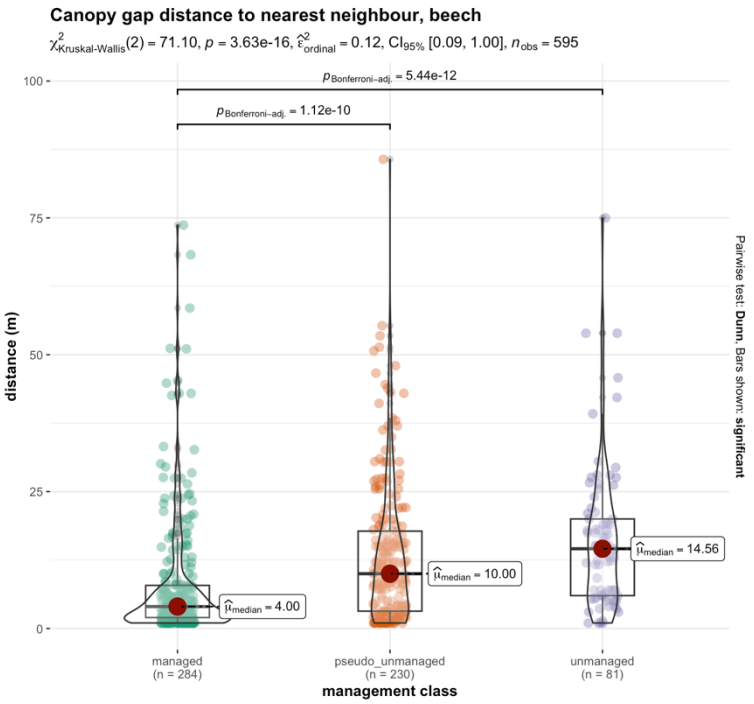

14b

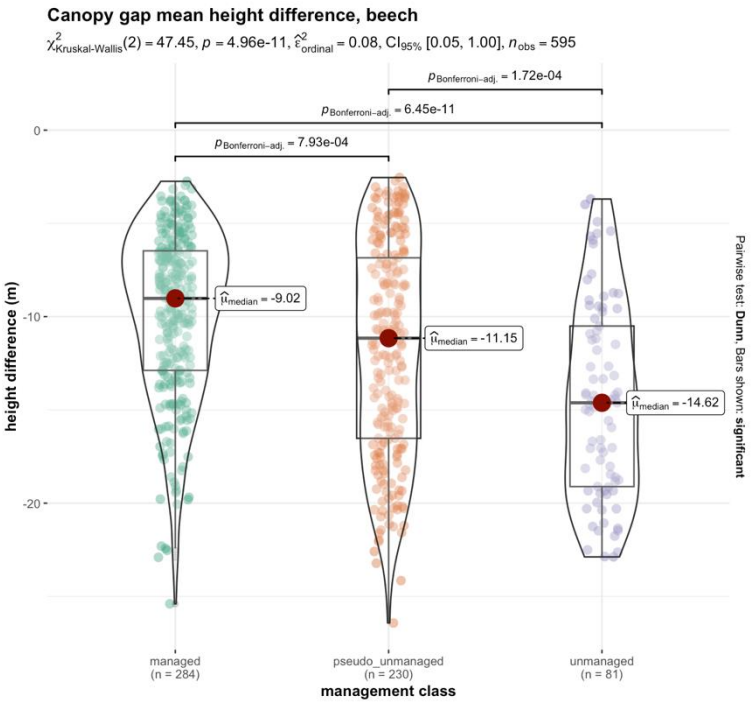

14c

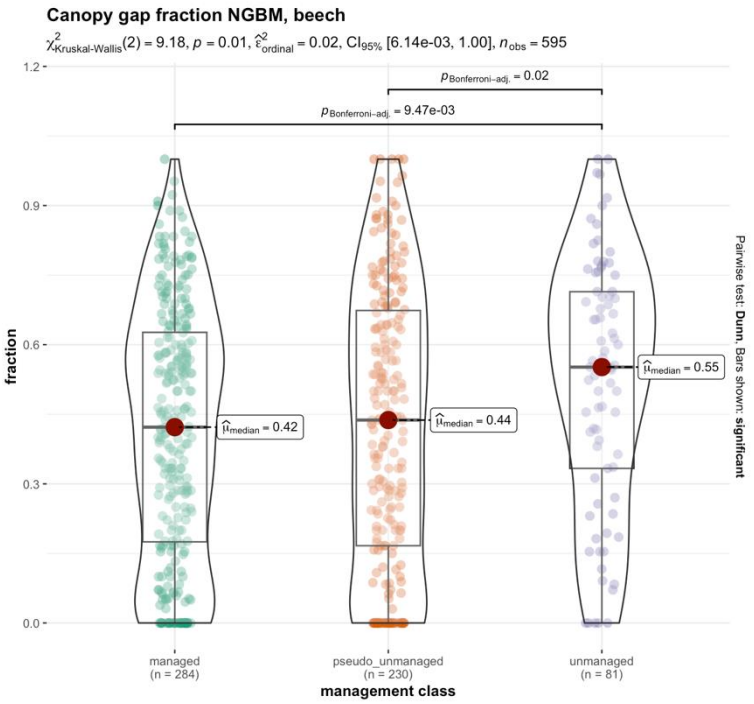

14d

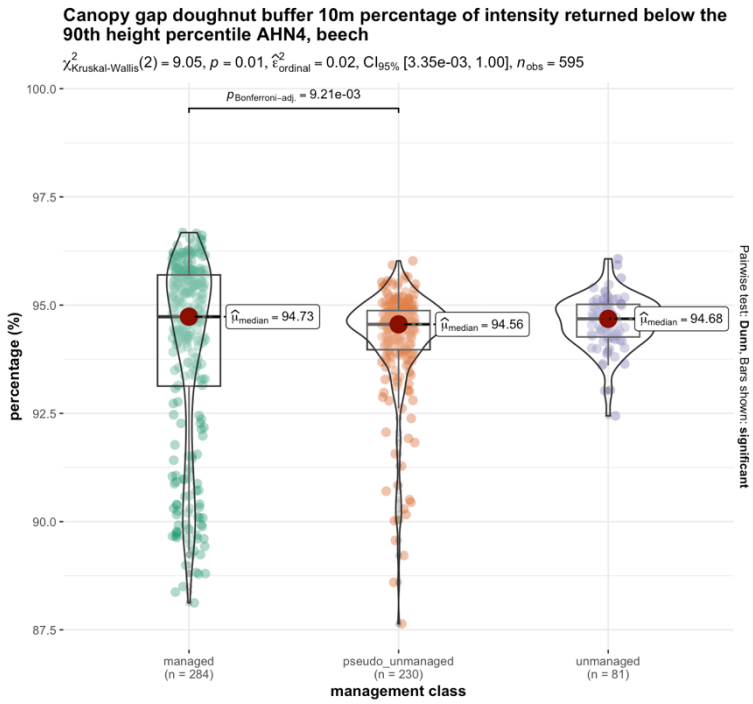

Figure 14 Statistical comparisons of management types for beech on canopy gap level for the variables distance to the nearest neighbour (14a), mean difference CHM (14b), fraction NGBM (14c), and 10 m doughnut buffer percentage of intensity returned below the 90th height percentile AHN4 (14d). For additional variable comparisons of management types for beech on canopy gap level, see Appendix G1.

15a

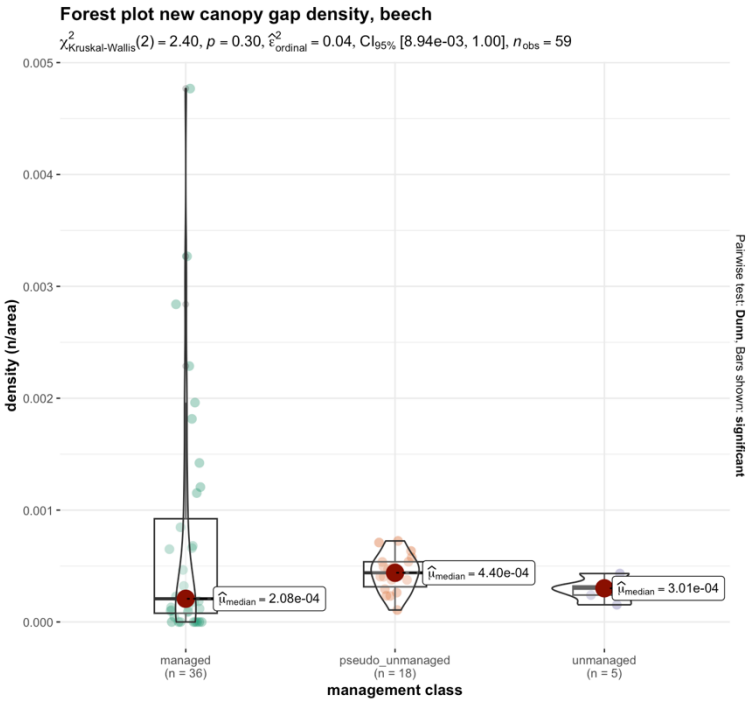

15b

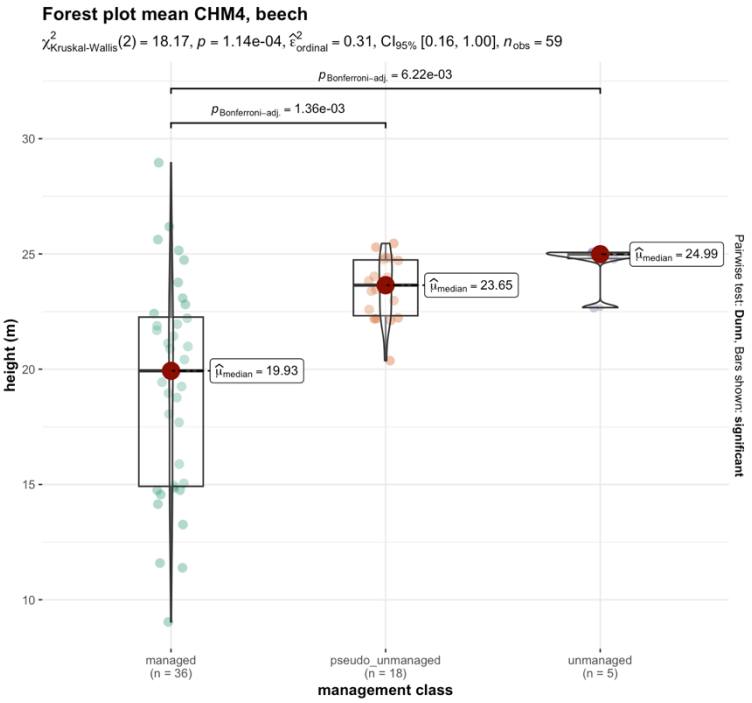

15c

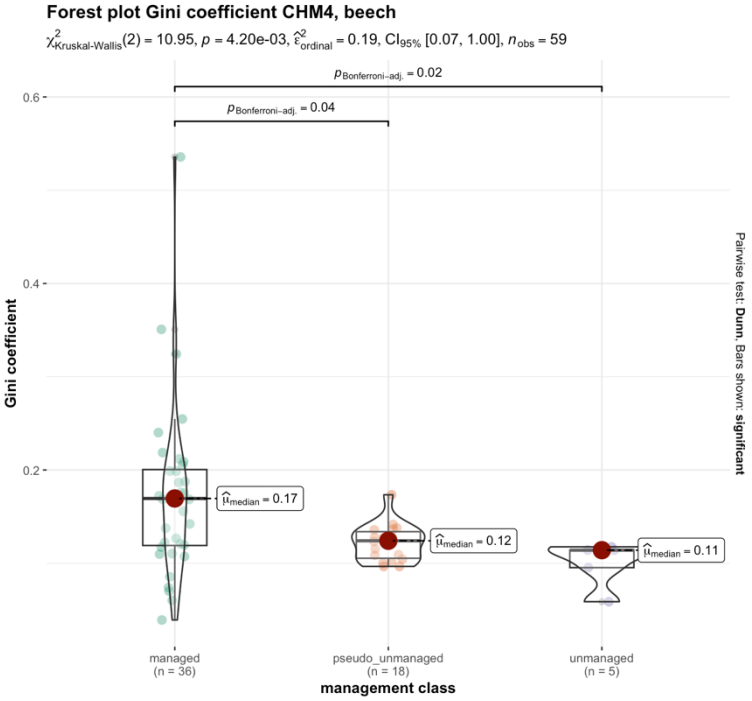

15d

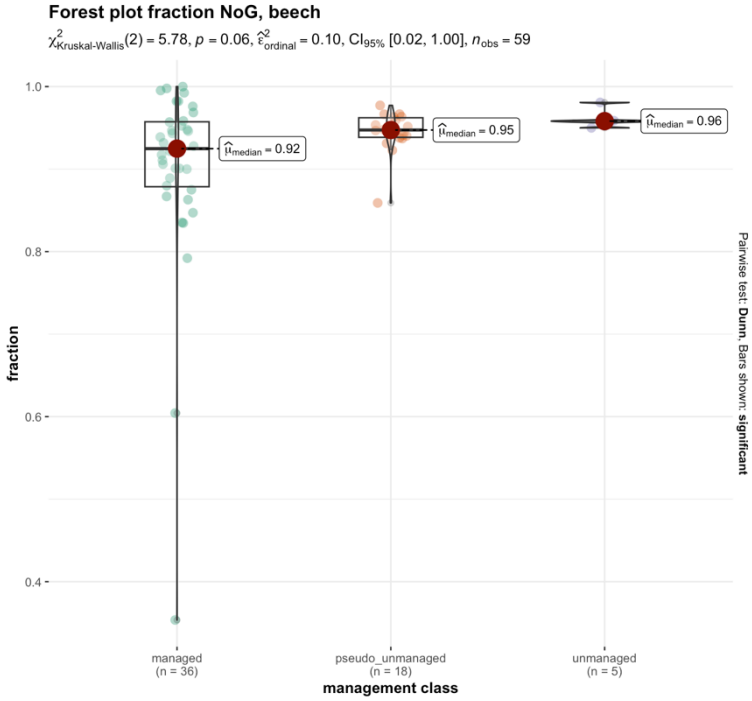

Figure 15 Statistical comparisons of management types of beech on forest plot level for the variables new gap density (15a), mean CHM4 (15b), Gini coefficient CHM4 (15c), and fraction NoG (15d). For additional variable comparisons of management types of beech on forest plot level, see Appendix G2.

3.2.7. Forest plot age

The number of new canopy gaps and forest plots per age class can be found in table 13. Managed forest plots were overrepresented in the lower age classes. The pseudo-unmanaged plots were represented in the 160-200 age class, as the registered germination date of these forest plots was 1835. The unmanaged plot were relatively evenly representation over the age classes, with a slight overrepresentation in the 160-200 age class. The tree species that were overrepresented in managed plots were also overrepresented in the lower age classes. Beech had a relatively even representation over the age classes compared to the other tree species, but it was slightly overrepresented in the 160-200 age class (Appendix I3 - I6).

Table 13 Number and area of new canopy gaps and forest plots per age class

Age class (y)	*Number of new canopy gaps*	*Number of forest plots*	*Area of new canopy gaps (m2)*	*Area in study area (m2)*	*Fraction of area in new canopy gap*
0-40	229	28	13957	248191	0.056
40-80	1525	101	92222	1319269	0.070
80-120	355	41	27622	538063	0.051
120-160	47	9	1309	90709	0.014
160-200	317	23	15353	814760	0.019
Total	2473	202	150463	3010992	0.050

3.2.7.1. New canopy gap level

The distance to the nearest neighbour of new canopy gaps in forest plots with the age classes 120-160 and 160-200 was significantly higher compared to the younger age classes (Figure 16). This pattern was also observed for the 5 and 10 m doughnut buffer overlap with neighbouring new canopy gaps (Appendix H1). There were observed significant differences in the mean difference CHM within the new canopy gaps between the different age classes, but no relation between forest plot age and mean CHM difference could be observed (Figure 16). The same could be said about the relation between forest plot age and mean CHM3 and CHM4 (Appendix H1). The only significant difference in fraction NGBM of new canopy gaps was between the age class 0-40 and 40-80, all other age classes did not differ significantly. Nonetheless, the median value of fraction NGBM was the highest for the age class 160-200 (Figure 16). The 10m ipcum90 in AHN4 was significantly higher in forest plots with age classes 120-160 and 160-200 compared to the other age classes (Figure 16). The same pattern was observed for the three other important variables in the management type RF model without forest plot variables (Appendix H1). No relation between age class and new canopy gap area or perimeter was observed (Appendix H1).

3.2.7.2. Forest plot level

There were no significant differences observed gap density between forest plots with different age classes. Nevertheless, the forest plots with older age classes had lower median gap density values compared to younger age classes (Figure 17). The forest plot mean CHM3 and CHM4 was observed to significantly increase with forest plot age, while the mean difference CHM was observed to significantly decrease with forest plot age (Figure 17, Appendix H2). The Gini coefficient of CHM4 was observed to be significantly lower in the oldest two age classes compared to the other age classes (Figure 17). The fraction NoG was observed to be significantly higher in the oldest two age classes compared to the other age classes (Figure 17).

The fraction VC of the fraction DG decreased significantly with increasing age class (Appendix H2).

16a

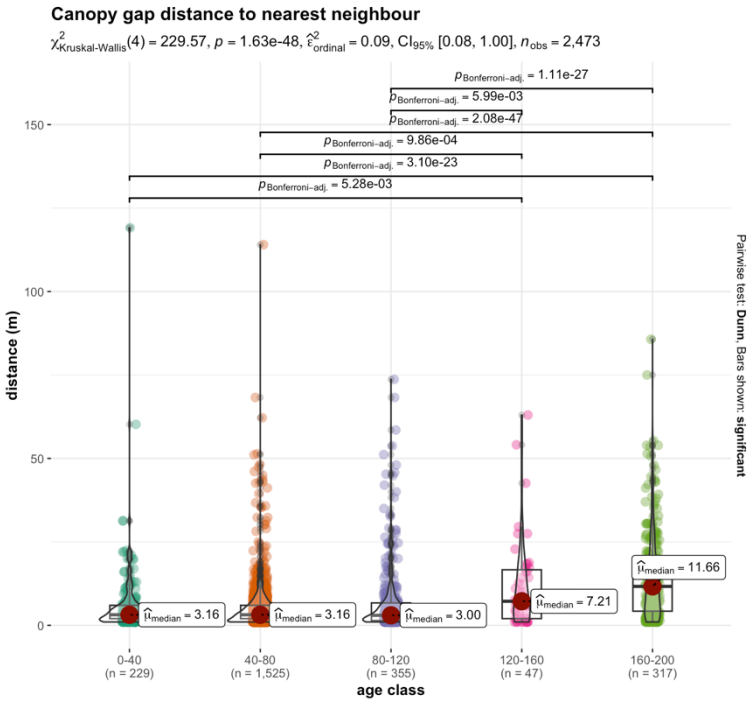

16b

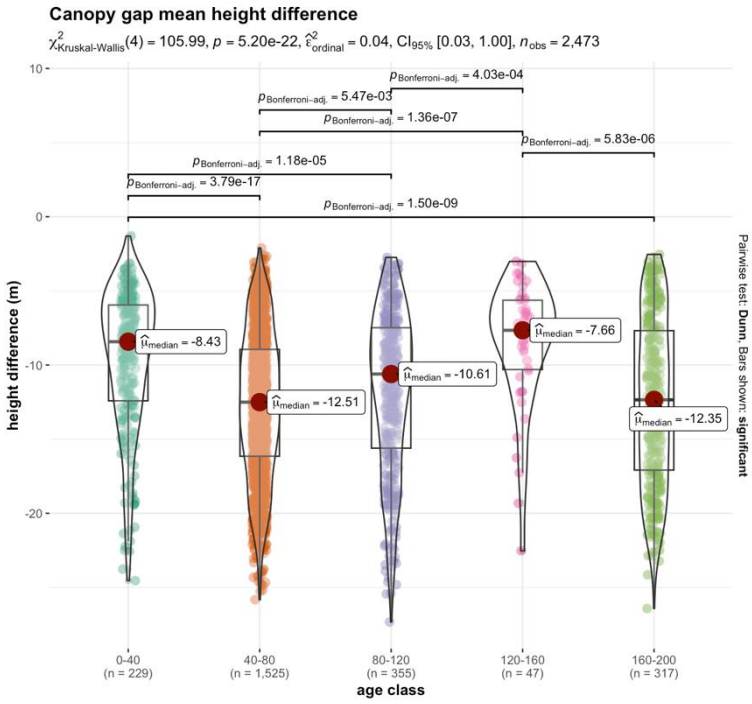

16c

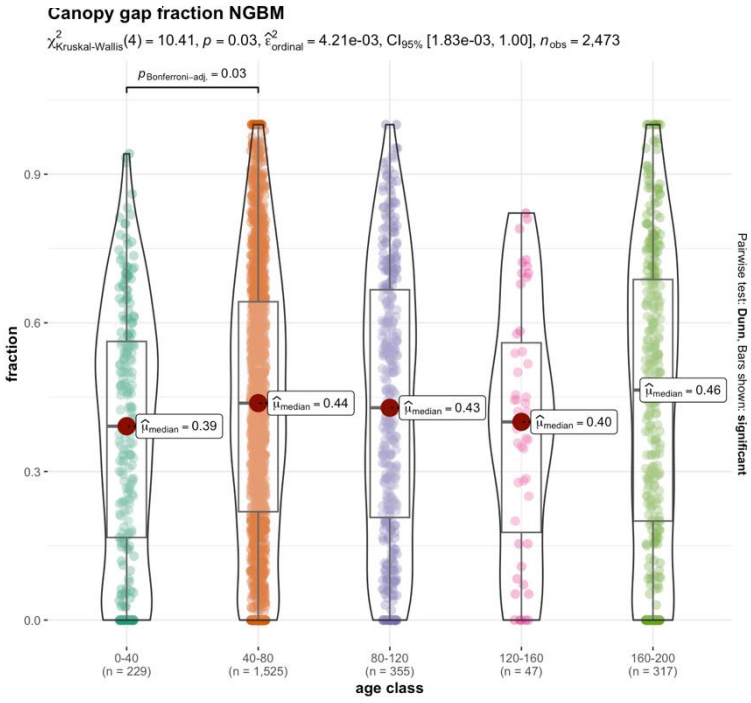

16d

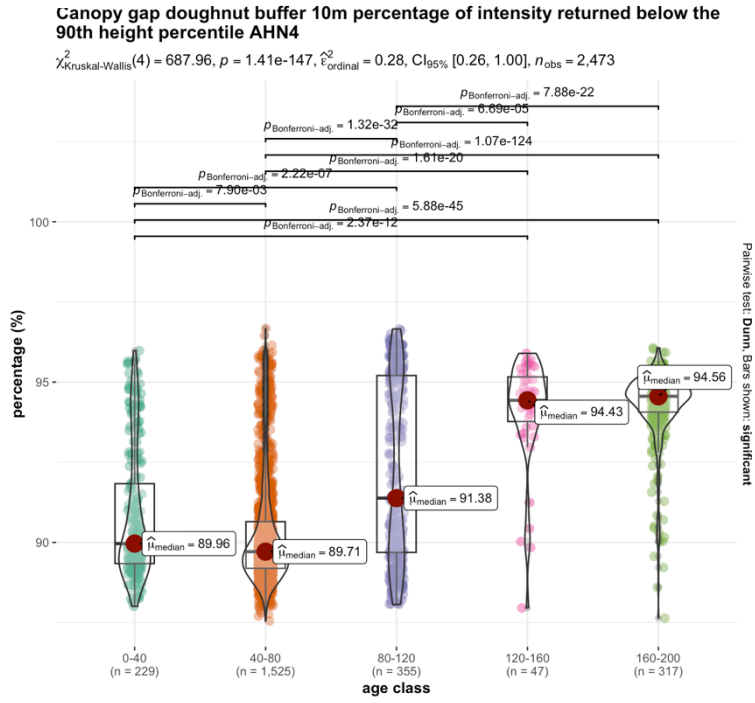

Figure 16 Statistical comparisons of age classes on canopy gap level for the variables distance to the nearest neighbour (16a), mean difference CHM (16b), fraction NGBM (16c) , and 10 m doughnut buffer percentage of intensity returned below the 90th height percentile AHN4 (16d). For additional variable comparisons of age classes on canopy gap level, see Appendix H1.

17a

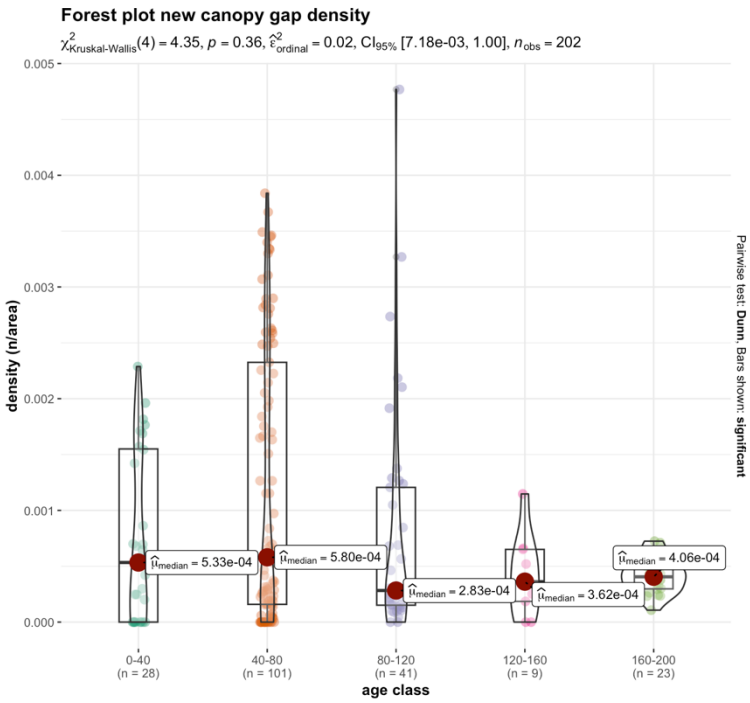

17b

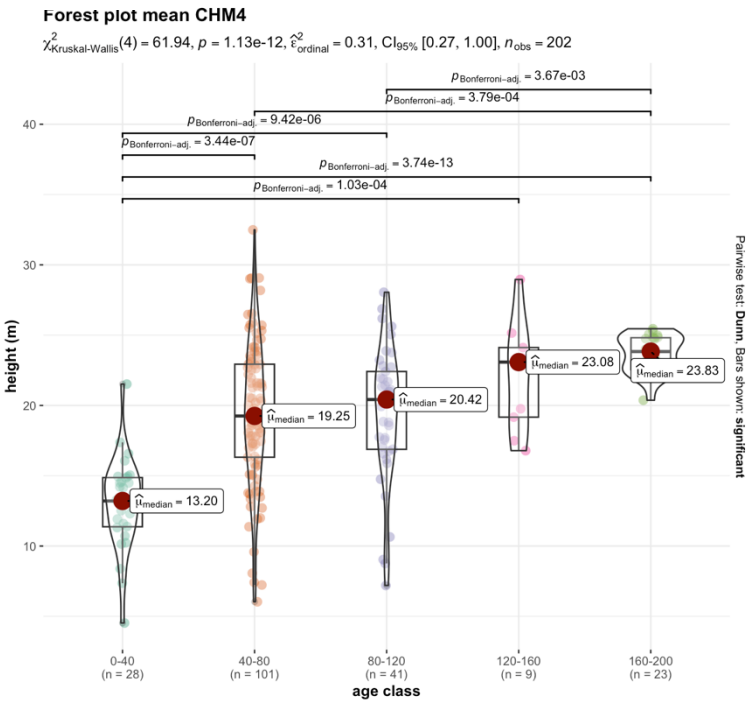

17c

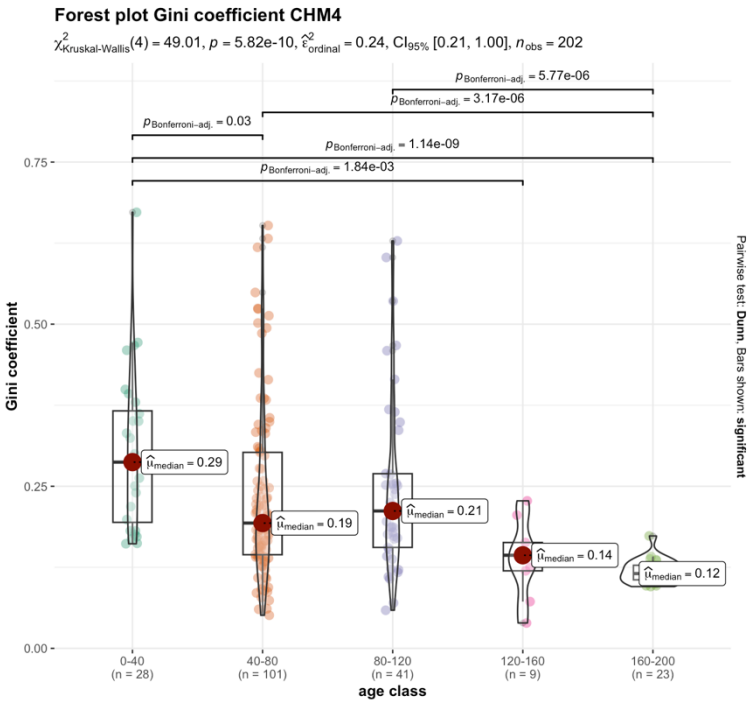

17d

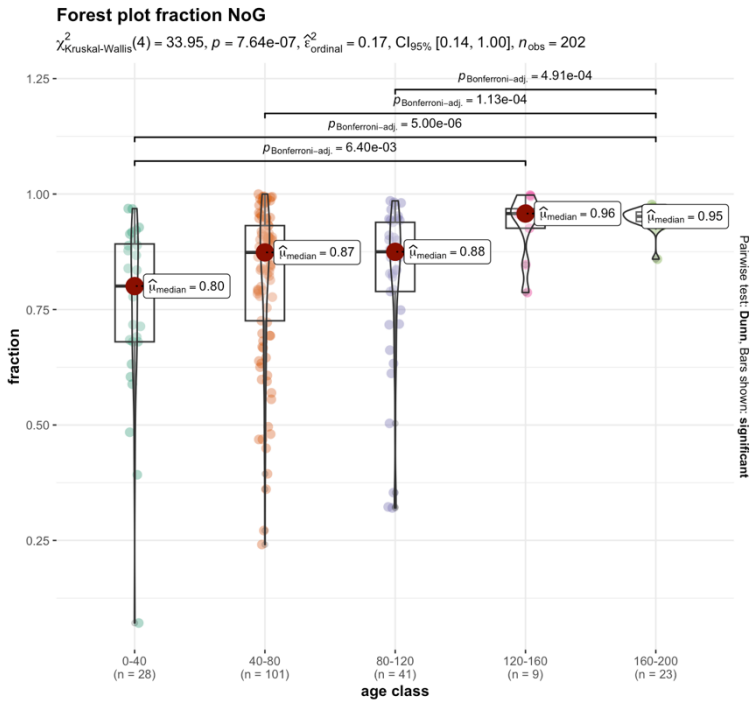

Figure 17 Statistical comparisons of age classes on forest plot level for the variables new gap density (17a), mean CHM4 (17b), Gini coefficient CHM4 (17c) , and fraction NoG (17d). For additional variable comparisons of age classes on forest plot level, see Appendix H2.

4. Discussion

4.1. Comparison Silva and Leitold method

At the start of the study, it was hypothesized that different canopy gap delineation methods would result in different spatial patterns of identified gaps, and that this difference would provide information of the ecological conditions in the canopy gaps. The Silva and the Leitold method are both conceptually simple methods to derive canopy gaps from a timeseries of two CHM versions. Both methods use a single threshold to binary split either one CHM version, Silva, or a difference CHM, Leitold, in areas in which new gaps have formed, or not (Leitold et al., 2018; Vepakomma et al., 2012). The Silva method uses a threshold, minimum vegetation height, to binary split each CHM version in gap areas and no gap areas. Thereafter, the binary gap output of both CHM versions is overlayed to derive areas in which new canopy gaps have formed. These areas have to be larger than the threshold for minimum new canopy gap area. The Leitold method requires one step less as the Silva method, and is therefore twice as fast to derive new canopy gaps. It uses a threshold, minimum canopy decrease, to directly identify new canopy gaps from the difference between the two CHM versions, the area of which must be again larger than the threshold for minimum new canopy gap area. As both methods are CHM-based, the computational time to derive canopy gaps is low compared to pointcloud-based methods (Gaulton & Malthus, 2010). This characteristic of the methods makes it suitable for upscaling to larger study areas. Moreover, ALS data, such as the AHN, can be used to determine canopy height with hight accuracy (Brede et al., 2017). Furthermore, because the Silva and Leitold methods are conceptually simple, the outcomes of the methods can easily be interpreted. However, the ecological effects of canopy gap emergence, such as tree species regeneration, is hard to investigate with these canopy gap detection methods based on the Brokaw definition (de Lima, 2005).

The use of the Silva and Leitold method in the study area revealed that the total area of new canopy gaps identified with the Leitold method is larger compared to the Silva method (Table 3, Figure 4). Nonetheless, the Silva method was able to identify areas with remaining canopy gaps and areas were canopy gaps have disappeared over time, whereas the Leitold method was unable to detect these canopy gap dynamic classes. The combination of the two methods revealed information about the fraction of the new canopy gap areas that were identified with both methods, with only the Leitold method, and with only the Silva method. These fractions provide information of the ecological impact of canopy gap formation, that cannot be derived from the Silva and Leitold method separately. The fraction of a new canopy gap that is detected with both methods is assumed to have no intact forest layer after the canopy gap emergence event, as the CHM4 is higher than 5 meter, whereas the fraction of a new canopy gap that is only detected with the Leitold method is assumed to still have an intact forest layer after the canopy gap emergence, as CHM4 is higher than 5 meter. New canopy gaps influence the light availability on the soil, and therefore they influence the micro climatic conditions, nutrient and water availability in the new gap (Lombard et al., 2019). Hence, it can be assumed that the fraction of the new canopy gaps that is only detected with the Leitold method has a lower impact on the forest ecosystem than the fraction of the new canopy gaps that is detected with both methods. This reveals that the combination of the Silva and Leitold method can provide ecologically relevant information about canopy gap dynamics, namely the presence of a tree layer in a canopy gap after the canopy gap emergence.

The first step of validating the identified new canopy gaps, derived from the combination of the Silva and Leitold methods, was the comparison with registered management interventions. This comparison revealed that large new canopy gaps, and clusters with high densities of new canopy gaps, are often situated in forest plots with registered management

interventions (Figure 6). This outcome was the first indication of the accuracy of the combination of the Silva and Leitold methods to detect canopy gaps. However, there were some discrepancies between the location of registered management interventions and of the detected large new canopy gaps, and clusters with high densities of new canopy gaps. This could best be explained by inaccuracies in management intervention registration, as the error margin of the AHN is on a centimetre scale. It is therefore unlikely that large new canopy gaps, and clusters with high densities of new canopy gaps, are incorrectly identified. It is more likely that there were inaccuracies in management intervention registration. To start, the map with the forest plot delineation did not always correspond with the field situation. The borders of the forests did not always correspond with the borders of plots of trees species with the same age class. Moreover, there were situations in which management interventions were registered in a forest plot with no identified new canopy gaps, neighbouring a forest plot were large numbers of canopy gaps were detected, even though in that forest plot no management interventions were registered. It is likely that the forest plot codes were mixed up during management intervention registration in this specific situation.

The second step of validating the identified new canopy gaps was a field visit of a selection of the new canopy gaps. During the field visit, the presence of all of the selected identified new canopy gaps was confirmed, which confirms the accuracy of the used canopy gap detection method. However, there were canopy gaps observed in the field that were not identified as new canopy gaps, or as remaining gaps. This can better be explained by the time interval between the acquisition of AHN4 and the field visit than by inaccuracies in the used canopy gap detection method. The field visit was conducted three years after the acquisition of AHN4. It is highly plausible that new gaps have formed in the visited forest plots in the time interval between the acquisition of AHN4 and the field visit.

4.2. Influence forest management on canopy gap dynamics

At the start of the study, it was hypothesized that in managed forest plots, the canopy gaps would be larger in area, higher in density, and more regularly shaped compared to canopy gaps in unmanaged forest plots (Muscolo et al., 2014; St-Onge et al., 2014). The influence of forest management on canopy gap dynamics was first exploratively investigated by labelling the identified new canopy gaps with a “number of trees” class. The variables of the new canopy gaps per “number of trees” class were statistically analysed, and the presence per “number of trees” class in each management type was analysed. Thereafter, the identified new canopy gaps in different management types were statistically compared. RF models were used to determine which variables were most important to distinguish new canopy gaps in different management types. The most important variables were then compared on canopy gap and forest plot level to disentangle the influence of forest management, dominant tree species and age on canopy gap dynamics. Overall, it could be said that the investigation of forest management on canopy gap dynamics revealed that it is possible to derive the influence of different forest conditions on canopy gap dynamics by using the AHN.

4.2.1. “Number of trees” class comparison

The classes “one tree” and “group of trees” are overrepresented in managed plots, while the class “part of tree” is relatively evenly distributed over the three management type. The class “group of trees” was rare in pseudo-unmanaged and unmanaged plots (Table 4). These proportions of new canopy gaps in different “number of trees” classes per management type indicates the higher new canopy gap size and density in managed plots compared to pseudo-unmanaged and unmanaged plots. Furthermore, it indicates that pseudo-unmanaged plots have a slightly higher new canopy gap size and density compared to unmanaged plots, as the

proportional occurrence of the class “group of trees” was higher in pseudo-unmanaged plots compared to unmanaged plots.

The “number of trees” RF model with all variables included had a total accuracy of 0.853 (Table 5). The fifteen most important variables in this model were pointcloud shape variables, forest plot variables, pointcloud variables and , 2D canopy gap shape variables (Figure 7). The planarity of the shape of AHN3 in the new canopy gaps was the most important variable in the “number of trees” classification. Planarity of AHN3 is the alignment of points whining a pane, before the emergence of the new canopy gap (Dobler et al., 2014). The “one tree” class has the lowest planarity. The “one tree” class is overrepresented in managed plots (Table 4), and in these managed plots, there is an overrepresentation of coniferous tree species. Coniferous tree species have a cone-shaped crown, and this can explain the low planarity of AHN3 in the “one tree class” (Liang et al., 2007). Deciduous trees are overrepresented in pseudo-unmanaged and unmanaged plots, and because the “part of tree” class had a higher proportional presence in these plots compared to the “one tree” class, the more planar shape of a deciduous tree can be an explanation for the higher planarity of the “part of tree” class compared to the “one tree” class. Continuous areas with multiple trees have a high planarity, and this can explain the “group of trees” class has the highest planarity (Dobler et al., 2014).

The next most important variables in the “number of trees” RF model were forest plot variables, namely the fraction NGCM, gap density, and fraction in gap. For these three variables, the classes “one tree” and “group of trees” have higher values compared to the “part of tree” class. This can be explained by the overrepresentation of the classes “one tree” and “group of trees” in managed plots, and relatively high presence of the “part of tree” class in pseudo-unmanaged and unmanaged plots, as the gap density and fraction in gap is higher in managed plots compared to pseudo-unmanaged and unmanaged plots (Table 10, Figure 11).

Two pointcloud variables are the next most important variables. The percentage of intensity returned below the 70^{th} and 90^{th} height percentile is higher in the “part of tree” class compared to the classes “one tree” and “group of trees”. This can be explained by the relatively high presence of the “part of tree” class in forest plots with deciduous tree species, and the relatively high presence of the classes “one tree” and “group of trees” in forest plots with coniferous species. This difference in intensity returned per percentile hight between the “number of trees” classes can be explained by the fact that the AHN is acquired during the leaf-off season. In this this season, the crown penetration of laser beams is higher in deciduous tree species compared to coniferous tree species (Liang et al., 2007). Deciduous tree species can therefore be distinguished from coniferous tree species with high precision during the leaf-off season (Reitberger et al., 2008).

The final most important variables in the “number of trees” classification are 2D shape variables derived from the area and perimeter of the new canopy gaps. The area and perimeter of the “group of trees” class are significantly larger compared to the other classes. This can be explained by the higher number of trees that have disappeared, and therefore new canopy gap area, in the “group of trees” class compared to the others. The area of the “one tree” class is significantly larger compared to the “part of tree” class, but the perimeter of “one tree” class is significantly smaller compared to the “part of tree” class. This suggests that the new canopy gaps in the “part of tree” class are more irregular compared to the ones in the “one tree” class. New canopy gaps that have emerged due to natural events are generally more irregularly shaped compared to gaps that have emerged due to management (St-Onge et al., 2014). As the “part of tree” class is proportionally more represented in pseudo-unmanaged and unmanaged plots, this can be an explanation why the new canopy gaps of the class “part of tree” are more irregularly shaped compared to the ones in the “one tee” class (Table 4).

The accuracy of the “number of trees” RF model with only the three most important variables included is 0.747, which is 0.109 lower compared to the model with all variables included (Table 6). In the selection of three most important variables, 2D shape variables are

not included. This makes it harder for the model to distinguish the "part of tree" class from the "one tree" class, and thus leads to a relatively low users accuracy of the "part of tree" class compared to the RF model with all variables included.

A drawback of the "number of trees" classes investigation was that the labelling of the new canopy gaps in the different "number of trees" classes was not validated in the field. The results of this analysis should therefore be viewed with precaution. Furthermore, in forest plots with deciduous species, it was hard to visually recognize individual tree species compared to forest plots with coniferous species, as deciduous tree species do not have the same recognizable cone shape as coniferous species (Liang et al., 2007). Accordingly, it was harder to determine whether in which "number of trees" class a new canopy gap fell in deciduous forest plots compared to coniferous plots.

4.2.2. Disentangling the influence of different forest plot characteristics

To derive the influence of forest management on canopy gap dynamics, the difference in dominant tree species and age class per management type had to be taken into account. The conditions in forest plots in different management types in the study area different considerably (Figure 1). Therefore, the influence of the difference in conditions between management classes first had to be separated from the influence of management to learn the influence of management on canopy gap dynamics.

The management type RF model with all variables included had a total accuracy of 0.990 (Table 7). Even though the accuracy of this model on test data was high, 0.986, the model was highly overfitted to the study area, which means that this model would perform considerably worse on test data outside the study area. However, interesting insights can be still derived from this management type RF model, as it shows which variables are most important in the classification of identified new canopy gaps in different management types. Of the fifteen most important variables in this model, thirteen were forest plot variables, and two were doughnut buffer pointcloud variables (Figure 8).

The forest plot variable that was most important in the management type RF model was the Gini coefficient of the AHN4. The Gini coefficient of CHM4 is significantly higher in managed plots compared to pseudo-unmanaged and managed plots (Figure 11). This can be interpreted as a higher tree size inequality in managed plots compared to pseudo-unmanaged and managed plots, which indicates larger disturbance events (Silva et al., 2019). This finding corresponds with the expectation that forest management leads to a higher density of new canopy gaps and larger new canopy gap area (Muscolo et al., 2014). Other findings, such as the difference in median value of gap density and fraction NoG between the different management types are as well in line with this expectation. The observation that forest management led to an increased gap density is also an explanation why the distance to the nearest neighbour was lower in managed plots compared to pseudo-unmanaged and unmanaged plots (Figure 10 & 14). It is unlikely that the difference between these forest plot variables are caused by other factors than forest management, such as dominant tree species or age class. The influence of dominant tree species was tested by comparing the different management types for beech plots only, and this comparison revealed that the fraction in gap was highest in managed plots, in-between in pseudo-unmanaged plots, and lowest in unmanaged plots (Table 12). Moreover, the Gini coefficient was highest in managed plots, in-between in pseudo-unmanaged plots, and lowest in unmanaged plots. The fraction NoG was lowest in managed plots, in-between in pseudo-unmanaged plots, and highest in unmanaged plots (Figure 15). The influence of forest plot age on forest plot variables was tested by comparing different age classes. This comparison revealed that the fraction in gap and the Gini coefficient decreased with forest plot age. Furthermore, the fraction NoG increased with forest plot age (Table 13, Figure 17). These findings contrasts with the expectation that the area and density of new canopy gaps increases with age (Spies, 1998). However, in the study area, older age classes are overrepresented by

pseudo-unmanaged and unmanaged plots, while the younger age classes are overrepresented by managed plots. Therefore, the difference in forest plot variables can best be explained by management type, instead of dominant tree species or age.

Of the in fifteen most important variables in the management type RF model with all variables included, two were doughnut buffer pointcloud variables (Figure 8). These variables both related to the percentage intensity returned at the x^{th} height percentile. The fifteen most important variables in the management type RF model without forest plot variables included were all doughnut buffer pointcloud variables. This suggested that the characteristics of the pointcloud directly neighbouring the new canopy gaps provided important information for the classification in different management types. However, it was found that not forest management, but dominant tree species caused this difference in doughnut buffer pointcloud variables between different management types. Deciduous species are overrepresented in the pseudo-unmanaged and unmanaged class, and coniferous species are overrepresented in the managed class, and the crown penetration differs considerably between these two tree types (Reitberger et al., 2008). The comparison of management types for only beech revealed that there were no significant differences in doughnut buffer pointcloud variables between different management classes (Figure 14). The observation that not the difference in management type, but the difference in dominant tree species caused the difference in doughnut buffer pointcloud variables can be an explanation why the user accuracy for pseudo-unmanaged and unmanaged plots is so low in the management type RF model without forest plot variables (Table 9). The question remains why the fifteen most important variables in the management type RF model without forest plot variables were doughnut buffer pointcloud variables, instead of pointcloud variables directly derived from the new canopy gaps. This might be explained by the difference in area between the two clips of the pointcloud, as the area of the two doughnut buffers was on average larger compared to the new canopy gaps.

When investigating the variable importance of the most important variables in the management type RF model, it can be observed that the importance of forest plot variables is considerably higher compared to doughnut buffer pointcloud variables (Figure 8). The variable importance decreased rapidly with decreasing variable importance rank. This finding suggests that the difference in forest plot variables between management types is actually caused by forest management, while the difference in doughnut buffer pointcloud metrics is caused by another factor, specifically dominant tree species. This, and the fact that the total accuracy of the management type RF model with only the four most important variables was higher compared to the model with all variables included, suggested that the pointcloud variables were noise in the classification of new canopy gap in different management types (Table 7 & 8).

A significant difference was observed in the mean difference CHM within the new canopy gaps between different management types (Figure 10). The mean difference CHM was higher in unmanaged plots compared to managed plots. However, it is expected that this difference was not caused by the difference in management type, but the difference in age between the forest plots in managed and unmanaged plots. With increasing age, the mean CHM3 and CHM4 increases on forest plot level (Figure 17). This makes sense, as trees grow over time. The older age classes are overrepresented in unmanaged plots, while the younger age classes are overrepresented in managed plots. It is therefore expected that when a canopy gap emerges in an unmanaged plot, the height difference in bigger compared to a new canopy gap in a managed plot.

The fraction NGBM of new canopy gaps was significantly higher in unmanaged forest plots compared to managed plots (Figure 10 & 14). Managed forests are generally described as monotone, even-aged stands with no different tree layers, while unmanaged forests are described as structured forests with multiple tree layers (Johann, 2006). It is therefore surprising that the fraction NGBM is lower in managed compared to unmanaged plots, as the fraction NGBM indicates the proportion of new canopy gaps in which no tree layer remains after the

canopy gap emergence event (CHM4 ≤ 5 m). A possible explanation for this result is the light availability under beech forests. Beech forests are considered to be dominant, climax species that can cover 99% of a forest under natural conditions (Feldmann et al., 2018). The light availability is low in beech forests, and therefore mature beech forests are associated with a low plant species diversity (Ottaviani et al., 2019). Many generalist species are not able to regenerate under a closed beech canopy. Even the highly shade tolerant saplings of beech need small gaps in the beech canopy to successfully regenerate (Naaf & Wulf, 2007). Consequently, in unmanaged, mature beech forests, it is unlikely that there are multiple tree layers in the forest structure. Another explanation for the difference in fraction NGBM between managed and unmanaged plots could be the influence of herbivory. The herbivory pressure is relatively high in the Speulderbos, and herbivory negatively influences beech regeneration, which prevents the formation of new tree layers under the mature beech canopy in unmanaged plots (Naaf & Wulf, 2007). However, the significant difference in fraction NGBM between pseudo-unmanaged and managed plots cannot be explained by this reasoning, as these management types are both overrepresented by beech. A possible explanation for the lower fraction NGBM in pseudo-unmanaged plots compared to unmanaged plots could be the girdling management practice in pseudo-unmanaged plots. Girdling leads to the slow decay of trees, and during this process, the light availability on the ground can increase due to the decay of the crown of the girdled tree. With this increased availability of light, a new tree layer could form under the girdled trees.

The fraction in gap is higher in pseudo-unmanaged plots compared to unmanaged plots (Table 10 & 12). This distance to nearest neighbour is significantly higher in unmanaged forest plots compared to pseudo-unmanaged plots (Figure 10 & 14). Even though the difference is not statistically significant, the gap density and Gini coefficient median values are higher in pseudo-unmanaged plots compared to unmanaged plots (Figure 11 & 15). These three observations can best explained by the girdling practice in pseudo-unmanaged plots, as the tree species composition and age class of pseudo-unmanaged and unmanaged forest plots are similar.

The area and perimeter of new canopy gaps did not significantly differ between different management types, even though it was expected that in managed plots, the area of new canopy gaps would be higher compared to unmanaged gaps (Muscolo et al., 2014). Moreover, it was observed that the relative presence of the "number of trees" class "group of trees" was considerably larger in managed plots compared to pseudo-unmanaged and unmanaged plots (Table 4). There are several factors that could possibly explain this absence of difference in area and perimeter between new canopy gaps in different management types. One explanation could be thinning operations in managed plots. Thinning operations often lead to the emergence of small new canopy gaps with high density (Wilkinson et al., 2016). The number of new canopy gaps in managed plots with the class "one tree" is almost twice as high as with the class "group of trees" (Table 4). Besides, the beech forests of pseudo-unmanaged and unmanaged plots are mature, so in case one tree disappears, a relatively large new gap is formed. Furthermore, it was observed in managed plots that small cohorts of young trees were removed in a thinning operation, leaving behind a relatively small new canopy gap, but receiving the label "group of trees". Additionally, observations of large clear-cuts and extensive thinning operations that led to large consecutive new canopy gaps were rare in the study area.

4.3. Recommendations

This study showed that CHM-based canopy gap detection methods, both the Silva method, the Leitold method, and a combination of these methods are suitable to study canopy gap dynamics derived from AHN data. The preferred method, or combination of methods, to study canopy gap dynamics derived from AHN data depends on the aim of the study. The Silva method reveals new canopy gaps in which no tree layer is intact after the canopy gap emergence. Besides, the Silva method is able to determine areas in the forest were canopy gaps have

remained over time, and were canopy gaps have disappeared. The Leitold method reveals all areas in the forest plot where the canopy was considerably lowered. The combination of these two method reveals the fractions of new canopy gap in which an intact tree layer is absent or present after the canopy gap emergence event. It is recommended that when analysing canopy gap dynamics derived from AHN data, especially on a larger spatial scale, to work with CHM-based canopy gap detection methods. The reasons for this is that ALS data is highly suitable to determine canopy height, and the computation time is considerably faster compared to pointcloud based methods. Moreover, CHM-based methods are conceptually simple and therefore easily interpretable (Brede et al., 2017; Gaulton & Malthus, 2010). In this study, the AHN pointclouds were processed to create DEMs and thereby CHMs. Further studies on canopy gap dynamics derived from the AHN can consider to directly download the derived DEMs from the AHN, depending on the research aim. Pointcloud variables are highly useful to discriminate different tree species, but do not provide insights in the differences between different management types.

The results of this study are influenced by the selected canopy gap thresholds. The threshold selection procedure is partly a subjective process, that is highly influenced by the aim of the research (Senecal et al., 2018). In further canopy gap dynamics studies with the AHN, the thresholds most be critically reviewed, and it must always be considered to what extent the set of thresholds fits to the aim of the study.

It is recommended that the AHN will be implemented in a monitoring scheme of canopy gap dynamic of Dutch forests. There are already four versions of the AHN, and a new version is currently under development. It can therefore be expected that the AHN will be regularly renewed, also in the future, which makes it possible to continuously monitor Dutch forests canopy gap dynamics with the AHN. The results of the validation of the identified new canopy gaps in this study revealed that the AHN is a reliable source to detect canopy gaps. The AHN is an open data source, and can therefore be implemented in forest monitoring projects without the need of large financial investments. This study revealed that the canopy gaps derived from the AHN can be used to make in-depth statistical comparisons between different types of forest plots. The AHN can therefore be used to study the influence of different factors on canopy gap dynamics, with the availability of additional datasets. In this study, data on forest plot level was used, but in further studies, data about e.g. land use type, soil type, hydrological conditions, nutrient availability or climatic conditions could be used to determine the its influence on canopy gap dynamics.

For forest terrain owners, the AHN could be used to transparently communicate the quantity of removed trees to the public. In the Netherlands, wood removal can be considered to be a politically-charged issue. In the current situation, in which terrain owners often do not have precise information on were new canopy gaps have emerged, there is little information available to the public about wood removal in the forest. The AHN makes it possible for terrain owners to fully transparently communicate about wood removal practices in their forests, and that can lead an increase in trust from the public (Auger, 2014).

5. Conclusion

In this study, it was aimed to uncover the potential of the AHN to study canopy gap dynamics by comparing two CHM-based canopy gap detection methods, the Silva and Leitold method, and to investigate the influence of forest management on canopy gap dynamics. It was found that the Leitold method identified a larger area of new canopy gaps compared to the Silva method, and that the Silva method was able to detect more canopy gap dynamics classes compared to the Leitold method. The combination of these methods was shown to identify new canopy gaps with high accuracy, and led to additional ecological understanding about the

identified canopy gaps by providing information about the presence of a forest layer in canopy gap after the canopy gap emergence event. The analysis of the influence of forest management on the identified new canopy gaps showed that forest management decreased the distance to the nearest neighbour, and increased the forest plot gap density. The other differences in new canopy gap characteristics between different management types were explained by other factors than management, namely the difference in dominant tree species and age of the forest plots in different management types in the study area. This study revealed that it is possible to derive the influence of different forest conditions on canopy gap dynamics by using the AHN.

Disclaimer

It would have been more appropriate to refer to the canopy gap detection method from two separate CHM versions as the Vepakomma method, instead of the Silva method, as Vepakomma et al. (2012) developed the method, while Silva et al. (2019) developed an implementation of the method in R.

References

Akay, A. E., Oguz, H., Karas, I. R., & Aruga, K. (2009, Apr). Using LiDAR technology in forestry activities. *Environmental Monitoring and Assessment, 151*(1-4), 117-125. https://doi.org/10.1007/s10661-008-0254-1

Alonso-Rego, C., Arellano-Perez, S., Guerra-Hernandez, J., Molina-Valero, J. A., Martinez-Calvo, A., Perez-Cruzado, C., Castedo-Dorado, F., Gonzalez-Ferreiro, E., alvarez-Gonzalez, J. G., & Ruiz-Gonzalez, A. D. (2021, Dec). Estimating Stand and Fire-Related Surface and Canopy Fuel Variables in Pine Stands Using Low-Density Airborne and Single-Scan Terrestrial Laser Scanning Data. *Remote Sensing, 13*(24), Article 5170. https://doi.org/10.3390/rs13245170

Auger, G. A. (2014). Trust Me, Trust Me Not: An Experimental Analysis of the Effect of Transparency on Organizations. *Journal of Public Relations Research, 26*(4), 325-343. https://doi.org/10.1080/1062726x.2014.908722

Beaudet, M., Messier, C., & Leduc, A. (2004, Apr). Understorey light profiles in temperate deciduous forests: recovery process following selection cutting. *Journal of Ecology, 92*(2), 328-338. https://doi.org/10.1111/j.0022-0477.2004.00869.x

Beck, H. E., Zimmermann, N. E., McVicar, T. R., Vergopolan, N., Berg, A., & Wood, E. F. (2018, Oct). Present and future Koppen-Geiger climate classification maps at 1-km resolution. *Scientific Data, 5*, Article 180214. https://doi.org/10.1038/sdata.2018.214

Blackburn, G. A., Abd Latif, Z., & Boyd, D. S. (2014, Nov). Forest disturbance and regeneration: a mosaic of discrete gap dynamics and openmatrix regimes? *Journal of Vegetation Science, 25*(6), 1341-1354. https://doi.org/10.1111/jvs.12201

Blackburn, G. A., & Milton, E. J. (1996, Jul-Sep). Filling the gaps: Remote sensing meets woodland ecology. *Global Ecology and Biogeography, 5*(4-5), 175-191. https://doi.org/10.2307/2997787

Bonan, G. B. (2008, Jun). Forests and climate change: Forcings, feedbacks, and the climate benefits of forests. *Science, 320*(5882), 1444-1449. https://doi.org/10.1126/science.1155121

Bonferroni, C. (1936). Teoria statistica delle classi e calcolo delle probabilita. *Pubblicazioni del R Istituto Superiore di Scienze Economiche e Commericiali di Firenze, 8*, 3-62. https://doi.org/10.4135/9781412961288.n455

Bonhomme, V., Picq, S., Gaucherel, C., & Claude, J. (2014, Feb). Momocs: Outline Analysis Using R. *Journal of Statistical Software, 56*(13), 1-24. https://doi.org/10.18637/jss.v056.i13

Bonnet, S., Gaulton, R., Lehaire, F., & Lejeune, P. (2015, Sep). Canopy Gap Mapping from Airborne Laser Scanning: An Assessment of the Positional and Geometrical Accuracy. *Remote Sensing, 7*(9), 11267-11294. https://doi.org/10.3390/rs70911267

Brede, B., Lau, A., Bartholomeus, H. M., & Kooistra, L. (2017, Oct). Comparing RIEGL RiCOPTER UAV LiDAR Derived Canopy Height and DBH with Terrestrial LiDAR. *Sensors, 17*(10), Article 2371. https://doi.org/10.3390/s17102371

Breiman, L. (2001). Random forests. *Machine learning*, *45*(1), 5-32.

Brokaw, N. V. L. (1982). THE DEFINITION OF TREEFALL GAP AND ITS EFFECT ON MEASURES OF FOREST DYNAMICS. *Biotropica*, *14*(2), 158-160. https://doi.org/10.2307/2387750

Cisneros Vaca, C., van der Tol, C., & Ghimire, C. P. (2018, Jul). The influence of long-term changes in canopy structure on rainfall interception loss: a case study in Speulderbos, the Netherlands. *Hydrology and Earth System Sciences*, *22*(7), 3701-3719. https://doi.org/10.5194/hess-22-3701-2018

da Cruz, D. C., Benayas, J. M. R., Ferreira, G. C., Santos, S. R., & Schwartz, G. (2021, Jan). An overview of forest loss and restoration in the Brazilian Amazon. *New Forests*, *52*(1), 1-16. https://doi.org/10.1007/s11056-020-09777-3

de Lima, R. A. F. (2005, Aug). Gap size measurement: The proposal of a new field method. *Forest Ecology and Management*, *214*(1-3), 413-419. https://doi.org/10.1016/j.foreco.2005.04.011

Demetriou, D., Stillwell, J., & See, L. (2013, May). A new methodology for measuring land fragmentation. *Computers Environment and Urban Systems*, *39*, 71-80. https://doi.org/10.1016/j.compenvurbsys.2013.02.001

Dobler, W., Steinbacher, F., Baran, R., & Aufleger, M. (2014). High Resolution Bathymetric Lidar Data to Hydraulic-Modelling a Mountain Stream by Bathymetric Lidar Data. https://doi.org/10.13140/2.1.4909.9529

Dorman, M. (2023). *nngeo: k-Nearest Neighbour Join for Spatial Data.* In https://github.com/michaeldorman/nngeo/

Du, Z. H., Zheng, G., Shen, G. C., & Moskal, L. M. (2021, Dec). Characterizing spatiotemporal variations of forest canopy gaps using aerial laser scanning data. *International Journal of Applied Earth Observation and Geoinformation*, *104*, Article 102588. https://doi.org/10.1016/j.jag.2021.102588

Dunn, O. J. (1964). MULTIPLE COMPARISONS USING RANK SUMS. *Technometrics*, *6*(3), 241-&. https://doi.org/10.2307/1266041

Feldmann, E., Drossler, L., Hauck, M., Kucbel, S., Pichler, V., & Leuschner, C. (2018, May). Canopy gap dynamics and tree understory release in a virgin beech forest, Slovakian Carpathians. *Forest Ecology and Management*, *415*, 38-46. https://doi.org/10.1016/j.foreco.2018.02.022

Franklin, W. R. (1973). Triangulated irregular network program. ftp://ftp.cs.rpi.edu/pub/franklin/tin73.tar.gz.

Frolking, S., Palace, M. W., Clark, D., Chambers, J. Q., Shugart, H., & Hurtt, G. C. (2009). Forest disturbance and recovery: A general review in the context of spaceborne remote sensing of impacts on aboveground biomass and canopy structure. *Journal of Geophysical Research: Biogeosciences*, *114*(G2). https://doi.org/10.1029/2008JG000911

Fujii, K., Funakawa, S., Hayakawa, C., & Kosaki, T. (2021, Oct). Effects of clearcutting and girdling on soil respiration and fluxes of dissolved organic carbon and nitrogen in a Japanese cedar plantation. *Forest Ecology and Management, 498*, Article 119520. https://doi.org/10.1016/j.foreco.2021.119520

Gaulton, R., & Malthus, T. J. (2010). LiDAR mapping of canopy gaps in continuous cover forests: A comparison of canopy height model and point cloud based techniques. *International Journal of Remote Sensing, 31*(5), 1193-1211. https://doi.org/10.1080/01431160903380565

Gini, C. (1921). Measurement of inequality of incomes. *The economic journal, 31*(121), 124-125.

Haddad, N. M., Brudvig, L. A., Clobert, J., Davies, K. F., Gonzalez, A., Holt, R. D., Lovejoy, T. E., Sexton, J. O., Austin, M. P., Collins, C. D., Cook, W. M., Damschen, E. I., Ewers, R. M., Foster, B. L., Jenkins, C. N., King, A. J., Laurance, W. F., Levey, D. J., Margules, C. R., Melbourne, B. A., Nicholls, A. O., Orrock, J. L., Song, D. X., & Townshend, J. R. (2015, Mar). Habitat fragmentation and its lasting impact on Earth's ecosystems. *Science Advances, 1*(2), Article e1500052. https://doi.org/10.1126/sciadv.1500052

Hasan, S. S., Zhang, Y., Chu, X., & Teng, Y. (2019). The role of big data in China's sustainable forest management. *Forestry Economics Review, 1*(1), 96-105. https://doi.org/10.1108/FER-04-2019-0013

Hijmans, R. J., Bivand, R., Forner, K., Ooms, J., Pebesma, E., & Sumner, M. D. (2023). *terra: Spatial Data Analysis.* In (Version 1.7-18) https://CRAN.R-project.org/package=terra

Huertas, C., Sabatier, D., Derroire, G., Ferry, B., Jackson, T. D., Pelissier, R., & Vincent, G. (2022, May). Mapping tree mortality rate in a tropical moist forest using multi-temporal LiDAR. *International Journal of Applied Earth Observation and Geoinformation, 109*, Article 102780. https://doi.org/10.1016/j.jag.2022.102780

Hunter, M. O., Keller, M., Morton, D., Cook, B., Lefsky, M., Ducey, M., Saleska, S., de Oliveira, R. C., & Schietti, J. (2015, Jul). Structural Dynamics of Tropical Moist Forest Gaps. *Plos One, 10*(7), Article e0132144. https://doi.org/10.1371/journal.pone.0132144

Jansen, H., Oosterbaan, A., Mohren, G., Goudzwaard, L., den Ouden, J., Schoonderwoerd, H., Thomassen, E., Schmidt, P., & Copini, P. (2018). *Opbrengsttabellen Nederland 2018*. Wageningen Academic Publishers. https://doi.org/10.3920/978-90-8686-876-6

Johann, E. (2006). Historical development of nature-based forestry in Central Europe. *Nature-based forestry in Central Europe. Alternatives to industrial forestry and strict preservation. Biotechnical Faculty, Department of Forestry and Renewable Forest Resources, Ljubljana, Slovenia*, 1-17.

Knevels, R., Brenning, A., Gingrich, S., Gruber, E., Lechner, T., Leopold, P., Petschko, H., & Plutzar, C. (2020). CULTURAL LANDSCAPE CHANGE: AN INDICATOR-BASED RETROSPECT INTO THE 19TH CENTURY. CASE STUDY OF THE MUNICIPALITIES WAIDHOFEN/YBBS AND PALDAU. *Mitteilungen Der Osterreichischen Geographischen Gesellschaft, 162*, 255-285. https://doi.org/10.1553/moegg162s255

Koukoulas, S., & Blackburn, G. A. (2004, Aug). Quantifying the spatial properties of forest canopy gaps using LiDAR imagery and GIS. *International Journal of Remote Sensing, 25*(15), 3049-3071. https://doi.org/10.1080/01431160310001657786

Kruskal, W. H., & Wallis, W. A. (1952). Use of ranks in one-criterion variance analysis. *Journal of the American statistical Association, 47*(260), 583-621. https://doi.org/10.1080/01621459.1952.10483441

Kuhn, M. (2008, Nov). Building Predictive Models in R Using the caret Package. *Journal of Statistical Software, 28*(5), 1-26. https://doi.org/10.18637/jss.v028.i05

Leiterer, R., Furrer, R., Schaepman, M. E., & Morsdorf, F. (2015, Dec). Forest canopy-structure characterization: A data-driven approach. *Forest Ecology and Management, 358*, 48-61. https://doi.org/10.1016/j.foreco.2015.09.003

Leitold, V., Morton, D. C., Longo, M., dos-Santos, M. N., Keller, M., & Scaranello, M. (2018, Aug). El Nino drought increased canopy turnover in Amazon forests. *New Phytologist, 219*(3), 959-971. https://doi.org/10.1111/nph.15110

Li, C. Y., Weiss, D., & Goldschmidt, E. E. (2003, Jul). Girdling affects carbohydrate-related gene expression in leaves, bark and roots of alternate-bearing citrus trees. *Annals of Botany, 92*(1), 137-143. https://doi.org/10.1093/aob/mcg108

Liang, X., Hyyppä, J., & Matikainen, L. (2007). Deciduous-coniferous tree classification using difference between first and last pulse laser signatures. *International Archives of Photogrammetry, Remote Sensing and Spatial Information Sciences, 36*(3/W52).

Lim, K., Treitz, P., Wulder, M., St-Onge, B., & Flood, M. (2003, Mar). LiDAR remote sensing of forest structure. *Progress in Physical Geography-Earth and Environment, 27*(1), 88-106. https://doi.org/10.1191/0309133303pp360ra

Lombard, L., Ismail, R., & Poona, N. (2019, Jan). Modelling forest canopy gaps using LiDAR-derived variables. *Geocarto International, 34*(2), 179-193. https://doi.org/10.1080/10106049.2017.1377775

Mao, X. G., Liang, Z., & Fan, W. Y. (2020, Mar). Object-Oriented Automatic Identification of Forest Gaps Using Digital Orthophoto Maps and LiDAR Data. *Canadian Journal of Remote Sensing, 46*(2), 177-192. https://doi.org/10.1080/07038992.2020.1768515

McCarthy, J. (2001). Gap dynamics of forest trees: a review with particular attention to boreal forests. *Environmental reviews, 9*(1), 1-59. https://doi.org/10-1139/enrev-9-1-1

Meijer, M., Rip, F., van Benthem, R., Clement, J., & van der Sande, C. (2015). *Boomkronen afleiden uit het Actueel Hoogtebestand Nederland* (2671). https://library.wur.nl/WebQuery/wurpubs/fulltext/362099

Muscolo, A., Bagnato, S., Sidari, M., & Mercurio, R. (2014, Dec). A review of the roles of forest canopy gaps. *Journal of Forestry Research, 25*(4), 725-736. https://doi.org/10.1007/s11676-014-0521-7

Naaf, T., & Wulf, M. (2007, Jun). Effects of gap size, light and herbivory on the herb layer vegetation in European beech forest gaps. *Forest Ecology and Management, 244*(1-3), 141-149. https://doi.org/10.1016/j.foreco.2007.04.020

Nolet, C., & Spliethof, N. (2020). *Bepaling van lokaal biomassapotentieel met de puntenwolk van het Actueel Hoogtebestand Nederland 3* (221). https://www.futurewater.nl/wp-content/uploads/2021/04/Biomassapotentieel_Puntenwolk_AHN3_Final.pdf

Ogle D.H., Doll J.C., Wheeler A.P., & A., D. (2023). *FSA: Simple Fisheries Stock Assessment Methods.* In https://CRAN.R-project.org/package=FSA

Ottaviani, G., Gotzenberger, L., Bacaro, G., Chiarucci, A., de Bello, F., & Marcantonio, M. (2019, Jul). A multifaceted approach for beech forest conservation: Environmental drivers of understory plant diversity. *Flora, 256*, 85-91. https://doi.org/10.1016/j.flora.2019.05.006

Patil, I. (2021). Visualizations with statistical details: The'ggstatsplot'approach. *Journal of Open Source Software, 6*(61), 3167. https://doi.org/10.21105/joss.03167

Patton, D. R. (1975). A diversity index for quantifying habitat" edge". *Wildlife Society Bulletin (1973-2006), 3*(4), 171-173. https://www.jstor.org/stable/3781151

Pearson, S. G., Elias, E. P. L., van Prooijen, B. C., van der Vegt, H., van der Spek, A. J. F., & Wang, Z. B. (2022, May). A novel approach to mapping ebb-tidal delta morphodynamics and stratigraphy. *Geomorphology, 405*, Article 108185. https://doi.org/10.1016/j.geomorph.2022.108185

Pebesma, E. (2018). Simple Features for R: Standardized Support for Spatial Vector Data. *The R Journal, 10*(1), 439-446. https://doi.org/10.32614/RJ-2018-009

QGIS Development Team. (2023). *QGIS Geographic Information System.* In Open Source Geospatial Foundation. http://qgis.org

R Core Team. (2023). *R: A language and environment for statistical computing.* In R Foundation for Statistical Computing. https://www.R-project.org/.

Reitberger, J., Krzystek, P., & Stilla, U. (2008). Analysis of full waveform LIDAR data for the classification of deciduous and coniferous trees. *International Journal of Remote Sensing, 29*(5), 1407-1431. https://doi.org/10.1080/01431160701736448

Ripple, W. J., Newsome, T. M., Wolf, C., Dirzo, R., Everatt, K. T., Galetti, M., Hayward, M. W., Kerley, G. I. H., Levi, T., Lindsey, P. A., Macdonald, D. W., Malhi, Y., Painter, L. E., Sandom, C. J., Terborgh, J., & Van Valkenburgh, B. (2015, May). Collapse of the world's largest herbivores. *Science Advances, 1*(4), Article e1400103. https://doi.org/10.1126/sciadv.1400103

Rosenvald, R., & Lohmus, A. (2008, Feb). For what, when, and where is green-tree retention better than clear-cutting? A review of the biodiversity aspects. *Forest Ecology and Management, 255*(1), 1-15. https://doi.org/10.1016/j.foreco.2007.09.016

Roussel, J. R., Auty, D., Coops, N. C., Tompalski, P., Goodbody, T. R. H., Meador, A. S., Bourdon, J. F., de Boissieu, F., & Achim, A. (2020, Dec). lidR: An R package for analysis of Airborne Laser Scanning (ALS) data. *Remote Sensing of Environment, 251*, Article 112061. https://doi.org/10.1016/j.rse.2020.112061

Runkle, J. R. (1981). Gap regeneration in some old-growth forests of the eastern United States. *Ecology, 62*(4), 1041-1051. https://www.jstor.org/stable/1937003

Ryan, C. M., & Williams, M. (2011). How does fire intensity and frequency affect miombo woodland tree populations and biomass? *Ecological Applications, 21*(1), 48-60. https://doi.org/10.1890/09-1489.1

Seidel, D., Ammer, C., & Puettmann, K. (2015, Nov). Describing forest canopy gaps efficiently, accurately, and objectively: New prospects through the use of terrestrial laser scanning. *Agricultural and Forest Meteorology, 213*, 23-32. https://doi.org/10.1016/j.agrformet.2015.06.006

Senecal, J. F., Doyon, F., & Messier, C. (2018, Feb). Management implications of varying gap detection height thresholds and other canopy dynamics processes in temperate deciduous forests. *Forest Ecology and Management, 410*, 84-94. https://doi.org/10.1016/j.foreco.2017.12.029

Shepard, D. (1968). *Proceedings of the 1968 23rd ACM National conference*

Silva, C. A., Valbuena, R., Pinage, E. R., Mohan, M., de Almeida, D. R. A., North, E., Jaafar, W., Papa, D. D. M., Cardil, A., & Klauberg, C. (2019, Aug). ForestGapR: An r Package for forest gap analysis from canopy height models. *Methods in Ecology and Evolution, 10*(8), 1347-1356. https://doi.org/10.1111/2041-210x.13211

Spies, T. A. (1998). Forest structure: A key to the ecosystem. *Northwest Science, 72*, 34-39. https://andrewsforest.oregonstate.edu/sites/default/files/lter/pubs/pdf/pub2564.pdf

St-Onge, B., Vepakomma, U., Sénécal, J.-F., Kneeshaw, D., & Doyon, F. (2014). Canopy gap detection and analysis with airborne laser scanning. In *Forestry Applications of Airborne Laser Scanning* (pp. 419-437). Springer, Dordrecht.

Steeneveld, G. J., Koopmans, S., Heusinkveld, B. G., van Hove, L. W. A., & Holtslag, A. A. M. (2011, Oct). Quantifying urban heat island effects and human comfort for cities of variable size and urban morphology in the Netherlands. *Journal of Geophysical Research-Atmospheres, 116*, Article D20129. https://doi.org/10.1029/2011jd015988

Subedi, V., Bhatta, K., Poudel, I., & Bhattarai, P. (2018). Application of silvicultural system, yield regulation and thinning practices in natural forests: Case study from western Terai. *Banko Janakari*, 92-97. https://doi.org/10.3126/banko.v27i3.20553

Swart, L. (2010). How the Up-to-date Height Model of the Netherlands (AHN) became a massive point data cloud. *NCG KNAW, 17*, 17-32. https://www.ncgeo.nl/downloads/49ncggroenpointclouds_03.pdf

Thiollay, J. M. (1992, Mar). INFLUENCE OF SELECTIVE LOGGING ON BIRD SPECIES-DIVERSITY IN A GUIANAN RAIN-FOREST. *Conservation Biology, 6*(1), 47-63. https://doi.org/10.1046/j.1523-1739.1992.610047.x

Valbuena, R., Maltamo, M., Mehtatalo, L., & Packalen, P. (2017, Jun). Key structural features of Boreal forests may be detected directly using L-moments from airborne lidar data. *Remote Sensing of Environment, 194*, 437-446. https://doi.org/10.1016/j.rse.2016.10.024

van der Sande, C., Soudarissanane, S., & Khoshelham, K. (2010, Sep). Assessment of Relative Accuracy of AHN-2 Laser Scanning Data Using Planar Features. *Sensors, 10*(9), 8198-8214. https://doi.org/10.3390/s100908198

Van Rossum, G. a. D., Fred L. (2009). *Python 3 Reference Manual.* In CreateSpace.

Vehmas, M., Packalen, P., Maltamo, M., & Eerikainen, K. (2011, Jun). Using airborne laser scanning data for detecting canopy gaps and their understory type in mature boreal forest. *Annals of Forest Science, 68*(4), 825-835. https://doi.org/10.1007/s13595-011-0079-x

Vepakomma, U., Kneeshaw, D., & Fortin, M. J. (2012, Sep). Spatial contiguity and continuity of canopy gaps in mixed wood boreal forests: persistence, expansion, shrinkage and displacement. *Journal of Ecology, 100*(5), 1257-1268. https://doi.org/10.1111/j.1365-2745.2012.01996.x

Vepakomma, U., St-Onge, B., & Kneeshaw, D. (2008, May). Spatially explicit characterization of boreal forest gap dynamics using multi-temporal lidar data. *Remote Sensing of Environment, 112*(5), 2326-2340. https://doi.org/10.1016/j.rse.2007.10.001

Weis, W., Rotter, V., & Gottlein, A. (2006, Apr). Water and element fluxes during the regeneration of Norway spruce with European beech: Effects of shelterwood-cut and clear-cut. *Forest Ecology and Management, 224*(3), 304-317. https://doi.org/10.1016/j.foreco.2005.12.040

White, J. C., Tompalski, P., Coops, N. C., & Wulder, M. A. (2018, Apr). Comparison of airborne laser scanning and digital stereo imagery for characterizing forest canopy gaps in coastal temperate rainforests. *Remote Sensing of Environment, 208*, 1-14. https://doi.org/10.1016/j.rse.2018.02.002

Wickham, H., Averick, M., Bryan, J., Chang, W., McGowan, L. D., François, R., Grolemund, G., Hayes, A., Henry, L., Hester, J., Kuhn, M., Pedersen, T. L., Miller, E., Bache, S. M., Müller, K., Ooms, J., Robinson, D., Seidel, D. P., Spinu, V., Takahashi, K., Vaughan, D., Wilke, C., Woo, K., & Yutani, H. (2019). Welcome to the Tidyverse. *Journal of Open Source Software, 4*(43). https://doi.org/10.21105/joss.01686

Wilkinson, M., Crow, P., Eaton, E. L., & Morison, J. I. L. (2016). Effects of management thinning on CO2 exchange by a plantation oak woodland in south-eastern England. *Biogeosciences, 13*(8), 2367-2378. https://doi.org/10.5194/bg-13-2367-2016

Zielewska-Buttner, K., Adler, P., Ehmann, M., & Braunisch, V. (2016, Mar). Automated Detection of Forest Gaps in Spruce Dominated Stands Using Canopy Height Models Derived from Stereo Aerial Imagery. *Remote Sensing, 8*(3), Article 175. https://doi.org/10.3390/rs8030175

Appendices

Appendix A: Relationship between tree height and diameter (A1), relationship between tree height and age (A2), and information per tree species (A3).

A1

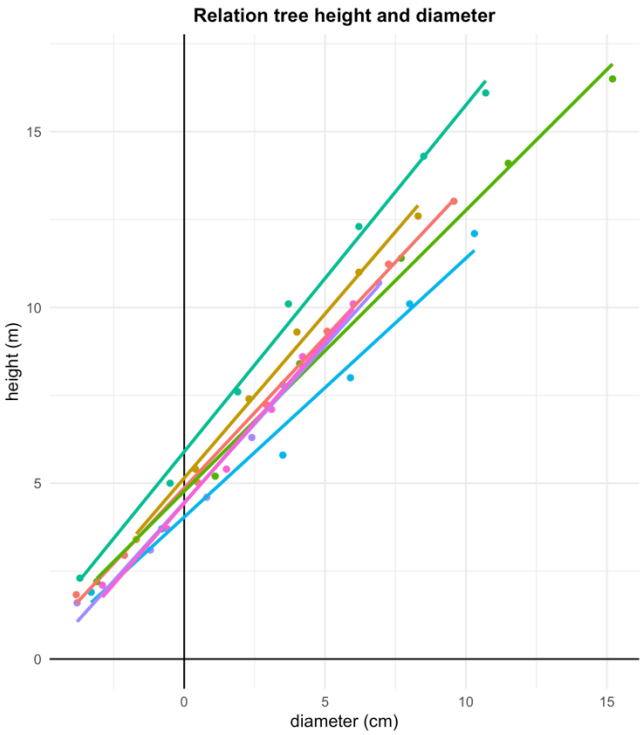

A2

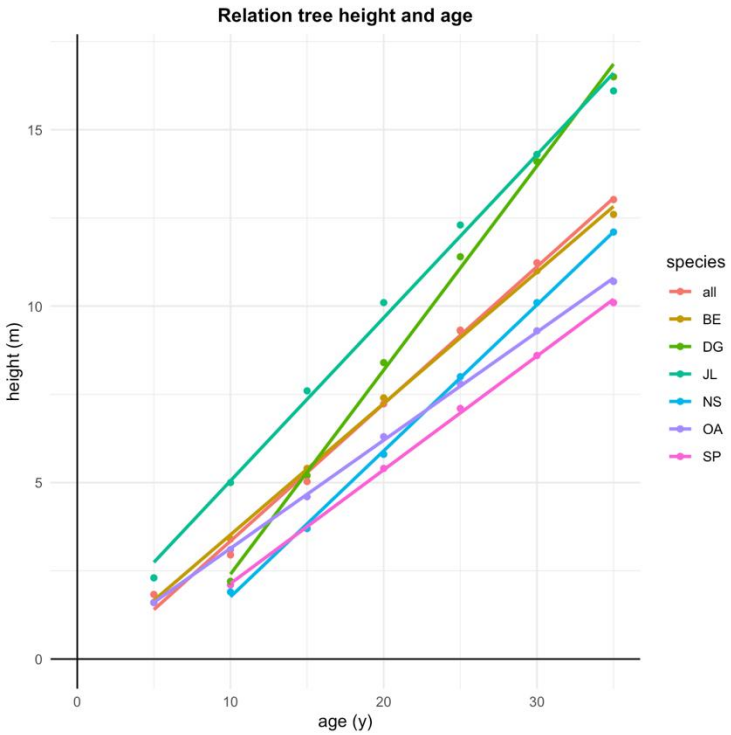

A3

Tree species	*Beech*	*Oak*	*Scotch pine*	*Japanese larch*	*Douglas fir*	*Norway spruce*	*Overall*
Tree height at DBH of 5 cm (m)	5.15	4.45	4.43	5.90	4.77	4.04	4.86
Tree height growth per year (m)	0.37	0.31	0.32	0.46	0.58	0.41	0.39
Tree height growth per 3 years (m)	1.12	0.92	0.97	1.39	1.73	1.24	1.17

The maximum vegetation height threshold was based on the tree height at a DBH of 5 cm. This height was determined by taking the intercept of the linear relationship between tree height and DBH. The DBH was first subtracted by 5 so that the intercept would be equal to the tree height at a DBH of 5 cm. The difference between lateral and vertical canopy gap closure was based on the maximal tree growth in three years. The yearly height growth was determined by taking the slope of the linear relationship between tree height and age.

Appendix B: Map of forest plots and new canopy gaps visited for validation in the study area.

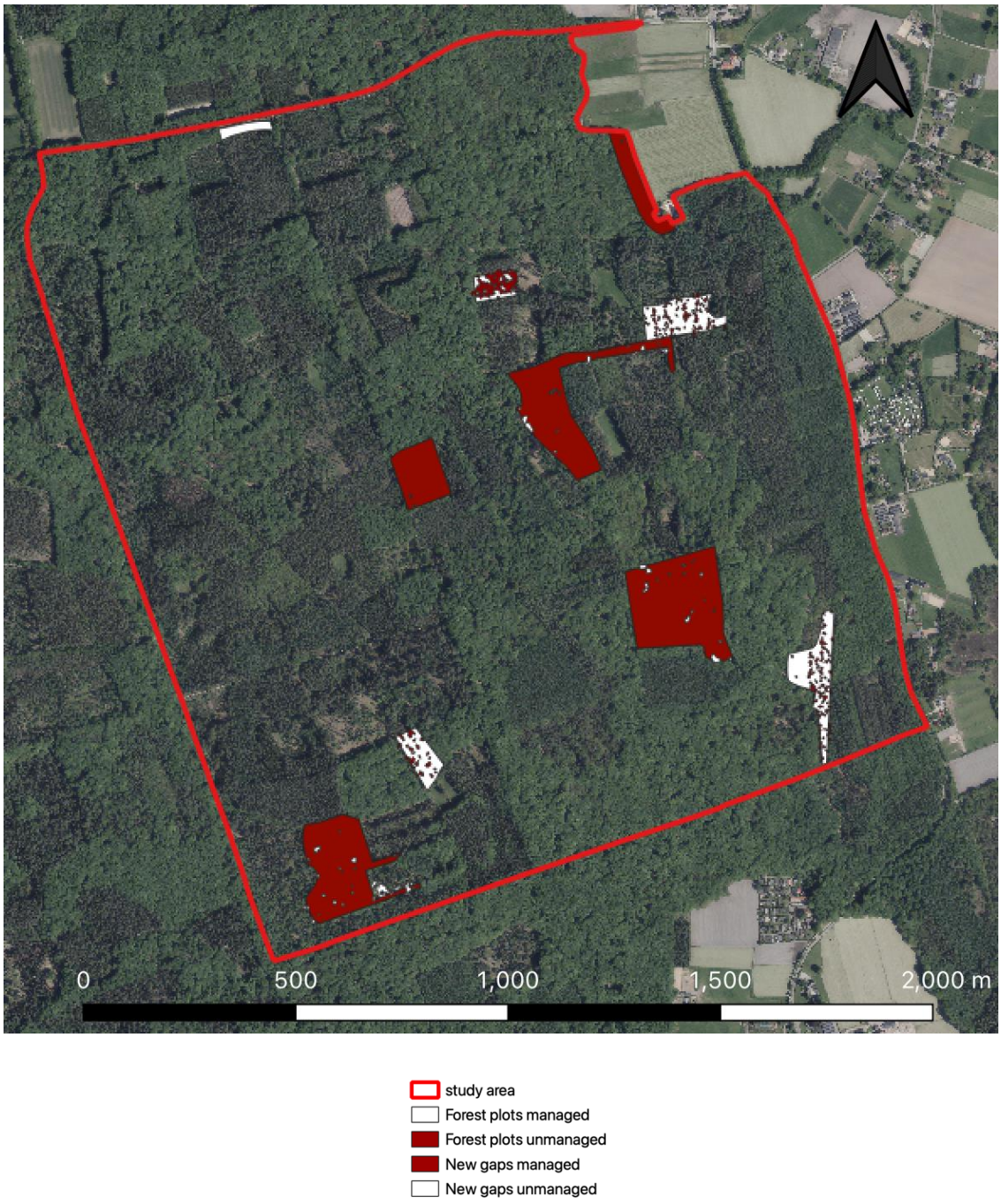

The location of ten randomly selected forest plots, five managed and five (pseudo-)unmanaged, and the location of identified new canopy gaps that intersect with these forest plots are shown in this map. The basemap is a 8 cm resolution areal orthophoto of the study area from the year 2021 provided by PDOK. Due to colour differences between different tree species, contours of different forest plots in the study area can be observed in this orthophoto. For the location of the study area in the Netherlands, see Figure 1.

Appendix C: Function sheet of attributes added to the new canopy gap and their sources. Function 1-11 were used to determine the 2D shape characteristics of the gaps. Function 12 – 15 were used to determine canopy gap characteristics of the forest plots

Number	*Function*	*Source*
1	$Gap\ Shape\ Complexity\ Index\ (GSCI) = \frac{perimeter}{2 * \sqrt{area * \pi}}$	Bonnet et al. (2015); Patton (1975)
2	$Circularity = \frac{perimeter^2}{area}$	Bonhomme et al. (2014)
3	$Roundness = \frac{perimeter^2}{4\pi\ * area}$	http://www.empix.com/ NE%20HELP/functions/ glossary/ morphometric_param.htm
4	$Shape\ Index\ (SI) = \frac{4\pi\ * area}{perimeter^2}$	Demetriou et al. (2013)
5	$Fractional\ Dimension\ (FD) = \frac{2 * \ln perimeter}{\ln area}$	Demetriou et al. (2013)
6	$Areal\ Form\ Factor\ (AFF) = \frac{area}{perimeter^2}$	Demetriou et al. (2013)
7	$Interior\ to\ Edge\ Ratio\ (IER) = \frac{perimeter}{area}$	Blackburn and Milton (1996)
8	$Solidity = \frac{area}{area\ convex\ hull}$	Bonhomme et al. (2014)
9	$Convexity = \frac{perimeter\ convex\ hull}{perimeter}$	Bonhomme et al. (2014)
10	$Equivalent\ Circular\ Diameter\ (ECD) = 2 * \sqrt{\frac{area}{\pi}}$	http://www.empix.com/ NE%20HELP/functions/ glossary/ morphometric_param.htm
11	$Euivalent\ Spherical\ Volume\ (ESV) = \frac{4}{3}\ *\ \pi\ * \sqrt{\frac{area}{\pi}^3}$	http://www.empix.com/ NE%20HELP/functions/ glossary/ morphometric_param.htm
12	$Percentage\ In\ Gap\ (PIG) = \frac{\sum area\ new\ gaps\ in\ plot}{area\ plot} * 100$	Blackburn and Milton (1996)
13	$Gap\ Density\ (GD) = \frac{number\ new\ gaps\ in\ plot}{area\ plot} * 100$	Blackburn and Milton (1996)
14	$Dispersion\ Index(DI) = 2 * \sqrt{GD} * \frac{\mu\ nearest\ neighbour\ distance\ new\ gaps\ in\ plot}{10}$	Blackburn and Milton (1996)
15	$Canopy\ Edge\ (CE) = \frac{\sum perimeter\ new\ gaps\ in\ plot}{\sum area\ new\ gaps\ in\ plot} * 100$	Blackburn and Milton (1996)

Appendix D: variable importance of the 5 RF models. For model 2 and 4, the difference between the classes per important variable is shown.

D1: “number of trees” model with all variables included

variable	*importance*
shape_AHN3_planarity	127.948198
shape_AHN3_linearity	98.3953374
ForestPlot_fraq_NGLM	77.9449865
ForestPlot_GD	51.5250249
shape_AHN3_eigen_medium	40.5939026
ForestPlot_PIG	36.3068979
ipcumzq90_AHN3	25.0343279
ipcumzq70_AHN3	20.234873
shape_IER	16.9803963
shape_FD	14.3488342
shape_AFF	12.6700546
shape_roundness	11.3660621
shape_GSCI	10.692241
shape_circularity	8.72628288
shape_SI	8.71340607
n_AHN3	7.73742527
Buffer5m_ipcumzq70_AHN4	7.03703061
shape_solidity	6.57620625
shape_convexity	6.3862045
itot_AHN3	6.31906003
zq45_AHN3	5.85037072
Buffer10m_area_AHN3	5.28643964
pzabove2_AHN3	5.27180717
shape_ESV	4.84058941
Buffer5m_area_AHN3	4.67250968
area_AHN3	4.50790004
zq40_AHN3	4.41349829
shape_ECD	4.23391063
shape_area	4.05181388
shape_AHN3_eigen_smallest	3.93134472
Buffer10m_zpcum9_AHN3	3.91654528
Buffer5m_area_AHN4	3.91220745
itot_AHN4	3.73880487
Buffer5m_itot_AHN4	3.45457418
ForestPlot_mean_CHM4	3.43209419
Buffer10m_area_AHN4	3.3465539
gini_CHM3	3.21498333
zq20_AHN3	3.03271761
pground_AHN3	3.02346436
zq50_AHN3	2.93040263
Buffer10m_ipcumzq30_AHN4	2.92089571
buffer10m_overlap_relative	2.91901108
zpcum1_AHN3	2.85658736
zpcum8_AHN3	2.82068396
ForestPlot_gini_CHM3	2.66333272

Buffer5m_n_AHN3	2.60212854
p2th_AHN3	2.52085907
shape_AHN3_sphericity	2.50899028
ForestPlot_gini_CHM4	2.48375264
ForestPlot_fraq_NoG	2.48021766
area_AHN4	2.47871828
Buffer5m_zpcum9_AHN3	2.4566476
Buffer10m_ipcumzq90_AHN4	2.43257094
ipground_AHN3	2.39785353
Buffer10m_ipcumzq70_AHN4	2.36238456
ForestPlot_mean_CHM3	2.36087724
Buffer10m_ipcumzq10_AHN4	2.35718198
zpcum7_AHN3	2.34667201
shape_AHN3_curvature	2.34291652
zskew_AHN3	2.33821482
shape_AHN4_eigen_smallest	2.32598327
Buffer10m_imean_AHN3	2.30908989
Buffer5m_ipcumzq90_AHN3	2.28096124
Buffer5m_p4th_AHN4	2.27335009
Buffer10m_ipcumzq90_AHN3	2.25431884
Buffer10m_n_AHN3	2.20643416
shape_AHN3_anisotropy	2.18508661
pzabovezmean_AHN3	2.17966568
zq15_AHN3	2.17942794
zq35_AHN3	2.15678782
Buffer5m_zpcum9_AHN4	2.12507823
Buffer5m_p3th_AHN4	2.09304326
zpcum6_AHN3	2.06046171
ipcumzq30_AHN4	2.03812982
zq25_AHN3	2.03095982
Buffer5m_p5th_AHN4	2.01399802
shape_perimeter	1.99668512
shape_AHN3_horizontality	1.9901801
ForestPlot_fraq_DG	1.97923698
Buffer5m_n_AHN4	1.94377163
Buffer10m_p5th_AHN4	1.92623003
ipcumzq10_AHN4	1.92092183
sd_CHM3	1.89254521
Buffer10m_zpcum9_AHN4	1.87595549
iskew_AHN3	1.87193167
zpcum9_AHN3	1.86731481
Buffer5m_imean_AHN4	1.85807522
p5th_AHN4	1.84465799
Buffer10m_p4th_AHN4	1.84185362
ForestPlot_max_CHM3	1.81389678
ipcumzq50_AHN3	1.7950297
Buffer10m_p5th_AHN3	1.78159564
imax_AHN4	1.77395396
ForestPlot_fraq_NGBM	1.75235737
Buffer5m_p1th_AHN4	1.75077535

Buffer5m_imean_AHN3	1.74662439
shape_AHN4_eigen_medium	1.72884107
Buffer5m_ipcumzq90_AHN4	1.72142041
ipcumzq10_AHN3	1.70680402
ForestPlot_max_CHM4	1.69589384
Buffer5m_p2th_AHN3	1.69549791
ForestPlot_fraq_VC	1.69515379
mean_CHMdiv	1.68749069
Buffer5m_zpcum7_AHN4	1.66460073
Buffer10m_itot_AHN3	1.64081887
Buffer10m_ipcumzq50_AHN4	1.62320427
Buffer5m_itot_AHN3	1.61141122
zq55_AHN3	1.60920381
Buffer10m_zpcum8_AHN4	1.5935395
Buffer10m_zpcum8_AHN3	1.58610794
max_CHMdiv	1.5855236
ForestPlot_range_CHM3	1.57344468
Buffer10m_p3th_AHN4	1.55759085
isd_AHN3	1.55453053
n_AHN4	1.55138316
Buffer5m_zpcum8_AHN3	1.55101128
zq75_AHN3	1.5288247
min_CHM4	1.50299323
zq65_AHN3	1.48757924
shape_AHN4_anisotropy	1.48696417
ForestPlot_range_CHM4	1.47543652
shape_AHN4_linearity	1.47372079
ForestPlot_DI	1.46572158
ForestPlot_CE	1.45130619
ikurt_AHN4	1.44260855
shape_AHN4_sphericity	1.43725761
shape_AHN4_curvature	1.42405572
Buffer10m_zq95_AHN3	1.42209684
Buffer10m_zsd_AHN3	1.41923532
Buffer5m_zsd_AHN3	1.38222795
ForestPlot_max_CHMdiv	1.38093118
Buffer10m_itot_AHN4	1.37306062
ForestPlot_sd_CHM4	1.36364182
Buffer5m_ipcumzq70_AHN3	1.35957848
min_CHM3	1.35086621
dist_nn	1.34541783
ikurt_AHN3	1.34097812
Buffer5m_ipcumzq10_AHN4	1.33715171
shape_AHN4_planarity	1.326976
Buffer5m_ipcumzq50_AHN3	1.32120925
Buffer10m_p2th_AHN3	1.31201441
imax_AHN3	1.29908301
isd_AHN4	1.28980522
Buffer5m_ikurt_AHN4	1.2876984
Buffer10m_n_AHN4	1.26554315

ipcumzq90_AHN4	1.26364899
zpcum2_AHN3	1.26322896
ipcumzq50_AHN4	1.25244235
Buffer10m_imax_AHN4	1.2508898
range_CHM3	1.2327257
imean_AHN4	1.23072552
Buffer5m_ipcumzq30_AHN4	1.22359198
ipcumzq30_AHN3	1.22180428
ForestPlot_min_CHMdiv	1.21320245
Buffer10m_isd_AHN3	1.21099952
p3th_AHN3	1.20717653
zq60_AHN3	1.20472558
zpcum9_AHN4	1.20089878
Buffer10m_zmax_AHN3	1.20013643
Buffer5m_isd_AHN3	1.18613402
gini_CHM4	1.18275299
Buffer10m_iskew_AHN4	1.18124619
ForestPlot_fraq_RG	1.16684223
p4th_AHN4	1.16222592
zq70_AHN3	1.1539547
p1th_AHN4	1.14209484
Buffer10m_zq5_AHN4	1.13659843
Buffer5m_imax_AHN4	1.13547047
shape_AHN4_horizontality	1.13282878
ForestPlot_sd_CHMdiv	1.12967636
zq30_AHN3	1.12159594
Buffer5m_iskew_AHN4	1.12128873
zq10_AHN3	1.11603369
Buffer10m_zpcum7_AHN4	1.10926798
Buffer5m_zpcum6_AHN4	1.10276673
Buffer10m_ipcumzq10_AHN3	1.10199334
Buffer10m_zkurt_AHN3	1.09612631
imean_AHN3	1.0939305
Buffer10m_zmax_AHN4	1.09369326
ForestPlot_range_CHMdiv	1.08229892
Buffer5m_iskew_AHN3	1.07568753
p2th_AHN4	1.0756579
Buffer10m_zpcum7_AHN3	1.06696949
Buffer10m_p1th_AHN4	1.05714956
ipcumzq70_AHN4	1.05609485
Buffer10m_imean_AHN4	1.04358534
Buffer10m_isd_AHN4	1.04258785
Buffer10m_zkurt_AHN4	1.0388525
shape_AHN3_eigen_largest	1.03703002
Buffer5m_zpcum1_AHN4	1.02473451
Buffer5m_p3th_AHN3	1.02236741
Buffer5m_isd_AHN4	1.01650969
Buffer5m_ipcumzq30_AHN3	1.01354264
Buffer5m_zskew_AHN4	1.01333626
zpcum3_AHN3	1.00587353

mean_CHM4	1.00309574
zpcum5_AHN3	1.00308048
Buffer5m_zpcum8_AHN4	0.97643345
zq80_AHN3	0.97181266
Buffer5m_imax_AHN3	0.96870352
Buffer5m_zpcum1_AHN3	0.95161365
Buffer5m_zq5_AHN4	0.94607547
Buffer5m_zpcum2_AHN4	0.94420648
zsd_AHN3	0.94306775
iskew_AHN4	0.9421904
Buffer10m_zq85_AHN3	0.94100351
Buffer5m_ipcumzq50_AHN4	0.94054832
fraq_NGBM	0.9387121
zq90_AHN3	0.93732285
p1th_AHN3	0.93380946
Buffer10m_p2th_AHN4	0.93152068
Buffer5m_zpcum7_AHN3	0.93113963
Buffer5m_pzabovezmean_AHN3	0.92776364
zq5_AHN4	0.92514609
p3th_AHN4	0.92413703
zq10_AHN4	0.92180201
ForestPlot_gini_CHMdiv	0.91582612
buffer5m_overlap_relative	0.90462387
p5th_AHN3	0.89486006
Buffer10m_zpcum6_AHN4	0.88589476
ForestPlot_mean_CHMdiv	0.87775405
Buffer5m_ipcumzq10_AHN3	0.87356047
gini_CHMdiv	0.87216838
fraq_NGLM	0.86829543
zmean_AHN3	0.85881785
Buffer5m_zpcum4_AHN4	0.85034799
zq15_AHN4	0.84692001
Buffer10m_ipcumzq30_AHN3	0.84282691
zkurt_AHN3	0.83848154
zq5_AHN3	0.83670941
zpcum4_AHN3	0.82785395
Buffer5m_zpcum5_AHN4	0.8253135
Buffer5m_zkurt_AHN4	0.81785514
ipground_AHN4	0.81340488
zq85_AHN3	0.81241653
Buffer10m_imax_AHN3	0.810855
Buffer10m_p4th_AHN3	0.80822247
Buffer10m_p1th_AHN3	0.806413
Buffer5m_zpcum6_AHN3	0.80098713
Buffer10m_zpcum4_AHN3	0.80082524
Buffer5m_zkurt_AHN3	0.79551489
Buffer5m_zmax_AHN3	0.79349774
Buffer10m_ikurt_AHN4	0.78797621
Buffer5m_zq20_AHN3	0.786856
ForestPlot_sd_CHM3	0.78087838

Buffer5m_pzabove2_AHN4	0.77861807
Buffer10m_zq90_AHN3	0.77678813
mean_CHM3	0.77530626
Buffer10m_zq80_AHN3	0.76905192
Buffer10m_ikurt_AHN3	0.76785408
Buffer5m_ipground_AHN4	0.76695945
ForestPlot_fraq_NGSM	0.76397651
Buffer5m_zpcum5_AHN3	0.74950249
Buffer10m_pzabovezmean_AHN3	0.74759078
Buffer5m_zq35_AHN4	0.74669704
zq80_AHN4	0.74633814
Buffer10m_zpcum4_AHN4	0.73987582
pzabovezmean_AHN4	0.73835266
Buffer5m_ikurt_AHN3	0.73820213
Buffer5m_p2th_AHN4	0.73446934
Buffer10m_ipcumzq50_AHN3	0.73434331
Buffer10m_zpcum2_AHN4	0.72636325
sd_CHMdiv	0.72633578
Buffer5m_p5th_AHN3	0.72607609
range_CHMdiv	0.72538516
zq60_AHN4	0.72408007
zq50_AHN4	0.71573106
Buffer5m_ipground_AHN3	0.71554355
zpcum7_AHN4	0.71371851
Buffer10m_zpcum1_AHN3	0.70742705
zq70_AHN4	0.70738724
ForestPlot_min_CHM3	0.70347997
zq25_AHN4	0.69638524
Buffer10m_zpcum5_AHN4	0.6958159
Buffer10m_ipcumzq70_AHN3	0.69276903
Buffer5m_zq10_AHN4	0.6870136
Buffer10m_zpcum1_AHN4	0.68028937
Buffer5m_pground_AHN3	0.67485884
zpcum8_AHN4	0.67374505
Buffer5m_zq10_AHN3	0.66726369
Buffer10m_zskew_AHN4	0.66319923
Buffer5m_pzabovezmean_AHN4	0.65259902
Buffer10m_zpcum5_AHN3	0.65217348
zq20_AHN4	0.64993574
p4th_AHN3	0.64421926
Buffer5m_zskew_AHN3	0.64374434
Buffer10m_p3th_AHN3	0.63908399
Buffer10m_zq10_AHN3	0.63856998
Buffer5m_zmax_AHN4	0.63602455
zpcum4_AHN4	0.62255146
Buffer5m_zq5_AHN3	0.61950353
Buffer10m_zq75_AHN3	0.61898985
Buffer5m_zq25_AHN3	0.61378709
min_CHMdiv	0.61113966
shape_AHN4_eigen_largest	0.60276591

Buffer10m_iskew_AHN3	0.60204281
Buffer10m_zpcum6_AHN3	0.60031288
Buffer5m_zq95_AHN3	0.59893201
Buffer5m_zq30_AHN4	0.59538475
Buffer5m_zpcum3_AHN4	0.59292019
zq35_AHN4	0.58655584
Buffer10m_zq20_AHN3	0.58446724
zq40_AHN4	0.58280442
Buffer5m_zq20_AHN4	0.57689316
Buffer5m_zpcum4_AHN3	0.57444174
ForestPlot_fraq_RGCM	0.5709781
sd_CHM4	0.56528033
zkurt_AHN4	0.56288483
Buffer5m_p4th_AHN3	0.55989473
zq75_AHN4	0.55984114
zq90_AHN4	0.55455922
zq95_AHN4	0.55447891
zq45_AHN4	0.5522119
max_CHM3	0.55202064
Buffer5m_p1th_AHN3	0.54932934
Buffer10m_ipground_AHN3	0.54929219
Buffer5m_zq50_AHN4	0.54812923
Buffer5m_pground_AHN4	0.54260779
Buffer10m_zpcum2_AHN3	0.54216112
Buffer10m_zq40_AHN3	0.53958501
Buffer10m_zq95_AHN4	0.53561738
Buffer10m_zmean_AHN4	0.53485837
Buffer10m_zq5_AHN3	0.53137845
Buffer10m_pzabovezmean_AHN4	0.53063232
zq85_AHN4	0.52925777
Buffer10m_zq30_AHN3	0.52906716
Buffer10m_zq10_AHN4	0.5249089
Buffer5m_zq90_AHN3	0.52461842
zmax_AHN4	0.51933095
Buffer10m_pground_AHN3	0.51885487
zpcum5_AHN4	0.51829765
Buffer10m_zpcum3_AHN3	0.51727121
zsd_AHN4	0.50946097
Buffer10m_zq15_AHN4	0.50555165
Buffer5m_zpcum3_AHN3	0.50480131
zpcum1_AHN4	0.50224373
Buffer5m_zpcum2_AHN3	0.50092287
max_CHM4	0.49601972
zmean_AHN4	0.48839234
Buffer10m_zq25_AHN3	0.48766088
Buffer10m_ipground_AHN4	0.48495566
zq65_AHN4	0.48247812
Buffer10m_zq60_AHN3	0.47928847
Buffer10m_zpcum3_AHN4	0.47774579
Buffer10m_zskew_AHN3	0.47670481

Buffer10m_zq60_AHN4	0.47025284
pground_AHN4	0.46874146
ForestPlot_min_CHM4	0.46666226
Buffer10m_zq35_AHN3	0.46599435
Buffer5m_zq75_AHN4	0.46060212
Buffer5m_pzabove2_AHN3	0.46037825
Buffer5m_zq40_AHN4	0.45631752
Buffer10m_zsd_AHN4	0.45573726
zq95_AHN3	0.45119844
Buffer5m_zq95_AHN4	0.44827275
Buffer5m_zmean_AHN4	0.43894659
Buffer10m_zq15_AHN3	0.43532649
range_CHM4	0.43521902
Buffer10m_zq20_AHN4	0.43220925
Buffer10m_zq65_AHN3	0.43117204
zpcum6_AHN4	0.42989286
zskew_AHN4	0.42668643
zq30_AHN4	0.42065244
Buffer10m_pzabove2_AHN3	0.41919552
zpcum2_AHN4	0.41833615
zq55_AHN4	0.41613521
Buffer5m_zq15_AHN3	0.41609845
Buffer10m_zq45_AHN4	0.41384856
Buffer10m_zq45_AHN3	0.41209971
Buffer5m_zq50_AHN3	0.41061621
zmax_AHN3	0.41007936
pzabove2_AHN4	0.40994574
Buffer5m_zq30_AHN3	0.40283812
Buffer10m_zq70_AHN3	0.38943782
Buffer10m_pground_AHN4	0.38631089
Buffer5m_zq65_AHN4	0.38623269
Buffer5m_zq85_AHN3	0.38327931
Buffer5m_zsd_AHN4	0.38214981
Buffer5m_zq60_AHN4	0.38207058
Buffer10m_zq40_AHN4	0.37167624
Buffer5m_zq45_AHN3	0.37163237
Buffer5m_zq35_AHN3	0.36516017
Buffer5m_zq80_AHN3	0.36215561
Buffer5m_zq55_AHN3	0.35212878
Buffer5m_zq25_AHN4	0.35065729
Buffer5m_zq80_AHN4	0.34727629
Buffer10m_zq90_AHN4	0.34720515
zpcum3_AHN4	0.34690035
Buffer10m_zq35_AHN4	0.34589447
Buffer10m_zq50_AHN4	0.34551372
Buffer5m_zq55_AHN4	0.33468703
Buffer5m_zq70_AHN4	0.33128757
Buffer5m_zmean_AHN3	0.32870517
Buffer5m_zq90_AHN4	0.32360288
Buffer10m_zq30_AHN4	0.31382198

Buffer5m_zq45_AHN4	0.30689962
Buffer10m_zq65_AHN4	0.30658182
Buffer10m_zq55_AHN3	0.30625429
Buffer10m_zq70_AHN4	0.30477834
Buffer10m_zq85_AHN4	0.29438566
Buffer5m_zq15_AHN4	0.29229573
Buffer10m_zmean_AHN3	0.29116139
Buffer10m_zq50_AHN3	0.28603149
Buffer10m_zq55_AHN4	0.2851455
Buffer5m_zq65_AHN3	0.27585743
Buffer5m_zq40_AHN3	0.26210126
Buffer10m_zq25_AHN4	0.24417661
Buffer5m_zq85_AHN4	0.23747181
Buffer10m_pzabove2_AHN4	0.22936846
Buffer10m_zq80_AHN4	0.22083158
Buffer5m_zq60_AHN3	0.21378557
Buffer5m_zq70_AHN3	0.20903902
Buffer10m_zq75_AHN4	0.20456607
Buffer5m_zq75_AHN3	0.18563211
fraq_RGCM	0.17962385
fraq_NGSM	0.16860162

D2: “number of trees” model with only the most important variables included

variable	*importance*
shape_AHN3_planarity	556.540363
ForestPlot_fraq_NGLM	239.952029
ForestPlot_GD	225.632386

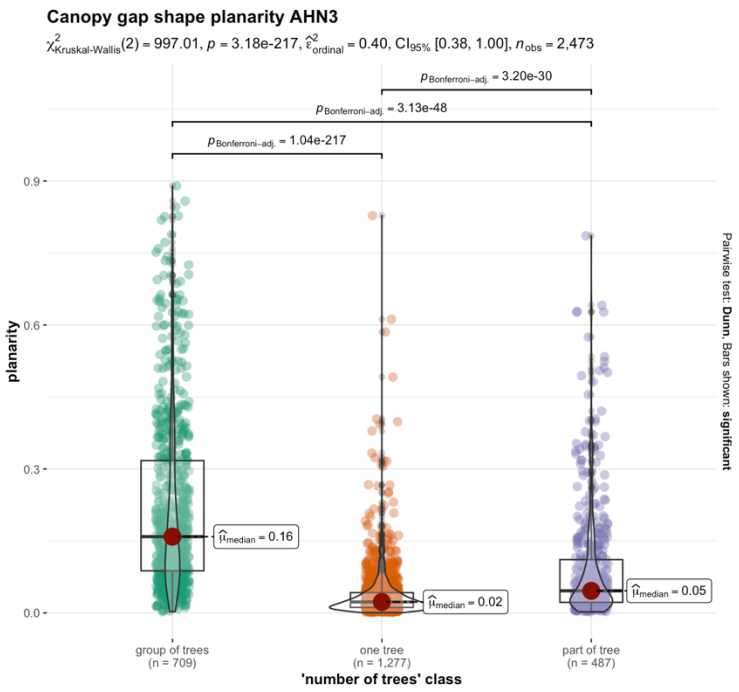

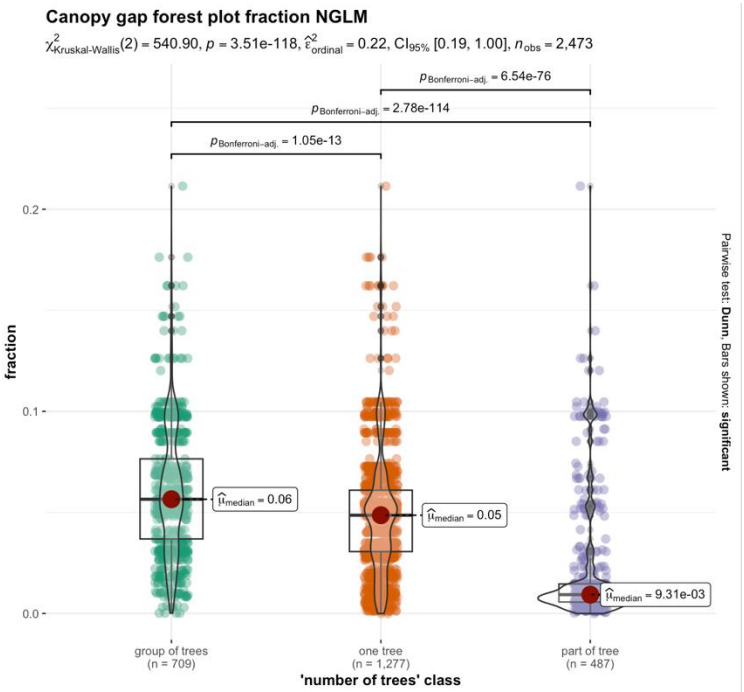

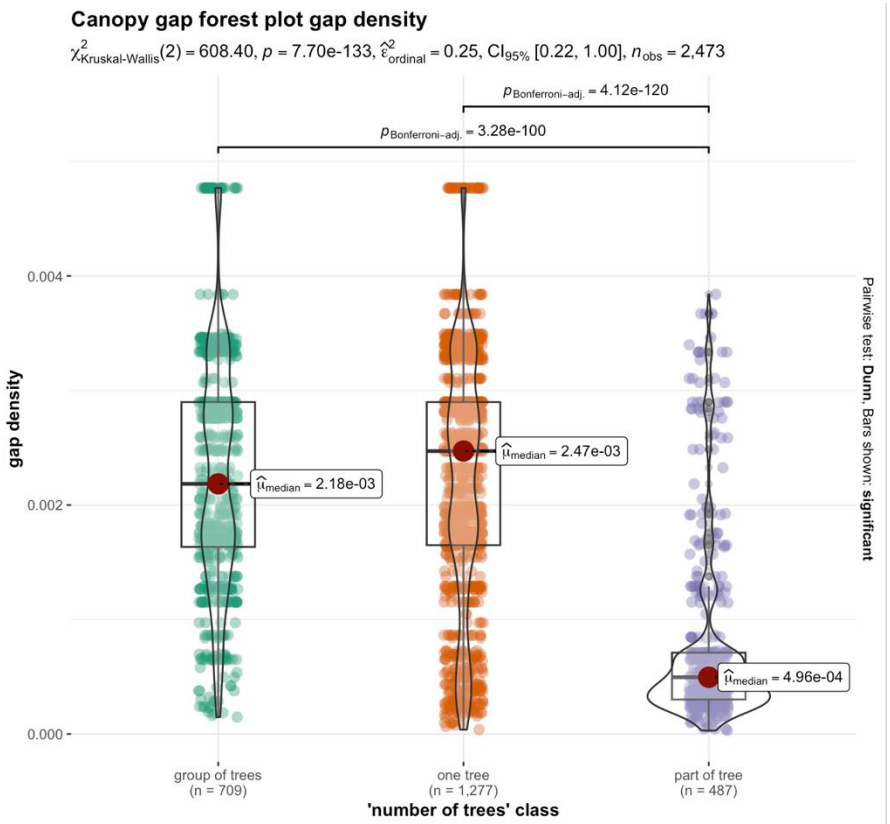

D3: management type model with all variables included

variable	*importance*
ForestPlot_gini_CHM4	152.787068
ForestPlot_fraq_NoG	41.0123291
ForestPlot_fraq_NGLM	28.8188507
ForestPlot_GD	19.2906064
ForestPlot_fraq_VC	13.2442281
ForestPlot_mean_CHMdiv	12.970866
ForestPlot_fraq_NGBM	12.4378948
ForestPlot_mean_CHM3	11.4290351
ForestPlot_gini_CHMdiv	7.28968015
ForestPlot_mean_CHM4	7.10472603
Buffer10m_ipcumzq30_AHN4	6.0811985
ForestPlot_sd_CHM4	4.72298554
ForestPlot_fraq_NGSM	4.3393727
Buffer5m_ipcumzq70_AHN4	3.77832042
Buffer10m_ipcumzq70_AHN3	3.77429692
Buffer10m_zq50_AHN4	3.04711779
ForestPlot_PIG	2.89526537
ForestPlot_gini_CHM3	2.80262763
Buffer10m_zmean_AHN4	2.72996115
Buffer10m_zpcum1_AHN3	2.66822777
Buffer10m_zkurt_AHN3	2.49311953
ForestPlot_range_CHMdiv	2.19920225
ForestPlot_max_CHMdiv	2.12591713
ForestPlot_min_CHMdiv	2.04619712

ForestPlot_min_CHM3	1.91993739
ForestPlot_max_CHM3	1.88596445
Buffer5m_ipcumzq90_AHN3	1.85970309
Buffer10m_zpcum3_AHN4	1.83594842
ForestPlot_range_CHM4	1.68442119
Buffer10m_ipcumzq70_AHN4	1.63789337
ForestPlot_min_CHM4	1.58748598
ForestPlot_max_CHM4	1.4875399
ForestPlot_range_CHM3	1.48508054
ForestPlot_sd_CHMdiv	1.43461776
Buffer10m_ipcumzq90_AHN4	1.27333711
Buffer10m_zpcum1_AHN4	1.25891973
Buffer10m_ipcumzq90_AHN3	1.24570201
ForestPlot_fraq_RG	1.16551264
Buffer10m_ipcumzq50_AHN3	1.15878451
ForestPlot_fraq_DG	1.01718996
Buffer5m_ipcumzq70_AHN3	1.00564038
Buffer5m_zpcum8_AHN3	0.9208675
ipcumzq50_AHN3	0.89006136
Buffer10m_zq45_AHN4	0.88213307
Buffer10m_p3th_AHN3	0.87390598
Buffer5m_zpcum9_AHN4	0.87251651
Buffer10m_zpcum9_AHN3	0.77768254
ForestPlot_fraq_RGCM	0.75772763
Buffer5m_zkurt_AHN3	0.75761698
Buffer10m_ipcumzq50_AHN4	0.75628635
Buffer5m_pzabovezmean_AHN4	0.73910683
Buffer10m_zpcum9_AHN4	0.71932648
ForestPlot_sd_CHM3	0.69546648
ipcumzq70_AHN3	0.67421668
Buffer10m_pground_AHN3	0.64477239
p2th_AHN3	0.5140113
Buffer10m_ipcumzq10_AHN4	0.50293877
Buffer5m_p3th_AHN3	0.43765663
imean_AHN3	0.42842577
Buffer10m_imax_AHN3	0.41980813
Buffer10m_p2th_AHN4	0.41134192
gini_CHM4	0.40718749
shape_AHN4_planarity	0.30348034
Buffer5m_zpcum9_AHN3	0.29160027
shape_AHN4_eigen_medium	0.28919737
Buffer5m_zpcum2_AHN4	0.28486227
Buffer5m_ipcumzq50_AHN4	0.2806899
Buffer10m_isd_AHN3	0.27901486
ipcumzq90_AHN3	0.27682906
Buffer10m_zpcum3_AHN3	0.26634898
pzabovezmean_AHN3	0.26573182
ipcumzq90_AHN4	0.2632257
Buffer5m_zq45_AHN4	0.25404966
Buffer10m_zpcum2_AHN3	0.25161366

Buffer5m_imax_AHN4	0.25019533
Buffer5m_zq30_AHN3	0.24986247
Buffer10m_zkurt_AHN4	0.24596231
dist_nn	0.23768351
Buffer5m_p1th_AHN3	0.22959026
Buffer5m_ipcumzq90_AHN4	0.22416675
Buffer10m_n_AHN3	0.20974149
Buffer10m_imax_AHN4	0.19428831
ipground_AHN3	0.19207246
Buffer5m_ipcumzq10_AHN4	0.18347242
Buffer10m_zskew_AHN4	0.18239564
Buffer10m_itot_AHN3	0.17510876
ipcumzq10_AHN4	0.17449835
Buffer10m_zq25_AHN3	0.1654139
p2th_AHN4	0.16236202
Buffer10m_p3th_AHN4	0.1578656
isd_AHN3	0.15761111
Buffer5m_zpcum1_AHN3	0.15728321
Buffer5m_ipcumzq50_AHN3	0.15581033
pzabove2_AHN3	0.14855486
Buffer10m_pzabovezmean_AHN4	0.14733101
Buffer10m_p4th_AHN4	0.14606978
Buffer10m_zq55_AHN4	0.14092842
Buffer5m_zpcum3_AHN4	0.13478713
Buffer10m_p1th_AHN4	0.13373749
Buffer10m_p1th_AHN3	0.13336271
Buffer10m_zmax_AHN3	0.12884369
Buffer5m_zpcum5_AHN4	0.12811519
Buffer5m_ipcumzq30_AHN4	0.12754118
Buffer10m_ipcumzq10_AHN3	0.12425962
Buffer5m_p3th_AHN4	0.1182395
sd_CHM3	0.1177501
Buffer5m_imax_AHN3	0.11657124
Buffer10m_n_AHN4	0.11400616
Buffer5m_p4th_AHN4	0.11338091
Buffer10m_zsd_AHN3	0.10759444
zq60_AHN4	0.10417568
Buffer5m_imean_AHN4	0.10288273
Buffer5m_n_AHN3	0.10164893
Buffer10m_zq5_AHN4	0.09894308
Buffer5m_isd_AHN4	0.09800963
p1th_AHN4	0.09457641
Buffer10m_zpcum7_AHN3	0.0941914
Buffer5m_p2th_AHN3	0.09326959
Buffer10m_isd_AHN4	0.09317415
gini_CHM3	0.09284786
shape_AHN4_linearity	0.09127044
Buffer10m_zq10_AHN4	0.0910562
zmax_AHN4	0.09083698
Buffer5m_imean_AHN3	0.08856818

p3th_AHN4	0.08721756
zskew_AHN4	0.08677786
Buffer5m_zq80_AHN3	0.08529279
Buffer5m_ikurt_AHN3	0.08450426
Buffer5m_zmax_AHN3	0.08417154
zsd_AHN3	0.08231293
Buffer5m_zq70_AHN3	0.08099194
Buffer5m_zq75_AHN3	0.08093124
Buffer10m_p5th_AHN4	0.08085398
Buffer10m_zq95_AHN4	0.08051986
fraq_NGBM	0.08001246
ipcumzq30_AHN3	0.07875656
Buffer10m_pzabovezmean_AHN3	0.07823897
Buffer5m_zq5_AHN3	0.07789409
Buffer10m_zq15_AHN4	0.07773953
Buffer10m_zpcum6_AHN4	0.07755622
zq15_AHN3	0.07701139
Buffer10m_zq95_AHN3	0.07609408
shape_ECD	0.07557834
Buffer10m_zq90_AHN3	0.07550676
Buffer10m_zmax_AHN4	0.07525666
Buffer5m_zq90_AHN4	0.07455344
Buffer10m_zq50_AHN3	0.07305927
Buffer10m_iskew_AHN4	0.07268213
iskew_AHN3	0.07234058
ikurt_AHN4	0.07165046
imax_AHN4	0.07134073
Buffer5m_zpcum8_AHN4	0.07129287
Buffer5m_zsd_AHN3	0.07100317
shape_IER	0.06912369
zq95_AHN4	0.06832716
Buffer10m_p2th_AHN3	0.06743773
zsd_AHN4	0.06707778
Buffer5m_p5th_AHN4	0.06690748
Buffer10m_zpcum8_AHN3	0.06582222
shape_AHN4_anisotropy	0.06555042
Buffer5m_area_AHN4	0.06533824
shape_AHN3_horizontality	0.06531875
Buffer10m_itot_AHN4	0.06528374
Buffer10m_zpcum7_AHN4	0.06483358
p3th_AHN3	0.06407013
shape_AHN3_eigen_smallest	0.06396419
Buffer10m_zpcum4_AHN4	0.06359307
zq65_AHN3	0.0635917
Buffer5m_ipcumzq10_AHN3	0.06351485
Buffer5m_itot_AHN4	0.06323898
Buffer10m_zq85_AHN3	0.06320998
Buffer10m_zq85_AHN4	0.06279192
Buffer10m_zq75_AHN3	0.06258246
itot_AHN3	0.06198711

Buffer10m_zpcum5_AHN3	0.06188015
Buffer10m_p4th_AHN3	0.06143377
zq5_AHN3	0.0610873
p1th_AHN3	0.06089708
zq70_AHN3	0.06020284
Buffer10m_zq5_AHN3	0.05968118
zmean_AHN4	0.05956752
shape_AHN3_curvature	0.05897133
zkurt_AHN3	0.05857733
Buffer10m_imean_AHN3	0.05843788
Buffer10m_ipcumzq30_AHN3	0.05823824
zq65_AHN4	0.05797143
Buffer10m_iskew_AHN3	0.05680996
Buffer5m_zq40_AHN4	0.0567919
Buffer5m_ikurt_AHN4	0.05645103
isd_AHN4	0.05630635
Buffer10m_ipground_AHN3	0.05580988
zpcum6_AHN3	0.05554944
Buffer10m_p5th_AHN3	0.0548435
iskew_AHN4	0.05469915
zq80_AHN3	0.05404737
zq50_AHN4	0.05392338
Buffer5m_zpcum6_AHN3	0.05378279
n_AHN4	0.05280556
pground_AHN3	0.0524514
Buffer5m_zq10_AHN4	0.0519974
Buffer5m_itot_AHN3	0.05179204
Buffer10m_zq30_AHN3	0.05076709
shape_ESV	0.0505477
shape_AHN4_sphericity	0.05011666
shape_perimeter	0.04984747
imean_AHN4	0.04980348
Buffer5m_zpcum2_AHN3	0.04919888
Buffer10m_area_AHN4	0.04842358
shape_FD	0.04817487
Buffer5m_zq20_AHN4	0.04762069
zq90_AHN3	0.04723725
Buffer5m_zq90_AHN3	0.04696785
shape_solidity	0.04555145
shape_SI	0.04554762
Buffer10m_ikurt_AHN3	0.04534478
shape_AHN3_linearity	0.04528581
shape_AHN3_anisotropy	0.04525585
zpcum8_AHN4	0.04515368
p4th_AHN3	0.04513548
Buffer5m_zskew_AHN3	0.04500611
zq15_AHN4	0.04480938
shape_AFF	0.04471661
zpcum6_AHN4	0.04464649
zpcum3_AHN3	0.04464169

zpcum7_AHN3	0.04431875
shape_AHN4_eigen_smallest	0.04428437
Buffer10m_zpcum6_AHN3	0.04423312
Buffer10m_zq90_AHN4	0.04399841
Buffer10m_zq15_AHN3	0.04358795
Buffer5m_zq35_AHN3	0.04350739
zpcum9_AHN4	0.04344636
Buffer10m_zpcum8_AHN4	0.0433536
zkurt_AHN4	0.0429364
zq95_AHN3	0.04237167
zq75_AHN3	0.04197143
min_CHMdiv	0.04193578
shape_AHN3_eigen_medium	0.04189507
Buffer5m_zpcum7_AHN4	0.04170726
Buffer5m_zpcum6_AHN4	0.04166855
max_CHM3	0.04156364
zq5_AHN4	0.04138517
Buffer10m_zq60_AHN3	0.04093333
zq10_AHN4	0.0409069
Buffer5m_area_AHN3	0.04061094
Buffer10m_zq65_AHN3	0.04055975
zpcum5_AHN4	0.04036667
pzabovezmean_AHN4	0.04033862
zpcum9_AHN3	0.04032285
Buffer5m_zq95_AHN3	0.04012248
Buffer5m_zmean_AHN3	0.0399342
zq25_AHN4	0.03991886
Buffer5m_zq65_AHN4	0.03954762
zq50_AHN3	0.03936173
p4th_AHN4	0.03924615
min_CHM4	0.03879798
Buffer5m_isd_AHN3	0.03869484
Buffer5m_zskew_AHN4	0.0386594
shape_circularity	0.03850014
sd_CHM4	0.03829403
zq70_AHN4	0.03823266
Buffer5m_zq5_AHN4	0.03801515
shape_AHN4_curvature	0.03800168
sd_CHMdiv	0.03780847
Buffer5m_zq85_AHN3	0.03768333
zq40_AHN3	0.0376601
Buffer5m_zq60_AHN3	0.03761866
shape_area	0.03747603
range_CHMdiv	0.03739169
zq55_AHN4	0.03716667
Buffer5m_zq80_AHN4	0.0370697
ipcumzq30_AHN4	0.03705117
Buffer10m_ikurt_AHN4	0.03679258
area_AHN4	0.03677427
Buffer10m_zmean_AHN3	0.03673333

zq75_AHN4	0.03658095
Buffer5m_iskew_AHN3	0.03630051
Buffer5m_zq55_AHN4	0.03629841
zq45_AHN3	0.03629741
n_AHN3	0.03613746
range_CHM3	0.03582963
Buffer5m_zq75_AHN4	0.03578626
Buffer10m_zpcum4_AHN3	0.03512632
zq35_AHN3	0.03511111
Buffer5m_zmax_AHN4	0.03503088
zq30_AHN3	0.03500566
Buffer5m_ipcumzq30_AHN3	0.03485519
imax_AHN3	0.03424267
Buffer10m_zq10_AHN3	0.03422787
Buffer10m_zq35_AHN3	0.03412381
Buffer10m_zq70_AHN4	0.03405
zpcum2_AHN3	0.03403493
Buffer10m_area_AHN3	0.03402472
shape_AHN3_sphericity	0.03355162
zpcum7_AHN4	0.0333539
Buffer10m_zq55_AHN3	0.03303333
Buffer5m_ipground_AHN4	0.03300317
shape_GSCI	0.03271429
Buffer5m_n_AHN4	0.03268494
Buffer5m_zpcum7_AHN3	0.03217663
mean_CHM4	0.03199664
Buffer5m_zq85_AHN4	0.03170909
Buffer10m_zq45_AHN3	0.03156667
Buffer5m_zq15_AHN4	0.03128889
fraq_NGM	0.03123142
max_CHMdiv	0.03119936
zskew_AHN3	0.03095559
Buffer5m_zsd_AHN4	0.03073333
ipcumzq10_AHN3	0.03069402
Buffer10m_zq80_AHN4	0.03068571
Buffer10m_imean_AHN4	0.0306381
Buffer5m_zpcum4_AHN3	0.03051429
Buffer10m_zskew_AHN3	0.03047879
zq60_AHN3	0.03040719
zpcum1_AHN4	0.03034762
zpcum4_AHN3	0.03004574
Buffer10m_pground_AHN4	0.03002417
zq35_AHN4	0.03
ipground_AHN4	0.02983827
Buffer5m_zq65_AHN3	0.029825
Buffer5m_zpcum5_AHN3	0.02977535
shape_AHN4_eigen_largest	0.02974762
Buffer5m_pzabove2_AHN3	0.0296804
zq20_AHN4	0.02934722
Buffer10m_zq40_AHN3	0.02836365

Buffer5m_zq30_AHN4	0.02835382
zpcum3_AHN4	0.02834685
Buffer5m_zq95_AHN4	0.02782222
zq30_AHN4	0.02663333
zq25_AHN3	0.02656531
Buffer5m_p1th_AHN4	0.02632418
Buffer10m_zpcum2_AHN4	0.02622095
shape_roundness	0.02588571
zpcum2_AHN4	0.02545364
gini_CHMdiv	0.02514514
pground_AHN4	0.02486667
Buffer10m_zq80_AHN3	0.02471515
ikurt_AHN3	0.02448889
area_AHN3	0.02441468
Buffer10m_zsd_AHN4	0.02422381
Buffer10m_zq30_AHN4	0.02403195
buffer5m_overlap_relative	0.02384329
zpcum1_AHN3	0.02376528
zq10_AHN3	0.02361686
zq80_AHN4	0.0235812
Buffer5m_zq40_AHN3	0.02352381
zq20_AHN3	0.02324762
Buffer10m_ipground_AHN4	0.02309229
Buffer10m_zq60_AHN4	0.02273333
Buffer5m_zkurt_AHN4	0.02247888
p5th_AHN3	0.02195204
buffer10m_overlap_relative	0.02175556
zq85_AHN3	0.02162487
zq55_AHN3	0.02128976
Buffer5m_zpcum1_AHN4	0.02119464
Buffer5m_pzabovezmean_AHN3	0.02103985
Buffer5m_zq45_AHN3	0.02060784
Buffer5m_zq70_AHN4	0.02049595
Buffer5m_iskew_AHN4	0.02028253
Buffer5m_pground_AHN3	0.02026032
Buffer10m_zq25_AHN4	0.02022222
Buffer5m_zmean_AHN4	0.01965359
Buffer5m_zq50_AHN4	0.01915238
zmean_AHN3	0.01889524
ipcumzq50_AHN4	0.01866667
Buffer5m_p2th_AHN4	0.01838702
Buffer5m_zq25_AHN3	0.01795122
p5th_AHN4	0.0178
ipcumzq70_AHN4	0.0177619
zq85_AHN4	0.01763361
Buffer10m_zq35_AHN4	0.01763333
Buffer10m_zq20_AHN3	0.01739394
Buffer5m_zq50_AHN3	0.01725439
Buffer10m_pzabove2_AHN4	0.0172193
mean_CHM3	0.0172

Buffer5m_zpcum3_AHN3	0.01702165
shape_convexity	0.01695905
Buffer5m_zq55_AHN3	0.01672018
Buffer5m_zq60_AHN4	0.0162403
zq40_AHN4	0.01593651
Buffer5m_zq10_AHN3	0.01585311
Buffer10m_zq40_AHN4	0.01573333
Buffer10m_zq65_AHN4	0.01537839
Buffer5m_zq35_AHN4	0.01533333
zq45_AHN4	0.015
Buffer5m_p4th_AHN3	0.01466667
pzabove2_AHN4	0.01466667
Buffer5m_zpcum4_AHN4	0.0146087
Buffer5m_pground_AHN4	0.01436667
Buffer5m_p5th_AHN3	0.01353187
Buffer10m_zq20_AHN4	0.01322564
Buffer10m_zpcum5_AHN4	0.01312281
zmax_AHN3	0.01286667
shape_AHN4_horizontality	0.0123355
Buffer5m_zq20_AHN3	0.01233333
Buffer10m_zq70_AHN3	0.01222222
Buffer5m_zq25_AHN4	0.01186667
Buffer5m_ipground_AHN3	0.01116667
Buffer5m_pzabove2_AHN4	0.0102619
itot_AHN4	0.01013333
shape_AHN3_eigen_largest	0.00968301
zq90_AHN4	0.0087619
zpcum8_AHN3	0.00866667
max_CHM4	0.00866667
Buffer10m_pzabove2_AHN3	0.00833333
zpcum4_AHN4	0.008
mean_CHMdiv	0.00709524
Buffer5m_zq15_AHN3	0.00666667
range_CHM4	0.00589189
shape_AHN3_planarity	0.00566667
zpcum5_AHN3	0.00266667
min_CHM3	0.00266667
Buffer10m_zq75_AHN4	0
fraq_NGSM	0
fraq_RGCM	0

D4: management type model with only the most important variables included

variable	*importance*
ForestPlot_gini_CHM4	134.17408
ForestPlot_fraq_NoG	114.41287
ForestPlot_fraq_NGLM	104.11153
ForestPlot_GD	61.21909

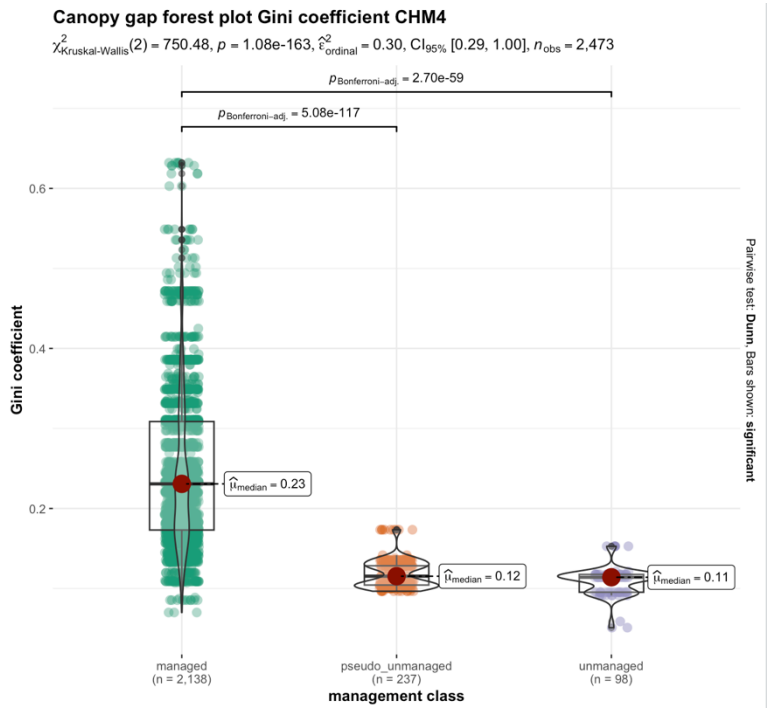

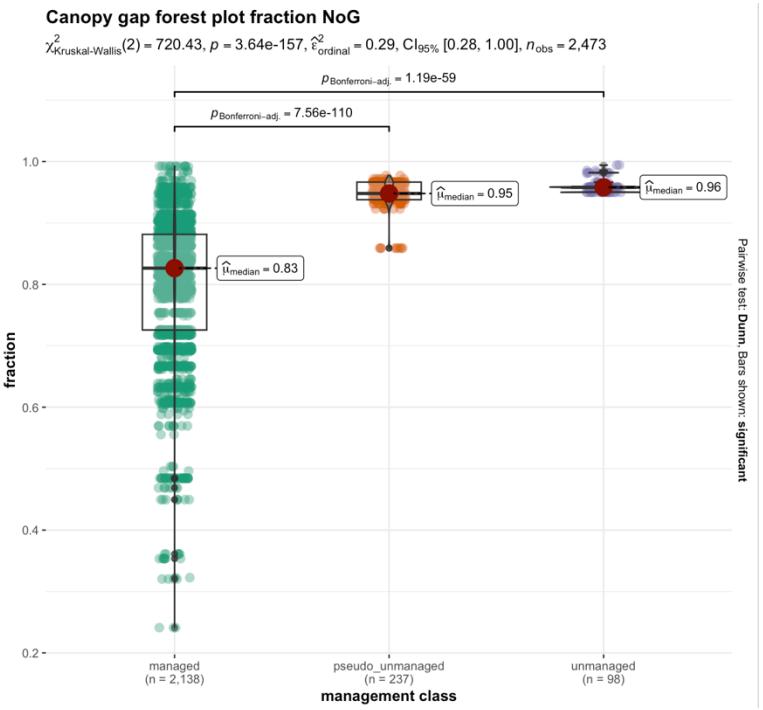

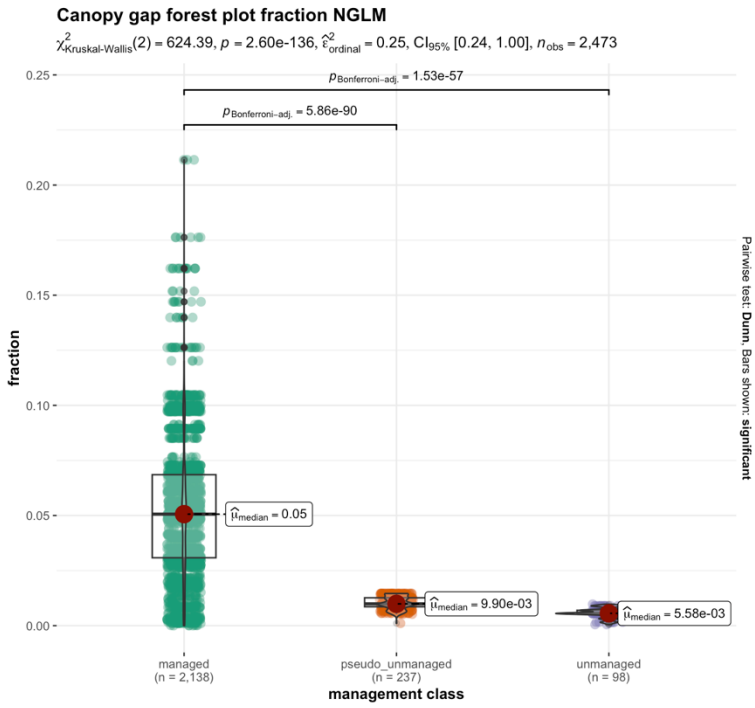

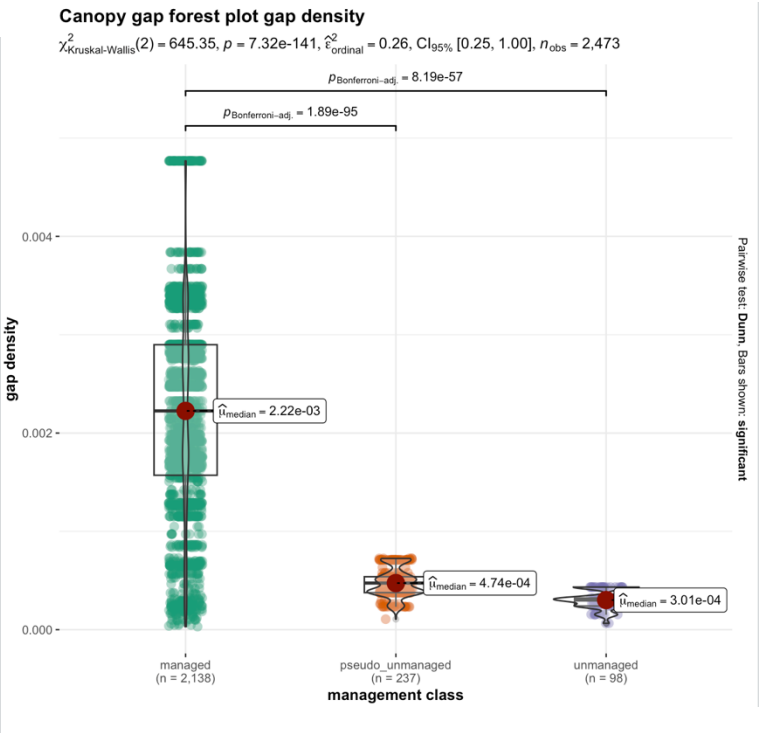

D5: management type model without forest plot variables included

variable	*importance*
Buffer10m_ipcumzq90_AHN4	4.92773978
Buffer10m_ipcumzq10_AHN4	4.2689557
Buffer5m_ipground_AHN4	4.04184966
Buffer10m_ipcumzq50_AHN4	3.8021842
Buffer5m_ipcumzq90_AHN4	3.46991955
Buffer10m_ipground_AHN3	3.46466745
Buffer5m_ipcumzq70_AHN4	3.41793246
Buffer10m_iskew_AHN4	3.41207591
Buffer10m_zq25_AHN3	3.33464116
Buffer5m_ipcumzq50_AHN4	3.28199769
Buffer5m_zq20_AHN3	3.21765873
Buffer10m_ipcumzq30_AHN4	3.13957376
ipground_AHN3	3.10499946
Buffer10m_ipcumzq50_AHN3	3.09252474
Buffer5m_ipcumzq50_AHN3	2.95358877
Buffer10m_ipcumzq90_AHN3	2.95042646
Buffer10m_zq35_AHN4	2.90819993
Buffer5m_ipcumzq30_AHN4	2.83703158
Buffer10m_ipcumzq70_AHN3	2.79484849
Buffer5m_ipcumzq90_AHN3	2.78388214
Buffer10m_ipcumzq70_AHN4	2.74601264
Buffer10m_zpcum7_AHN3	2.74372165
Buffer10m_zq20_AHN3	2.67245384
ipcumzq50_AHN3	2.6502374
Buffer10m_zpcum8_AHN4	2.63292524
Buffer5m_p3th_AHN3	2.59392825
Buffer10m_zq40_AHN4	2.58299837
Buffer5m_ipcumzq10_AHN4	2.53477598
Buffer10m_zpcum8_AHN3	2.44892117
Buffer5m_zpcum9_AHN3	2.40654057
ipcumzq70_AHN3	2.36185851
Buffer10m_pzabove2_AHN4	2.33913094
Buffer10m_zkurt_AHN4	2.33182307
Buffer10m_zpcum6_AHN3	2.32964101
zq20_AHN3	2.31748692
Buffer5m_zq35_AHN4	2.28388546
pground_AHN3	2.25275549
Buffer10m_ipcumzq30_AHN3	2.23265068
Buffer10m_zq30_AHN4	2.23249184
Buffer10m_zsd_AHN4	2.18022317
Buffer10m_p1th_AHN3	2.17918184
Buffer10m_zpcum9_AHN3	2.14104088
Buffer5m_ipground_AHN3	2.04496897
Buffer5m_zq15_AHN3	2.03268885
Buffer10m_p4th_AHN3	1.9982754
Buffer5m_zpcum7_AHN3	1.99718081
Buffer5m_pground_AHN4	1.97272506
Buffer5m_zq45_AHN4	1.97105806

Buffer5m_ipcumzq30_AHN3	1.96402758
Buffer5m_pzabove2_AHN4	1.9424562
Buffer10m_zq75_AHN3	1.92360551
Buffer5m_isd_AHN3	1.90021777
Buffer10m_zq90_AHN3	1.90015717
Buffer5m_ipcumzq10_AHN3	1.8999643
Buffer5m_zpcum9_AHN4	1.89662476
Buffer5m_zq30_AHN4	1.86772301
Buffer10m_zpcum7_AHN4	1.85839674
Buffer10m_zq45_AHN4	1.82984061
Buffer10m_zq80_AHN3	1.82143603
zq15_AHN3	1.81927304
Buffer5m_zpcum1_AHN4	1.80305404
Buffer10m_zq60_AHN4	1.75767601
Buffer5m_zq40_AHN4	1.75102732
Buffer5m_pground_AHN3	1.74956284
Buffer5m_ipcumzq70_AHN3	1.74667649
Buffer10m_zq90_AHN4	1.74038904
Buffer10m_zq15_AHN3	1.73905602
Buffer5m_zq70_AHN3	1.73165382
Buffer5m_zpcum8_AHN3	1.7281357
Buffer5m_zq25_AHN4	1.7213616
Buffer10m_zq75_AHN4	1.69317881
Buffer10m_iskew_AHN3	1.68783167
buffer10m_overlap_relative	1.68441297
Buffer10m_ipground_AHN4	1.68411174
Buffer5m_zq85_AHN3	1.67660227
Buffer10m_zpcum1_AHN4	1.6711432
Buffer10m_zq65_AHN4	1.66173033
Buffer10m_zq55_AHN3	1.64901604
Buffer10m_zq70_AHN4	1.64499421
Buffer5m_zq65_AHN3	1.64044566
Buffer10m_zmean_AHN3	1.62398964
Buffer10m_zsd_AHN3	1.62281567
ipcumzq10_AHN3	1.62121429
Buffer10m_p3th_AHN3	1.61694614
Buffer10m_zpcum9_AHN4	1.61487555
Buffer10m_zq15_AHN4	1.6057637
Buffer10m_isd_AHN3	1.60137236
Buffer10m_ipcumzq10_AHN3	1.59115032
Buffer5m_zsd_AHN4	1.59081246
Buffer5m_zsd_AHN3	1.58087604
ipcumzq30_AHN3	1.57291268
Buffer10m_zq20_AHN4	1.55549879
Buffer5m_pzabove2_AHN3	1.53190307
Buffer10m_zq60_AHN3	1.51864749
Buffer10m_zq70_AHN3	1.5160187
Buffer10m_p4th_AHN4	1.51456601
Buffer10m_zpcum3_AHN4	1.51407
Buffer5m_zq20_AHN4	1.50347572

isd_AHN3	1.49477553
Buffer10m_pground_AHN4	1.48115184
Buffer5m_zpcum6_AHN3	1.4749647
Buffer10m_zq85_AHN3	1.46919328
Buffer10m_ikurt_AHN4	1.46776722
zq30_AHN3	1.43782107
Buffer10m_zkurt_AHN3	1.43147146
Buffer5m_zmean_AHN3	1.42868118
Buffer10m_zq50_AHN3	1.42802225
zq25_AHN3	1.42608451
Buffer10m_pground_AHN3	1.42499436
zmax_AHN4	1.41339358
Buffer10m_p2th_AHN4	1.41147813
Buffer5m_zq30_AHN3	1.40845503
Buffer5m_p4th_AHN4	1.39826673
Buffer10m_zq85_AHN4	1.38956086
Buffer10m_zq10_AHN3	1.38747012
Buffer10m_zq80_AHN4	1.38640647
Buffer5m_zq75_AHN4	1.37615256
Buffer10m_p3th_AHN4	1.37565323
Buffer5m_zq50_AHN4	1.36651486
Buffer5m_isd_AHN4	1.36580033
Buffer5m_zq25_AHN3	1.3612136
Buffer5m_p1th_AHN3	1.35596757
Buffer10m_p1th_AHN4	1.32897114
Buffer5m_zkurt_AHN4	1.32407784
zq10_AHN4	1.31373862
Buffer10m_zskew_AHN4	1.30555334
Buffer10m_zq25_AHN4	1.30394864
Buffer5m_zq90_AHN3	1.30296208
Buffer10m_zq65_AHN3	1.29108748
Buffer5m_zq55_AHN3	1.29038885
Buffer10m_zq10_AHN4	1.28844938
pzabove2_AHN3	1.28642897
Buffer10m_zq95_AHN3	1.28369773
Buffer10m_zq30_AHN3	1.27461367
zq40_AHN3	1.27157699
Buffer10m_zpcum6_AHN4	1.26366985
Buffer10m_zpcum4_AHN4	1.25883059
Buffer5m_zmax_AHN4	1.25761463
Buffer5m_zskew_AHN4	1.25058778
Buffer5m_zq90_AHN4	1.24462601
ipcumzq90_AHN4	1.21603934
Buffer10m_zq45_AHN3	1.21541442
Buffer10m_imean_AHN4	1.20890423
zsd_AHN3	1.20364069
Buffer10m_pzabovezmean_AHN4	1.19912414
max_CHM4	1.19555443
zq35_AHN3	1.19437437
Buffer10m_zq95_AHN4	1.19308734

Buffer10m_ikurt_AHN3	1.19139125
dist_nn	1.18782026
Buffer10m_pzabove2_AHN3	1.17903758
Buffer5m_zq60_AHN3	1.16628645
Buffer5m_zq95_AHN4	1.1642485
Buffer5m_zpcum8_AHN4	1.16249531
zq50_AHN3	1.15522881
zq65_AHN3	1.14860265
Buffer10m_zpcum5_AHN3	1.14325643
ipground_AHN4	1.14047084
Buffer5m_p3th_AHN4	1.12796964
Buffer10m_zpcum5_AHN4	1.12392791
Buffer10m_zq40_AHN3	1.12265305
Buffer5m_p1th_AHN4	1.11422322
Buffer5m_zq75_AHN3	1.11409456
Buffer10m_zq5_AHN4	1.10870183
Buffer10m_zpcum3_AHN3	1.10459375
Buffer5m_zq70_AHN4	1.09895698
Buffer5m_ikurt_AHN4	1.09859572
Buffer5m_zpcum4_AHN4	1.0944349
Buffer10m_isd_AHN4	1.092934
ipcumzq90_AHN3	1.08801186
Buffer5m_zq85_AHN4	1.08506118
Buffer10m_zmax_AHN4	1.07782459
Buffer5m_zq55_AHN4	1.07529777
Buffer5m_zq50_AHN3	1.06211545
mean_CHM3	1.04679952
zq95_AHN3	1.04449634
Buffer5m_zq95_AHN3	1.04273888
Buffer10m_imax_AHN3	1.04174197
zq10_AHN3	1.03217319
zmean_AHN3	1.03207538
Buffer10m_zq5_AHN3	1.02761269
zq5_AHN4	1.02138916
Buffer5m_zkurt_AHN3	1.01918095
Buffer10m_p5th_AHN4	1.00174459
Buffer5m_iskew_AHN3	1.00143574
Buffer5m_zq80_AHN4	0.98897571
Buffer10m_zpcum2_AHN4	0.98278776
Buffer5m_iskew_AHN4	0.97655131
Buffer5m_zpcum4_AHN3	0.97312908
Buffer5m_zq65_AHN4	0.95914991
Buffer5m_zpcum3_AHN4	0.9550592
Buffer5m_zmax_AHN3	0.95051594
Buffer5m_p4th_AHN3	0.94980652
zq45_AHN3	0.94917169
Buffer10m_pzabovezmean_AHN3	0.94683492
Buffer10m_zq55_AHN4	0.94350967
p1th_AHN3	0.94179011
Buffer10m_zmean_AHN4	0.94163972

Buffer5m_zpcum2_AHN4	0.93448202
Buffer5m_zpcum7_AHN4	0.93433891
shape_AHN3_eigen_largest	0.93284915
zq60_AHN3	0.93208051
pzabovezmean_AHN3	0.9262294
Buffer10m_zmax_AHN3	0.92348517
zpcum2_AHN3	0.90569046
Buffer10m_zskew_AHN3	0.89886463
zq85_AHN3	0.89660134
zkurt_AHN3	0.89420609
Buffer5m_pzabovezmean_AHN4	0.89024465
Buffer5m_zq5_AHN4	0.88700904
Buffer5m_p5th_AHN3	0.87205357
zpcum3_AHN3	0.8644849
gini_CHM3	0.86383144
shape_IER	0.85560301
Buffer5m_imax_AHN3	0.85470049
Buffer5m_p5th_AHN4	0.85438412
Buffer10m_p5th_AHN3	0.85421882
ipcumzq70_AHN4	0.85100387
zq15_AHN4	0.84406923
Buffer5m_zq80_AHN3	0.8407322
imean_AHN3	0.82029239
Buffer5m_zq10_AHN3	0.81861694
zskew_AHN3	0.81753984
Buffer10m_zq50_AHN4	0.81676487
max_CHM3	0.81533114
Buffer5m_zskew_AHN3	0.80866119
buffer5m_overlap_relative	0.80820043
iskew_AHN3	0.80089254
Buffer5m_zq15_AHN4	0.80039125
Buffer5m_zq35_AHN3	0.79925598
Buffer5m_zpcum1_AHN3	0.79806883
Buffer5m_zq45_AHN3	0.79483316
zq20_AHN4	0.79454779
zq95_AHN4	0.79340334
Buffer5m_imax_AHN4	0.79106881
zpcum4_AHN3	0.78685188
p3th_AHN3	0.78576321
zq75_AHN3	0.78507384
zpcum5_AHN3	0.78136038
Buffer5m_zpcum6_AHN4	0.77101623
Buffer5m_zq60_AHN4	0.77044493
Buffer5m_zpcum5_AHN4	0.77003791
zq5_AHN3	0.7697371
Buffer5m_pzabovezmean_AHN3	0.76759285
Buffer5m_ikurt_AHN3	0.76489374
zq45_AHN4	0.75705803
min_CHM3	0.7566565
Buffer5m_zpcum3_AHN3	0.75511328

p3th_AHN4	0.7541195
p2th_AHN3	0.75251577
shape_solidity	0.74777567
pground_AHN4	0.74586924
Buffer5m_zpcum5_AHN3	0.74575227
shape_AHN3_sphericity	0.74566657
zq80_AHN4	0.74523339
Buffer5m_p2th_AHN4	0.74517613
min_CHMdiv	0.74299307
Buffer10m_zpcum4_AHN3	0.74059223
zpcum1_AHN3	0.73526077
range_CHMdiv	0.73327151
shape_FD	0.73311046
Buffer5m_zq40_AHN3	0.7310422
zq25_AHN4	0.72533046
zq50_AHN4	0.72170485
zsd_AHN4	0.72095103
sd_CHM3	0.71863222
sd_CHM4	0.71332012
shape_AHN3_curvature	0.71292799
Buffer10m_zpcum1_AHN3	0.71202443
Buffer5m_zmean_AHN4	0.7084665
zq70_AHN3	0.70751808
imax_AHN3	0.70555514
ipcumzq50_AHN4	0.70515362
zq90_AHN3	0.70407637
ipcumzq30_AHN4	0.70229751
Buffer5m_zpcum2_AHN3	0.70224736
p1th_AHN4	0.70015882
zq90_AHN4	0.69881502
mean_CHM4	0.69814961
zq85_AHN4	0.69470671
zmax_AHN3	0.69455124
Buffer5m_zq5_AHN3	0.69374744
range_CHM4	0.69177106
zq75_AHN4	0.69122572
Buffer10m_imean_AHN3	0.69009061
zq70_AHN4	0.68986056
zq55_AHN3	0.68295663
ipcumzq10_AHN4	0.68051493
gini_CHM4	0.67334487
sd_CHMdiv	0.66810336
shape_AHN4_eigen_largest	0.66098258
zq65_AHN4	0.65916317
mean_CHMdiv	0.65245553
p2th_AHN4	0.65087427
zpcum8_AHN3	0.65027338
Buffer5m_zq10_AHN4	0.64680599
Buffer10m_imax_AHN4	0.64209765
Buffer5m_imean_AHN4	0.63713327

zpcum9_AHN3	0.63659495
p4th_AHN4	0.63394532
zq40_AHN4	0.63299848
p4th_AHN3	0.63127458
Buffer5m_n_AHN3	0.62848853
gini_CHMdiv	0.62590802
Buffer10m_zpcum2_AHN3	0.62319188
zpcum7_AHN3	0.61917371
zpcum2_AHN4	0.61714608
shape_AHN3_anisotropy	0.61699995
Buffer5m_imean_AHN3	0.61450906
imax_AHN4	0.60632044
zq35_AHN4	0.60594842
Buffer10m_zq35_AHN3	0.60535672
imean_AHN4	0.60474969
shape_convexity	0.60280036
range_CHM3	0.60080695
Buffer10m_p2th_AHN3	0.60077442
zkurt_AHN4	0.59800267
zq55_AHN4	0.59721167
zq80_AHN3	0.59395576
zq30_AHN4	0.59033326
ikurt_AHN3	0.58867837
shape_AHN3_linearity	0.5858635
n_AHN3	0.58390214
shape_AHN4_anisotropy	0.58330259
zq60_AHN4	0.58151185
Buffer5m_p2th_AHN3	0.57905751
max_CHMdiv	0.57507009
shape_roundness	0.57283236
p5th_AHN3	0.57174681
iskew_AHN4	0.57172845
itot_AHN3	0.56931015
shape_SI	0.5643051
shape_circularity	0.56157304
itot_AHN4	0.56015364
zpcum6_AHN3	0.55989389
zskew_AHN4	0.55955519
min_CHM4	0.55561457
shape_AHN4_curvature	0.55240982
zpcum1_AHN4	0.55177042
Buffer10m_itot_AHN3	0.54932633
isd_AHN4	0.54785073
shape_AFF	0.54578886
Buffer5m_itot_AHN3	0.54206216
zpcum4_AHN4	0.54021155
shape_AHN4_horizontality	0.53800497
pzabove2_AHN4	0.53319787
zpcum6_AHN4	0.52802011
zmean_AHN4	0.52545154

fraq_NGLM	0.52080456
zpcum5_AHN4	0.52078251
zpcum3_AHN4	0.51824288
shape_AHN4_sphericity	0.51791953
zpcum7_AHN4	0.51750481
Buffer5m_itot_AHN4	0.51747765
Buffer5m_area_AHN3	0.51597644
shape_AHN3_eigen_smallest	0.51543899
Buffer10m_area_AHN3	0.51256694
shape_AHN3_horizontality	0.50627512
Buffer5m_area_AHN4	0.50382341
shape_AHN4_linearity	0.50171686
zpcum8_AHN4	0.50031324
shape_AHN3_planarity	0.50018116
Buffer5m_n_AHN4	0.4981758
shape_ECD	0.49072078
shape_AHN3_eigen_medium	0.48816323
Buffer10m_n_AHN3	0.48053836
shape_AHN4_eigen_smallest	0.47529074
shape_GSCI	0.47091421
Buffer10m_n_AHN4	0.46098356
Buffer10m_itot_AHN4	0.45907797
shape_area	0.45806937
shape_AHN4_planarity	0.45590968
area_AHN3	0.44975593
Buffer10m_area_AHN4	0.44835249
shape_AHN4_eigen_medium	0.43912111
ikurt_AHN4	0.43812708
area_AHN4	0.43327449
pzabovezmean_AHN4	0.43123292
zpcum9_AHN4	0.42772761
shape_ESV	0.42250656
fraq_NGBM	0.40942944
shape_perimeter	0.40909462
p5th_AHN4	0.40875161
n_AHN4	0.40370925
fraq_RGCM	0.19547263
fraq_NGSM	0.15836321

Appendix E: Statistical comparisons to determine influence of management type for selection of variables on canopy gap level (E1) and on forest plot level (E2).

E1

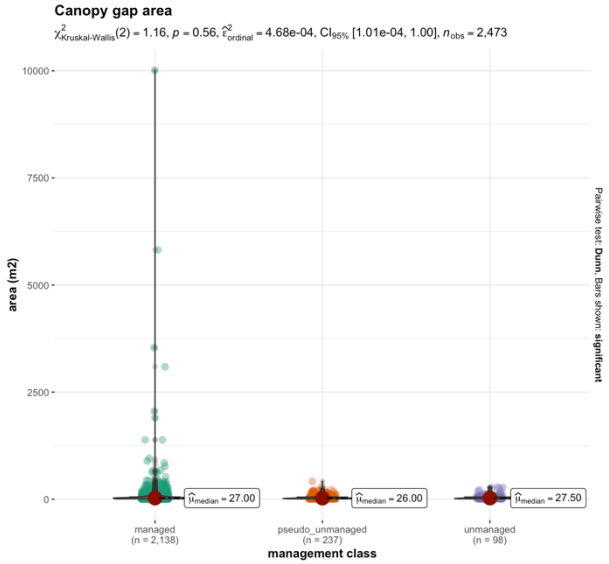

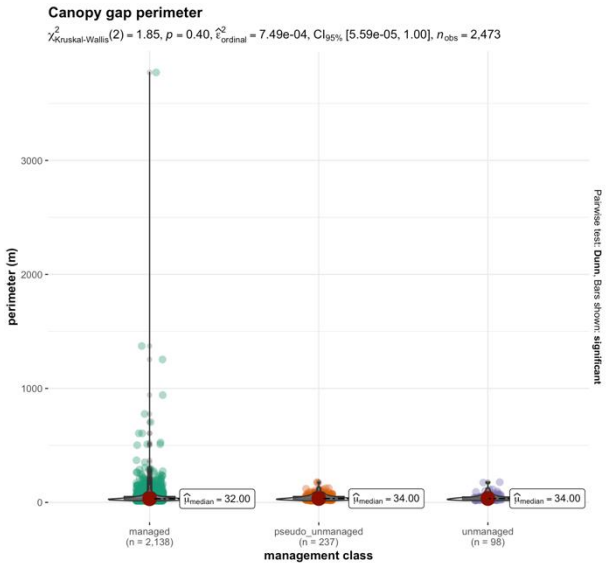

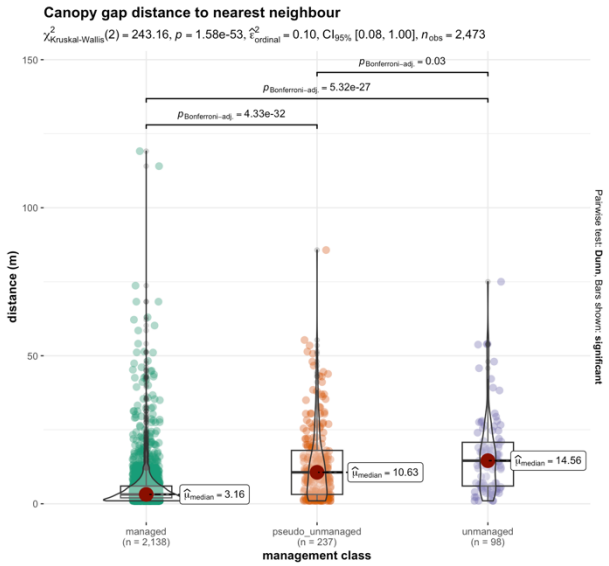

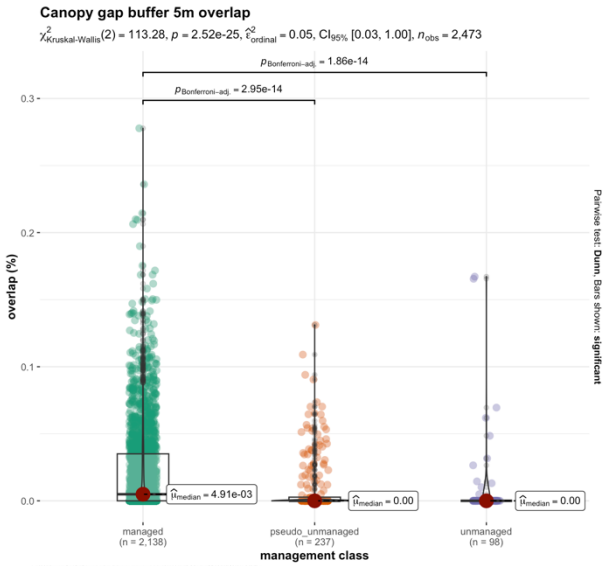

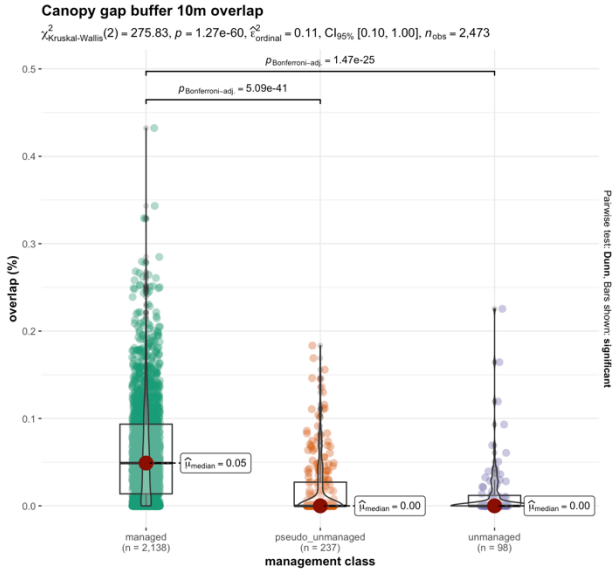

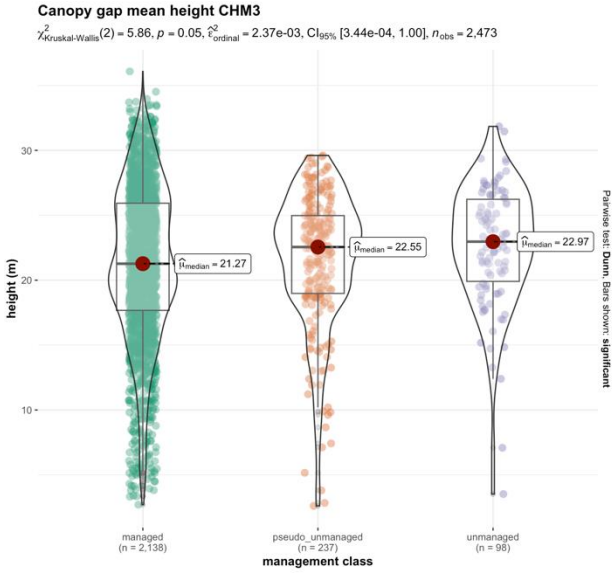

Canopy gap mean height CHM4

$\chi^2_{Kruskal\text{-}Wallis}(2) = 3.03$, $p = 0.22$, $\hat{\epsilon}^2_{ordinal} = 1.23e\text{-}03$, $CI_{95\%}$ [1.79e-04, 1.00], $n_{obs} = 2,473$

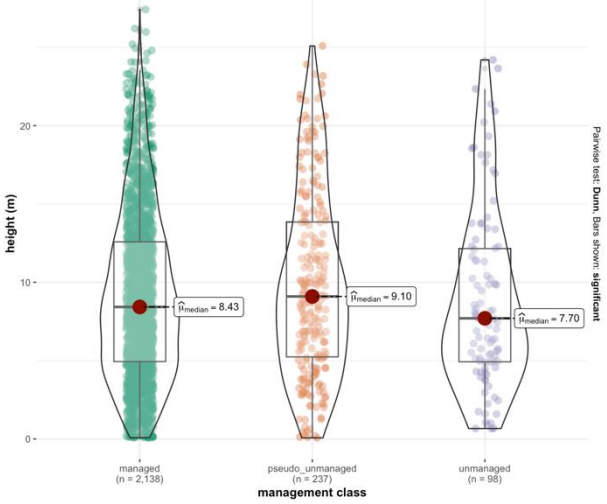

Canopy gap mean height difference

$\chi^2_{Kruskal\text{-}Wallis}(2) = 10.92$, $p = 4.25e\text{-}03$, $\hat{\epsilon}^2_{ordinal} = 4.42e\text{-}03$, $CI_{95\%}$ [1.54e-03, 1.00], $n_{obs} = 2,473$

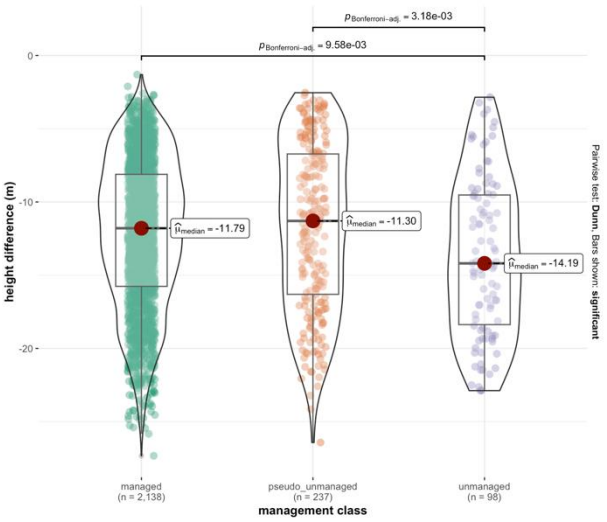

Canopy gap fraction NGBM

$\chi^2_{Kruskal\text{-}Wallis}(2) = 9.02$, $p = 0.01$, $\hat{\epsilon}^2_{ordinal} = 3.65e\text{-}03$, $CI_{95\%}$ [6.28e-04, 1.00], $n_{obs} = 2,473$

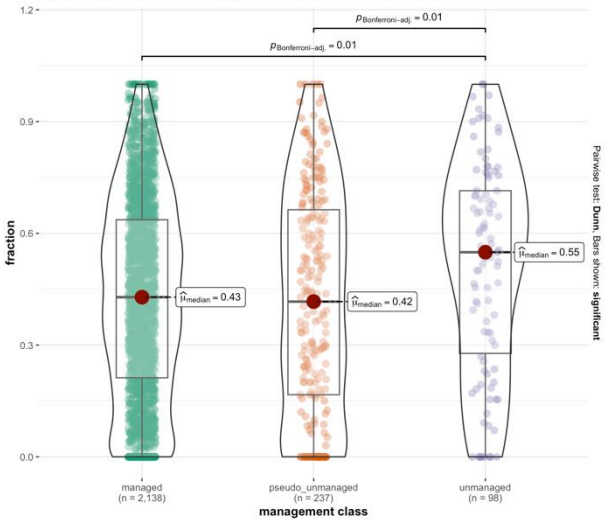

Canopy gap fraction NGLM

$\chi^2_{Kruskal\text{-}Wallis}(2) = 6.19$, $p = 0.05$, $\hat{\epsilon}^2_{ordinal} = 2.50e\text{-}03$, $CI_{95\%}$ [2.98e-04, 1.00], $n_{obs} = 2,473$

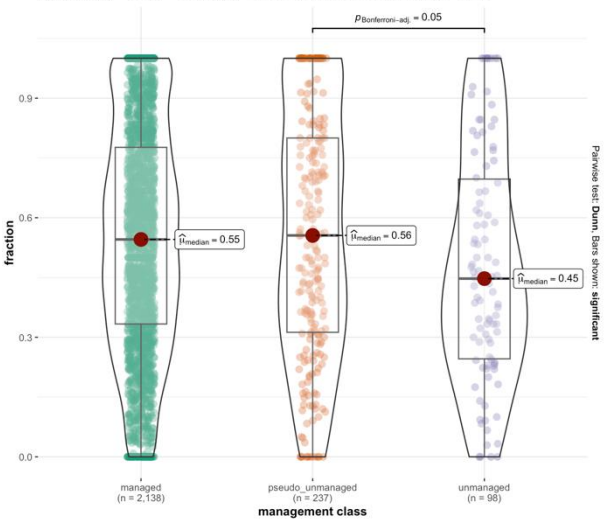

Canopy gap doughnut buffer 10m percentage of intensity returned below the 90th height percentile AHN4

$\chi^2_{Kruskal\text{-}Wallis}(2) = 474.37$, $p = 9.79e\text{-}104$, $\hat{\epsilon}^2_{ordinal} = 0.19$, $CI_{95\%}$ [0.17, 1.00], $n_{obs} = 2,473$

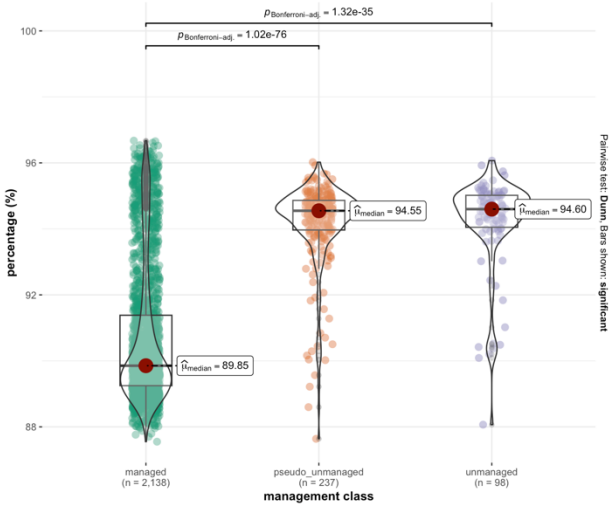

Canopy gap doughnut buffer 5m percentage of intensity returned by points classified as 'ground' AHN4

$\chi^2_{Kruskal\text{-}Wallis}(2) = 376.35$, $p = 1.89e\text{-}82$, $\hat{\epsilon}^2_{ordinal} = 0.15$, $CI_{95\%}$ [0.14, 1.00], $n_{obs} = 2,473$

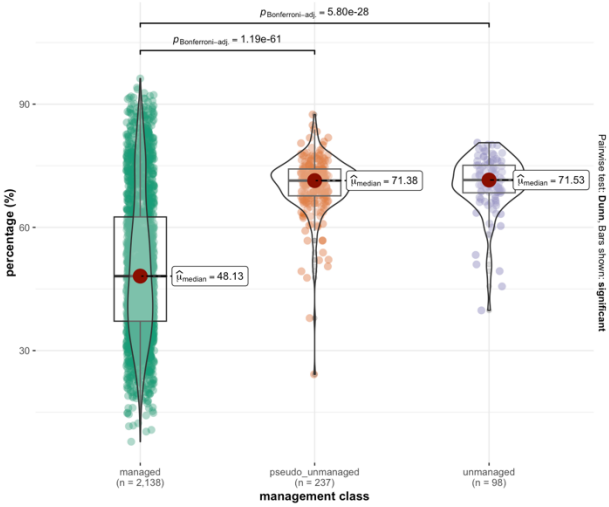

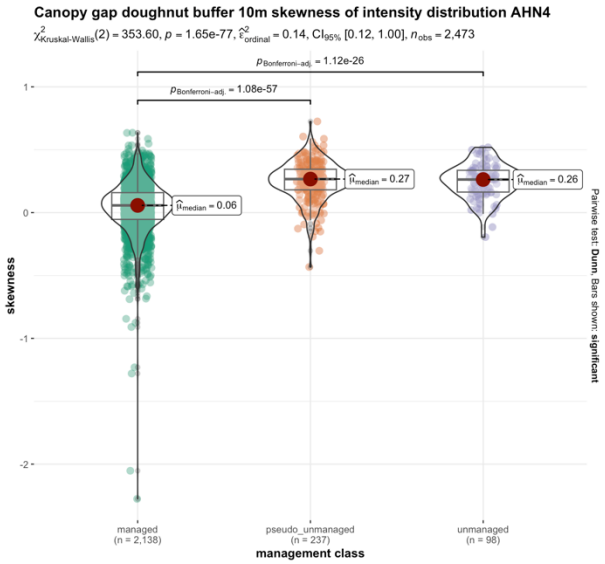
Canopy gap doughnut buffer 10m skewness of intensity distribution AHN4
$\chi^2_{Kruskal\text{-}Wallis}(2) = 353.60$, $p = 1.65e\text{-}77$, $\hat{\varepsilon}^2_{ordinal} = 0.14$, $CI_{95\%}$ [0.12, 1.00], $n_{obs} = 2,473$
$p_{Bonferroni\text{-}adj.} = 1.12e\text{-}26$
$p_{Bonferroni\text{-}adj.} = 1.08e\text{-}57$
skewness
$\hat{\mu}_{median} = 0.06$
$\hat{\mu}_{median} = 0.27$
$\hat{\mu}_{median} = 0.26$
managed (n = 2,138)
pseudo_unmanaged (n = 237)
unmanaged (n = 98)
management class
Pairwise test: Dunn, Bars shown: significant

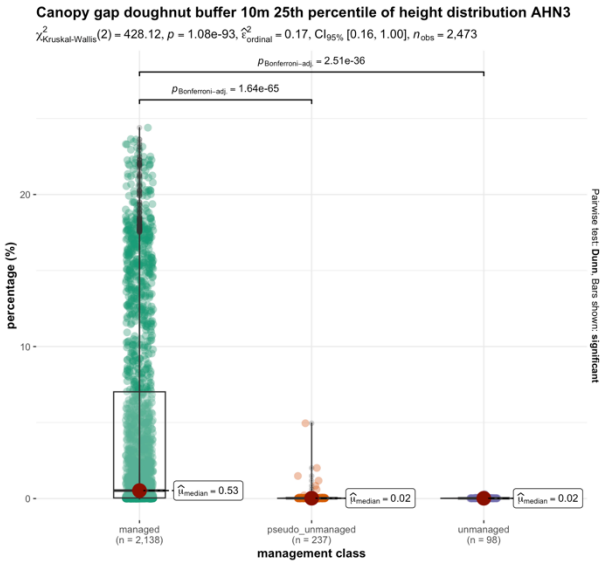
Canopy gap doughnut buffer 10m 25th percentile of height distribution AHN3
$\chi^2_{Kruskal\text{-}Wallis}(2) = 428.12$, $p = 1.08e\text{-}93$, $\hat{\varepsilon}^2_{ordinal} = 0.17$, $CI_{95\%}$ [0.16, 1.00], $n_{obs} = 2,473$
$p_{Bonferroni\text{-}adj.} = 2.51e\text{-}36$
$p_{Bonferroni\text{-}adj.} = 1.64e\text{-}65$
percentage (%)
$\hat{\mu}_{median} = 0.53$
$\hat{\mu}_{median} = 0.02$
$\hat{\mu}_{median} = 0.02$
managed (n = 2,138)
pseudo_unmanaged (n = 237)
unmanaged (n = 98)
management class
Pairwise test: Dunn, Bars shown: significant

E2

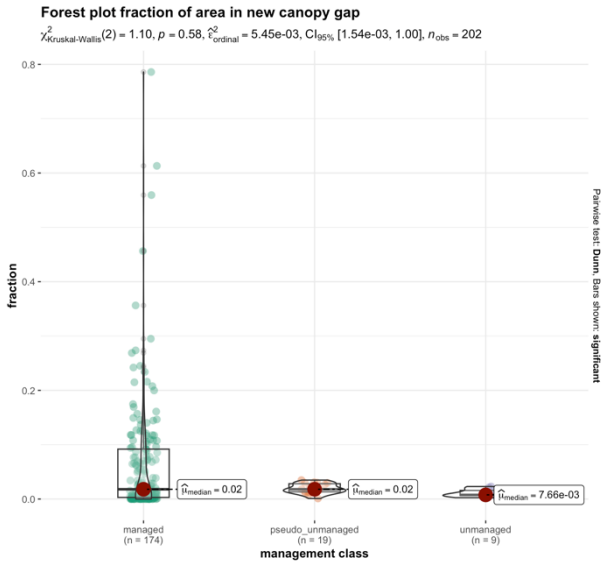
Forest plot fraction of area in new canopy gap
$\chi^2_{Kruskal\text{-}Wallis}(2) = 1.10$, $p = 0.58$, $\hat{\varepsilon}^2_{ordinal} = 5.45e\text{-}03$, $CI_{95\%}$ [1.54e-03, 1.00], $n_{obs} = 202$
fraction
$\hat{\mu}_{median} = 0.02$
$\hat{\mu}_{median} = 0.02$
$\hat{\mu}_{median} = 7.66e\text{-}03$
managed (n = 174)
pseudo_unmanaged (n = 19)
unmanaged (n = 9)
management class
Pairwise test: Dunn, Bars shown: significant

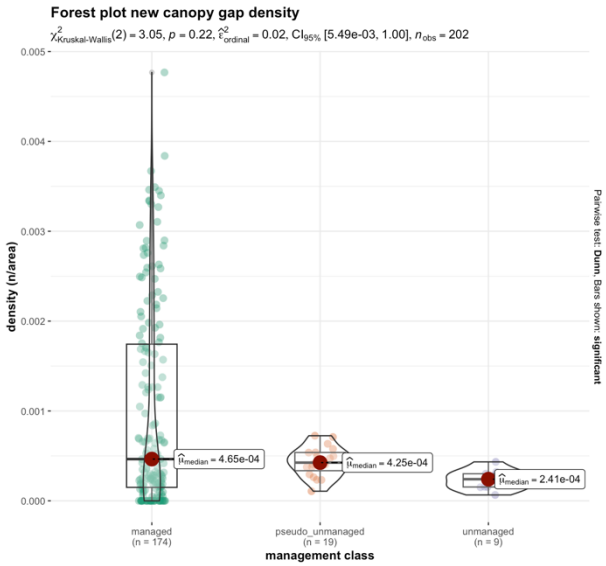
Forest plot new canopy gap density
$\chi^2_{Kruskal\text{-}Wallis}(2) = 3.05$, $p = 0.22$, $\hat{\varepsilon}^2_{ordinal} = 0.02$, $CI_{95\%}$ [5.49e-03, 1.00], $n_{obs} = 202$
density (n/area)
$\hat{\mu}_{median} = 4.65e\text{-}04$
$\hat{\mu}_{median} = 4.25e\text{-}04$
$\hat{\mu}_{median} = 2.41e\text{-}04$
managed (n = 174)
pseudo_unmanaged (n = 19)
unmanaged (n = 9)
management class
Pairwise test: Dunn, Bars shown: significant

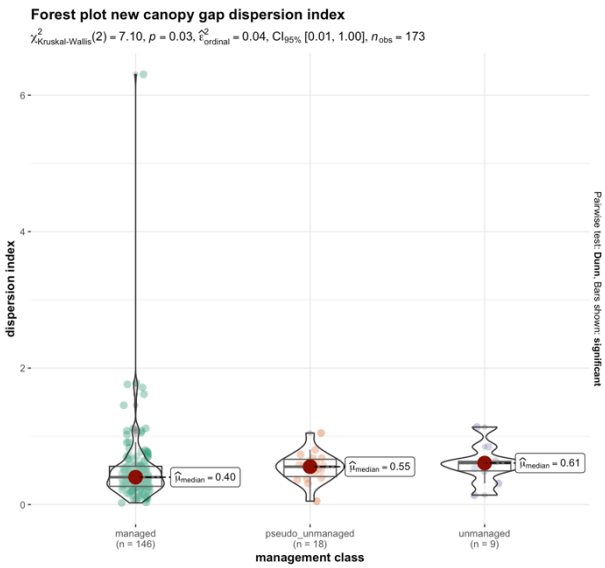
Forest plot new canopy gap dispersion index
$\chi^2_{Kruskal\text{-}Wallis}(2) = 7.10$, $p = 0.03$, $\hat{\varepsilon}^2_{ordinal} = 0.04$, $CI_{95\%}$ [0.01, 1.00], $n_{obs} = 173$
dispersion index
$\hat{\mu}_{median} = 0.40$
$\hat{\mu}_{median} = 0.55$
$\hat{\mu}_{median} = 0.61$
managed (n = 146)
pseudo_unmanaged (n = 18)
unmanaged (n = 9)
management class
Pairwise test: Dunn, Bars shown: significant

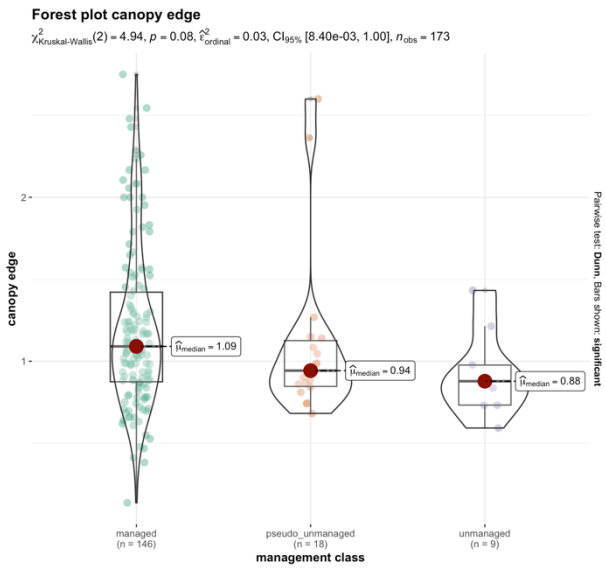
Forest plot canopy edge
$\chi^2_{Kruskal\text{-}Wallis}(2) = 4.94$, $p = 0.08$, $\hat{\varepsilon}^2_{ordinal} = 0.03$, $CI_{95\%}$ [8.40e-03, 1.00], $n_{obs} = 173$
canopy edge
$\hat{\mu}_{median} = 1.09$
$\hat{\mu}_{median} = 0.94$
$\hat{\mu}_{median} = 0.88$
managed (n = 146)
pseudo_unmanaged (n = 18)
unmanaged (n = 9)
management class
Pairwise test: Dunn, Bars shown: significant

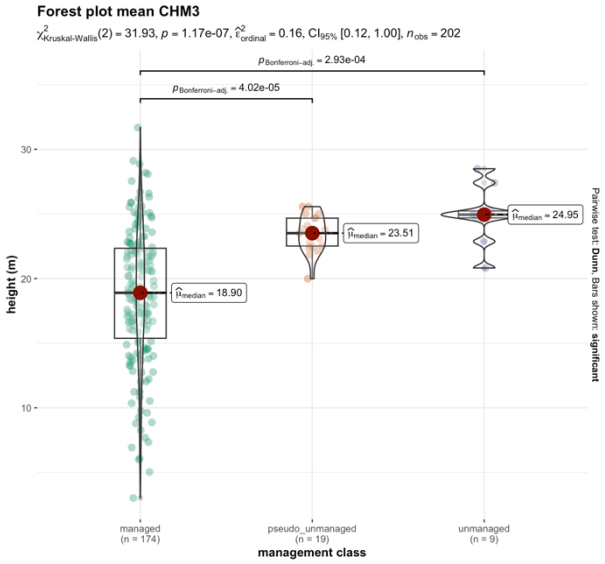
Forest plot mean CHM3
$\chi^2_{Kruskal-Wallis}(2) = 31.93$, $p = 1.17e-07$, $\hat{\epsilon}^2_{ordinal} = 0.16$, $CI_{95\%}$ [0.12, 1.00], $n_{obs} = 202$
$p_{Bonferroni-adj.} = 2.93e-04$
$p_{Bonferroni-adj.} = 4.02e-05$
$\hat{\mu}_{median} = 18.90$
$\hat{\mu}_{median} = 23.51$
$\hat{\mu}_{median} = 24.95$
height (m)
30
20
10
managed (n = 174)
pseudo_unmanaged (n = 19)
unmanaged (n = 9)
management class
Pairwise test: Dunn, Bars shown: significant

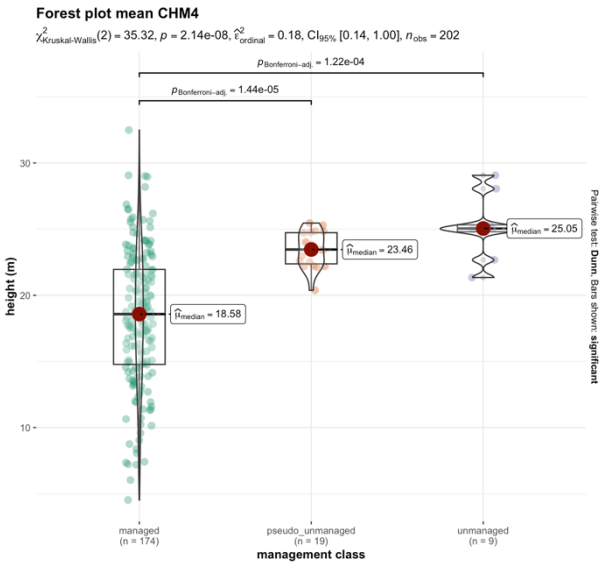
Forest plot mean CHM4
$\chi^2_{Kruskal-Wallis}(2) = 35.32$, $p = 2.14e-08$, $\hat{\epsilon}^2_{ordinal} = 0.18$, $CI_{95\%}$ [0.14, 1.00], $n_{obs} = 202$
$p_{Bonferroni-adj.} = 1.22e-04$
$p_{Bonferroni-adj.} = 1.44e-05$
$\hat{\mu}_{median} = 18.58$
$\hat{\mu}_{median} = 23.46$
$\hat{\mu}_{median} = 25.05$
height (m)
30
20
10
managed (n = 174)
pseudo_unmanaged (n = 19)
unmanaged (n = 9)
management class
Pairwise test: Dunn, Bars shown: significant

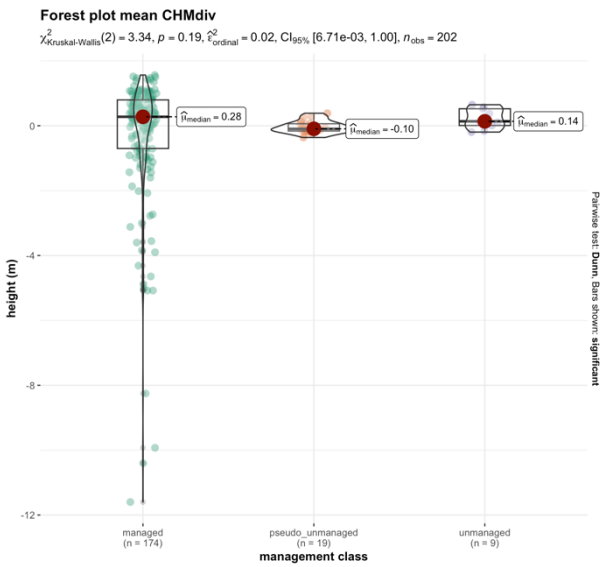
Forest plot mean CHMdiv
$\chi^2_{Kruskal-Wallis}(2) = 3.34$, $p = 0.19$, $\hat{\epsilon}^2_{ordinal} = 0.02$, $CI_{95\%}$ [6.71e-03, 1.00], $n_{obs} = 202$
$\hat{\mu}_{median} = 0.28$
$\hat{\mu}_{median} = -0.10$
$\hat{\mu}_{median} = 0.14$
height (m)
0
-4
-8
-12
managed (n = 174)
pseudo_unmanaged (n = 19)
unmanaged (n = 9)
management class
Pairwise test: Dunn, Bars shown: significant

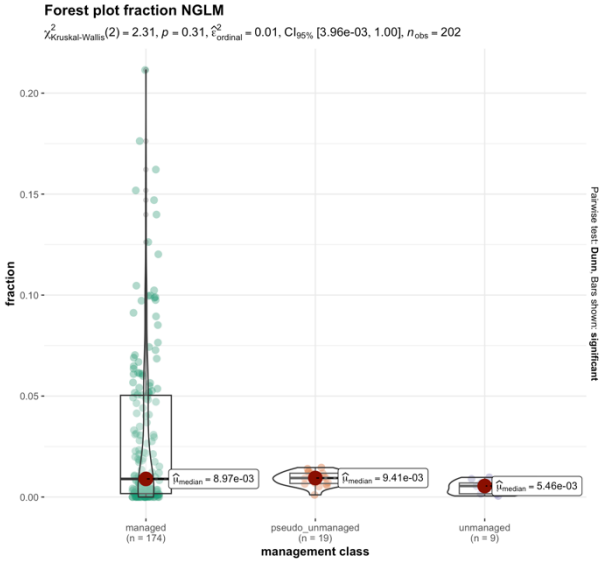
Forest plot fraction NGLM
$\chi^2_{Kruskal-Wallis}(2) = 2.31$, $p = 0.31$, $\hat{\epsilon}^2_{ordinal} = 0.01$, $CI_{95\%}$ [3.96e-03, 1.00], $n_{obs} = 202$
$\hat{\mu}_{median} = 8.97e-03$
$\hat{\mu}_{median} = 9.41e-03$
$\hat{\mu}_{median} = 5.46e-03$
fraction
0.20
0.15
0.10
0.05
0.00
managed (n = 174)
pseudo_unmanaged (n = 19)
unmanaged (n = 9)
management class
Pairwise test: Dunn, Bars shown: significant

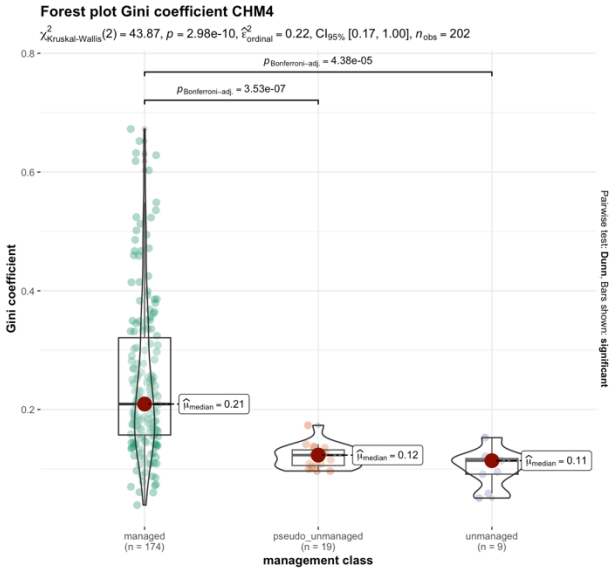
Forest plot Gini coefficient CHM4
$\chi^2_{Kruskal-Wallis}(2) = 43.87$, $p = 2.98e-10$, $\hat{\epsilon}^2_{ordinal} = 0.22$, $CI_{95\%}$ [0.17, 1.00], $n_{obs} = 202$
$p_{Bonferroni-adj.} = 4.38e-05$
$p_{Bonferroni-adj.} = 3.53e-07$
$\hat{\mu}_{median} = 0.21$
$\hat{\mu}_{median} = 0.12$
$\hat{\mu}_{median} = 0.11$
Gini coefficient
0.8
0.6
0.4
0.2
managed (n = 174)
pseudo_unmanaged (n = 19)
unmanaged (n = 9)
management class
Pairwise test: Dunn, Bars shown: significant

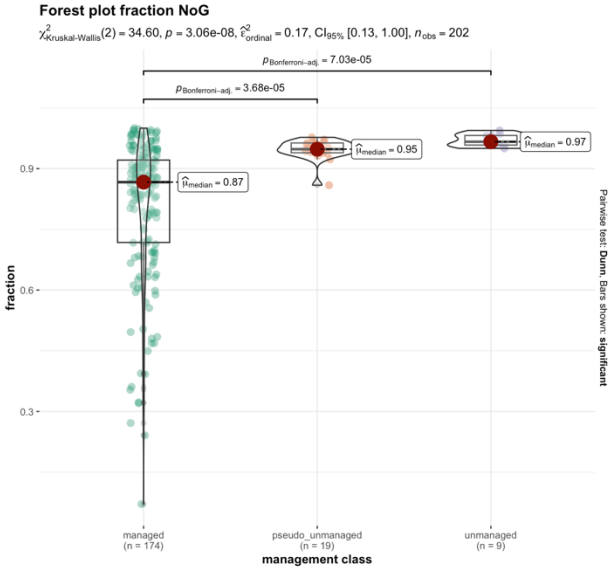
Forest plot fraction NoG
$\chi^2_{Kruskal-Wallis}(2) = 34.60$, $p = 3.06e-08$, $\hat{\epsilon}^2_{ordinal} = 0.17$, $CI_{95\%}$ [0.13, 1.00], $n_{obs} = 202$
$p_{Bonferroni-adj.} = 7.03e-05$
$p_{Bonferroni-adj.} = 3.68e-05$
$\hat{\mu}_{median} = 0.87$
$\hat{\mu}_{median} = 0.95$
$\hat{\mu}_{median} = 0.97$
fraction
0.9
0.6
0.3
managed (n = 174)
pseudo_unmanaged (n = 19)
unmanaged (n = 9)
management class
Pairwise test: Dunn, Bars shown: significant

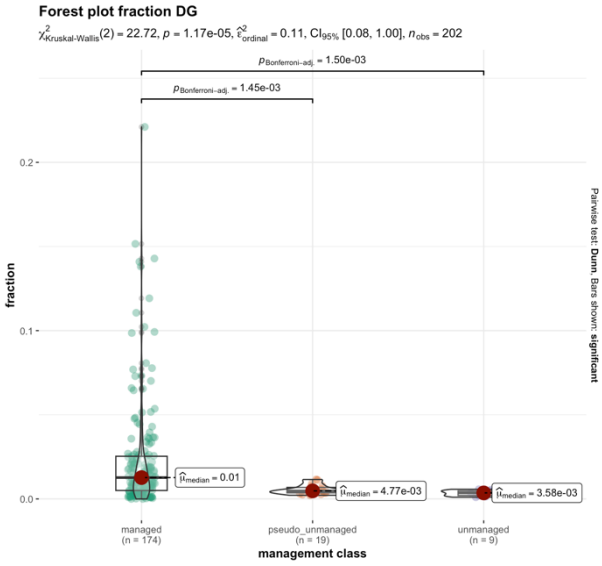
Forest plot fraction DG
$\chi^2_{Kruskal\text{-}Wallis}(2) = 22.72$, $p = 1.17e\text{-}05$, $\hat{\epsilon}^2_{ordinal} = 0.11$, $CI_{95\%}$ [0.08, 1.00], $n_{obs} = 202$
$p_{Bonferroni\text{-}adj.} = 1.50e\text{-}03$
$p_{Bonferroni\text{-}adj.} = 1.45e\text{-}03$
fraction
0.0
0.1
0.2
$\hat{\mu}_{median} = 0.01$
$\hat{\mu}_{median} = 4.77e\text{-}03$
$\hat{\mu}_{median} = 3.58e\text{-}03$
managed (n = 174)
pseudo_unmanaged (n = 19)
unmanaged (n = 9)
management class
Pairwise test: Dunn. Bars shown: significant

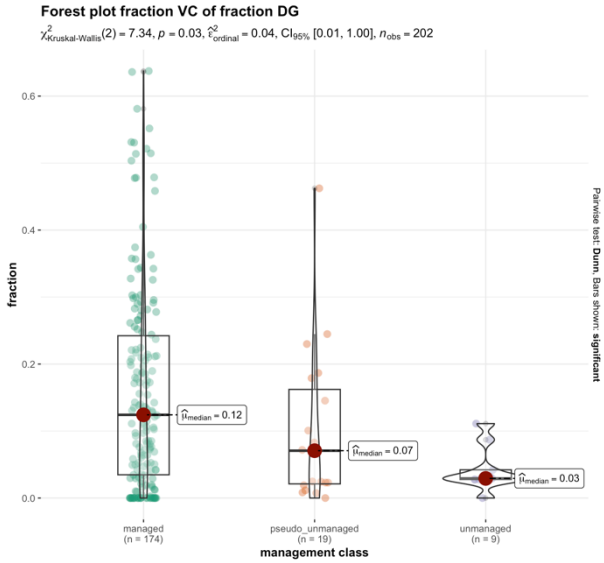
Forest plot fraction VC of fraction DG
$\chi^2_{Kruskal\text{-}Wallis}(2) = 7.34$, $p = 0.03$, $\hat{\epsilon}^2_{ordinal} = 0.04$, $CI_{95\%}$ [0.01, 1.00], $n_{obs} = 202$
fraction
0.0
0.2
0.4
0.6
$\hat{\mu}_{median} = 0.12$
$\hat{\mu}_{median} = 0.07$
$\hat{\mu}_{median} = 0.03$
managed (n = 174)
pseudo_unmanaged (n = 19)
unmanaged (n = 9)
management class
Pairwise test: Dunn. Bars shown: significant

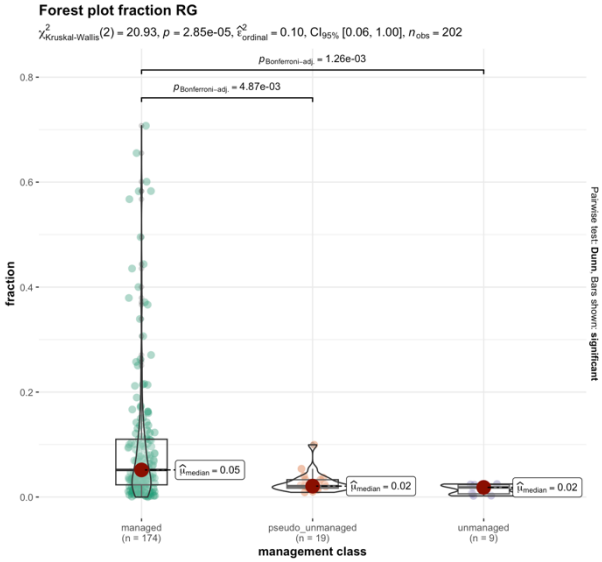
Forest plot fraction RG
$\chi^2_{Kruskal\text{-}Wallis}(2) = 20.93$, $p = 2.85e\text{-}05$, $\hat{\epsilon}^2_{ordinal} = 0.10$, $CI_{95\%}$ [0.06, 1.00], $n_{obs} = 202$
$p_{Bonferroni\text{-}adj.} = 1.26e\text{-}03$
$p_{Bonferroni\text{-}adj.} = 4.87e\text{-}03$
fraction
0.0
0.2
0.4
0.6
0.8
$\hat{\mu}_{median} = 0.05$
$\hat{\mu}_{median} = 0.02$
$\hat{\mu}_{median} = 0.02$
managed (n = 174)
pseudo_unmanaged (n = 19)
unmanaged (n = 9)
management class
Pairwise test: Dunn. Bars shown: significant

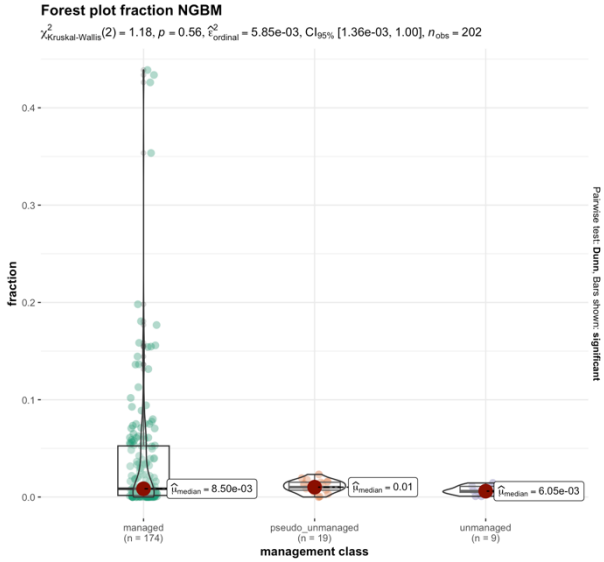
Forest plot fraction NGBM
$\chi^2_{Kruskal\text{-}Wallis}(2) = 1.18$, $p = 0.56$, $\hat{\epsilon}^2_{ordinal} = 5.85e\text{-}03$, $CI_{95\%}$ [1.36e-03, 1.00], $n_{obs} = 202$
fraction
0.0
0.1
0.2
0.3
0.4
$\hat{\mu}_{median} = 8.50e\text{-}03$
$\hat{\mu}_{median} = 0.01$
$\hat{\mu}_{median} = 6.05e\text{-}03$
managed (n = 174)
pseudo_unmanaged (n = 19)
unmanaged (n = 9)
management class
Pairwise test: Dunn. Bars shown: significant

Appendix F: Statistical comparisons to determine influence of dominant tree species for selection of variables on canopy gap level (F1) and on forest plot level (F2).

F1

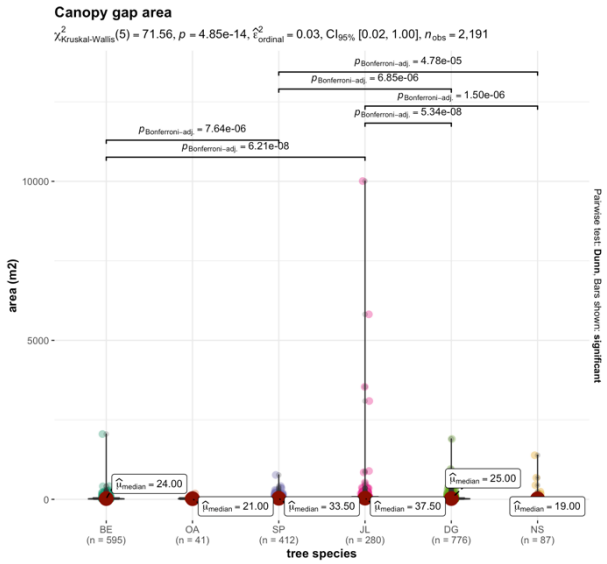

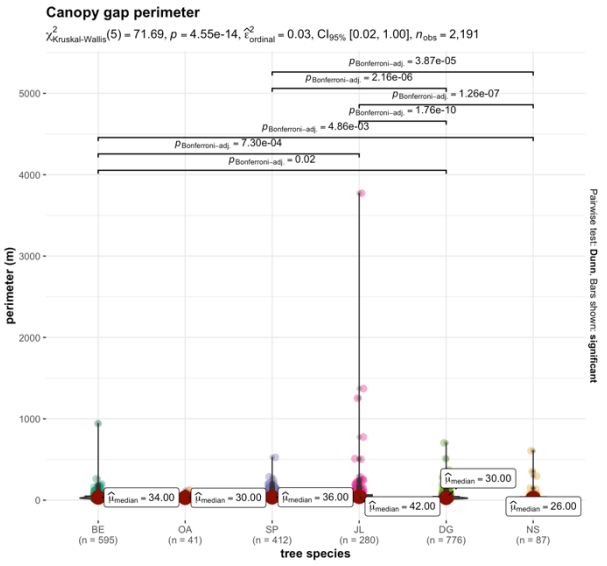

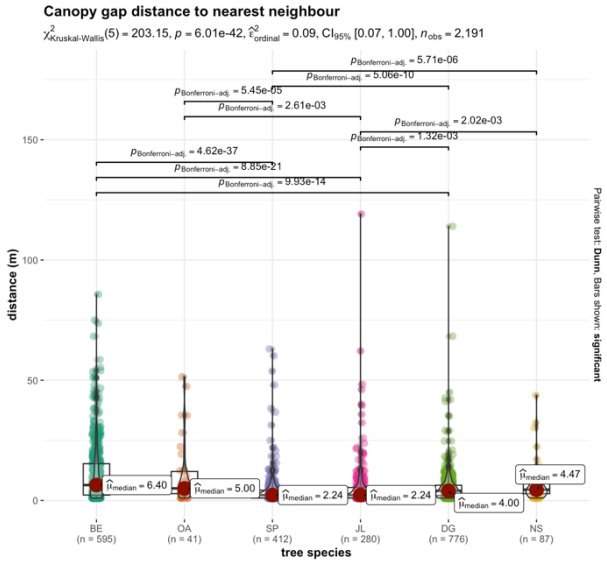

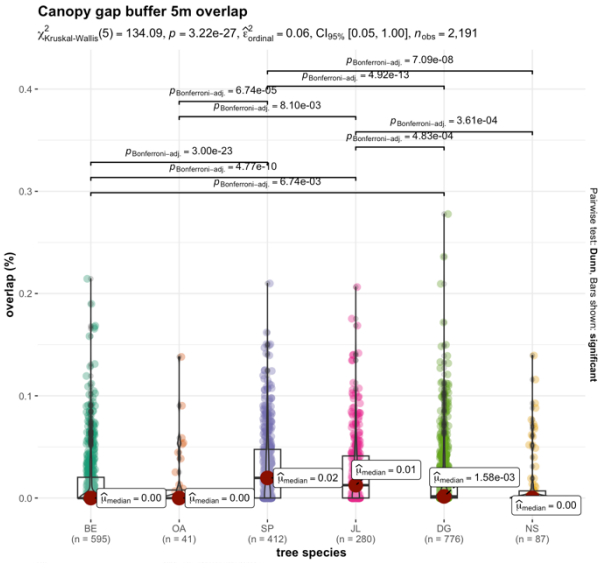

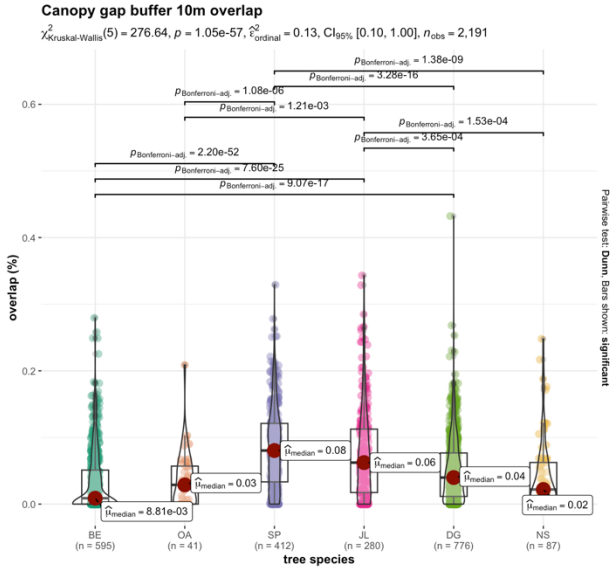

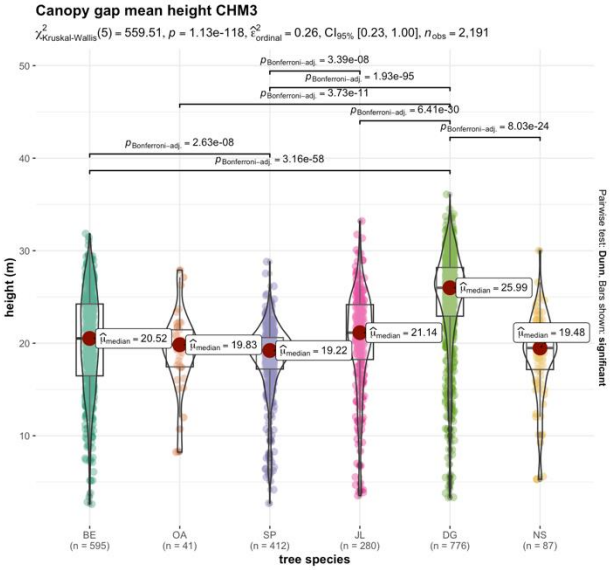

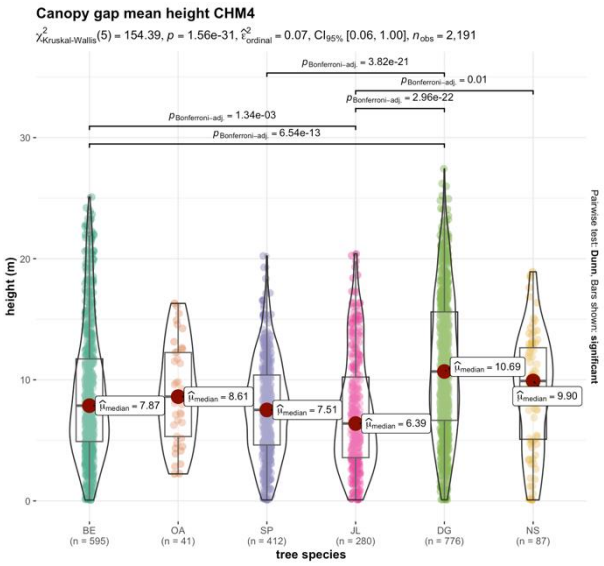
Canopy gap mean height CHM4
$\chi^2_{Kruskal\text{-}Wallis}(5) = 154.39$, $p = 1.56e\text{-}31$, $\hat{\varepsilon}^2_{ordinal} = 0.07$, $CI_{95\%}$ [0.06, 1.00], $n_{obs} = 2,191$
$p_{Bonferroni\text{-}adj.} = 3.82e\text{-}21$
$p_{Bonferroni\text{-}adj.} = 0.01$
$p_{Bonferroni\text{-}adj.} = 2.96e\text{-}22$
$p_{Bonferroni\text{-}adj.} = 1.34e\text{-}03$
$p_{Bonferroni\text{-}adj.} = 6.54e\text{-}13$
height (m)
$\hat{\mu}_{median} = 7.87$
$\hat{\mu}_{median} = 8.61$
$\hat{\mu}_{median} = 7.51$
$\hat{\mu}_{median} = 6.39$
$\hat{\mu}_{median} = 10.69$
$\hat{\mu}_{median} = 9.90$
BE (n = 595)
OA (n = 41)
SP (n = 412)
JL (n = 280)
DG (n = 776)
NS (n = 87)
tree species
Pairwise test: Dunn. Bars shown: significant

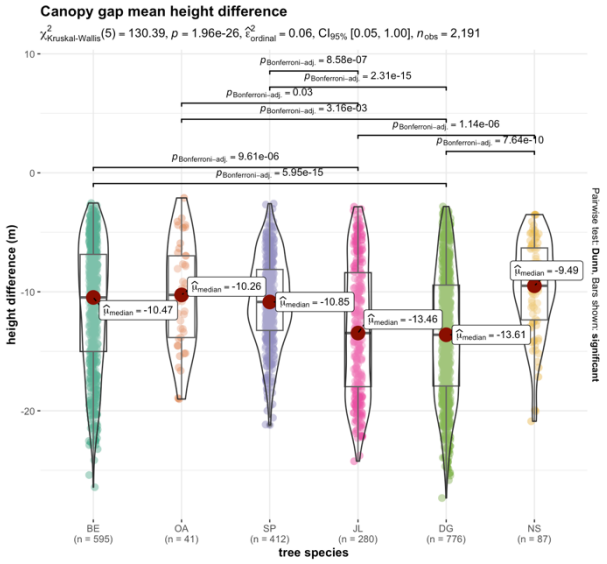
Canopy gap mean height difference
$\chi^2_{Kruskal\text{-}Wallis}(5) = 130.39$, $p = 1.96e\text{-}26$, $\hat{\varepsilon}^2_{ordinal} = 0.06$, $CI_{95\%}$ [0.05, 1.00], $n_{obs} = 2,191$
$p_{Bonferroni\text{-}adj.} = 8.58e\text{-}07$
$p_{Bonferroni\text{-}adj.} = 2.31e\text{-}15$
$p_{Bonferroni\text{-}adj.} = 0.03$
$p_{Bonferroni\text{-}adj.} = 3.16e\text{-}03$
$p_{Bonferroni\text{-}adj.} = 1.14e\text{-}06$
$p_{Bonferroni\text{-}adj.} = 7.64e\text{-}10$
$p_{Bonferroni\text{-}adj.} = 9.61e\text{-}06$
$p_{Bonferroni\text{-}adj.} = 5.95e\text{-}15$
height difference (m)
$\hat{\mu}_{median} = -10.47$
$\hat{\mu}_{median} = -10.26$
$\hat{\mu}_{median} = -10.85$
$\hat{\mu}_{median} = -13.46$
$\hat{\mu}_{median} = -13.61$
$\hat{\mu}_{median} = -9.49$
BE (n = 595)
OA (n = 41)
SP (n = 412)
JL (n = 280)
DG (n = 776)
NS (n = 87)
tree species
Pairwise test: Dunn. Bars shown: significant

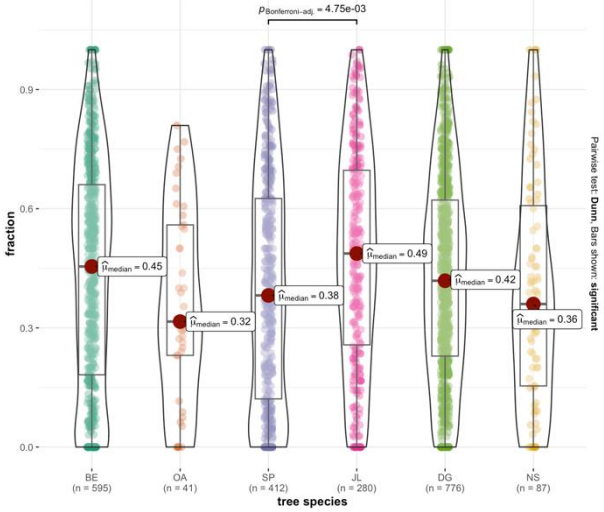
Canopy gap fraction NGBM
$\chi^2_{Kruskal\text{-}Wallis}(5) = 17.58$, $p = 3.52e\text{-}03$, $\hat{\varepsilon}^2_{ordinal} = 8.03e\text{-}03$, $CI_{95\%}$ [5.21e-03, 1.00], $n_{obs} = 2,191$
$p_{Bonferroni\text{-}adj.} = 4.75e\text{-}03$
fraction
$\hat{\mu}_{median} = 0.45$
$\hat{\mu}_{median} = 0.32$
$\hat{\mu}_{median} = 0.38$
$\hat{\mu}_{median} = 0.49$
$\hat{\mu}_{median} = 0.42$
$\hat{\mu}_{median} = 0.36$
BE (n = 595)
OA (n = 41)
SP (n = 412)
JL (n = 280)
DG (n = 776)
NS (n = 87)
tree species
Pairwise test: Dunn. Bars shown: significant

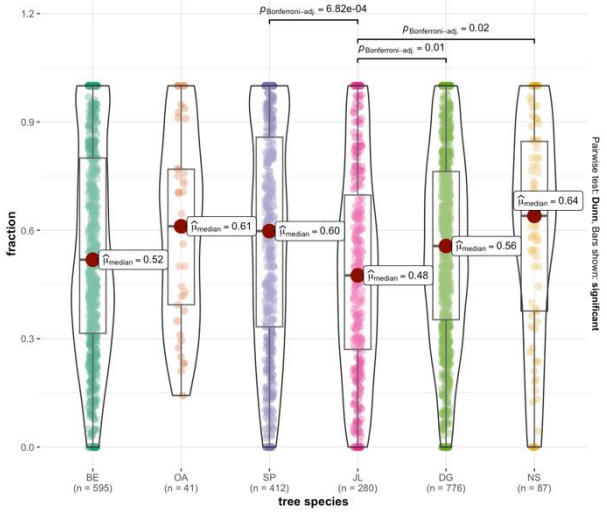
Canopy gap fraction NGLM
$\chi^2_{Kruskal\text{-}Wallis}(5) = 21.51$, $p = 6.48e\text{-}04$, $\hat{\varepsilon}^2_{ordinal} = 9.82e\text{-}03$, $CI_{95\%}$ [4.97e-03, 1.00], $n_{obs} = 2,191$
$p_{Bonferroni\text{-}adj.} = 6.82e\text{-}04$
$p_{Bonferroni\text{-}adj.} = 0.02$
$p_{Bonferroni\text{-}adj.} = 0.01$
fraction
$\hat{\mu}_{median} = 0.52$
$\hat{\mu}_{median} = 0.61$
$\hat{\mu}_{median} = 0.60$
$\hat{\mu}_{median} = 0.48$
$\hat{\mu}_{median} = 0.56$
$\hat{\mu}_{median} = 0.64$
BE (n = 595)
OA (n = 41)
SP (n = 412)
JL (n = 280)
DG (n = 776)
NS (n = 87)
tree species
Pairwise test: Dunn. Bars shown: significant

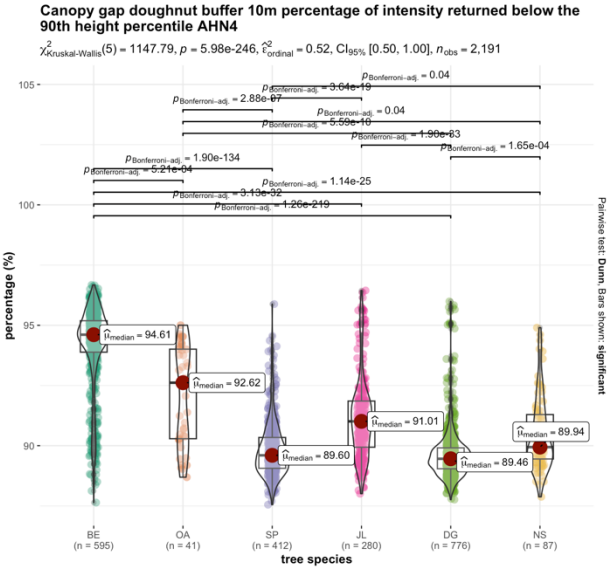
Canopy gap doughnut buffer 10m percentage of intensity returned below the 90th height percentile AHN4
$\chi^2_{Kruskal\text{-}Wallis}(5) = 1147.79$, $p = 5.98e\text{-}246$, $\hat{\varepsilon}^2_{ordinal} = 0.52$, $CI_{95\%}$ [0.50, 1.00], $n_{obs} = 2,191$
$p_{Bonferroni\text{-}adj.} = 0.04$
$p_{Bonferroni\text{-}adj.} = 3.64e\text{-}19$
$p_{Bonferroni\text{-}adj.} = 2.88e\text{-}87$
$p_{Bonferroni\text{-}adj.} = 0.04$
$p_{Bonferroni\text{-}adj.} = 5.59e\text{-}10$
$p_{Bonferroni\text{-}adj.} = 1.90e\text{-}63$
$p_{Bonferroni\text{-}adj.} = 1.65e\text{-}04$
$p_{Bonferroni\text{-}adj.} = 1.90e\text{-}134$
$p_{Bonferroni\text{-}adj.} = 5.21e\text{-}04$
$p_{Bonferroni\text{-}adj.} = 1.14e\text{-}25$
$p_{Bonferroni\text{-}adj.} = 3.13e\text{-}32$
$p_{Bonferroni\text{-}adj.} = 1.26e\text{-}219$
percentage (%)
$\hat{\mu}_{median} = 94.61$
$\hat{\mu}_{median} = 92.62$
$\hat{\mu}_{median} = 89.60$
$\hat{\mu}_{median} = 91.01$
$\hat{\mu}_{median} = 89.46$
$\hat{\mu}_{median} = 89.94$
BE (n = 595)
OA (n = 41)
SP (n = 412)
JL (n = 280)
DG (n = 776)
NS (n = 87)
tree species
Pairwise test: Dunn. Bars shown: significant

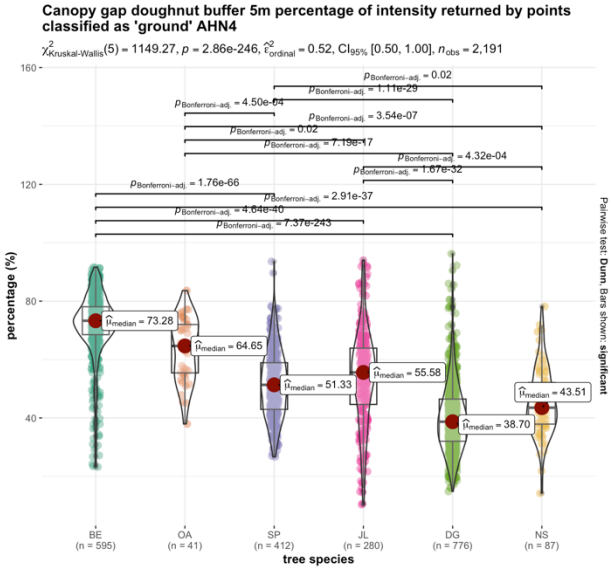
Canopy gap doughnut buffer 5m percentage of intensity returned by points classified as 'ground' AHN4
$\chi^2_{Kruskal\text{-}Wallis}(5) = 1149.27$, $p = 2.86e\text{-}246$, $\hat{\varepsilon}^2_{ordinal} = 0.52$, $CI_{95\%}$ [0.50, 1.00], $n_{obs} = 2,191$
$p_{Bonferroni\text{-}adj.} = 0.02$
$p_{Bonferroni\text{-}adj.} = 1.11e\text{-}29$
$p_{Bonferroni\text{-}adj.} = 4.50e\text{-}04$
$p_{Bonferroni\text{-}adj.} = 3.54e\text{-}07$
$p_{Bonferroni\text{-}adj.} = 0.02$
$p_{Bonferroni\text{-}adj.} = 7.19e\text{-}17$
$p_{Bonferroni\text{-}adj.} = 4.32e\text{-}04$
$p_{Bonferroni\text{-}adj.} = 1.67e\text{-}32$
$p_{Bonferroni\text{-}adj.} = 1.76e\text{-}66$
$p_{Bonferroni\text{-}adj.} = 2.91e\text{-}37$
$p_{Bonferroni\text{-}adj.} = 4.64e\text{-}40$
$p_{Bonferroni\text{-}adj.} = 7.37e\text{-}243$
percentage (%)
$\hat{\mu}_{median} = 73.28$
$\hat{\mu}_{median} = 64.65$
$\hat{\mu}_{median} = 51.33$
$\hat{\mu}_{median} = 55.58$
$\hat{\mu}_{median} = 38.70$
$\hat{\mu}_{median} = 43.51$
BE (n = 595)
OA (n = 41)
SP (n = 412)
JL (n = 280)
DG (n = 776)
NS (n = 87)
tree species
Pairwise test: Dunn. Bars shown: significant

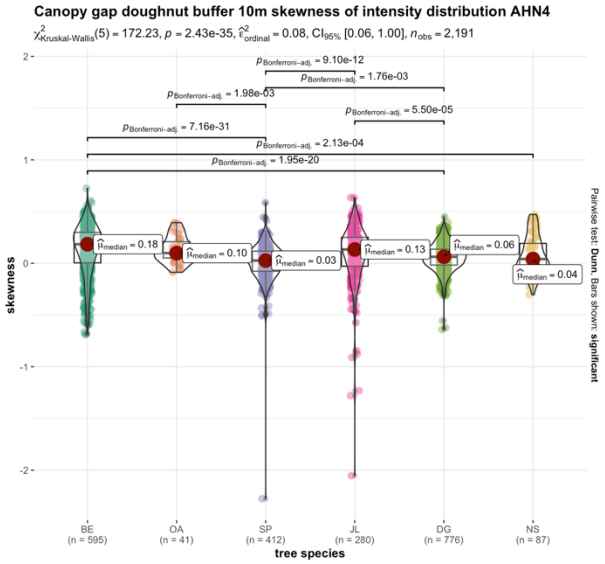
Canopy gap doughnut buffer 10m skewness of intensity distribution AHN4
skewness
tree species
Pairwise test: Dunn. Bars shown: significant

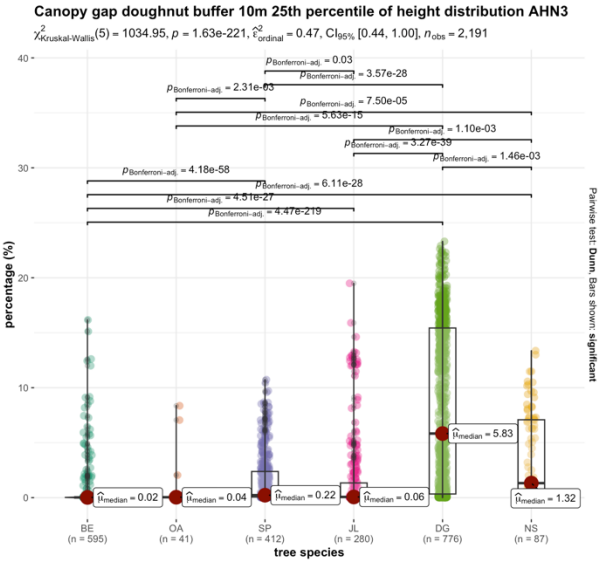
Canopy gap doughnut buffer 10m 25th percentile of height distribution AHN3
percentage (%)
tree species
Pairwise test: Dunn. Bars shown: significant

F2

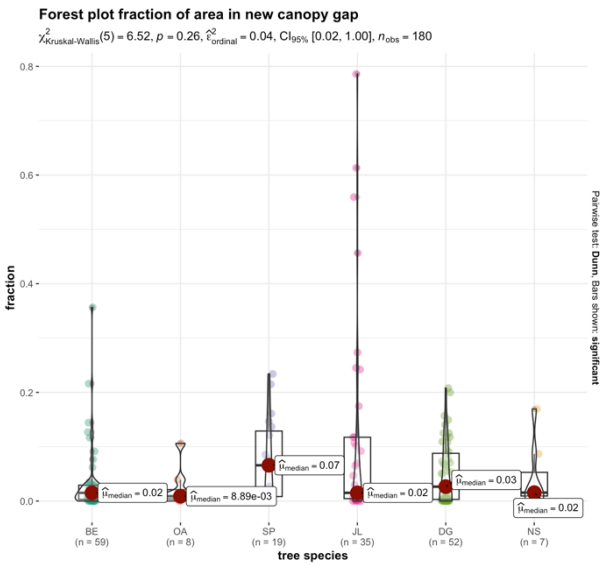
Forest plot fraction of area in new canopy gap
fraction
tree species
Pairwise test: Dunn. Bars shown: significant

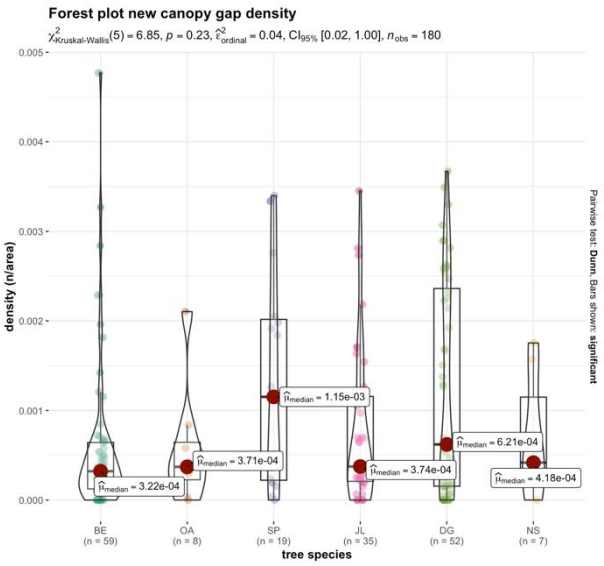
Forest plot new canopy gap density
density (n/area)
tree species
Pairwise test: Dunn. Bars shown: significant

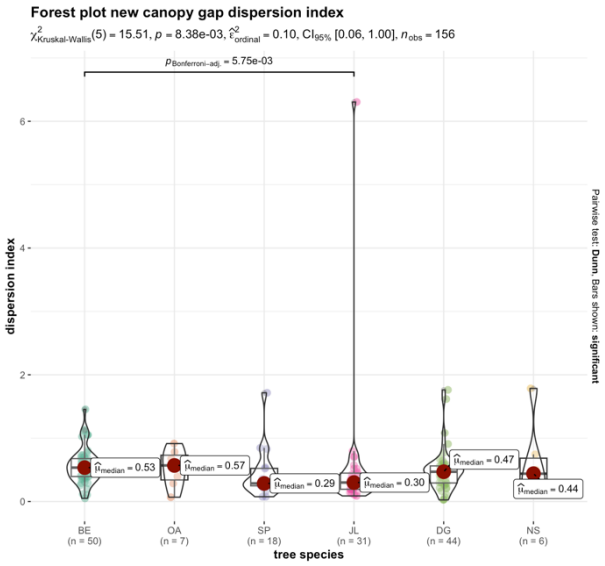
Forest plot new canopy gap dispersion index
dispersion index
tree species
Pairwise test: Dunn. Bars shown: significant

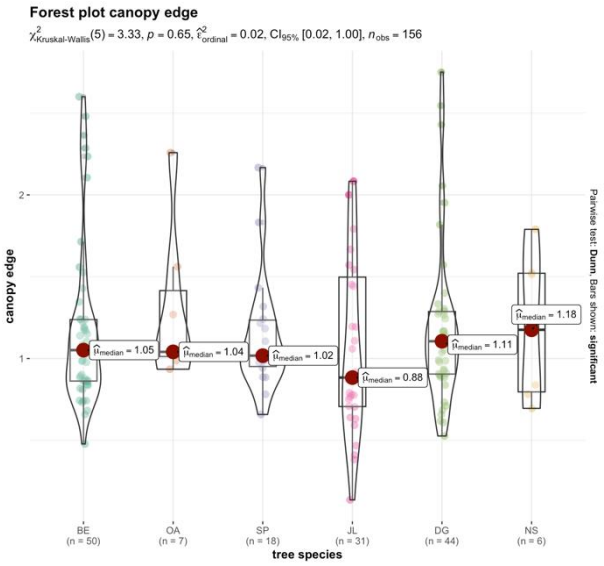
Forest plot canopy edge
canopy edge
tree species
Pairwise test: Dunn. Bars shown: significant

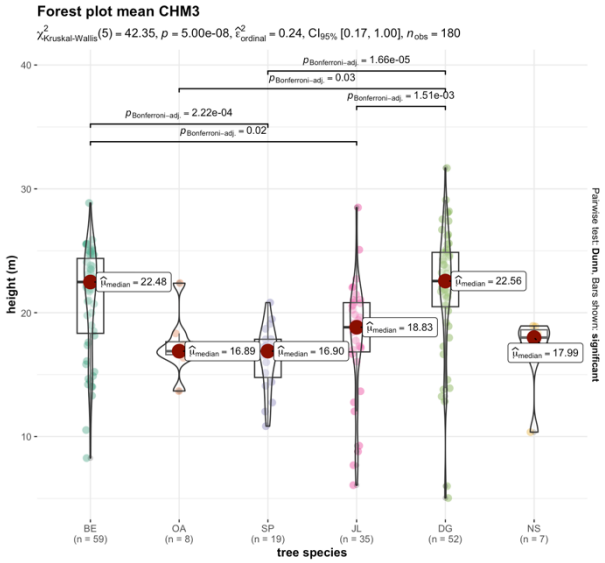
Forest plot mean CHM3
$\chi^2_{Kruskal-Wallis}(5) = 42.35$, $p = 5.00e-08$, $\hat{\epsilon}^2_{ordinal} = 0.24$, $CI_{95\%}$ [0.17, 1.00], $n_{obs} = 180$
$p_{Bonferroni-adj.} = 1.66e-05$
$p_{Bonferroni-adj.} = 0.03$
$p_{Bonferroni-adj.} = 1.51e-03$
$p_{Bonferroni-adj.} = 2.22e-04$
$p_{Bonferroni-adj.} = 0.02$
$\hat{\mu}_{median} = 22.48$
$\hat{\mu}_{median} = 16.89$
$\hat{\mu}_{median} = 16.90$
$\hat{\mu}_{median} = 18.83$
$\hat{\mu}_{median} = 22.56$
$\hat{\mu}_{median} = 17.99$
height (m)
40
30
20
10
BE (n = 59)
OA (n = 8)
SP (n = 19)
JL (n = 35)
DG (n = 52)
NS (n = 7)
tree species
Pairwise test: Dunn, Bars shown: significant

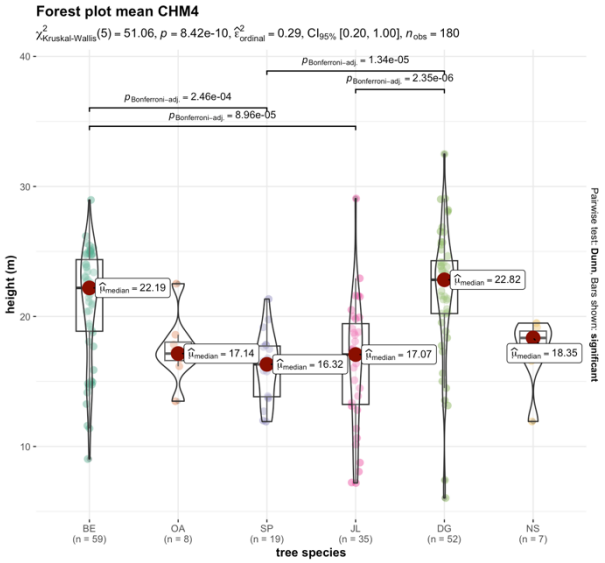
Forest plot mean CHM4
$\chi^2_{Kruskal-Wallis}(5) = 51.06$, $p = 8.42e-10$, $\hat{\epsilon}^2_{ordinal} = 0.29$, $CI_{95\%}$ [0.20, 1.00], $n_{obs} = 180$
$p_{Bonferroni-adj.} = 1.34e-05$
$p_{Bonferroni-adj.} = 2.35e-06$
$p_{Bonferroni-adj.} = 2.46e-04$
$p_{Bonferroni-adj.} = 8.96e-05$
$\hat{\mu}_{median} = 22.19$
$\hat{\mu}_{median} = 17.14$
$\hat{\mu}_{median} = 16.32$
$\hat{\mu}_{median} = 17.07$
$\hat{\mu}_{median} = 22.82$
$\hat{\mu}_{median} = 18.35$
height (m)
40
30
20
10
BE (n = 59)
OA (n = 8)
SP (n = 19)
JL (n = 35)
DG (n = 52)
NS (n = 7)
tree species
Pairwise test: Dunn, Bars shown: significant

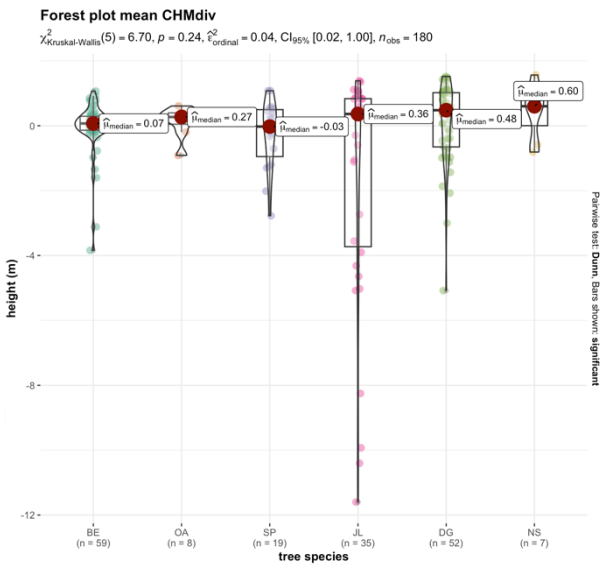
Forest plot mean CHMdiv
$\chi^2_{Kruskal-Wallis}(5) = 6.70$, $p = 0.24$, $\hat{\epsilon}^2_{ordinal} = 0.04$, $CI_{95\%}$ [0.02, 1.00], $n_{obs} = 180$
$\hat{\mu}_{median} = 0.07$
$\hat{\mu}_{median} = 0.27$
$\hat{\mu}_{median} = -0.03$
$\hat{\mu}_{median} = 0.36$
$\hat{\mu}_{median} = 0.48$
$\hat{\mu}_{median} = 0.60$
height (m)
0
-4
-8
-12
BE (n = 59)
OA (n = 8)
SP (n = 19)
JL (n = 35)
DG (n = 52)
NS (n = 7)
tree species
Pairwise test: Dunn, Bars shown: significant

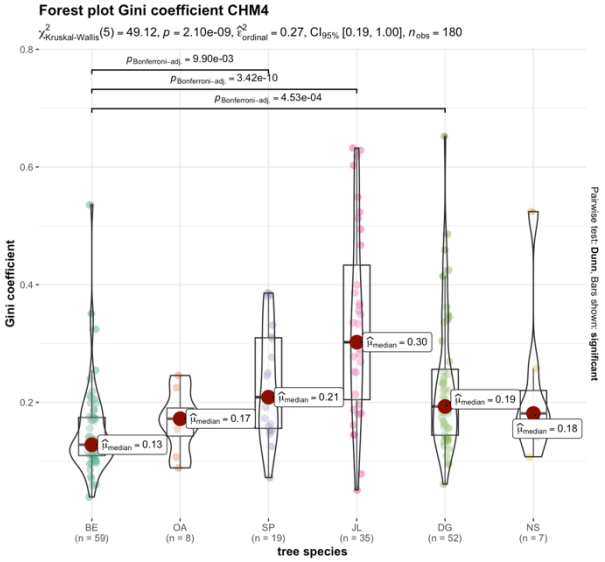
Forest plot Gini coefficient CHM4
$\chi^2_{Kruskal-Wallis}(5) = 49.12$, $p = 2.10e-09$, $\hat{\epsilon}^2_{ordinal} = 0.27$, $CI_{95\%}$ [0.19, 1.00], $n_{obs} = 180$
$p_{Bonferroni-adj.} = 9.90e-03$
$p_{Bonferroni-adj.} = 3.42e-10$
$p_{Bonferroni-adj.} = 4.53e-04$
$\hat{\mu}_{median} = 0.13$
$\hat{\mu}_{median} = 0.17$
$\hat{\mu}_{median} = 0.21$
$\hat{\mu}_{median} = 0.30$
$\hat{\mu}_{median} = 0.19$
$\hat{\mu}_{median} = 0.18$
Gini coefficient
0.8
0.6
0.4
0.2
BE (n = 59)
OA (n = 8)
SP (n = 19)
JL (n = 35)
DG (n = 52)
NS (n = 7)
tree species
Pairwise test: Dunn, Bars shown: significant

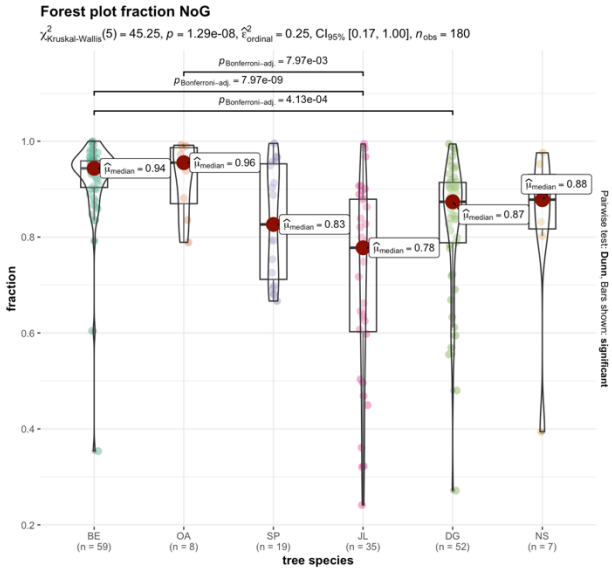
Forest plot fraction NoG
$\chi^2_{Kruskal-Wallis}(5) = 45.25$, $p = 1.29e-08$, $\hat{\epsilon}^2_{ordinal} = 0.25$, $CI_{95\%}$ [0.17, 1.00], $n_{obs} = 180$
$p_{Bonferroni-adj.} = 7.97e-03$
$p_{Bonferroni-adj.} = 7.97e-09$
$p_{Bonferroni-adj.} = 4.13e-04$
$\hat{\mu}_{median} = 0.94$
$\hat{\mu}_{median} = 0.96$
$\hat{\mu}_{median} = 0.83$
$\hat{\mu}_{median} = 0.78$
$\hat{\mu}_{median} = 0.87$
$\hat{\mu}_{median} = 0.88$
fraction
1.0
0.8
0.6
0.4
0.2
BE (n = 59)
OA (n = 8)
SP (n = 19)
JL (n = 35)
DG (n = 52)
NS (n = 7)
tree species
Pairwise test: Dunn, Bars shown: significant

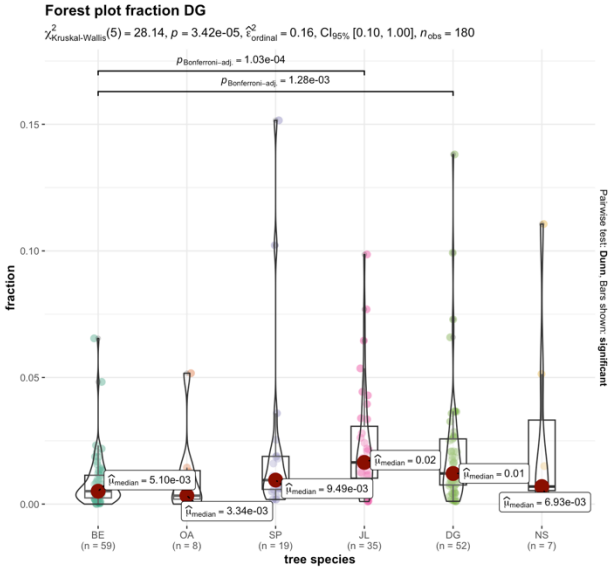
Forest plot fraction DG
$\chi^2_{Kruskal-Wallis}(5) = 28.14$, $p = 3.42e-05$, $\hat{\epsilon}^2_{ordinal} = 0.16$, $CI_{95\%}$ [0.10, 1.00], $n_{obs} = 180$
$p_{Bonferroni-adj.} = 1.03e-04$
$p_{Bonferroni-adj.} = 1.28e-03$
$\hat{\mu}_{median} = 5.10e-03$
$\hat{\mu}_{median} = 3.34e-03$
$\hat{\mu}_{median} = 9.49e-03$
$\hat{\mu}_{median} = 0.02$
$\hat{\mu}_{median} = 0.01$
$\hat{\mu}_{median} = 6.93e-03$
fraction
0.15
0.10
0.05
0.00
BE (n = 59)
OA (n = 8)
SP (n = 19)
JL (n = 35)
DG (n = 52)
NS (n = 7)
tree species
Pairwise test: Dunn, Bars shown: significant

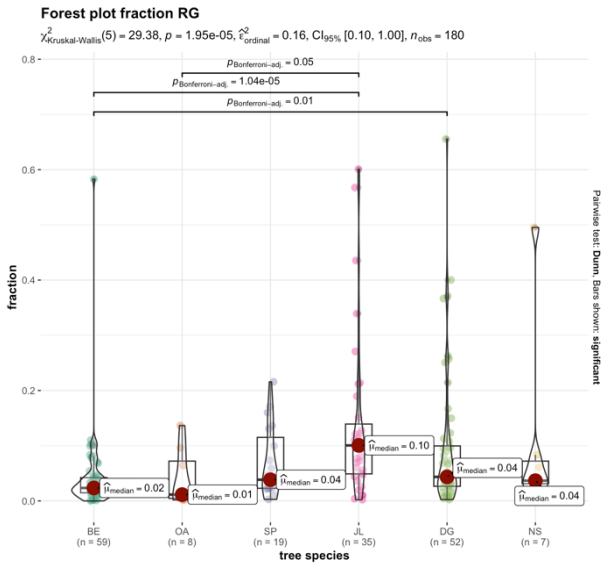
Forest plot fraction RG
$\chi^2_{Kruskal\text{-}Wallis}(5) = 29.38$, $p = 1.95e\text{-}05$, $\hat{\varepsilon}^2_{ordinal} = 0.16$, $CI_{95\%}$ [0.10, 1.00], $n_{obs} = 180$
$p_{Bonferroni\text{-}adj.} = 0.05$
$p_{Bonferroni\text{-}adj.} = 1.04e\text{-}05$
$p_{Bonferroni\text{-}adj.} = 0.01$
fraction
tree species
BE (n = 59)
OA (n = 8)
SP (n = 19)
JL (n = 35)
DG (n = 52)
NS (n = 7)
$\hat{\mu}_{median} = 0.02$
$\hat{\mu}_{median} = 0.01$
$\hat{\mu}_{median} = 0.04$
$\hat{\mu}_{median} = 0.10$
$\hat{\mu}_{median} = 0.04$
$\hat{\mu}_{median} = 0.04$
Pairwise test: Dunn. Bars shown: significant

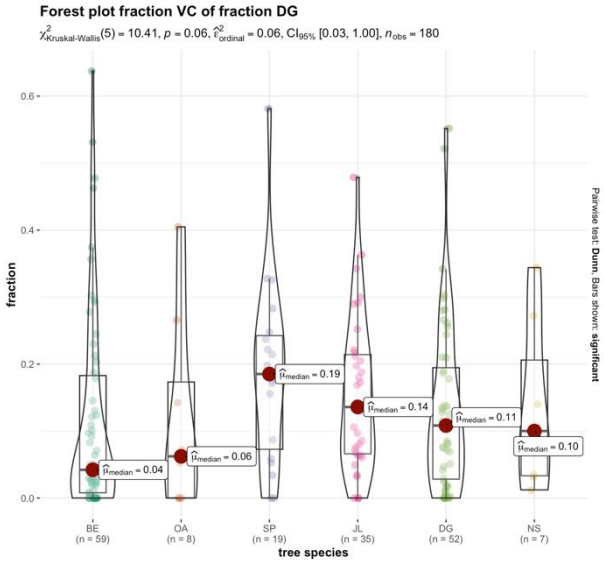
Forest plot fraction VC of fraction DG
$\chi^2_{Kruskal\text{-}Wallis}(5) = 10.41$, $p = 0.06$, $\hat{\varepsilon}^2_{ordinal} = 0.06$, $CI_{95\%}$ [0.03, 1.00], $n_{obs} = 180$
fraction
tree species
BE (n = 59)
OA (n = 8)
SP (n = 19)
JL (n = 35)
DG (n = 52)
NS (n = 7)
$\hat{\mu}_{median} = 0.04$
$\hat{\mu}_{median} = 0.06$
$\hat{\mu}_{median} = 0.19$
$\hat{\mu}_{median} = 0.14$
$\hat{\mu}_{median} = 0.11$
$\hat{\mu}_{median} = 0.10$
Pairwise test: Dunn. Bars shown: significant

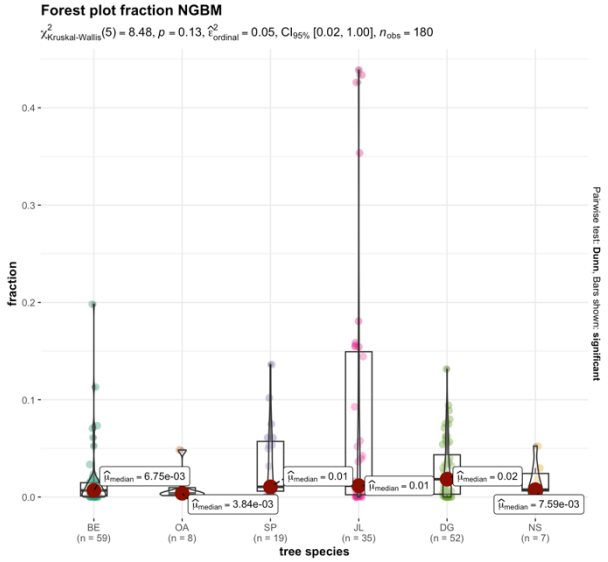
Forest plot fraction NGBM
$\chi^2_{Kruskal\text{-}Wallis}(5) = 8.48$, $p = 0.13$, $\hat{\varepsilon}^2_{ordinal} = 0.05$, $CI_{95\%}$ [0.02, 1.00], $n_{obs} = 180$
fraction
tree species
BE (n = 59)
OA (n = 8)
SP (n = 19)
JL (n = 35)
DG (n = 52)
NS (n = 7)
$\hat{\mu}_{median} = 6.75e\text{-}03$
$\hat{\mu}_{median} = 3.84e\text{-}03$
$\hat{\mu}_{median} = 0.01$
$\hat{\mu}_{median} = 0.01$
$\hat{\mu}_{median} = 0.02$
$\hat{\mu}_{median} = 7.59e\text{-}03$
Pairwise test: Dunn. Bars shown: significant

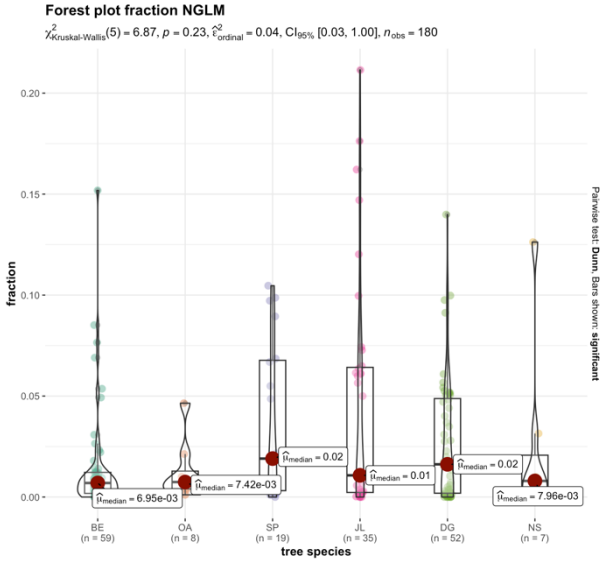
Forest plot fraction NGLM
$\chi^2_{Kruskal\text{-}Wallis}(5) = 6.87$, $p = 0.23$, $\hat{\varepsilon}^2_{ordinal} = 0.04$, $CI_{95\%}$ [0.03, 1.00], $n_{obs} = 180$
fraction
tree species
BE (n = 59)
OA (n = 8)
SP (n = 19)
JL (n = 35)
DG (n = 52)
NS (n = 7)
$\hat{\mu}_{median} = 6.95e\text{-}03$
$\hat{\mu}_{median} = 7.42e\text{-}03$
$\hat{\mu}_{median} = 0.02$
$\hat{\mu}_{median} = 0.01$
$\hat{\mu}_{median} = 0.02$
$\hat{\mu}_{median} = 7.96e\text{-}03$
Pairwise test: Dunn. Bars shown: significant

Appendix G: Statistical comparisons to determine influence of management type for beech for selection of variables on canopy gap level (G1) and on forest plot level (G2).

G1

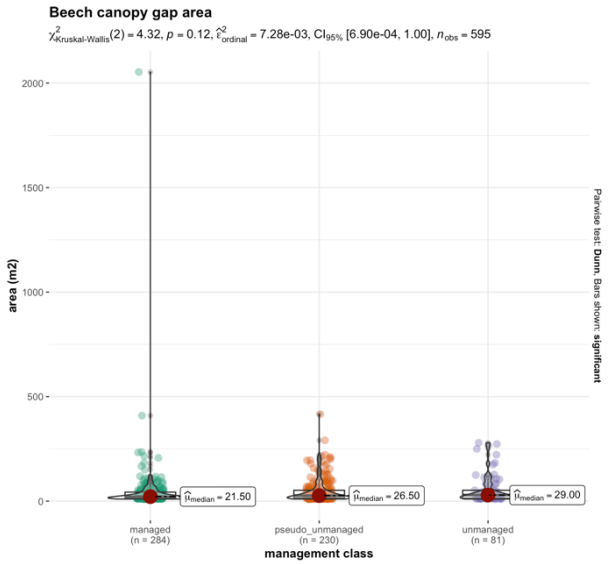

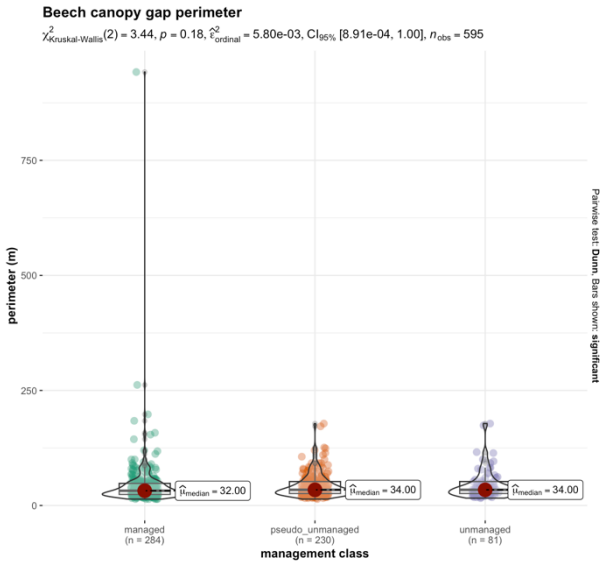

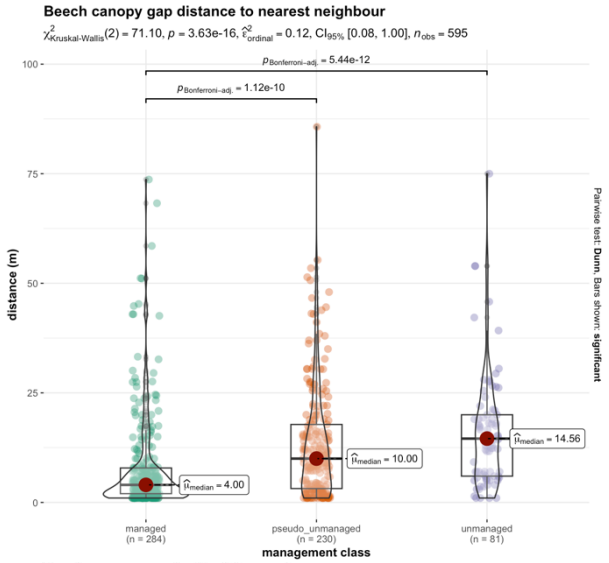

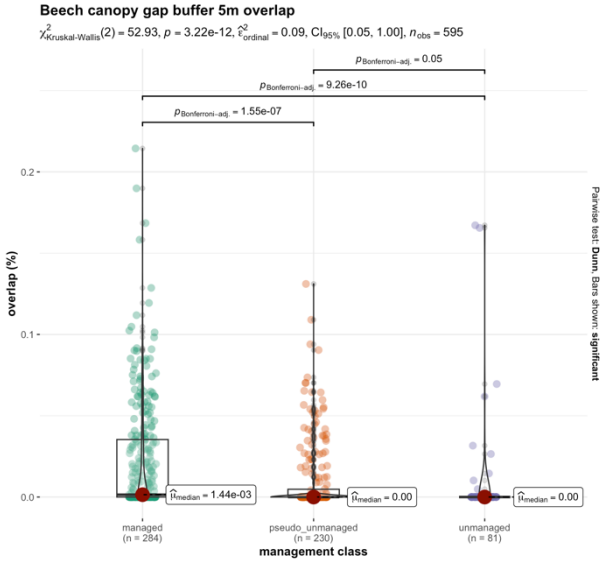

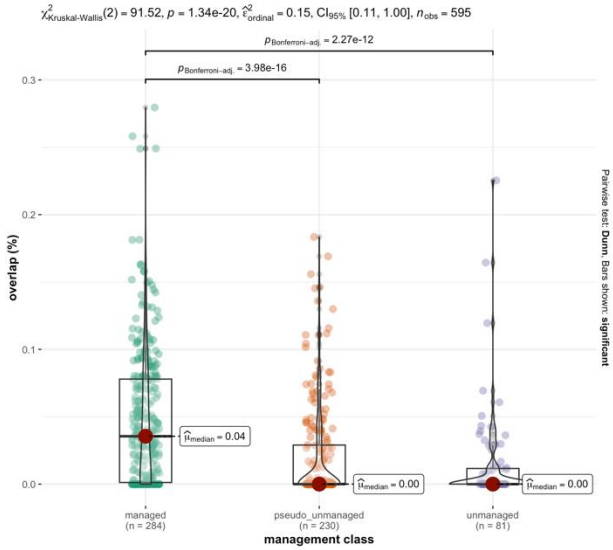

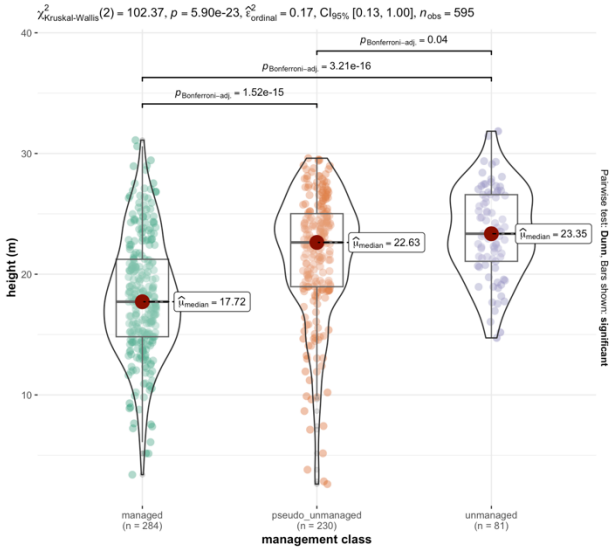

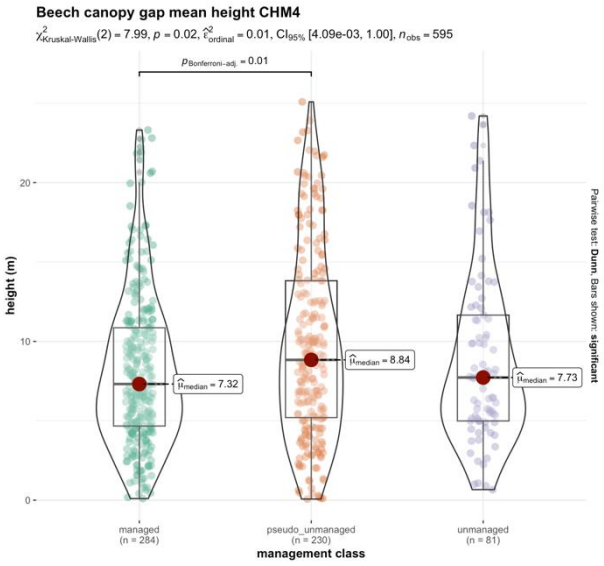
Beech canopy gap mean height CHM4
$\chi^2_{Kruskal\text{-}Wallis}(2) = 7.99$, $p = 0.02$, $\hat{\varepsilon}^2_{ordinal} = 0.01$, $CI_{95\%}$ [4.09e-03, 1.00], $n_{obs} = 595$
$p_{Bonferroni\text{-}adj.} = 0.01$
height (m)
20
10
0
$\hat{\mu}_{median} = 7.32$
$\hat{\mu}_{median} = 8.84$
$\hat{\mu}_{median} = 7.73$
managed (n = 284)
pseudo_unmanaged (n = 230)
unmanaged (n = 81)
management class
Pairwise test: Dunn. Bars shown: significant

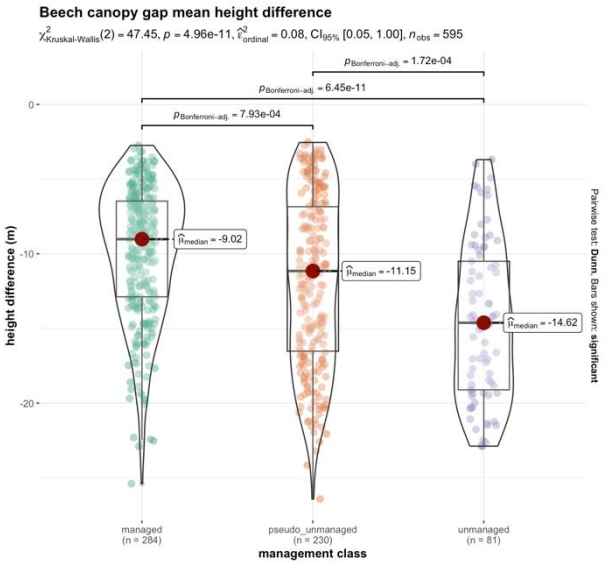
Beech canopy gap mean height difference
$\chi^2_{Kruskal\text{-}Wallis}(2) = 47.45$, $p = 4.96e\text{-}11$, $\hat{\varepsilon}^2_{ordinal} = 0.08$, $CI_{95\%}$ [0.05, 1.00], $n_{obs} = 595$
$p_{Bonferroni\text{-}adj.} = 1.72e\text{-}04$
$p_{Bonferroni\text{-}adj.} = 6.45e\text{-}11$
$p_{Bonferroni\text{-}adj.} = 7.93e\text{-}04$
height difference (m)
0
-10
-20
$\hat{\mu}_{median} = -9.02$
$\hat{\mu}_{median} = -11.15$
$\hat{\mu}_{median} = -14.62$
managed (n = 284)
pseudo_unmanaged (n = 230)
unmanaged (n = 81)
management class
Pairwise test: Dunn. Bars shown: significant

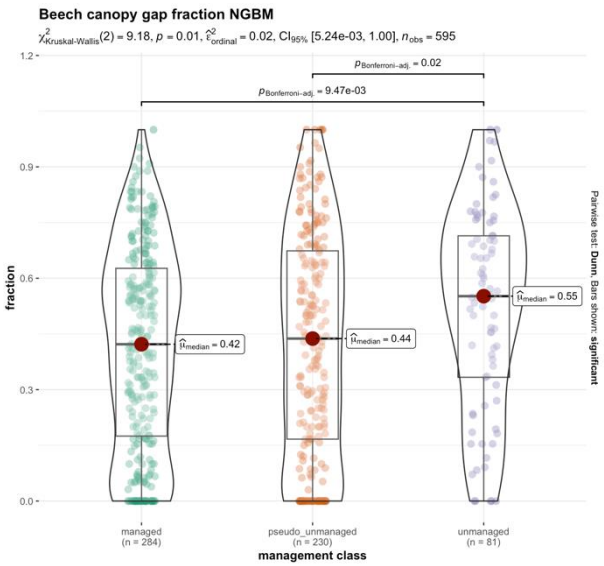
Beech canopy gap fraction NGBM
$\chi^2_{Kruskal\text{-}Wallis}(2) = 9.18$, $p = 0.01$, $\hat{\varepsilon}^2_{ordinal} = 0.02$, $CI_{95\%}$ [5.24e-03, 1.00], $n_{obs} = 595$
$p_{Bonferroni\text{-}adj.} = 0.02$
$p_{Bonferroni\text{-}adj.} = 9.47e\text{-}03$
fraction
1.2
0.9
0.6
0.3
0.0
$\hat{\mu}_{median} = 0.42$
$\hat{\mu}_{median} = 0.44$
$\hat{\mu}_{median} = 0.55$
managed (n = 284)
pseudo_unmanaged (n = 230)
unmanaged (n = 81)
management class
Pairwise test: Dunn. Bars shown: significant

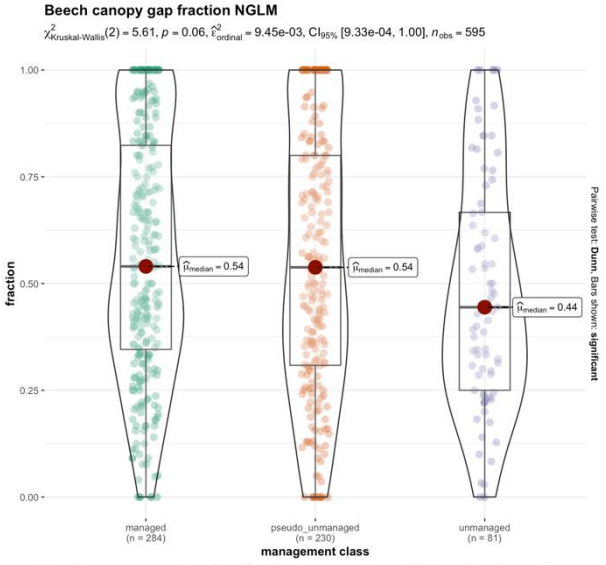
Beech canopy gap fraction NGLM
$\chi^2_{Kruskal\text{-}Wallis}(2) = 5.61$, $p = 0.06$, $\hat{\varepsilon}^2_{ordinal} = 9.45e\text{-}03$, $CI_{95\%}$ [9.33e-04, 1.00], $n_{obs} = 595$
fraction
1.00
0.75
0.50
0.25
0.00
$\hat{\mu}_{median} = 0.54$
$\hat{\mu}_{median} = 0.54$
$\hat{\mu}_{median} = 0.44$
managed (n = 284)
pseudo_unmanaged (n = 230)
unmanaged (n = 81)
management class
Pairwise test: Dunn. Bars shown: significant

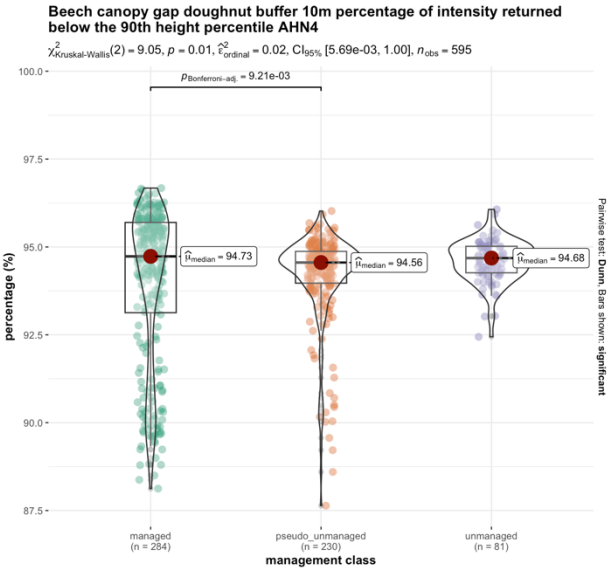
Beech canopy gap doughnut buffer 10m percentage of intensity returned below the 90th height percentile AHN4
$\chi^2_{Kruskal\text{-}Wallis}(2) = 9.05$, $p = 0.01$, $\hat{\varepsilon}^2_{ordinal} = 0.02$, $CI_{95\%}$ [5.69e-03, 1.00], $n_{obs} = 595$
$p_{Bonferroni\text{-}adj.} = 9.21e\text{-}03$
percentage (%)
100.0
97.5
95.0
92.5
90.0
87.5
$\hat{\mu}_{median} = 94.73$
$\hat{\mu}_{median} = 94.56$
$\hat{\mu}_{median} = 94.68$
managed (n = 284)
pseudo_unmanaged (n = 230)
unmanaged (n = 81)
management class
Pairwise test: Dunn. Bars shown: significant

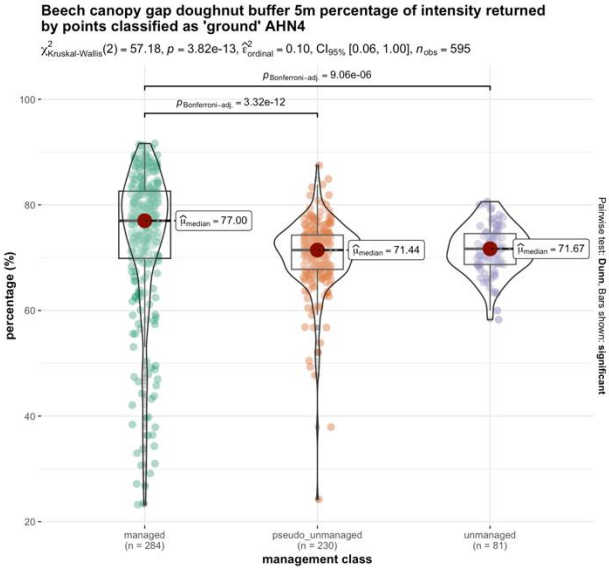
Beech canopy gap doughnut buffer 5m percentage of intensity returned by points classified as 'ground' AHN4
$\chi^2_{Kruskal\text{-}Wallis}(2) = 57.18$, $p = 3.82e\text{-}13$, $\hat{\varepsilon}^2_{ordinal} = 0.10$, $CI_{95\%}$ [0.06, 1.00], $n_{obs} = 595$
$p_{Bonferroni\text{-}adj.} = 9.06e\text{-}06$
$p_{Bonferroni\text{-}adj.} = 3.32e\text{-}12$
percentage (%)
100
80
60
40
20
$\hat{\mu}_{median} = 77.00$
$\hat{\mu}_{median} = 71.44$
$\hat{\mu}_{median} = 71.67$
managed (n = 284)
pseudo_unmanaged (n = 230)
unmanaged (n = 81)
management class
Pairwise test: Dunn. Bars shown: significant

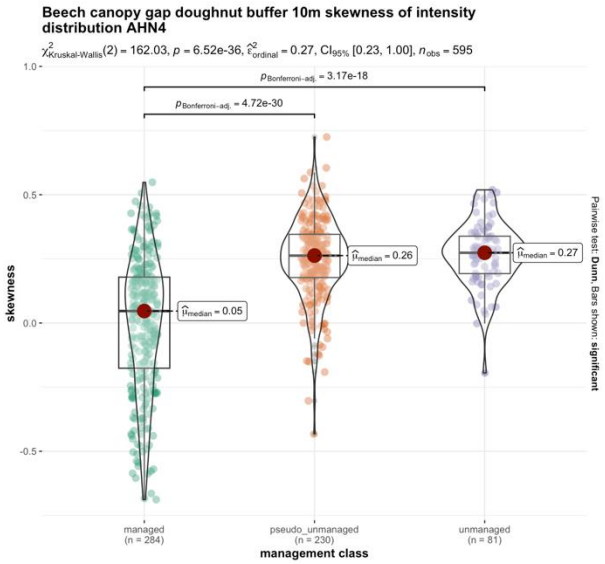
Beech canopy gap doughnut buffer 10m skewness of intensity distribution AHN4
$\chi^2_{Kruskal\text{-}Wallis}(2) = 162.03$, $p = 6.52e\text{-}36$, $\hat{\epsilon}^2_{ordinal} = 0.27$, $CI_{95\%}$ [0.23, 1.00], $n_{obs} = 595$
$p_{Bonferroni\text{-}adj.} = 3.17e\text{-}18$
$p_{Bonferroni\text{-}adj.} = 4.72e\text{-}30$
skewness
1.0
0.5
0.0
-0.5
$\hat{\mu}_{median} = 0.05$
$\hat{\mu}_{median} = 0.26$
$\hat{\mu}_{median} = 0.27$
managed (n = 284)
pseudo_unmanaged (n = 230)
unmanaged (n = 81)
management class
Pairwise test: Dunn, Bars shown: significant

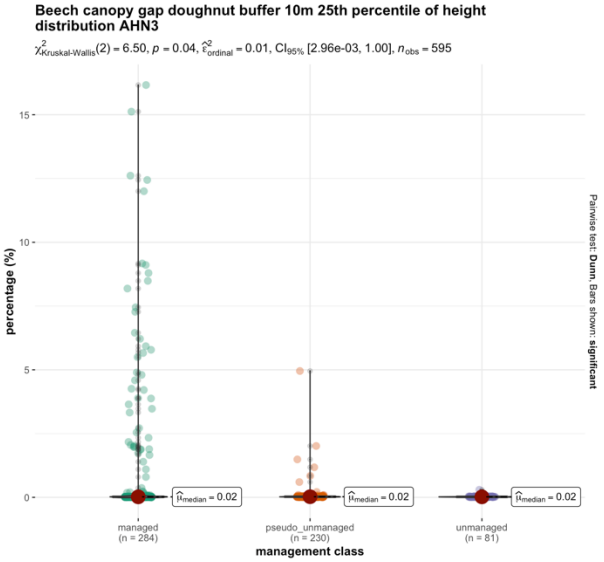
Beech canopy gap doughnut buffer 10m 25th percentile of height distribution AHN3
$\chi^2_{Kruskal\text{-}Wallis}(2) = 6.50$, $p = 0.04$, $\hat{\epsilon}^2_{ordinal} = 0.01$, $CI_{95\%}$ [2.96e-03, 1.00], $n_{obs} = 595$
percentage (%)
15
10
5
0
$\hat{\mu}_{median} = 0.02$
$\hat{\mu}_{median} = 0.02$
$\hat{\mu}_{median} = 0.02$
managed (n = 284)
pseudo_unmanaged (n = 230)
unmanaged (n = 81)
management class
Pairwise test: Dunn, Bars shown: significant

G2

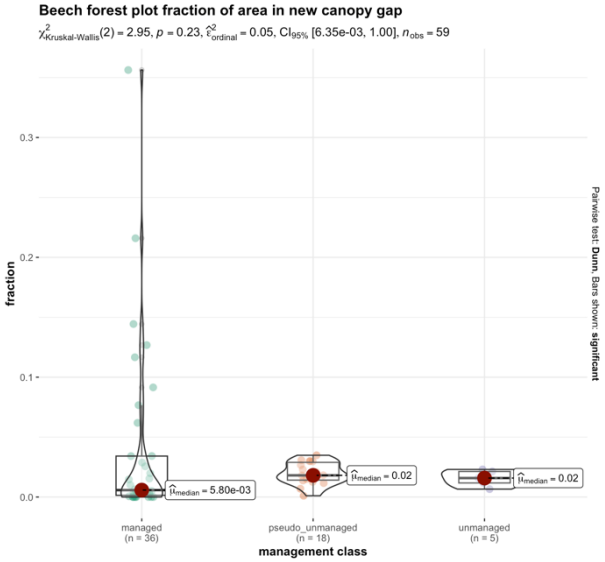
Beech forest plot fraction of area in new canopy gap
$\chi^2_{Kruskal\text{-}Wallis}(2) = 2.95$, $p = 0.23$, $\hat{\epsilon}^2_{ordinal} = 0.05$, $CI_{95\%}$ [6.35e-03, 1.00], $n_{obs} = 59$
fraction
0.3
0.2
0.1
0.0
$\hat{\mu}_{median} = 5.80e\text{-}03$
$\hat{\mu}_{median} = 0.02$
$\hat{\mu}_{median} = 0.02$
managed (n = 36)
pseudo_unmanaged (n = 18)
unmanaged (n = 5)
management class
Pairwise test: Dunn, Bars shown: significant

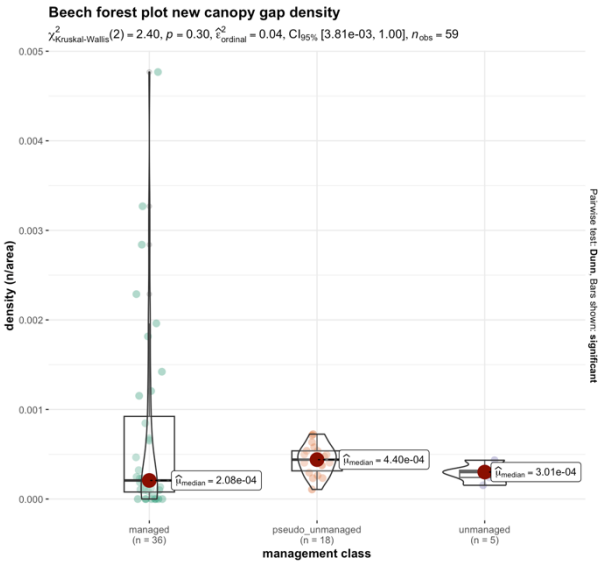
Beech forest plot new canopy gap density
$\chi^2_{Kruskal\text{-}Wallis}(2) = 2.40$, $p = 0.30$, $\hat{\epsilon}^2_{ordinal} = 0.04$, $CI_{95\%}$ [3.81e-03, 1.00], $n_{obs} = 59$
density (n/area)
0.005
0.004
0.003
0.002
0.001
0.000
$\hat{\mu}_{median} = 2.08e\text{-}04$
$\hat{\mu}_{median} = 4.40e\text{-}04$
$\hat{\mu}_{median} = 3.01e\text{-}04$
managed (n = 36)
pseudo_unmanaged (n = 18)
unmanaged (n = 5)
management class
Pairwise test: Dunn, Bars shown: significant

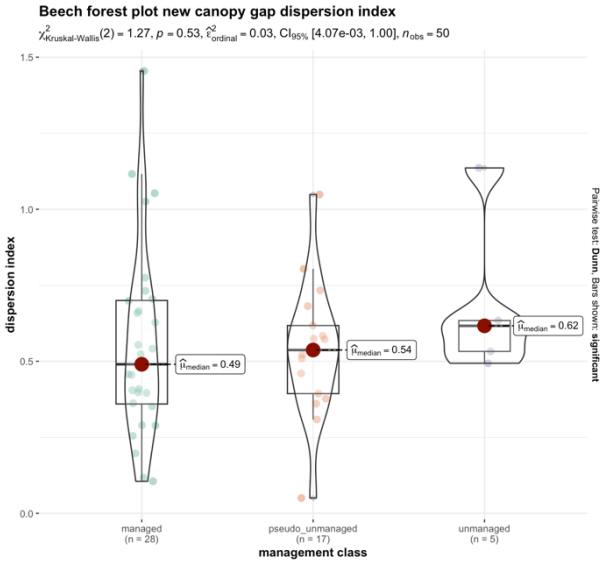
Beech forest plot new canopy gap dispersion index
$\chi^2_{Kruskal\text{-}Wallis}(2) = 1.27$, $p = 0.53$, $\hat{\epsilon}^2_{ordinal} = 0.03$, $CI_{95\%}$ [4.07e-03, 1.00], $n_{obs} = 50$
dispersion index
1.5
1.0
0.5
0.0
$\hat{\mu}_{median} = 0.49$
$\hat{\mu}_{median} = 0.54$
$\hat{\mu}_{median} = 0.62$
managed (n = 28)
pseudo_unmanaged (n = 17)
unmanaged (n = 5)
management class
Pairwise test: Dunn, Bars shown: significant

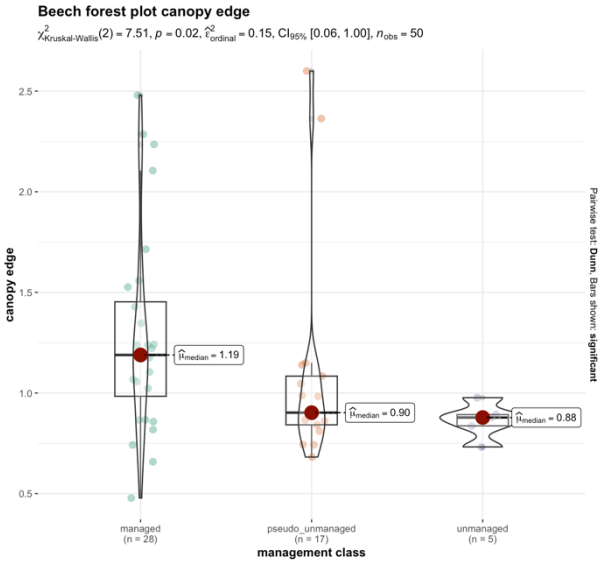
Beech forest plot canopy edge
$\chi^2_{Kruskal\text{-}Wallis}(2) = 7.51$, $p = 0.02$, $\hat{\epsilon}^2_{ordinal} = 0.15$, $CI_{95\%}$ [0.06, 1.00], $n_{obs} = 50$
canopy edge
2.5
2.0
1.5
1.0
0.5
$\hat{\mu}_{median} = 1.19$
$\hat{\mu}_{median} = 0.90$
$\hat{\mu}_{median} = 0.88$
managed (n = 28)
pseudo_unmanaged (n = 17)
unmanaged (n = 5)
management class
Pairwise test: Dunn, Bars shown: significant

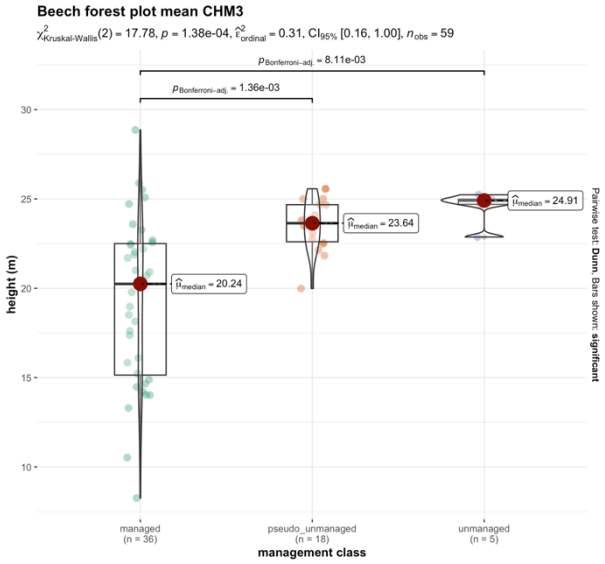
Beech forest plot mean CHM3
$\chi^2_{Kruskal-Wallis}(2) = 17.78$, $p = 1.38e-04$, $\hat{\epsilon}^2_{ordinal} = 0.31$, $CI_{95\%}$ [0.16, 1.00], $n_{obs} = 59$
$p_{Bonferroni-adj.} = 8.11e-03$
$p_{Bonferroni-adj.} = 1.36e-03$
$\hat{\mu}_{median} = 20.24$
$\hat{\mu}_{median} = 23.64$
$\hat{\mu}_{median} = 24.91$
height (m)
30
25
20
15
10
managed (n = 36)
pseudo_unmanaged (n = 18)
unmanaged (n = 5)
management class
Pairwise test: Dunn, Bars shown: significant

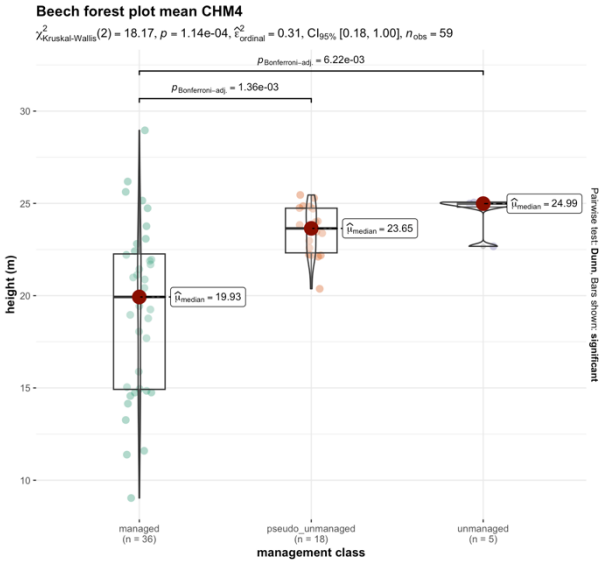
Beech forest plot mean CHM4
$\chi^2_{Kruskal-Wallis}(2) = 18.17$, $p = 1.14e-04$, $\hat{\epsilon}^2_{ordinal} = 0.31$, $CI_{95\%}$ [0.18, 1.00], $n_{obs} = 59$
$p_{Bonferroni-adj.} = 6.22e-03$
$p_{Bonferroni-adj.} = 1.36e-03$
$\hat{\mu}_{median} = 19.93$
$\hat{\mu}_{median} = 23.65$
$\hat{\mu}_{median} = 24.99$
height (m)
30
25
20
15
10
managed (n = 36)
pseudo_unmanaged (n = 18)
unmanaged (n = 5)
management class
Pairwise test: Dunn, Bars shown: significant

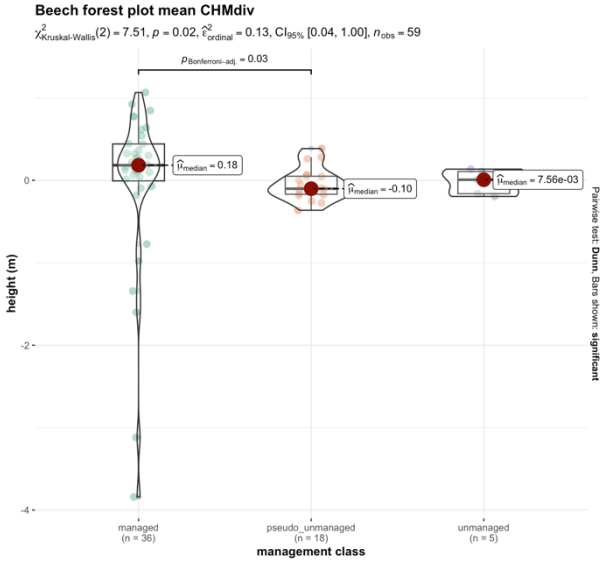
Beech forest plot mean CHMdiv
$\chi^2_{Kruskal-Wallis}(2) = 7.51$, $p = 0.02$, $\hat{\epsilon}^2_{ordinal} = 0.13$, $CI_{95\%}$ [0.04, 1.00], $n_{obs} = 59$
$p_{Bonferroni-adj.} = 0.03$
$\hat{\mu}_{median} = 0.18$
$\hat{\mu}_{median} = -0.10$
$\hat{\mu}_{median} = 7.56e-03$
height (m)
0
-2
-4
managed (n = 36)
pseudo_unmanaged (n = 18)
unmanaged (n = 5)
management class
Pairwise test: Dunn, Bars shown: significant

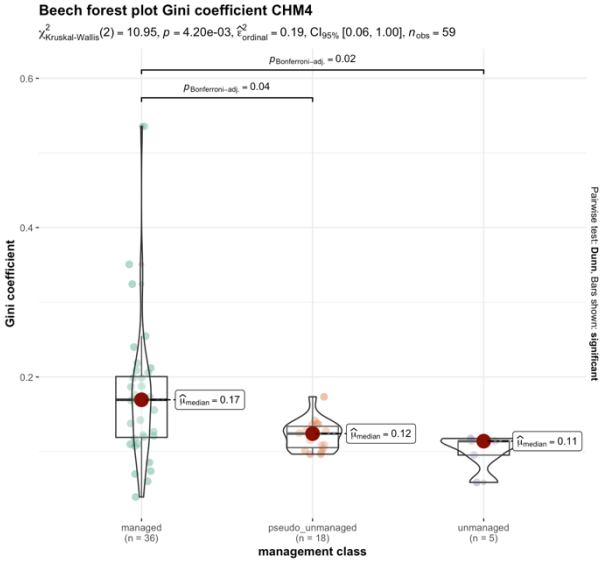
Beech forest plot Gini coefficient CHM4
$\chi^2_{Kruskal-Wallis}(2) = 10.95$, $p = 4.20e-03$, $\hat{\epsilon}^2_{ordinal} = 0.19$, $CI_{95\%}$ [0.06, 1.00], $n_{obs} = 59$
$p_{Bonferroni-adj.} = 0.02$
$p_{Bonferroni-adj.} = 0.04$
$\hat{\mu}_{median} = 0.17$
$\hat{\mu}_{median} = 0.12$
$\hat{\mu}_{median} = 0.11$
Gini coefficient
0.6
0.4
0.2
managed (n = 36)
pseudo_unmanaged (n = 18)
unmanaged (n = 5)
management class
Pairwise test: Dunn, Bars shown: significant

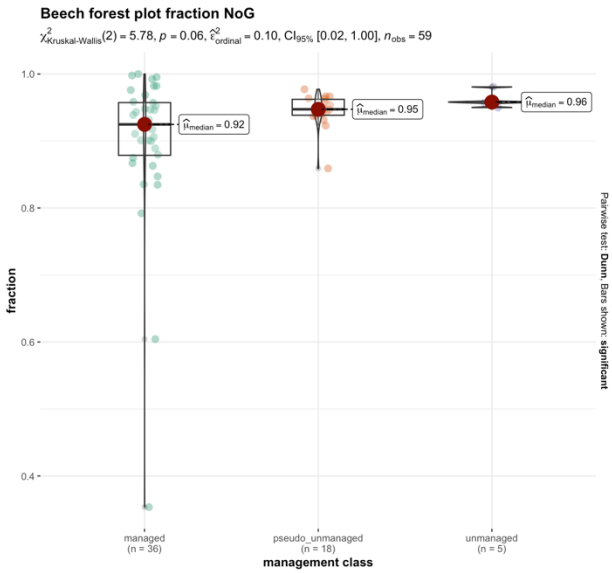
Beech forest plot fraction NoG
$\chi^2_{Kruskal-Wallis}(2) = 5.78$, $p = 0.06$, $\hat{\epsilon}^2_{ordinal} = 0.10$, $CI_{95\%}$ [0.02, 1.00], $n_{obs} = 59$
$\hat{\mu}_{median} = 0.92$
$\hat{\mu}_{median} = 0.95$
$\hat{\mu}_{median} = 0.96$
fraction
1.0
0.8
0.6
0.4
managed (n = 36)
pseudo_unmanaged (n = 18)
unmanaged (n = 5)
management class
Pairwise test: Dunn, Bars shown: significant

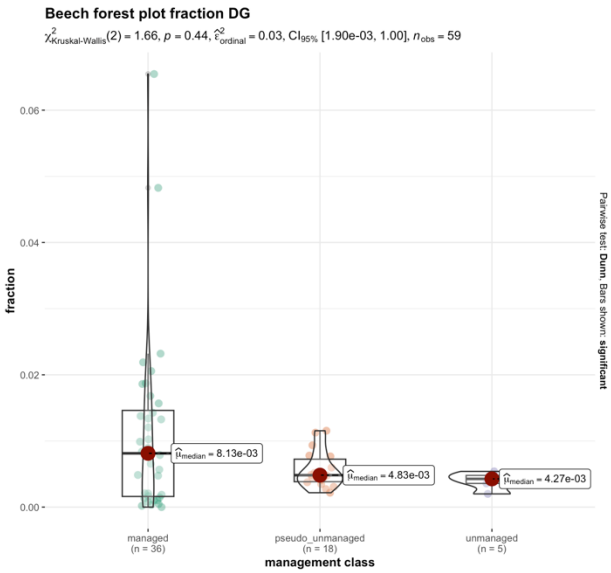
Beech forest plot fraction DG
$\chi^2_{Kruskal-Wallis}(2) = 1.66$, $p = 0.44$, $\hat{\epsilon}^2_{ordinal} = 0.03$, $CI_{95\%}$ [1.90e-03, 1.00], $n_{obs} = 59$
$\hat{\mu}_{median} = 8.13e-03$
$\hat{\mu}_{median} = 4.83e-03$
$\hat{\mu}_{median} = 4.27e-03$
fraction
0.06
0.04
0.02
0.00
managed (n = 36)
pseudo_unmanaged (n = 18)
unmanaged (n = 5)
management class
Pairwise test: Dunn, Bars shown: significant

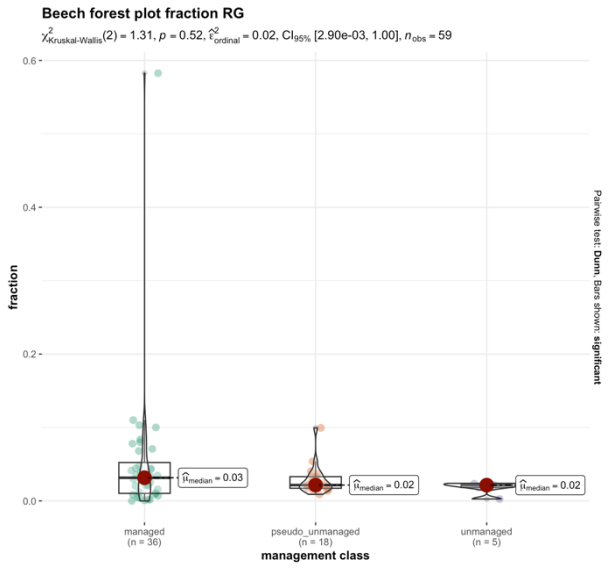
Beech forest plot fraction RG
$\chi^2_{Kruskal\text{-}Wallis}(2) = 1.31$, $p = 0.52$, $\hat{\epsilon}^2_{ordinal} = 0.02$, $CI_{95\%}$ [2.90e-03, 1.00], $n_{obs} = 59$
fraction
0.6
0.4
0.2
0.0
$\hat{\mu}_{median} = 0.03$
$\hat{\mu}_{median} = 0.02$
$\hat{\mu}_{median} = 0.02$
managed (n = 36)
pseudo_unmanaged (n = 18)
unmanaged (n = 5)
management class
Pairwise test: Dunn. Bars shown: significant

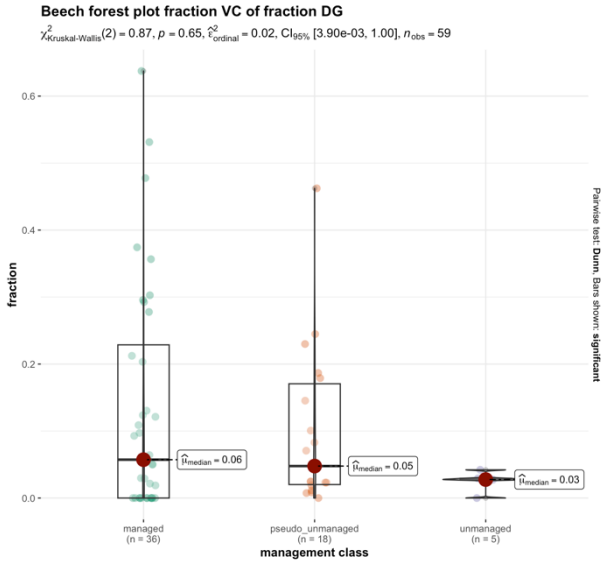
Beech forest plot fraction VC of fraction DG
$\chi^2_{Kruskal\text{-}Wallis}(2) = 0.87$, $p = 0.65$, $\hat{\epsilon}^2_{ordinal} = 0.02$, $CI_{95\%}$ [3.90e-03, 1.00], $n_{obs} = 59$
fraction
0.6
0.4
0.2
0.0
$\hat{\mu}_{median} = 0.06$
$\hat{\mu}_{median} = 0.05$
$\hat{\mu}_{median} = 0.03$
managed (n = 36)
pseudo_unmanaged (n = 18)
unmanaged (n = 5)
management class
Pairwise test: Dunn. Bars shown: significant

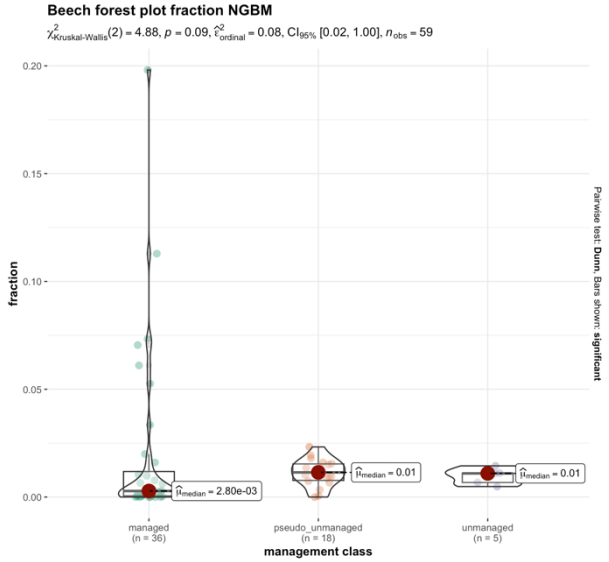
Beech forest plot fraction NGBM
$\chi^2_{Kruskal\text{-}Wallis}(2) = 4.88$, $p = 0.09$, $\hat{\epsilon}^2_{ordinal} = 0.08$, $CI_{95\%}$ [0.02, 1.00], $n_{obs} = 59$
fraction
0.20
0.15
0.10
0.05
0.00
$\hat{\mu}_{median} = 2.80e\text{-}03$
$\hat{\mu}_{median} = 0.01$
$\hat{\mu}_{median} = 0.01$
managed (n = 36)
pseudo_unmanaged (n = 18)
unmanaged (n = 5)
management class
Pairwise test: Dunn. Bars shown: significant

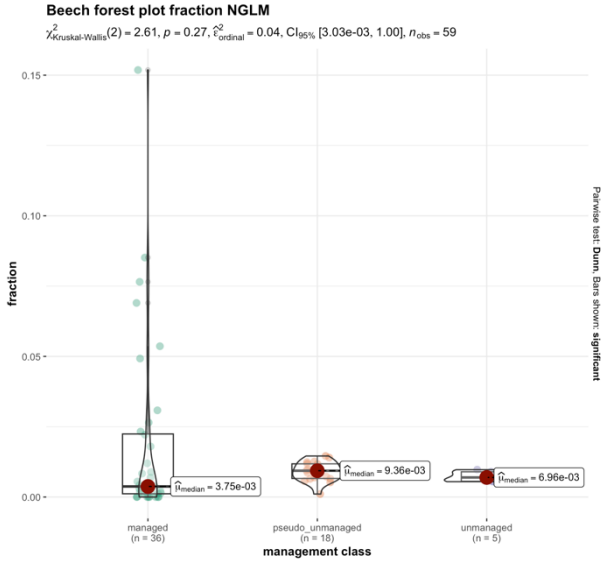
Beech forest plot fraction NGLM
$\chi^2_{Kruskal\text{-}Wallis}(2) = 2.61$, $p = 0.27$, $\hat{\epsilon}^2_{ordinal} = 0.04$, $CI_{95\%}$ [3.03e-03, 1.00], $n_{obs} = 59$
fraction
0.15
0.10
0.05
0.00
$\hat{\mu}_{median} = 3.75e\text{-}03$
$\hat{\mu}_{median} = 9.36e\text{-}03$
$\hat{\mu}_{median} = 6.96e\text{-}03$
managed (n = 36)
pseudo_unmanaged (n = 18)
unmanaged (n = 5)
management class
Pairwise test: Dunn. Bars shown: significant

Appendix H: Statistical comparisons to determine influence of forest plot age for selection of variables on canopy gap level (H1) and on forest plot level (H2).

H1

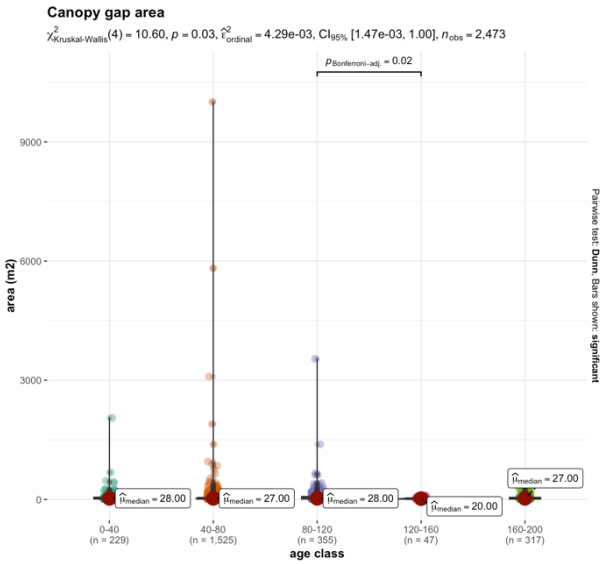

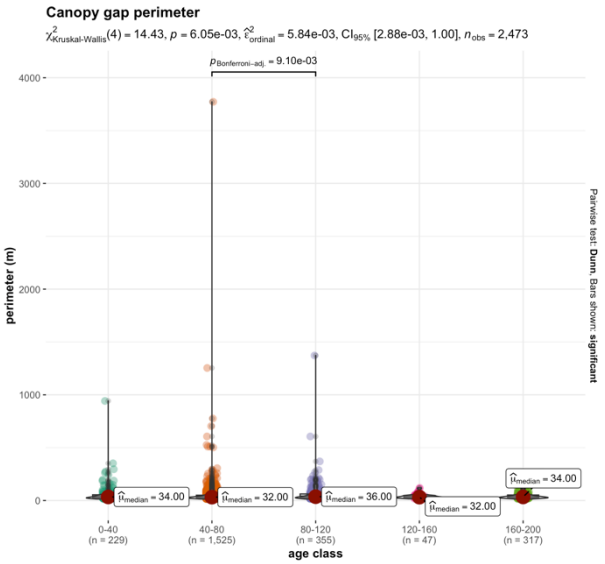

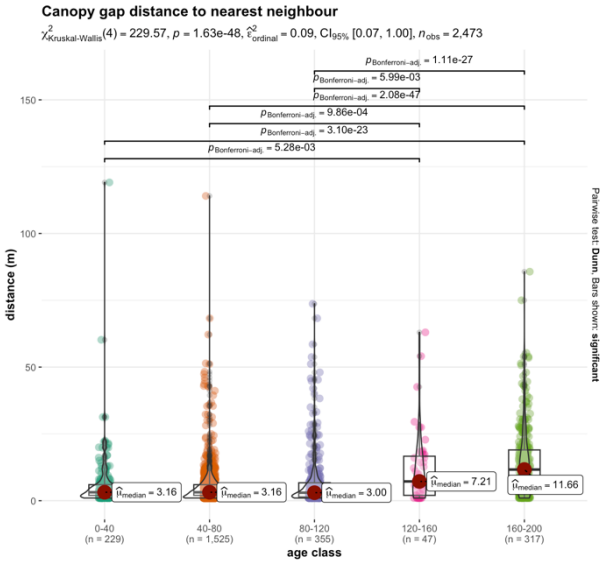

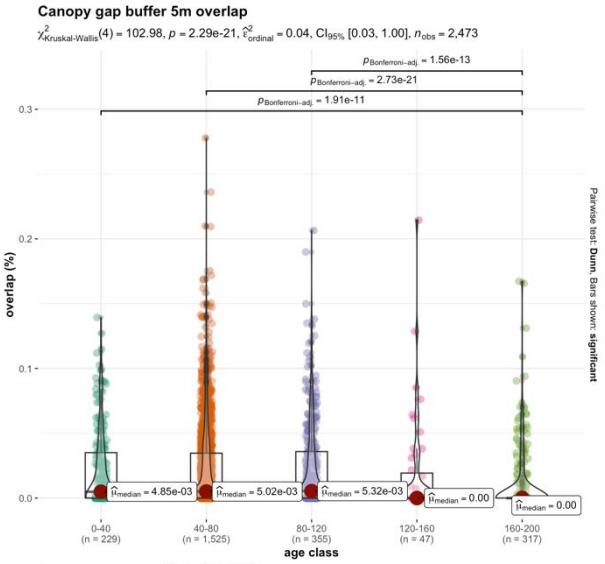

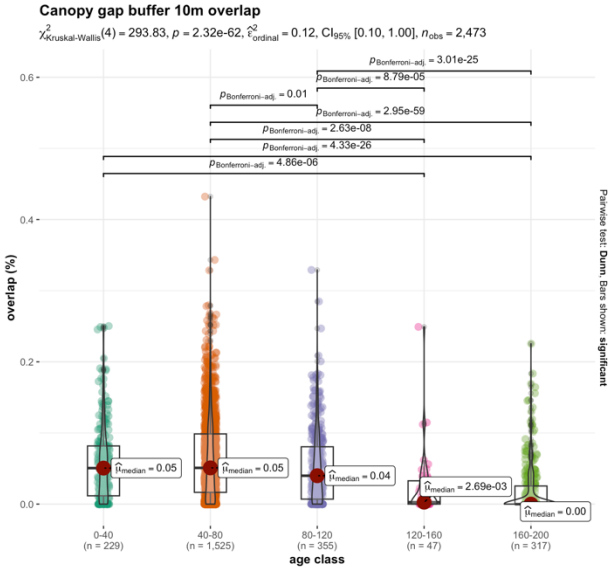

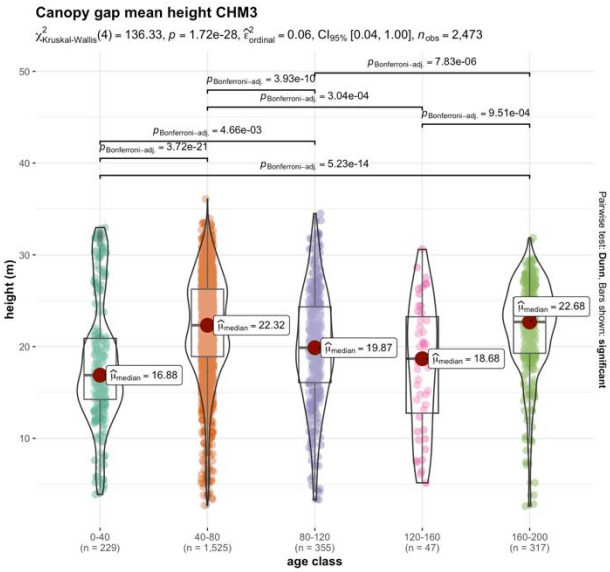

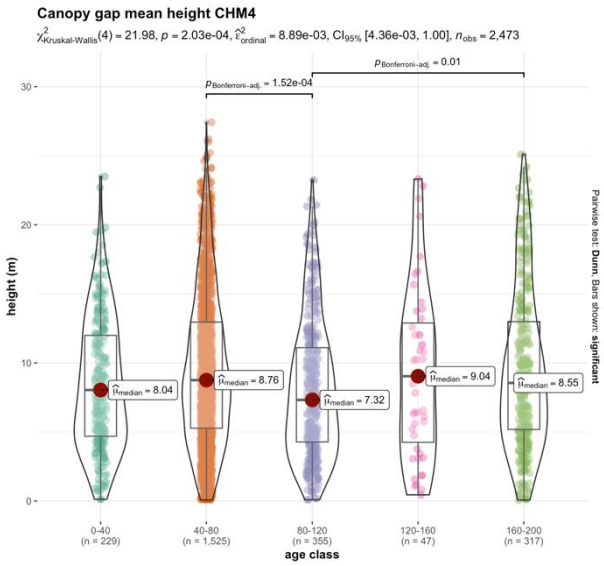
Canopy gap mean height CHM4
$\chi^2_{Kruskal-Wallis}(4) = 21.98$, $p = 2.03e-04$, $\hat{\epsilon}^2_{ordinal} = 8.89e-03$, $CI_{95\%}$ [4.36e-03, 1.00], $n_{obs} = 2,473$
$p_{Bonferroni-adj.} = 0.01$
$p_{Bonferroni-adj.} = 1.52e-04$
$\hat{\mu}_{median} = 8.04$
$\hat{\mu}_{median} = 8.76$
$\hat{\mu}_{median} = 7.32$
$\hat{\mu}_{median} = 9.04$
$\hat{\mu}_{median} = 8.55$
height (m)
30
20
10
0
0-40 (n = 229)
40-80 (n = 1,525)
80-120 (n = 355)
120-160 (n = 47)
160-200 (n = 317)
age class
Pairwise test: Dunn, Bars shown: significant

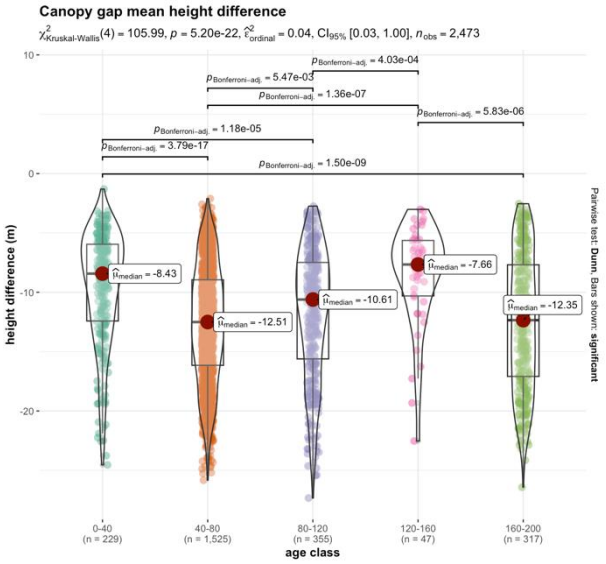
Canopy gap mean height difference
$\chi^2_{Kruskal-Wallis}(4) = 105.99$, $p = 5.20e-22$, $\hat{\epsilon}^2_{ordinal} = 0.04$, $CI_{95\%}$ [0.03, 1.00], $n_{obs} = 2,473$
$p_{Bonferroni-adj.} = 4.03e-04$
$p_{Bonferroni-adj.} = 5.47e-03$
$p_{Bonferroni-adj.} = 1.36e-07$
$p_{Bonferroni-adj.} = 5.83e-06$
$p_{Bonferroni-adj.} = 1.18e-05$
$p_{Bonferroni-adj.} = 3.79e-17$
$p_{Bonferroni-adj.} = 1.50e-09$
$\hat{\mu}_{median} = -8.43$
$\hat{\mu}_{median} = -12.51$
$\hat{\mu}_{median} = -10.61$
$\hat{\mu}_{median} = -7.66$
$\hat{\mu}_{median} = -12.35$
height difference (m)
10
0
-10
-20
0-40 (n = 229)
40-80 (n = 1,525)
80-120 (n = 355)
120-160 (n = 47)
160-200 (n = 317)
age class
Pairwise test: Dunn, Bars shown: significant

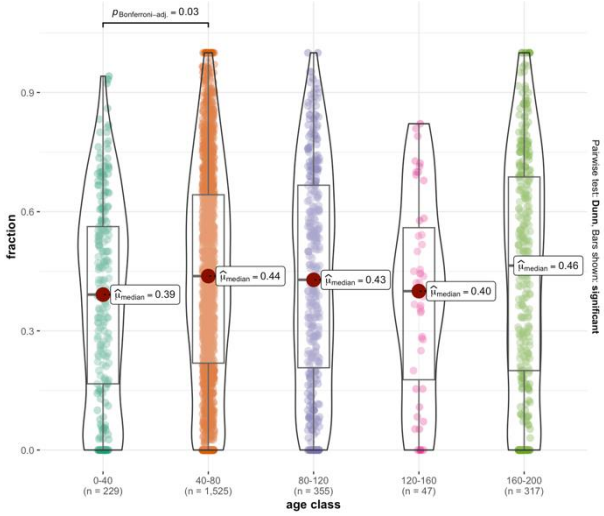
Canopy gap fraction NGBM
$\chi^2_{Kruskal-Wallis}(4) = 10.41$, $p = 0.03$, $\hat{\epsilon}^2_{ordinal} = 4.21e-03$, $CI_{95\%}$ [1.72e-03, 1.00], $n_{obs} = 2,473$
$p_{Bonferroni-adj.} = 0.03$
$\hat{\mu}_{median} = 0.39$
$\hat{\mu}_{median} = 0.44$
$\hat{\mu}_{median} = 0.43$
$\hat{\mu}_{median} = 0.40$
$\hat{\mu}_{median} = 0.46$
fraction
0.9
0.6
0.3
0.0
0-40 (n = 229)
40-80 (n = 1,525)
80-120 (n = 355)
120-160 (n = 47)
160-200 (n = 317)
age class
Pairwise test: Dunn, Bars shown: significant

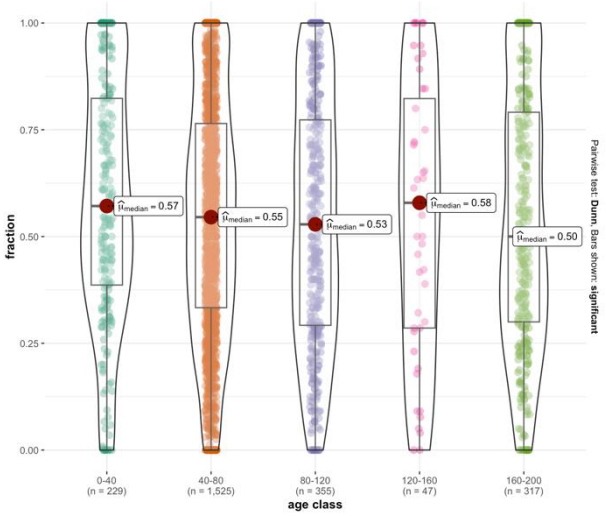
Canopy gap fraction NGLM
$\chi^2_{Kruskal-Wallis}(4) = 5.87$, $p = 0.21$, $\hat{\epsilon}^2_{ordinal} = 2.38e-03$, $CI_{95\%}$ [6.69e-04, 1.00], $n_{obs} = 2,473$
$\hat{\mu}_{median} = 0.57$
$\hat{\mu}_{median} = 0.55$
$\hat{\mu}_{median} = 0.53$
$\hat{\mu}_{median} = 0.58$
$\hat{\mu}_{median} = 0.50$
fraction
1.00
0.75
0.50
0.25
0.00
0-40 (n = 229)
40-80 (n = 1,525)
80-120 (n = 355)
120-160 (n = 47)
160-200 (n = 317)
age class
Pairwise test: Dunn, Bars shown: significant

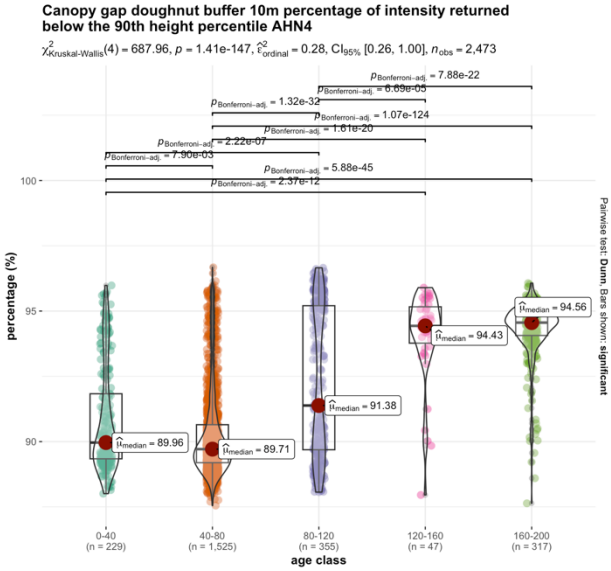
Canopy gap doughnut buffer 10m percentage of intensity returned below the 90th height percentile AHN4
$\chi^2_{Kruskal-Wallis}(4) = 687.96$, $p = 1.41e-147$, $\hat{\epsilon}^2_{ordinal} = 0.28$, $CI_{95\%}$ [0.26, 1.00], $n_{obs} = 2,473$
$p_{Bonferroni-adj.} = 7.88e-22$
$p_{Bonferroni-adj.} = 6.69e-03$
$p_{Bonferroni-adj.} = 1.32e-32$
$p_{Bonferroni-adj.} = 1.07e-124$
$p_{Bonferroni-adj.} = 1.61e-20$
$p_{Bonferroni-adj.} = 2.22e-07$
$p_{Bonferroni-adj.} = 7.90e-03$
$p_{Bonferroni-adj.} = 5.88e-45$
$p_{Bonferroni-adj.} = 2.37e-12$
$\hat{\mu}_{median} = 89.96$
$\hat{\mu}_{median} = 89.71$
$\hat{\mu}_{median} = 91.38$
$\hat{\mu}_{median} = 94.43$
$\hat{\mu}_{median} = 94.56$
percentage (%)
100
95
90
0-40 (n = 229)
40-80 (n = 1,525)
80-120 (n = 355)
120-160 (n = 47)
160-200 (n = 317)
age class
Pairwise test: Dunn, Bars shown: significant

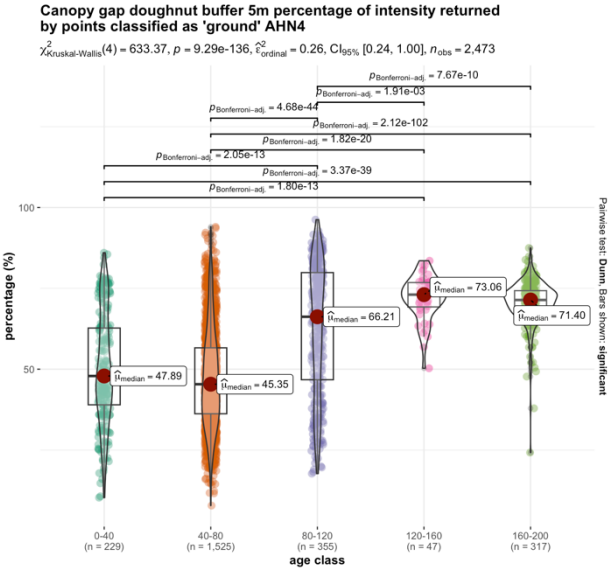
Canopy gap doughnut buffer 5m percentage of intensity returned by points classified as 'ground' AHN4
$\chi^2_{Kruskal-Wallis}(4) = 633.37$, $p = 9.29e-136$, $\hat{\epsilon}^2_{ordinal} = 0.26$, $CI_{95\%}$ [0.24, 1.00], $n_{obs} = 2,473$
$p_{Bonferroni-adj.} = 7.67e-10$
$p_{Bonferroni-adj.} = 1.91e-03$
$p_{Bonferroni-adj.} = 4.68e-44$
$p_{Bonferroni-adj.} = 2.12e-102$
$p_{Bonferroni-adj.} = 1.82e-20$
$p_{Bonferroni-adj.} = 2.05e-13$
$p_{Bonferroni-adj.} = 3.37e-39$
$p_{Bonferroni-adj.} = 1.80e-13$
$\hat{\mu}_{median} = 47.89$
$\hat{\mu}_{median} = 45.35$
$\hat{\mu}_{median} = 66.21$
$\hat{\mu}_{median} = 73.06$
$\hat{\mu}_{median} = 71.40$
percentage (%)
100
50
0-40 (n = 229)
40-80 (n = 1,525)
80-120 (n = 355)
120-160 (n = 47)
160-200 (n = 317)
age class
Pairwise test: Dunn, Bars shown: significant

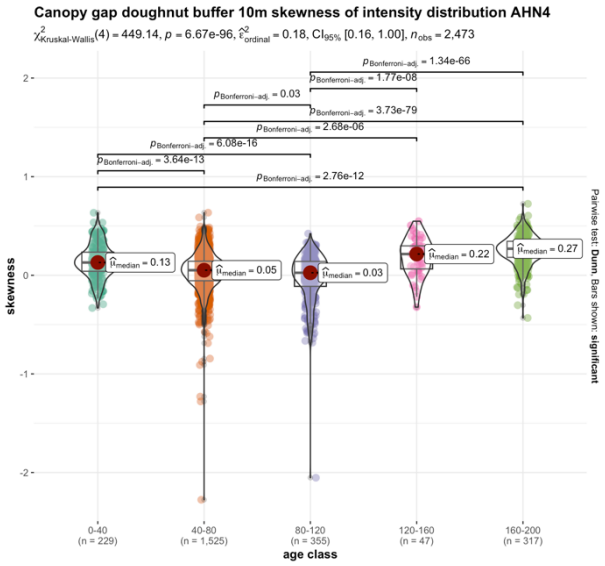
Canopy gap doughnut buffer 10m skewness of intensity distribution AHN4
$\chi^2_{Kruskal\text{-}Wallis}(4) = 449.14$, $p = 6.67e\text{-}96$, $\hat{\varepsilon}^2_{ordinal} = 0.18$, $CI_{95\%}$ [0.16, 1.00], $n_{obs} = 2,473$
skewness
age class
Pairwise test: Dunn, Bars shown: significant

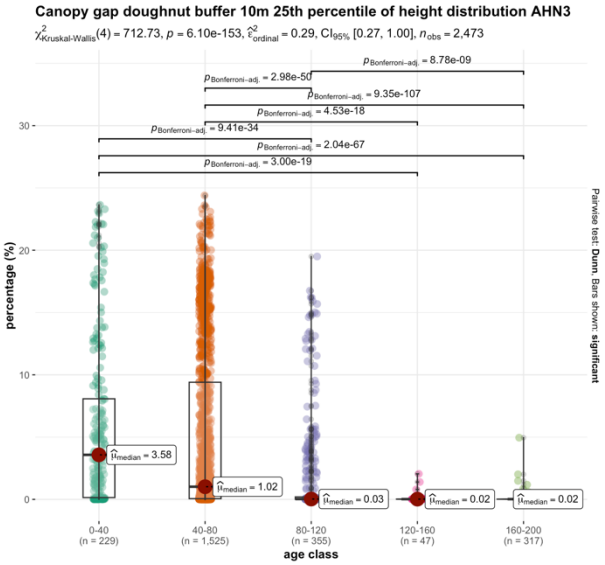
Canopy gap doughnut buffer 10m 25th percentile of height distribution AHN3
$\chi^2_{Kruskal\text{-}Wallis}(4) = 712.73$, $p = 6.10e\text{-}153$, $\hat{\varepsilon}^2_{ordinal} = 0.29$, $CI_{95\%}$ [0.27, 1.00], $n_{obs} = 2,473$
percentage (%)
age class
Pairwise test: Dunn, Bars shown: significant

H2

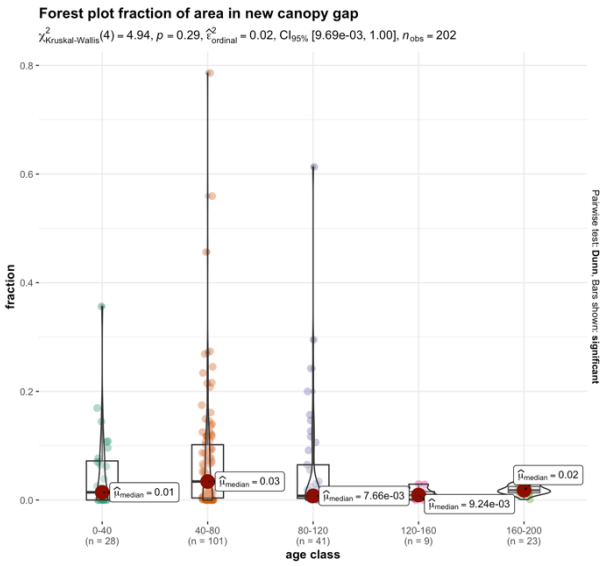
Forest plot fraction of area in new canopy gap
$\chi^2_{Kruskal\text{-}Wallis}(4) = 4.94$, $p = 0.29$, $\hat{\varepsilon}^2_{ordinal} = 0.02$, $CI_{95\%}$ [9.69e-03, 1.00], $n_{obs} = 202$
fraction
age class
Pairwise test: Dunn, Bars shown: significant

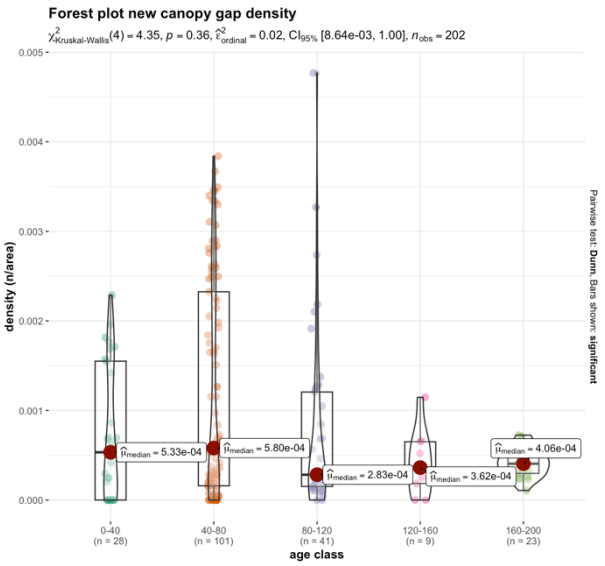
Forest plot new canopy gap density
$\chi^2_{Kruskal\text{-}Wallis}(4) = 4.35$, $p = 0.36$, $\hat{\varepsilon}^2_{ordinal} = 0.02$, $CI_{95\%}$ [8.64e-03, 1.00], $n_{obs} = 202$
density (n/area)
age class
Pairwise test: Dunn, Bars shown: significant

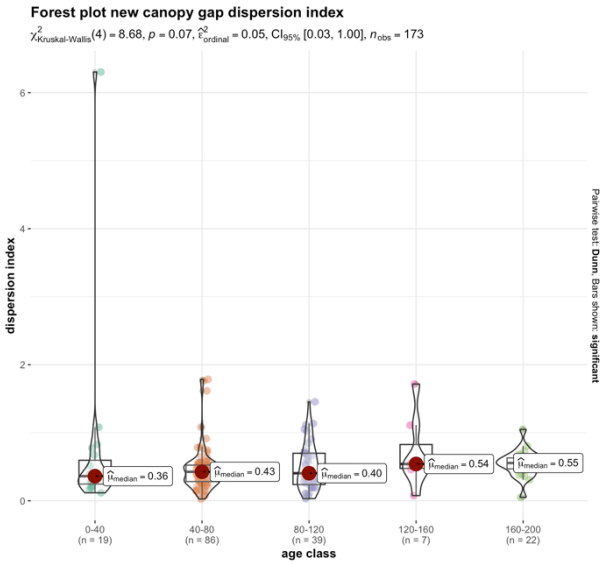
Forest plot new canopy gap dispersion index
$\chi^2_{Kruskal\text{-}Wallis}(4) = 8.68$, $p = 0.07$, $\hat{\varepsilon}^2_{ordinal} = 0.05$, $CI_{95\%}$ [0.03, 1.00], $n_{obs} = 173$
dispersion index
age class
Pairwise test: Dunn, Bars shown: significant

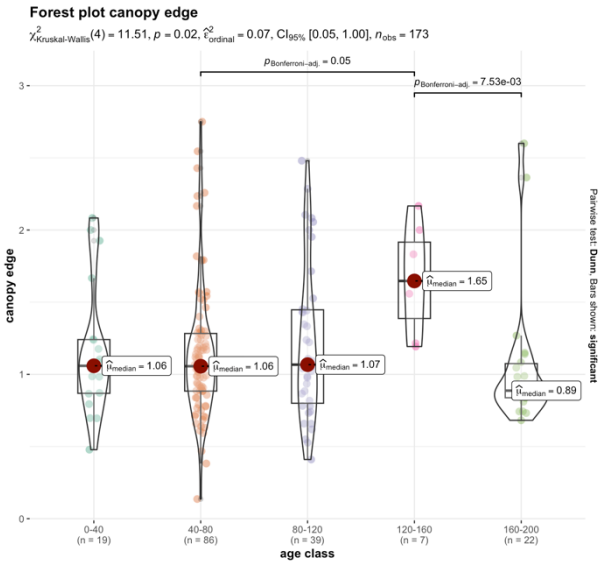
Forest plot canopy edge
$\chi^2_{Kruskal\text{-}Wallis}(4) = 11.51$, $p = 0.02$, $\hat{\varepsilon}^2_{ordinal} = 0.07$, $CI_{95\%}$ [0.05, 1.00], $n_{obs} = 173$
canopy edge
age class
Pairwise test: Dunn, Bars shown: significant

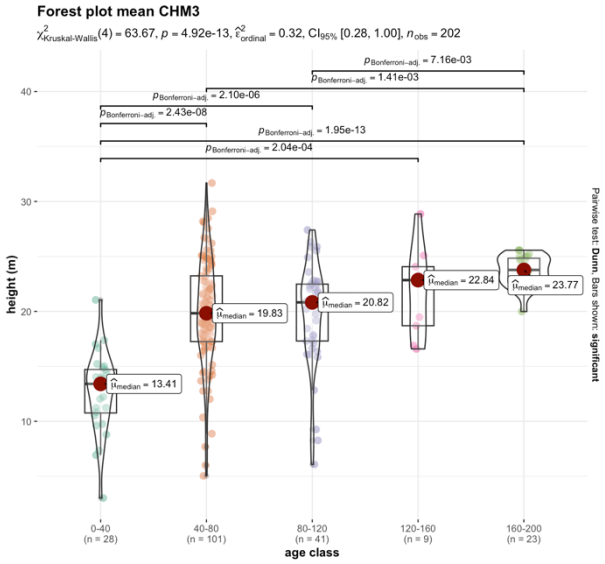
Forest plot mean CHM3
$\chi^2_{Kruskal\text{-}Wallis}(4) = 63.67$, $p = 4.92e\text{-}13$, $\hat{\epsilon}^2_{ordinal} = 0.32$, $CI_{95\%}$ [0.28, 1.00], $n_{obs} = 202$
$p_{Bonferroni\text{-}adj.} = 7.16e\text{-}03$
$p_{Bonferroni\text{-}adj.} = 1.41e\text{-}03$
$p_{Bonferroni\text{-}adj.} = 2.10e\text{-}06$
$p_{Bonferroni\text{-}adj.} = 2.43e\text{-}08$
$p_{Bonferroni\text{-}adj.} = 1.95e\text{-}13$
$p_{Bonferroni\text{-}adj.} = 2.04e\text{-}04$
$\hat{\mu}_{median} = 13.41$
$\hat{\mu}_{median} = 19.83$
$\hat{\mu}_{median} = 20.82$
$\hat{\mu}_{median} = 22.84$
$\hat{\mu}_{median} = 23.77$
height (m)
40
30
20
10
0-40 (n = 28)
40-80 (n = 101)
80-120 (n = 41)
120-160 (n = 9)
160-200 (n = 23)
age class
Pairwise test: Dunn, Bars shown: significant

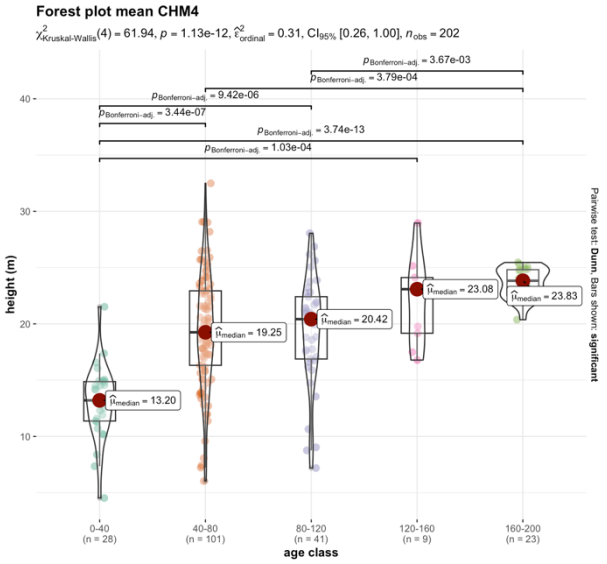
Forest plot mean CHM4
$\chi^2_{Kruskal\text{-}Wallis}(4) = 61.94$, $p = 1.13e\text{-}12$, $\hat{\epsilon}^2_{ordinal} = 0.31$, $CI_{95\%}$ [0.26, 1.00], $n_{obs} = 202$
$p_{Bonferroni\text{-}adj.} = 3.67e\text{-}03$
$p_{Bonferroni\text{-}adj.} = 3.79e\text{-}04$
$p_{Bonferroni\text{-}adj.} = 9.42e\text{-}06$
$p_{Bonferroni\text{-}adj.} = 3.44e\text{-}07$
$p_{Bonferroni\text{-}adj.} = 3.74e\text{-}13$
$p_{Bonferroni\text{-}adj.} = 1.03e\text{-}04$
$\hat{\mu}_{median} = 13.20$
$\hat{\mu}_{median} = 19.25$
$\hat{\mu}_{median} = 20.42$
$\hat{\mu}_{median} = 23.08$
$\hat{\mu}_{median} = 23.83$
height (m)
40
30
20
10
0-40 (n = 28)
40-80 (n = 101)
80-120 (n = 41)
120-160 (n = 9)
160-200 (n = 23)
age class
Pairwise test: Dunn, Bars shown: significant

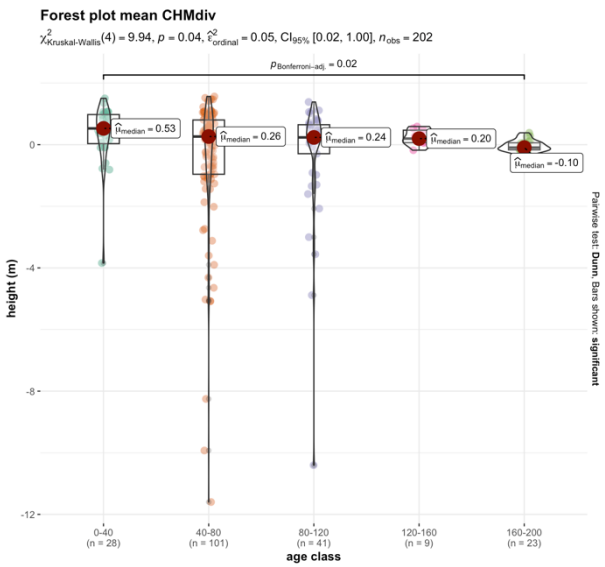
Forest plot mean CHMdiv
$\chi^2_{Kruskal\text{-}Wallis}(4) = 9.94$, $p = 0.04$, $\hat{\epsilon}^2_{ordinal} = 0.05$, $CI_{95\%}$ [0.02, 1.00], $n_{obs} = 202$
$p_{Bonferroni\text{-}adj.} = 0.02$
$\hat{\mu}_{median} = 0.53$
$\hat{\mu}_{median} = 0.26$
$\hat{\mu}_{median} = 0.24$
$\hat{\mu}_{median} = 0.20$
$\hat{\mu}_{median} = -0.10$
height (m)
0
-4
-8
-12
0-40 (n = 28)
40-80 (n = 101)
80-120 (n = 41)
120-160 (n = 9)
160-200 (n = 23)
age class
Pairwise test: Dunn, Bars shown: significant

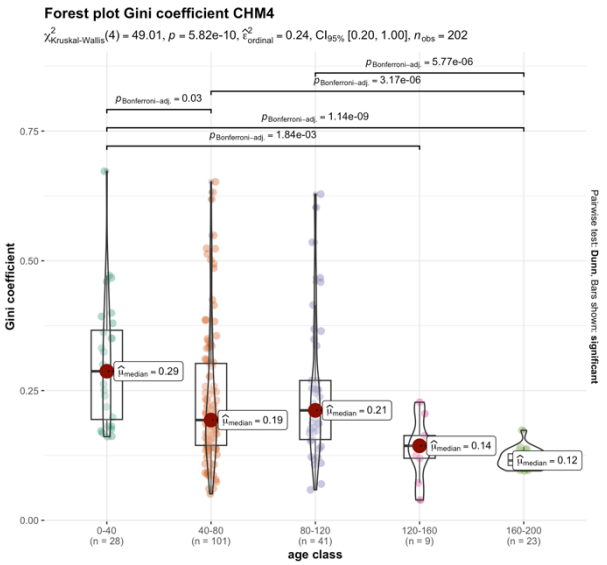
Forest plot Gini coefficient CHM4
$\chi^2_{Kruskal\text{-}Wallis}(4) = 49.01$, $p = 5.82e\text{-}10$, $\hat{\epsilon}^2_{ordinal} = 0.24$, $CI_{95\%}$ [0.20, 1.00], $n_{obs} = 202$
$p_{Bonferroni\text{-}adj.} = 5.77e\text{-}06$
$p_{Bonferroni\text{-}adj.} = 3.17e\text{-}06$
$p_{Bonferroni\text{-}adj.} = 0.03$
$p_{Bonferroni\text{-}adj.} = 1.14e\text{-}09$
$p_{Bonferroni\text{-}adj.} = 1.84e\text{-}03$
$\hat{\mu}_{median} = 0.29$
$\hat{\mu}_{median} = 0.19$
$\hat{\mu}_{median} = 0.21$
$\hat{\mu}_{median} = 0.14$
$\hat{\mu}_{median} = 0.12$
Gini coefficient
0.75
0.50
0.25
0.00
0-40 (n = 28)
40-80 (n = 101)
80-120 (n = 41)
120-160 (n = 9)
160-200 (n = 23)
age class
Pairwise test: Dunn, Bars shown: significant

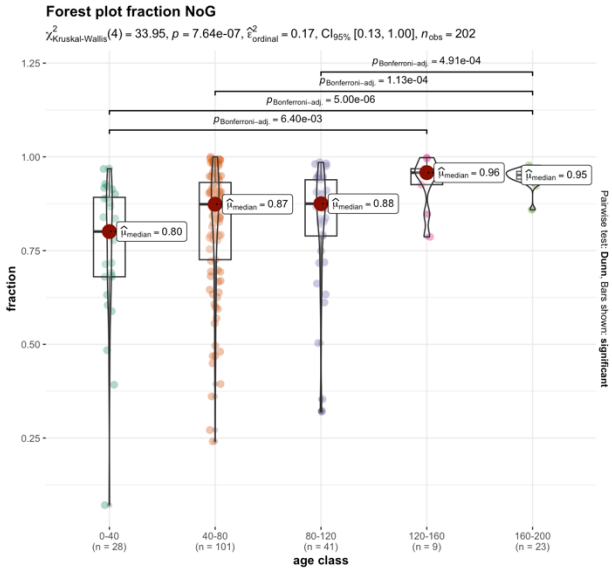
Forest plot fraction NoG
$\chi^2_{Kruskal\text{-}Wallis}(4) = 33.95$, $p = 7.64e\text{-}07$, $\hat{\epsilon}^2_{ordinal} = 0.17$, $CI_{95\%}$ [0.13, 1.00], $n_{obs} = 202$
$p_{Bonferroni\text{-}adj.} = 4.91e\text{-}04$
$p_{Bonferroni\text{-}adj.} = 1.13e\text{-}04$
$p_{Bonferroni\text{-}adj.} = 5.00e\text{-}06$
$p_{Bonferroni\text{-}adj.} = 6.40e\text{-}03$
$\hat{\mu}_{median} = 0.80$
$\hat{\mu}_{median} = 0.87$
$\hat{\mu}_{median} = 0.88$
$\hat{\mu}_{median} = 0.96$
$\hat{\mu}_{median} = 0.95$
fraction
1.25
1.00
0.75
0.50
0.25
0-40 (n = 28)
40-80 (n = 101)
80-120 (n = 41)
120-160 (n = 9)
160-200 (n = 23)
age class
Pairwise test: Dunn, Bars shown: significant

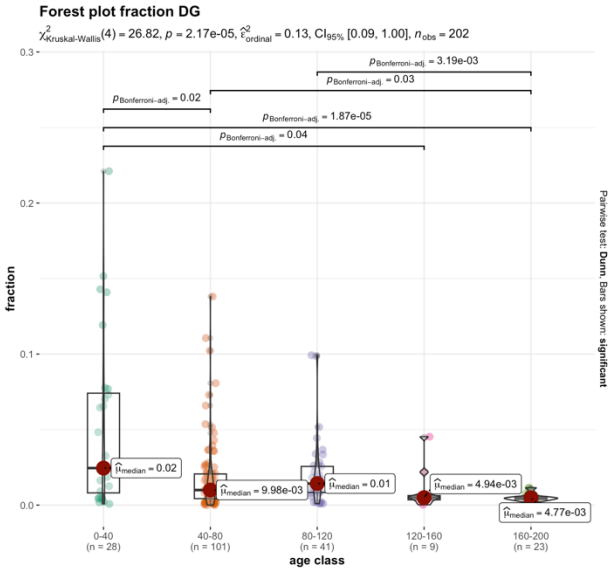
Forest plot fraction DG
$\chi^2_{Kruskal\text{-}Wallis}(4) = 26.82$, $p = 2.17e\text{-}05$, $\hat{\epsilon}^2_{ordinal} = 0.13$, $CI_{95\%}$ [0.09, 1.00], $n_{obs} = 202$
$p_{Bonferroni\text{-}adj.} = 3.19e\text{-}03$
$p_{Bonferroni\text{-}adj.} = 0.03$
$p_{Bonferroni\text{-}adj.} = 0.02$
$p_{Bonferroni\text{-}adj.} = 1.87e\text{-}05$
$p_{Bonferroni\text{-}adj.} = 0.04$
$\hat{\mu}_{median} = 0.02$
$\hat{\mu}_{median} = 9.98e\text{-}03$
$\hat{\mu}_{median} = 0.01$
$\hat{\mu}_{median} = 4.94e\text{-}03$
$\hat{\mu}_{median} = 4.77e\text{-}03$
fraction
0.3
0.2
0.1
0.0
0-40 (n = 28)
40-80 (n = 101)
80-120 (n = 41)
120-160 (n = 9)
160-200 (n = 23)
age class
Pairwise test: Dunn, Bars shown: significant

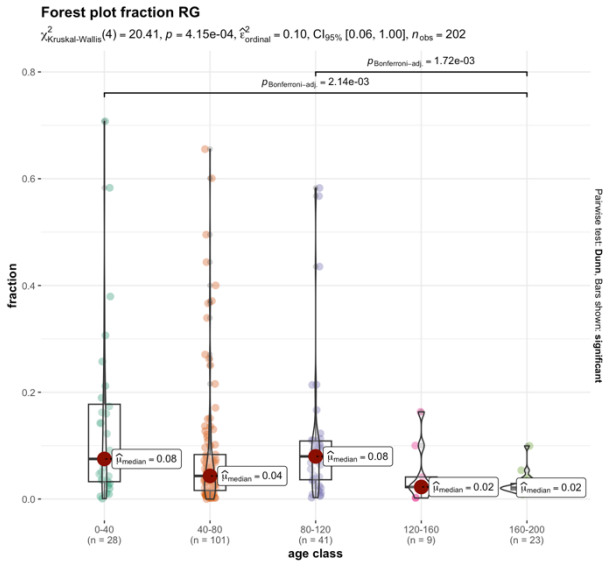
Forest plot fraction RG
$\chi^2_{Kruskal-Wallis}(4) = 20.41$, $p = 4.15e-04$, $\hat{\epsilon}^2_{ordinal} = 0.10$, $CI_{95\%}$ [0.06, 1.00], $n_{obs} = 202$
$p_{Bonferroni-adj.} = 1.72e-03$
$p_{Bonferroni-adj.} = 2.14e-03$
fraction
age class
0-40 (n = 28)
40-80 (n = 101)
80-120 (n = 41)
120-160 (n = 9)
160-200 (n = 23)
$\hat{\mu}_{median} = 0.08$
$\hat{\mu}_{median} = 0.04$
$\hat{\mu}_{median} = 0.08$
$\hat{\mu}_{median} = 0.02$
$\hat{\mu}_{median} = 0.02$
Pairwise test: Dunn, Bars shown: significant

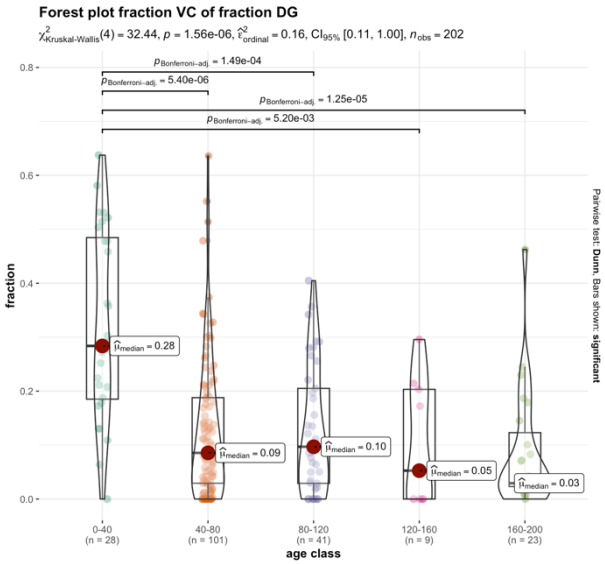
Forest plot fraction VC of fraction DG
$\chi^2_{Kruskal-Wallis}(4) = 32.44$, $p = 1.56e-06$, $\hat{\epsilon}^2_{ordinal} = 0.16$, $CI_{95\%}$ [0.11, 1.00], $n_{obs} = 202$
$p_{Bonferroni-adj.} = 1.49e-04$
$p_{Bonferroni-adj.} = 5.40e-06$
$p_{Bonferroni-adj.} = 1.25e-05$
$p_{Bonferroni-adj.} = 5.20e-03$
fraction
age class
0-40 (n = 28)
40-80 (n = 101)
80-120 (n = 41)
120-160 (n = 9)
160-200 (n = 23)
$\hat{\mu}_{median} = 0.28$
$\hat{\mu}_{median} = 0.09$
$\hat{\mu}_{median} = 0.10$
$\hat{\mu}_{median} = 0.05$
$\hat{\mu}_{median} = 0.03$
Pairwise test: Dunn, Bars shown: significant

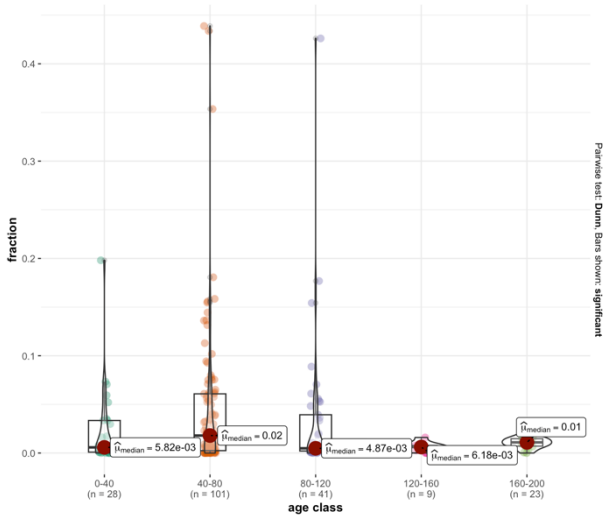
Forest plot fraction NGBM
$\chi^2_{Kruskal-Wallis}(4) = 7.79$, $p = 0.10$, $\hat{\epsilon}^2_{ordinal} = 0.04$, $CI_{95\%}$ [0.02, 1.00], $n_{obs} = 202$
fraction
age class
0-40 (n = 28)
40-80 (n = 101)
80-120 (n = 41)
120-160 (n = 9)
160-200 (n = 23)
$\hat{\mu}_{median} = 5.82e-03$
$\hat{\mu}_{median} = 0.02$
$\hat{\mu}_{median} = 4.87e-03$
$\hat{\mu}_{median} = 6.18e-03$
$\hat{\mu}_{median} = 0.01$
Pairwise test: Dunn, Bars shown: significant

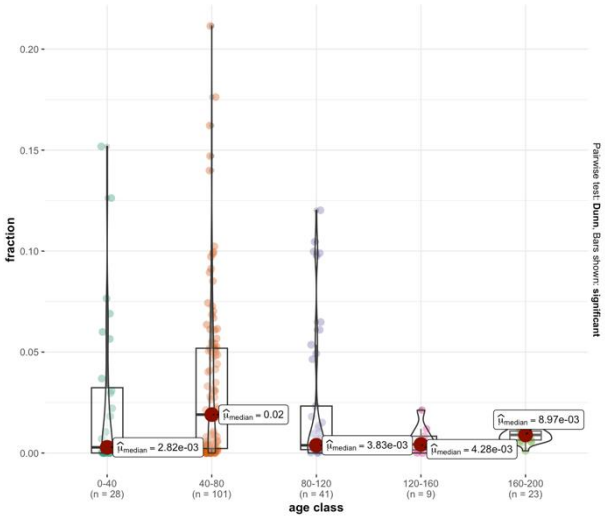
Forest plot fraction NGLM
$\chi^2_{Kruskal-Wallis}(4) = 7.87$, $p = 0.10$, $\hat{\epsilon}^2_{ordinal} = 0.04$, $CI_{95\%}$ [0.01, 1.00], $n_{obs} = 202$
fraction
age class
0-40 (n = 28)
40-80 (n = 101)
80-120 (n = 41)
120-160 (n = 9)
160-200 (n = 23)
$\hat{\mu}_{median} = 2.82e-03$
$\hat{\mu}_{median} = 0.02$
$\hat{\mu}_{median} = 3.83e-03$
$\hat{\mu}_{median} = 4.28e-03$
$\hat{\mu}_{median} = 8.97e-03$
Pairwise test: Dunn, Bars shown: significant

Appendix I: Number of canopy gaps and forest plots per tree species per management type (I1 & I2), per tree species and age class (I3 & I4), and per management type and age class (I5 & I6)

I1: Canopy gaps per tree species per management type

Tree species	*Managed*	*Pseudo-unmanaged*	*Unmanaged*	*Total*
Beech	284	230	81	595
Oak	34	7	0	41
Scotch pine	407	0	5	412
Japanese larch	278	0	2	280
Douglas fir	774	0	2	776
Norway spruce	87	0	0	87

I2: Forest plots per tree species per management type

Tree species	*Managed*	*Pseudo-unmanaged*	*Unmanaged*	*Total*
Beech	36	18	5	59
Oak	7	1	0	8
Scotch pine	18	0	1	19
Japanese larch	34	0	1	35
Douglas fir	51	0	1	52
Norway spruce	7	0	0	7

I3: Canopy gaps per tree species per age class

Tree species	*0-40 (y)*	*40-80 (y)*	*80-120 (y)*	*120-160 (y)*	*160-200 (y)*	*Total*
Beech	49	70	130	36	310	595
Oak	0	16	18	0	7	41
Scotch pine	4	352	49	7	0	412
Japanese larch	61	184	35	0	0	280
Douglas fir	31	637	108	0	0	776
Norway spruce	18	69	0	0	0	87
Total	163	1328	340	43	317	2191

I4: Forest plots per tree species per age class

Tree species	*0-40 (y)*	*40-80 (y)*	*80-120 (y)*	*120-160 (y)*	*160-200 (y)*	*Total*
Beech	8	8	18	3	22	59
Oak	0	5	2	0	1	8
Scotch pine	1	12	2	4	0	19
Japanese larch	6	20	9	0	0	35
Douglas fir	2	41	9	0	0	52
Norway spruce	1	6	0	0	0	7
Total	18	92	40	7	23	180

I5: Canopy gaps per management type per age class

Management type	*0-40 (y)*	*40-80 (y)*	*80-120 (y)*	*120-160 (y)*	*160-200 (y)*	*Total*
Managed	229	1515	347	47	0	2138
Pseudo-unmanaged	0	0	0	0	237	237
Unmanaged	0	10	8	0	80	98
Total	229	1525	355	47	317	2473

I6: Forest plots per management type per age class

Management type	*0-40 (y)*	*40-80 (y)*	*80-120 (y)*	*120-160 (y)*	*160-200 (y)*	*Total*
Managed	28	99	38	9	0	174
Pseudo-unmanaged	0	0	0	0	19	19
Unmanaged	0	2	3	0	4	9
Total	28	101	41	9	23	202

Appendix J: Statistical comparisons of the fifteen most important new canopy gap variables in the “number of trees” classification.

J1

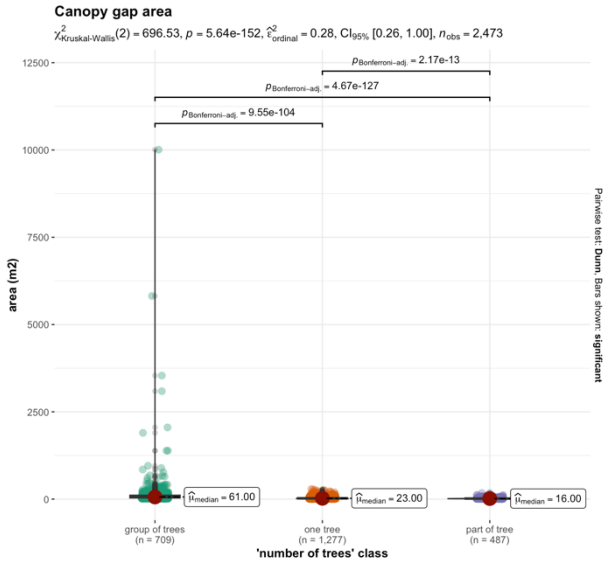

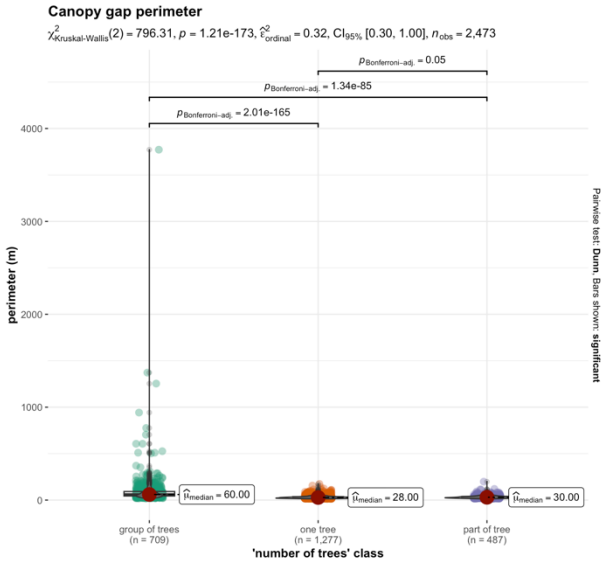

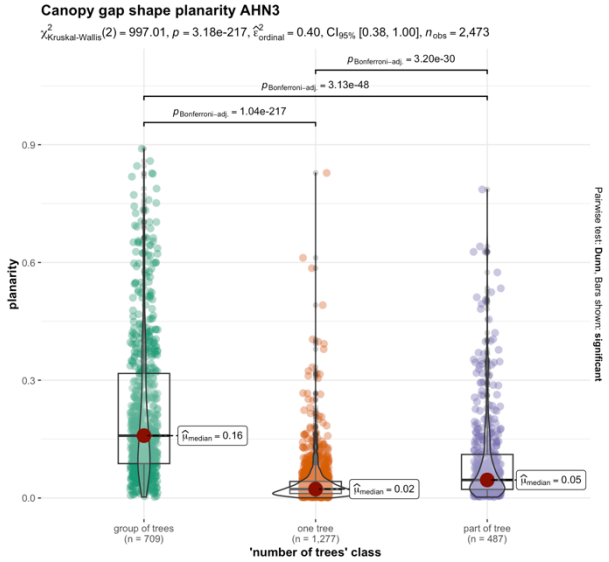

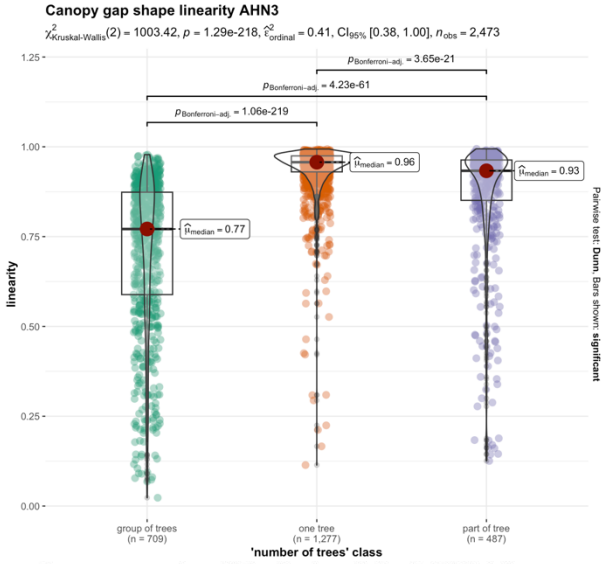

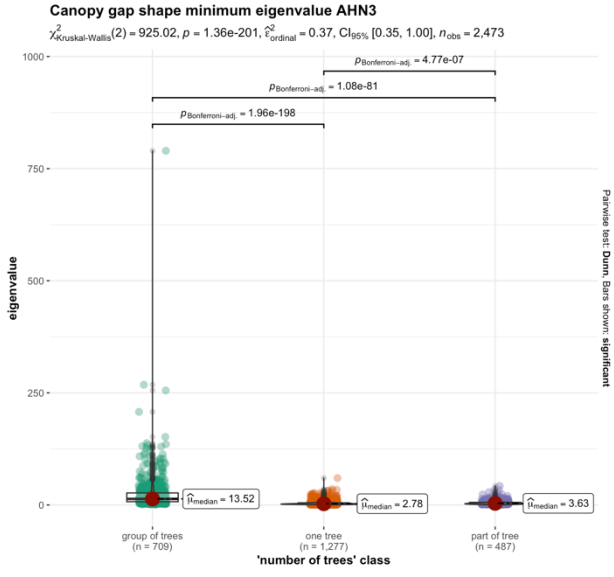

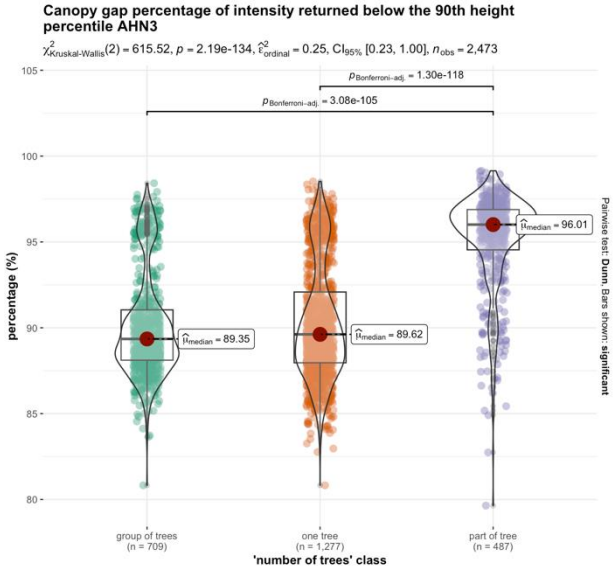

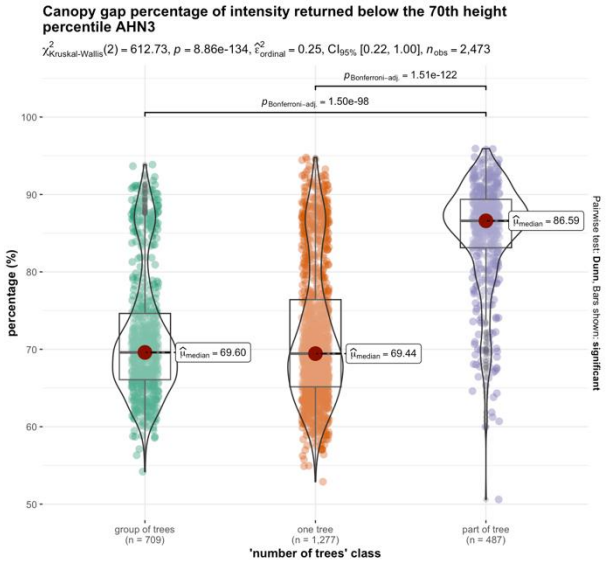
Canopy gap percentage of intensity returned below the 70th height percentile AHN3
$\chi^2_{Kruskal-Wallis}(2) = 612.73$, $p = 8.86e-134$, $\hat{\epsilon}^2_{ordinal} = 0.25$, $CI_{95\%}$ [0.22, 1.00], $n_{obs} = 2,473$
$p_{Bonferroni-adj.} = 1.51e-122$
$p_{Bonferroni-adj.} = 1.50e-98$
percentage (%)
$\hat{\mu}_{median} = 69.60$
$\hat{\mu}_{median} = 69.44$
$\hat{\mu}_{median} = 86.59$
group of trees (n = 709)
one tree (n = 1,277)
part of tree (n = 487)
'number of trees' class
Pairwise test: Dunn, Bars shown: significant

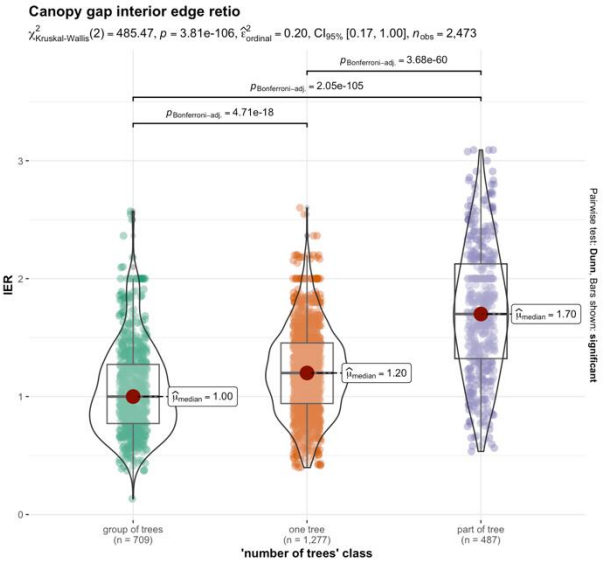
Canopy gap interior edge retio
$\chi^2_{Kruskal-Wallis}(2) = 485.47$, $p = 3.81e-106$, $\hat{\epsilon}^2_{ordinal} = 0.20$, $CI_{95\%}$ [0.17, 1.00], $n_{obs} = 2,473$
$p_{Bonferroni-adj.} = 3.68e-60$
$p_{Bonferroni-adj.} = 2.05e-105$
$p_{Bonferroni-adj.} = 4.71e-18$
IER
$\hat{\mu}_{median} = 1.00$
$\hat{\mu}_{median} = 1.20$
$\hat{\mu}_{median} = 1.70$
group of trees (n = 709)
one tree (n = 1,277)
part of tree (n = 487)
'number of trees' class
Pairwise test: Dunn, Bars shown: significant

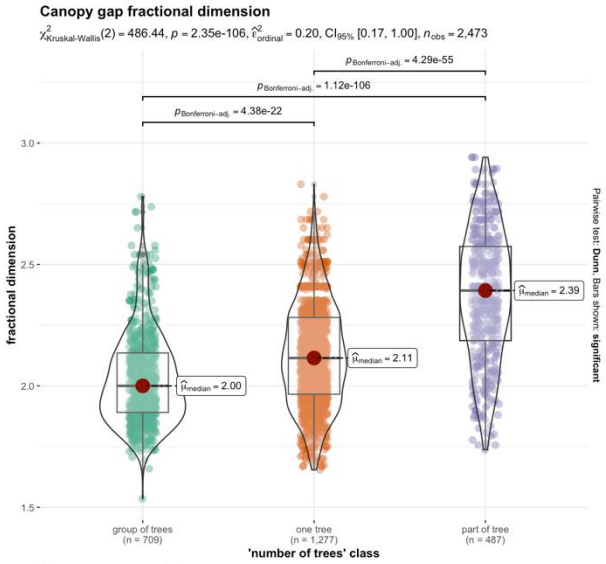
Canopy gap fractional dimension
$\chi^2_{Kruskal-Wallis}(2) = 486.44$, $p = 2.35e-106$, $\hat{\epsilon}^2_{ordinal} = 0.20$, $CI_{95\%}$ [0.17, 1.00], $n_{obs} = 2,473$
$p_{Bonferroni-adj.} = 4.29e-55$
$p_{Bonferroni-adj.} = 1.12e-106$
$p_{Bonferroni-adj.} = 4.38e-22$
fractional dimension
$\hat{\mu}_{median} = 2.00$
$\hat{\mu}_{median} = 2.11$
$\hat{\mu}_{median} = 2.39$
group of trees (n = 709)
one tree (n = 1,277)
part of tree (n = 487)
'number of trees' class
Pairwise test: Dunn, Bars shown: significant

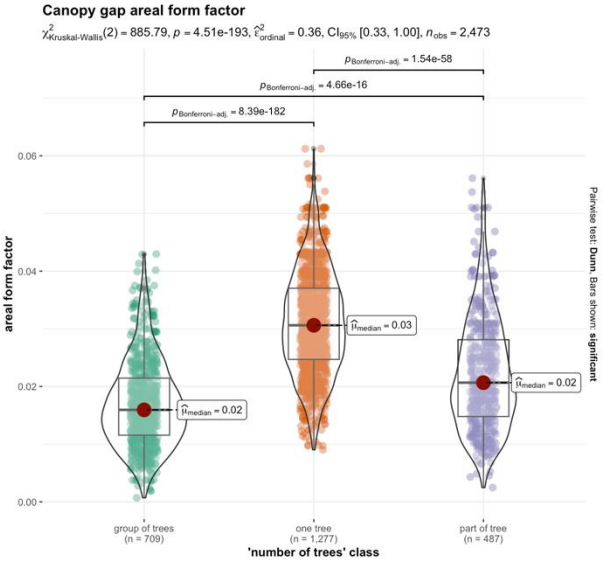
Canopy gap areal form factor
$\chi^2_{Kruskal-Wallis}(2) = 885.79$, $p = 4.51e-193$, $\hat{\epsilon}^2_{ordinal} = 0.36$, $CI_{95\%}$ [0.33, 1.00], $n_{obs} = 2,473$
$p_{Bonferroni-adj.} = 1.54e-58$
$p_{Bonferroni-adj.} = 4.66e-16$
$p_{Bonferroni-adj.} = 8.39e-182$
areal form factor
$\hat{\mu}_{median} = 0.02$
$\hat{\mu}_{median} = 0.03$
$\hat{\mu}_{median} = 0.02$
group of trees (n = 709)
one tree (n = 1,277)
part of tree (n = 487)
'number of trees' class
Pairwise test: Dunn, Bars shown: significant

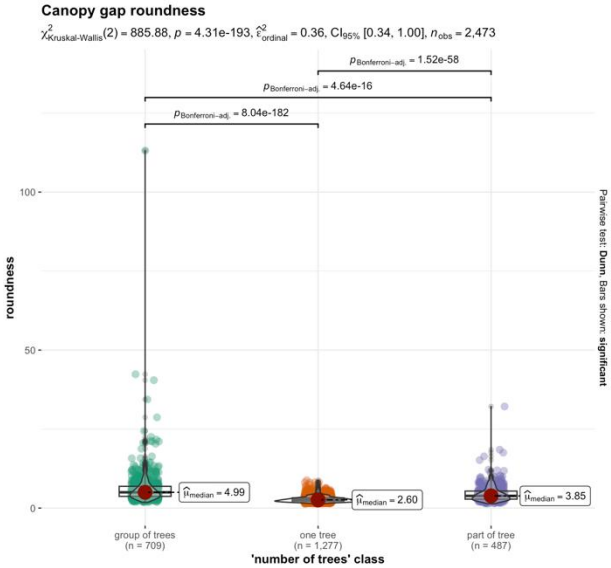
Canopy gap roundness
$\chi^2_{Kruskal-Wallis}(2) = 885.88$, $p = 4.31e-193$, $\hat{\epsilon}^2_{ordinal} = 0.36$, $CI_{95\%}$ [0.34, 1.00], $n_{obs} = 2,473$
$p_{Bonferroni-adj.} = 1.52e-58$
$p_{Bonferroni-adj.} = 4.64e-16$
$p_{Bonferroni-adj.} = 8.04e-182$
roundness
$\hat{\mu}_{median} = 4.99$
$\hat{\mu}_{median} = 2.60$
$\hat{\mu}_{median} = 3.85$
group of trees (n = 709)
one tree (n = 1,277)
part of tree (n = 487)
'number of trees' class
Pairwise test: Dunn, Bars shown: significant

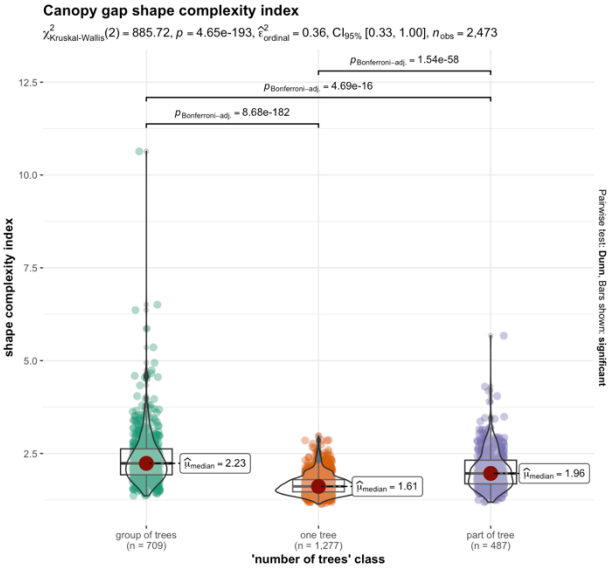
Canopy gap shape complexity index
$\chi^2_{Kruskal-Wallis}(2) = 885.72$, $p = 4.65e-193$, $\hat{\epsilon}^2_{ordinal} = 0.36$, $CI_{95\%}$ [0.33, 1.00], $n_{obs} = 2,473$
$p_{Bonferroni-adj.} = 1.54e-58$
$p_{Bonferroni-adj.} = 4.69e-16$
$p_{Bonferroni-adj.} = 8.68e-182$
shape complexity index
$\hat{\mu}_{median} = 2.23$
$\hat{\mu}_{median} = 1.61$
$\hat{\mu}_{median} = 1.96$
group of trees (n = 709)
one tree (n = 1,277)
part of tree (n = 487)
'number of trees' class
Pairwise test: Dunn, Bars shown: significant

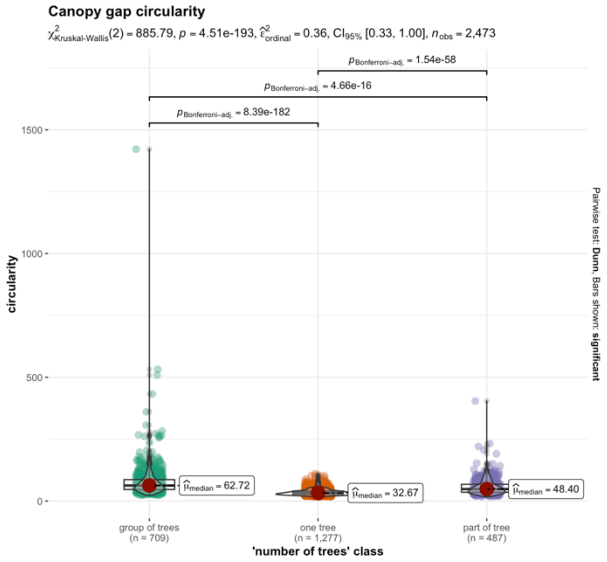
Canopy gap circularity
$\chi^2_{Kruskal-Wallis}(2) = 885.79$, $p = 4.51e-193$, $\hat{\epsilon}^2_{ordinal} = 0.36$, $CI_{95\%}$ [0.33, 1.00], $n_{obs} = 2,473$
$p_{Bonferroni-adj.} = 1.54e-58$
$p_{Bonferroni-adj.} = 4.66e-16$
$p_{Bonferroni-adj.} = 8.39e-182$
circularity
1500
1000
500
0
$\hat{\mu}_{median} = 62.72$
$\hat{\mu}_{median} = 32.67$
$\hat{\mu}_{median} = 48.40$
group of trees (n = 709)
one tree (n = 1,277)
part of tree (n = 487)
'number of trees' class
Pairwise test: Dunn, Bars shown: significant

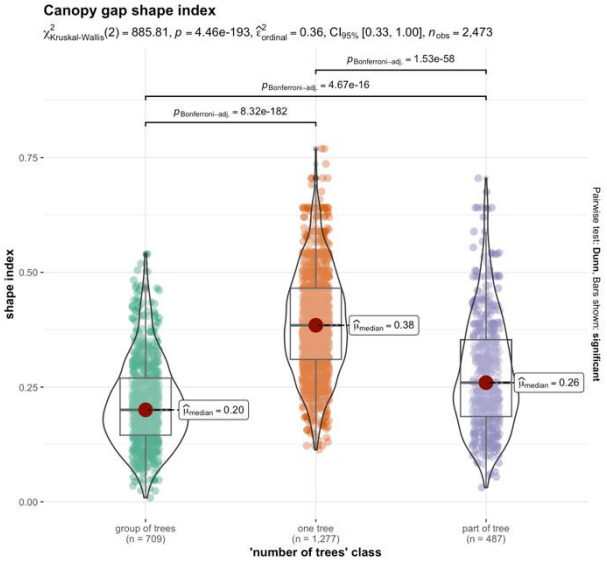
Canopy gap shape index
$\chi^2_{Kruskal-Wallis}(2) = 885.81$, $p = 4.46e-193$, $\hat{\epsilon}^2_{ordinal} = 0.36$, $CI_{95\%}$ [0.33, 1.00], $n_{obs} = 2,473$
$p_{Bonferroni-adj.} = 1.53e-58$
$p_{Bonferroni-adj.} = 4.67e-16$
$p_{Bonferroni-adj.} = 8.32e-182$
shape index
0.75
0.50
0.25
0.00
$\hat{\mu}_{median} = 0.20$
$\hat{\mu}_{median} = 0.38$
$\hat{\mu}_{median} = 0.26$
group of trees (n = 709)
one tree (n = 1,277)
part of tree (n = 487)
'number of trees' class
Pairwise test: Dunn, Bars shown: significant

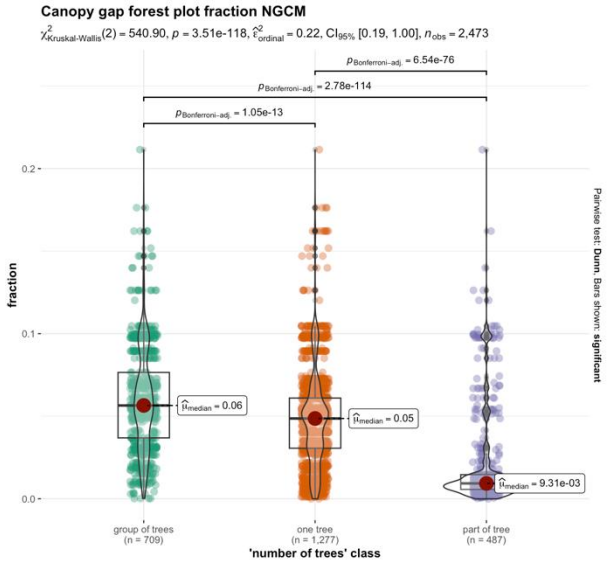
Canopy gap forest plot fraction NGCM
$\chi^2_{Kruskal-Wallis}(2) = 540.90$, $p = 3.51e-118$, $\hat{\epsilon}^2_{ordinal} = 0.22$, $CI_{95\%}$ [0.19, 1.00], $n_{obs} = 2,473$
$p_{Bonferroni-adj.} = 6.54e-76$
$p_{Bonferroni-adj.} = 2.78e-114$
$p_{Bonferroni-adj.} = 1.05e-13$
fraction
0.2
0.1
0.0
$\hat{\mu}_{median} = 0.06$
$\hat{\mu}_{median} = 0.05$
$\hat{\mu}_{median} = 9.31e-03$
group of trees (n = 709)
one tree (n = 1,277)
part of tree (n = 487)
'number of trees' class
Pairwise test: Dunn, Bars shown: significant

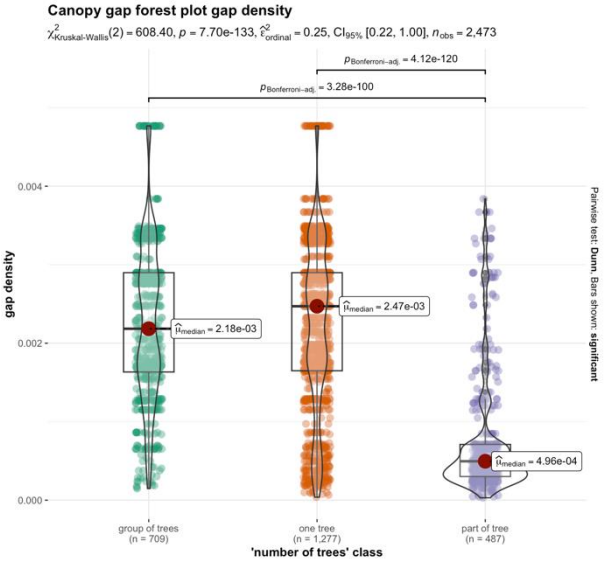
Canopy gap forest plot gap density
$\chi^2_{Kruskal-Wallis}(2) = 608.40$, $p = 7.70e-133$, $\hat{\epsilon}^2_{ordinal} = 0.25$, $CI_{95\%}$ [0.22, 1.00], $n_{obs} = 2,473$
$p_{Bonferroni-adj.} = 4.12e-120$
$p_{Bonferroni-adj.} = 3.28e-100$
gap density
0.004
0.002
0.000
$\hat{\mu}_{median} = 2.18e-03$
$\hat{\mu}_{median} = 2.47e-03$
$\hat{\mu}_{median} = 4.96e-04$
group of trees (n = 709)
one tree (n = 1,277)
part of tree (n = 487)
'number of trees' class
Pairwise test: Dunn, Bars shown: significant

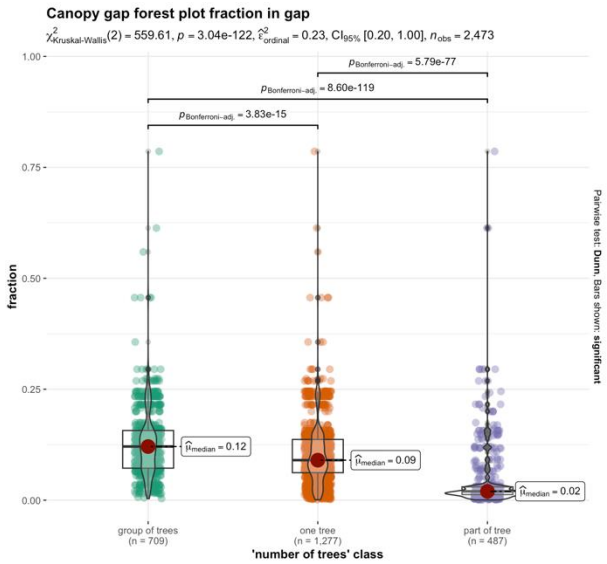
Canopy gap forest plot fraction in gap
$\chi^2_{Kruskal-Wallis}(2) = 559.61$, $p = 3.04e-122$, $\hat{\epsilon}^2_{ordinal} = 0.23$, $CI_{95\%}$ [0.20, 1.00], $n_{obs} = 2,473$
$p_{Bonferroni-adj.} = 5.79e-77$
$p_{Bonferroni-adj.} = 8.60e-119$
$p_{Bonferroni-adj.} = 3.83e-15$
fraction
1.00
0.75
0.50
0.25
0.00
$\hat{\mu}_{median} = 0.12$
$\hat{\mu}_{median} = 0.09$
$\hat{\mu}_{median} = 0.02$
group of trees (n = 709)
one tree (n = 1,277)
part of tree (n = 487)
'number of trees' class
Pairwise test: Dunn, Bars shown: significant